

ENGINEERING SYSTEMICALLY BIOAVAILABLE
ANALOGS OF ENDOGENOUS
NEUROPEPTIDES

by

Brad Reed Green

A thesis submitted to the faculty of
The University of Utah
in partial fulfillment of the requirements for the degree of

Master of Science

Department of Medicinal Chemistry

The University of Utah

December 2010

Copyright © Brad Reed Green 2010

All Rights Reserved

The University of Utah Graduate School

STATEMENT OF THESIS APPROVAL

The thesis of _____ Brad Reed Green _____

has been approved by the following supervisory committee members:

_____ Grzegorz Bulaj _____, Chair _____ 20-Oct-2010 _____
Date Approved

_____ Kuberan Balagurunathan _____, Member _____ 20-Oct-2010 _____
Date Approved

_____ H. Steve White _____, Member _____ 20-Oct-2010 _____
Date Approved

_____ Darin Y. Furgeson _____, Member _____ 20-Oct-2010 _____
Date Approved

and by _____ Darrell Davis _____, Chair of
the Department of _____ Medicinal Chemistry _____

and by Charles A. Wight, Dean of The Graduate School.

ABSTRACT

A significant amount of effort has been put into the research and development of peptide-based drugs for the treatment of human disease. The use of anticonvulsant neuropeptides for the treatment of pain and epilepsy has recently shown promise. Neuropeptides such as galanin (Gal), neuropeptide Y (NPY), neurotensin (NT), and neuropeptide W (NPW) modulate their biological activities through their respective receptor targets in the brain. Introduced intracerebroventricularly, these compounds have been shown to reduce pain and seizure activity. Upon systemic administration, however, these compounds do not exhibit the same potency. The metabolic instability and inability to penetrate the blood-brain barrier (BBB) has precluded their widespread use as drugs for neurological disorders. This work will describe the application of the lipidization-cationization strategy to several endogenous neuropeptides towards increasing their metabolic stability and improving systemic bioavailability. Based on existing structure activity relationship (SAR) information, analogs of Gal, NPY NT, and NPW were designed and chemically synthesized. The combination of increased cationic character (oligo-Lys motifs) and increased lipophilicity (lipoamino acid) resulted in analogs with increased octanol-water partitioning coefficients (logD), significantly improved metabolic stabilities, while retaining high affinities for their native receptors. Furthermore, these analogs were shown to modulate seizure activity in animal models of epilepsy upon systemic administration. Our results suggest that the cationization-

lipidization strategy may be broadly applicable across a wide variety of neuropeptides, opening up a large repertoire of new drug candidates for the treatment of neurological disorders.

TABLE OF CONTENTS

| | |
|--|-----|
| ABSTRACT | iii |
| LIST OF FIGURES | vii |
| LIST OF TABLES | x |
| LIST OF ABBREVIATIONS | xii |
| Chapter | |
| 1 INTRODUCTION | 1 |
| 1.1 Literature Review | 1 |
| 1.2 Initial Work | 8 |
| 1.3 Research Objectives | 11 |
| 1.4 References | 14 |
| 2 DEVELOPMENT OF SYSTEMICALLY-BIOAVAILABLE GALANIN ANALOGS | 17 |
| 2.1 Abstract | 17 |
| 2.2 Introduction | 18 |
| 2.3 General Methods and Materials | 21 |
| 2.4 Results and Discussion | 21 |
| 2.5 Publications | 31 |
| 2.6 Conclusions | 68 |
| 2.7 References | 69 |
| 3 INTRODUCTION OF LIPIDIZATION-CATIONIZATION MOTIFS AFFORDS SYSTEMICALLY BIOAVAILABLE NEUROPEPTIDE Y AND NEUROTENSIN ANALOGS WITH ANTICONVULSANT ACTIVITIES | 72 |
| 3.1 Introduction | 73 |
| 3.2 Materials and Methods | 74 |
| 3.3 Discussion | 78 |
| 3.4 References | 80 |

| | |
|--|-----|
| 4. ANALGESIC NEUROPEPTIDE W SUPPRESSES SEIZURES IN THE BRAIN REVEALED BY RATIONAL REPOSITIONING AND PEPTIDE ENGINEERING | 83 |
| 4.1 Abstract | 83 |
| 4.2 Introduction | 84 |
| 4.3 Materials and Methods | 86 |
| 4.4 Results | 93 |
| 4.5 Discussion | 103 |
| 4.6 Acknowledgements | 108 |
| 4.7 References | 109 |
| 5. INTRODUCTION OF LIPIDIZATION-CATIONIZATION MOTIFS INTO CYCLIC PEPTIDES: DESIGN, SYNTHESIS AND OXIDATION OF SOMATOSTATIN AND ERYTHROPOIETIN | 113 |
| 5.1 Abstract | 113 |
| 5.2 Introduction | 114 |
| 5.3 Materials and Methods | 117 |
| 5.4 Results and Discussion | 123 |
| 5.5 Conclusions | 123 |
| 5.6 References | 126 |
| 6. PERSPECTIVES AND CONCLUSIONS | 129 |
| 6.1 Perspectives | 129 |
| 6.2 Conclusions | 138 |
| 6.3 References | 140 |

LIST OF FIGURES

| Figure | Page |
|--|------|
| 1.1 Overview of the lipidization-cationization strategy | 9 |
| 1.2 Effects of differing logD values on CNS bioavailability | 10 |
| 2.1 Serum stability of modified galanin analogs | 24 |
| 2.2 Correlation between HPLC retention times and logD | 27 |
| 2.3 Effects of the lipidization-cationization strategy on logD values | 29 |
| 2.4 Developing systemically active galanin receptor ligands | 35 |
| 2.5 Characterization of the Gal-B2 analog | 37 |
| 2.6 In vitro serum stability assay | 38 |
| 2.7 Galanin receptor binding studies | 39 |
| 2.8 Anticonvulsant screening of the galanin analogs | 39 |
| 2.9 Separation of the potency and toxicity of the Gal-B2 analog | 40 |
| 2.10 Structures of Gal-B2 and LAAs used in this SAR study | 45 |
| 2.11 Relationships between the aliphatic chain length of LAAs in Gal-B2 | 47 |
| 2.12 In vitro serum stability assay for the galanin analogs | 48 |
| 2.13 Anticonvulsant activity of the galanin analogs | 49 |
| 2.14 Structures of selected galanin ligands and receptor binding affinities | 55 |

| | | |
|------|---|-----|
| 2.15 | Anticonvulsant activity of NAX 5055 (Gal-B2) | 56 |
| 2.16 | Bioavailability of NAX 5055 (Gal-B2) | 56 |
| 2.17 | Pharmacokinetic analysis of NAX 5055 (Gal-B2) in CF-1 mice | 58 |
| 2.18 | Structures of the N-terminus of GalR1/GalR2 preferring analogs | 64 |
| 2.19 | Receptor binding curves of Gal-B2 and [N-Me,des-Sar]Gal-B2 | 65 |
| 2.20 | Agonist activity of galanin analogs determined by Ca ²⁺ mobilization | 66 |
| 3.1 | Rational design of systemically-active NPY analogs | 75 |
| 3.2 | Rational design of systemically active NT analogs | 77 |
| 3.3 | LogD values of NT and NPY analogs | 77 |
| 3.4 | Helical properties of NPW-BBB2 | 77 |
| 3.5 | Metabolic stability of NT and NPY analogs | 78 |
| 3.6 | Pharmacological characterization of NPY and NT analogs | 79 |
| 4.1 | Comparison of the primary amino acid structures of neuropeptide W and neuropeptide B | 87 |
| 4.2 | Summary of anticonvulsant activities of hNPW-23 and NPB-29 following i.c.v. administration | 94 |
| 4.3 | Examples of endogenous neuropeptides and the modified peptide analogs containing the lipidization-cationization motif | 96 |
| 4.4 | Design strategy for NPW-based analogs | 97 |
| 4.5 | Comparison of the relative hydrophobicities of hNPW-23 and NPW-B1 | 101 |

| | | |
|-----|--|-----|
| 4.6 | Comparison of the metabolic stabilities of full-length hNPW-23 versus NPW-B1 | 102 |
| 4.7 | Dose-response curve for NPW-B1 | 105 |
| 5.1 | Schematic representations of different topologies exhibited by cyclized peptides | 115 |
| 5.2 | Design strategy for somatostatin analogs | 119 |
| 5.3 | Design strategy for erythropoietin analogs | 121 |
| 5.4 | Oxidative of cyclic peptides containing lipidization-cationization motifs | 124 |
| 6.1 | Potential outcomes/directions of the lipidization-cationization strategy | 130 |

LIST OF TABLES

| Table | Page |
|--|------|
| 1.1 Description of strategies commonly used to increase metabolic stability and improve bioavailability of peptide-based drugs | 7 |
| 2.1 Summary of in vitro serum stability data for galanin analogs | 23 |
| 2.2 Summary of the relative lipophilicities of galanin analogs | 28 |
| 2.3 Selected galanin-based ligands and their affinities to the galanin receptors | 35 |
| 2.4 Sequences, mass spectrometry data, HPLC retention times, and logD values for the galanin analogs | 36 |
| 2.5 Summary of the CD spectrometry and the in vitro serum stability analyses | 37 |
| 2.6 In vitro and in vivo pharmacological properties of the galanin analogs | 39 |
| 2.7 Structures of LAAs used for SPPS of the systemically active galanin analogs | 46 |
| 2.8 Structure and properties of the galanin analogs | 47 |
| 2.9 In vitro and in vivo pharmacological properties of galanin analogs | 49 |
| 2.10 Anticonvulsant profile of NAX 5055 (Gal-B2) | 55 |

| | | |
|------|--|-----|
| 2.11 | Comparative anticonvulsant activity of NAX 5055 (Gal-B2) and several control analogs | 57 |
| 2.12 | Anticonvulsant profile of NAX 5055 (Gal-B2) compared to other antiepileptic drugs in the 6 Hz model | 59 |
| 2.13 | Summary of galanin receptor agonists | 64 |
| 2.14 | Peptide sequences, calculated logD, and their stability in rat serum described in this work | 65 |
| 2.15 | In vivo pharmacology and in vitro receptor binding results | 66 |
| 3.1 | Summary of sequences, mass spectrometry data, HPLC retention times, and logD values for NT and NPY analogs | 76 |
| 3.2 | Pharmacological properties of NT and NPY analogs | 79 |
| 3.2 | Summary of physicochemical and pharmacological properties of three lead anticonvulsant neuropeptides | 80 |
| 3.3 | Examples of neuroactive peptides that may be modified with lipidization-cationization motifs | 80 |
| 4.1 | Examples of neuropeptides possessing both analgesic and antiepileptic activities in animal models of pain and epilepsy | 85 |
| 4.2 | Summary of sequences and physicochemical properties of neuropeptide W analogs | 99 |
| 4.3 | Summary of in vivo anticonvulsant activity for modified NPW analogs | 103 |
| 6.1 | Examples of endogenous neuropeptides that may be modified for analgesic effect | 133 |
| 6.2 | Strategies for improving CNS delivery of peptides | 137 |

LIST OF ABBREVIATIONS

| | |
|-------|--|
| ACN | acetonitrile |
| AED | antiepileptic drug |
| Ahx | 6-aminohexanoic acid |
| AUC | area under the curve |
| Ava | 5-aminovaleric acid |
| BBB | blood-brain barrier |
| CBZ | carbamazepine |
| CD | circular dichroism |
| CMC | critical micelle concentration |
| CNS | central nervous system |
| DCC | <i>N,N'</i> -dicyclohexylcarbodiimide |
| DIPEA | <i>N,N'</i> -diisopropylethylamine |
| EMP | erythropoietin mimetic peptide |
| EPO | erythropoietin |
| Fmoc | <i>N</i> -(9-fluorenyl)methoxycarbonyl |
| GABA | γ -aminobutyric acid |
| GAL | galanin |
| GalR | galanin receptor subtype |
| GPCR | G-coupled protein receptor |

| | |
|-------------------|---|
| HPLC | high pressure liquid chromatography |
| icv | intracerebroventricular |
| ip | intraperitoneal |
| it | intrathecal |
| k' | capacity factor |
| Kp | N ^ε -palmitoyl-L-lysine |
| LAA | lipoamino acid |
| logD | partitioning coefficient at pH 7.4 |
| MALDI-TOF | matrix-assisted laser desorption/ionization time-of-flight mass spectrometry |
| μM | micromolar |
| mM | millimolar |
| nH ₂ O | nanopure water |
| NMDA | N-methyl-D-aspartic acid |
| NPFF | neuropeptide FF |
| NPW | neuropeptide W |
| NPY | neuropeptide Y |
| NRP | non-ribosomal peptide |
| NT | neurotensin |
| NTR | neurotensin receptor |
| O ₂ Oc | 8-amino-3,6-dioxaoctanoic acid |
| PBS | phosphate buffered saline |
| PEG | polyethylene glycol |

| | |
|----------------|---|
| PNS | peripheral nervous system |
| PTX | pertussis toxin |
| PyBOP | (benzotriazol-1-yloxy)tripyrrolidinophosphonium hexafluorophosphate |
| Sar | sarcosine (<i>N</i> -methyl-glycine) |
| SAR | structure-activity relationship |
| SDS | sodium dodecyl sulfate |
| SOM | somatostatin |
| SPPS | solid phase peptide synthesis |
| $t_{1/2}$ | serum half-life |
| TFA | trifluoroacetic acid |
| TFE | 2,2,2-trifluoroethanol |
| TPE | time to peak effect |
| UV | ultraviolet |
| Y ₂ | neuropeptide Y receptor subtype 2 |
| Z | pyroglutamic acid |

CHAPTER 1

INTRODUCTION

1.1 Literature Review

1.1.1 Past and Present Treatments for Pain and Epilepsy

Excessive, uncontrolled firing of neurons (hyperexcitability) in the central nervous system (CNS) or peripheral nervous system (PNS) may result in a number of different neurological disorders. Hyperexcitability is often caused by decreased amounts of the anticonvulsant compound gamma-aminobutyric acid (GABA), or through disruptions in the cellular machinery responsible for maintaining $\text{Na}^+/\text{Ca}^{2+}$ homeostasis (1). If localized to the brain, individuals may suffer from seizure. Hyperexcitability in neurons associated with the spinal cord may result in painful neuropathies. As the underlying mechanisms of seizure activity and neuropathic pain are similar, the approaches taken towards treatment are often overlapping. For example, numerous first and second-generation anticonvulsant compounds, such as lamotrigine and gabapentin, have shown promise in treating neuropathic pain (1).

Neuropathic pain is a form of pain that can arise either from insult to the CNS/PNS, or by dysfunction of the nerve itself caused by illness or by the treatment of some illnesses (e.g., chemotherapy). Since neuropathic pain is not characterized as a

single disease, rather a spectrum of disorders all resulting in similar outcomes, treatment of neuropathies has been difficult (2). Of the analgesic compounds used for the treatment of acute pain, whether opioid or nonopioid, many have proven ineffective in alleviating some forms of neuropathic pain (3). It is estimated neuropathic pain affects approximately 1.5% of the total world population (4). Additionally, of this fraction of the population affected by neuropathic pain, only about one-third of people respond to currently available treatments (2). The most common treatment of neuropathic pain has been the administration of opioid-based drugs. However, opioids possess a number of undesirable side effects, including tolerance, constipation, high rates of abuse, respiratory depression, etc. (2). Aside from opioid-based drugs, antidepressants, anticonvulsants, N-methyl-D-aspartic acid (NMDA) receptor antagonists, and cannabinoids have also been explored (2). Despite the effectiveness of some of these approaches, the search continues for analgesic compounds with increased specificity, improved efficacy, and lower toxicity for the treatment of painful neuropathies.

Epilepsy is broadly classified as the occurrence of unprovoked seizures. Similar to what is observed in neuropathic pain, seizures commonly result from hyperexcitability of neurons. Affecting nearly 50 million individuals worldwide, epilepsy is the second most common neurological disorder, second only to stroke (5). In developed countries, it is estimated that epilepsy affects approximately 50 out of 100,000 people per year (6, 7).

The earliest antiepileptic drug (AED), potassium bromide, was reported in 1857 by Sir Charles Locock (8). The next advance in the generation of AEDs came in 1912 when Albert Hauptmann recommended the use of barbiturates (phenobarbital) to suppress seizure activity (8). Through the use of animal models of epilepsy, Merritt and

Putnam discovered the antiepileptic properties of phenytoin in 1938. This compound showed promise in treating seizures in individuals that did not respond to either potassium bromide or phenobarbital. However, phenytoin was later found to exhibit several undesirable properties including toxicity, carcinogenicity, unpredictable pharmacokinetics and adverse drug interactions (8). The next development in antiepileptic drug discovery came in 1963 with the description of the anticonvulsant properties of carbamazepine (CBZ) by Lorge and coworkers. CBZ had been found to be the most effective compound for suppression of partial seizure. As with previous AEDs side effects were discovered including: rash, blood toxicity, thrombocytopenia and Stevens-Johnson syndrome (8). Shortly after discovery of CBZ, valproate acid was characterized. Valproate was found to be efficacious against a wide range of epilepsies including idiopathic and symptomatic epilepsy. Nearly a quarter-century after the discovery of CBZ (1989), vigabatrin, the first of many next-generation AEDs was developed. This compound acted to selectively inhibit the enzyme responsible for breaking down gamma aminobutyric acid (GABA) (8). GABA serves to modulate neuronal excitability; as such, compounds that prevent the metabolism of GABA may dampen excitatory behaviors like those observed in seizure. The following 20 years of AED research resulted in a number of compounds that inhibited epileptic seizure by targeting the GABAergic system or by modulating ion flow in specific ion channels. To date, there are 20 compounds approved by the U.S. Food and Drug Administration for the treatment of epileptic seizure.

Though epilepsy is generally considered treatable using currently available AEDs, a significant portion of the patient population will either develop drug resistance or will

be completely unresponsive to AED treatments (pharmacoresistant epilepsy). Additionally, most of the currently prescribed AEDs exhibit cognitive impairment as a common side effect. It is estimated, that of the total number of those who suffer from active epilepsy, nearly 30% will not respond to available drug treatments (9). As alternatives to drug treatment for the control of seizure activity, patients are relegated to more invasive therapies such as implantable stimulation devices or resection of affected brain tissues (10). In light of pharmacoresistant epilepsy, it is apparent that there is still an unmet need for alternative treatments for controlling seizures.

1.1.2 Advantages of Peptide-Based Drugs as First-In-Class Therapies

Alternative drug treatments are currently being explored due to the lack of receptor specificity of current drugs in treating neuropathic pain, or the inability to effectively treat a significant population of people suffering from pharmacoresistant epilepsy. Our group has sought to treat pain and/or epilepsy using a peptide-based drug approach. There are numerous advantages of peptide-based drugs over their small molecule counterparts. First, peptides are extremely specific ligands for their molecular targets, and as a result, show less of the off-target effects exhibited by many small molecule drugs (11). Second, the structural and chemical diversity of synthetic peptides has drastically increased since the advent of solid phase peptide synthesis (SPPS) by Merrifield in 1963 (12). Beyond the naturally-occurring 20 amino acid repertoire available through recombinant methods, SPPS has provided the incorporation of numerous non-natural amino acids including glycoamino acids, backbone spacer units, fluorescent markers, lipoamino acids, and others. In addition to increasing the potential

for structural diversity amongst synthetic peptides, the advent of SPPS also increased the ease of synthesis of these compounds as amino acid building blocks are incorporated through repeated dehydration reactions using Fmoc or Boc chemistries. Finally, peptides are attractive drug candidates because of their low toxicity profiles (11). It is well known that peptides and proteins are biodegraded into smaller cleavage products, or even into individual amino acids for use in synthesis of new biomolecules or for excretion. As such, peptide-based drugs present attractive therapeutics because the metabolites of such compounds may either be used directly or removed completely from the system (13, 14).

1.1.3 Hurdles in the Development of Peptides as Therapeutics

On the surface, the use of peptides as potential treatments for disease appears appealing; however, there are also innate properties of these compounds that have slowed or precluded their widespread use. The major issues facing the development of peptide drugs are their low metabolic stabilities, which in turn results in poor bioavailability. Because of the large number of peptidases, serum half-lives for unmodified peptide-based drugs are relatively short, typically ranging from minutes to a few hours (15). Short half-lives often prevent intact peptides from reaching their intended targets. Numerous strategies have been employed towards increasing the metabolic stabilities of peptides. These include: N-terminal modifications (e.g., N-acylation), use of D-amino acids, conformational constraint (e.g., cyclization), side-chain/backbone modification, and others (15, 16). By making the peptide more resistant to proteolytic degradation, the likelihood of the drug reaching its intended target is greatly increased.

As a result of rapid rates of proteolytic degradation, peptide drugs also possess poor bioavailability following systemic administration. Bioavailability is defined as “the rate and extent to which the active ingredient or moiety is absorbed from a drug product and becomes available at the site of action” (17). In the case of peptide drugs targeting the CNS, the major obstacle to CNS delivery of peptides to their targets is the blood-brain barrier (BBB). The BBB can best be described as a highly selective barrier between the CNS and the rest of the body. The BBB is comprised of three tightly packed cell types at the capillary level. Furthermore, tight junctions between endothelial cells prevent paracellular transport. The BBB prevents passage of nearly all molecules except those nutrients that are small and lipophilic. Receptors on the surface of the BBB facilitate the controlled passage of larger macromolecules such as glucose and some amino acids from the blood into the brain, but all other macromolecules are excluded. A large number of efflux pumps on the surface of the BBB expel exogenous substances into the blood stream (17). This highly selective barrier serves to protect the brain from exogenous substances, such as toxins, that may otherwise damage brain tissues (18). Much in the same way that peptides have been modified for increased metabolic stability, numerous efforts have been made to circumvent the BBB to gain therapeutic access to the brain. Some of these methods have included: lipidization, increased metabolic stability through structural modifications, glycosylation, use of nutrient transporters, prodrug strategies, vector-based delivery, cationization, and conjugation to polymer systems (16). Many of these strategies take advantage of the inherent properties of the BBB to facilitate penetration into the brain (Table 1.1).

Table 1.1 Description of strategies commonly used to increase metabolic stability and improve bioavailability of peptide-based drugs (15, 16).

| | |
|---|-----------------------|
| N- or C-terminal modification | Glycosylation |
| Amino acid replacement | Nutrient transporters |
| Cyclization | Prodrug strategies |
| Increased molecular mass (polymer conjugation) | Vector-based delivery |
| Sustained delivery systems | Cationization |
| Lipidization | Polymer conjugation |
| Increased metabolic stability | |

1.2 Initial Work

1.2.1 The Cationization-Lipidization Strategy

It is the overall hypothesis of this work that analogs of endogenous neuropeptides can be engineered to increase metabolic stability and improve bioavailability upon systemic administration. Our work has focused on the lipidization and cationization of the bioactive fragments of galanin (GAL), neuropeptide Y (NPY), neurotensin (NT), neuropeptide W (NPW), somatostatin (SOM), and erythropoietin mimetic peptides (EPM). As mentioned previously, the strategies of cationization and lipidization have been employed separately towards overcoming the barriers facing peptide delivery into the CNS. However, we observed that the combination of these strategies resulted in peptide analogs with improved serum half-lives, increased partitioning coefficients (logD), and were active in the 6 Hz mouse model of pharmaco-resistant epilepsy (Figure 1.1).

Attachment of fatty acid motifs increased the overall lipophilic character of the modified peptide. Witt et al suggested that increased lipophilicity may facilitate passive diffusion of drugs across the BBB (16) (Figure 1.2). They reported that lipophilicity, reflected by larger logD values, could be increased by altering the ratio between polar and nonpolar groups within a molecule (16, 19). Furthermore, it has been reported that long chain fatty acids, such as palmitate, bind to serum albumin which may contribute to increased serum half-lives (20). This information may aid in explaining our results where it was observed that conjugation of the modified lipoamino acid N^ε-palmitoyl lysine (Kp)

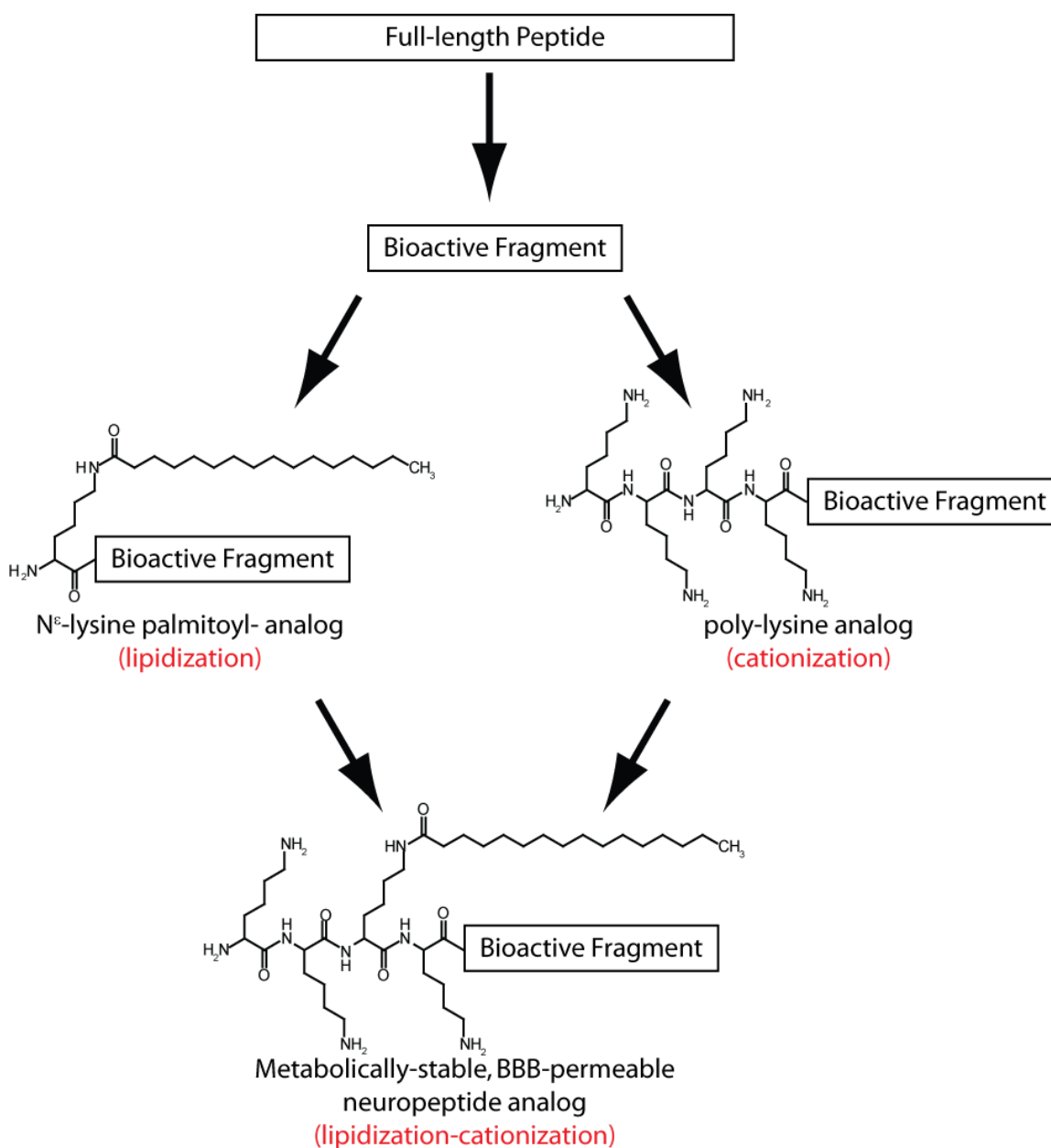


Figure 1.1 Overview of the lipidization-cationization strategy. Using the minimal number of amino acid residues required for biological activity, lipoamino acid and poly-lysine motifs were conjugated either centrally, or at the N- or C-terminus. These strategies were then combined to afford peptide analogs with increased lipophilicity (logD), improved metabolic stability, and that were active in an animal model of pharmaco-resistant epilepsy following intraperitoneal administration.

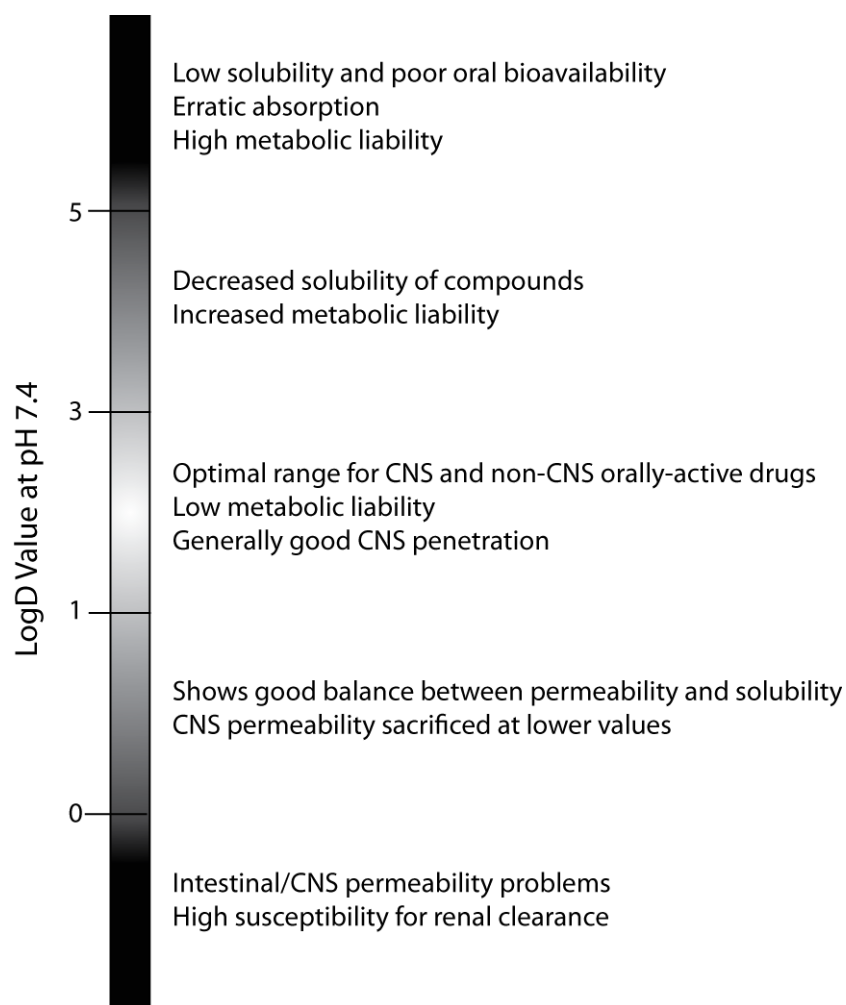


Figure 1.2 Effects of differing logD values on CNS bioavailability. The optimal range for compounds targeted to the brain spans logD values between 1 and 3. Lower values result in compounds with lower permeability, while values above this range result in compounds with poor solubility and high metabolic liability. Figure adapted from (17).

resulted in analogs with substantially increased logD and improved half-life ($t_{1/2}$) values in an in vitro serum stability assay (21-25).

Cationization of peptides has also been employed towards creating metabolically-stable, BBB-permeable peptide analogs of peptide-based drugs. It has been suggested that increased cationic character may assist in the delivery of peptides across biological membranes such as the BBB via absorptive-mediated endocytosis (16). Increased metabolic stability may well result from increased binding of the peptides to serum albumin (26). It is still unclear where cationic peptides bind to albumin; but, Svenson and coworkers reported that cationic peptides ranging from three (cationic antibacterial peptide) to nine (vasopressin) amino acids bound to both human and bovine serum albumin with similar low micromolar affinities (26). Applied independently, the strategies of cationization and lipidization have been shown to improve both metabolic stability and lipophilicity of peptide-based compounds. However, this thesis will set out to illustrate that the combination of these two approaches resulted in analogs of endogenous neuropeptides with improved lipophilicity and increased metabolic stability that were also found to exhibit potent antiepileptic activity in the 6 Hz model of epilepsy following intraperitoneal (ip) administration.

1.3 Research Objectives

Nearly 30% of individuals that suffer from seizures are resistant to available treatments for epilepsy. Furthermore, a rapidly increasing number of individuals suffer from chronic neuropathic pain. As such, the need for alternative treatments for these neurological disorders goes unmet. The primary goal of our research is to develop first-

in-class therapeutics for the treatment of pain and epilepsy. Therefore, we hypothesized that metabolically-stable, systemically-bioavailable analogs of endogenous neuropeptides could be generated using the combination of lipidization and cationization motifs. Testing of the overall hypothesis of this work was accomplished in the following four specific aims:

1.3.1 Specific Aim I

This aim tested the hypothesis that *modification of the biologically-active fragment could improve upon the physicochemical and pharmacological properties of the known anticonvulsant neuropeptide galanin*. Analogs containing lipidization and cationization motifs were designed and synthesized. Following synthesis structural, physicochemical, and pharmacological characterization of the analogs was conducted to determine which modifications lead to improved metabolic stability, BBB-permeability and anticonvulsant activities.

1.3.2 Specific Aim II

This aim focused on the extension of the lipidization-cationization strategy to other neuropeptides. The hypothesis of this aim was that *the lipidization-cationization strategy could be applied towards creation of metabolically-stable, BBB-permeable analogs of neurotensin and neuropeptide Y*. Similar to the galanin analogs described in Specific Aim I, these analogs will be examined for improved physicochemical and pharmacological properties.

1.3.3 Specific Aim III

This aim tested the hypothesis that *the lipidization-cationization strategy could be applied for the repositioning of analgesic peptides for use as anticonvulsants due to the common origins of the two neurological disorders*. Studies in support of this aim focused on the application of lipidization and cationization motifs to the analgesic peptide neuropeptide W. Since neuropeptide W has been previously shown to modulate neuronal hyperexcitability, the underlying cause of both neuropathic pain and epilepsy, we explored the hypothesis that this endogenous neuropeptide could be *repositioned* for the treatment of seizure. Analogs were designed, synthesized, and characterized with the aim of creating metabolically-stable, orally-bioavailable NPW analogs.

1.3.4 Specific Aim IV

Specific Aim IV tested the hypothesis that *lipidization and cationization motifs could be coupled to peptides with single disulfide bridges towards creation of BBB-permeable cyclic peptides*. As proof-of-concept that single disulfide bridge-containing peptides could be modified with lipidization-cationization motifs, analogs of somatostatin and erythropoietin were constructed. Numerous pharmacologically-active peptides contain disulfide bridges necessary for their biological activities. Construction of BBB-permeable cyclic peptides may provide a framework for the design and synthesis of other pharmacologically-active peptidic compounds such as conotoxins, non-ribosomal (NRP) and ribosomal peptide (RP) natural products, and others.

1.4 References

1. Finnerup, N. B., Gottrup, H., and Jensen, T. S. (2002) Anticonvulsants in central pain, *Expert Opin. Pharmacother.* 3, 1411-1420.
2. Jensen, T. S., Madsen, C. S., and Finnerup, N. B. (2009) Pharmacology and treatment of neuropathic pain, *Curr. Opin. Neurol.* 22, 467-474.
3. Perret, D., and Luo, Z. D. (2009) Targeting voltage-gated calcium channels for neuropathic pain management, *Neurotherapeutics* 6, 679-692.
4. Taylor, R. S. (2006) Epidemiology of refractory neuropathic pain, *Pain Pract.* 6, 22-26.
5. Pitkänen, A., and Lukasiuk, K. (2009) Molecular and cellular basis of epileptogenesis in symptomatic epilepsy, *Epilepsy Behav.* 14, 16-25.
6. Hirtz, D., Thurman, D. J., Gwinn-Hardy, K., Mohamed, M., Chaudhuri, A. R., and Zalutsky, R. (2007) How common are the "common" neurologic disorders?, *Neurology* 68, 326-337.
7. Sander, J. W. (2003) The epidemiology of epilepsy revisited, *Curr. Opin. Neurol.* 16, 165-170.
8. Arzimanoglou, A., Ben-Menachem, E., Cramer, J., Glauser, T., Seeruthun, R., and Harrison, M. (2010) The evolution of antiepileptic drug development and regulation, *Epileptic Disord.* 12, 3-15.
9. Schmidt, D., and Löscher, W. (2005) Drug resistance in epilepsy: Putative neurobiological and clinical mechanisms, *Epilepsia* 46, 858-877.
10. Epilepsy Research Foundation. What is Epilepsy?
<http://www.epilepsyfoundation.org> (accessed 10/01/10).
11. Sewald, N., and Jakubke, H.-D. (2002) *Peptides: Chemistry and biology*, Wiley-VCH Verlag GmbH & Co., Weinheim.
12. Merrifield, R. B. (1963) Solid phase peptide synthesis I. The synthesis of a tetrapeptide, *J. Am. Chem. Soc.* 85, 2149-2154.
13. Bellmann-Sickert, K., and Beck-Sickinger, A. G. (2010) Peptide drugs to target G protein-coupled receptors, *Trends Pharmacol. Sci.*
14. Rawlings, N. D., and Barrett, A. J. (1993) Evolutionary families of peptidases, *Biochem. J.* 290, 205-218.

15. Werle, W., and Bernkop-Schnürch, A. (2006) Strategies to improve plasma half life time of peptide and protein drugs, *Amino Acids* 30, 351-367.
16. Witt, K. A., Gillespie, T. J., Huber, J. D., Egleton, R. D., and Davis, T. P. (2001) Peptide drug modifications to enhance bioavailability and blood-brain barrier permeability, *Peptides* 22, 2329-2343.
17. van de Waterbeemd, H., Lennernäs, H., and Artursson, P. (2003) *Drug Bioavailability: Estimation of solubility, permeability, absorption and bioavailability*, Wiley-VCH Verlag GmbH & Co., Weinheim.
18. Rubin, L. L., and Staddon, J. M. (1999) The cell biology of the blood-brain barrier, *Annu. Rev. Neurosci.* 22, 11-28.
19. Egleton, R. D., and Davis, T. P. (1997) Bioavailability and transport of peptides and peptide drugs into the brain, *Peptides* 18, 1431-1439.
20. Kragh-Hansen, U. (1981) Molecular aspects of ligand binding to serum albumin, *Pharmacol. Rev.* 33, 17-53.
21. Bulaj, G., Green, B. R., Lee, H. K., Robertson, C. R., White, K., Zhang, L., Sochanska, M., Flynn, S. P., Scholl, E. A., Pruess, T. H., Smith, M. D., and White, H. S. (2008) Design, synthesis, and characterization of high-affinity, systemically-active galanin analogues with potent anticonvulsant activities, *J. Med. Chem.* 51, 8038-8047.
22. Zhang, L., Robertson, C. R., Green, B. R., Pruess, T. H., White, H. S., and Bulaj, G. (2009) Structural requirements for a lipoamino acid in modulating the anticonvulsant activities of systemically active galanin analogues, *J. Med. Chem.* 52, 1310-1316.
23. Robertson, C. R., Scholl, E. A., Pruess, T. H., Green, B. R., White, H. S., and Bulaj, G. (2009) Engineering galanin analogues that discriminate between GalR1 and GalR2 receptor subtypes and exhibit anticonvulsant activity following systemic delivery, *J. Med. Chem.* 53, 1871-1875.
24. White, H. S., Scholl, E. A., Klein, B. D., Flynn, S. P., Pruess, T. H., Green, B. R., Zhang, L., and Bulaj, G. (2009) Developing novel antiepileptic drugs: characterization of NAX 5055, a systemically-active galanin analog, in epilepsy models, *Neurotherapeutics* 6, 372-380.
25. Green, B. R., White, K. L., McDougale, D. R., Zhang, L., Klein, B., Scholl, E. A., Pruess, T. H., White, H. S., and Bulaj, G. (2010) Introduction of lipidization-cationization motifs affords systemically bioavailable neuropeptide Y and neurotensin analogs with anticonvulsant activities, *J. Pept. Sci.* 16, 486-495.

26. Svenson, J., Brandsdal, B.-O., Stensen, W., and Svendsen, J. S. (2007) Albumin binding of short cationic antimicrobial micropeptides and its influence in the in vitro bactericidal effect, *J. Med. Chem.* 50, 3334-3339.

CHAPTER 2

GENERATING METABOLICALLY-STABLE, SYSTEMICALLY BIOAVAILABLE GALANIN ANALOGS

2.1 Abstract

Galanin is a multifaceted, endogenous neuropeptide that has been shown to modulate anticonvulsant behavior. However, its use as an antiepileptic drug has been hindered by a lack of serum stability as well as poor CNS bioavailability. We have sought to improve upon the physicochemical and pharmacological properties of this peptide through a combination strategy of cationization and lipidization. As such, we identified a modified galanin analog (Gal-B2) which possessed improved metabolic stability, increased *n*-octanol/water partitioning (logD), and exhibited potent anticonvulsant activity in the 6 Hz mouse model of pharmaco-resistant epilepsy. My contribution to these efforts, described in the following chapter, illustrated how modifications of the Gal (1-16) active fragment influenced physicochemical properties such as serum stability and logD values. This was accomplished through the use of two *in vitro* assays that monitored peptide stability and relative lipophilicity. Furthermore, I examined the correlation between increases in these two properties and improved pharmacological activity in a mouse model of epilepsy.

2.2 Introduction

2.2.1 Galanin and Gal-receptors as Targets for Pain and Epilepsy

Human galanin is an endogenous neuropeptide consisting of 30 amino acid residues (sequence: GWTLNSAGYLLGPHAVGNHRSFSDKNGLTS-COOH). Galanin was first isolated from porcine intestinal tissues in 1983 by Tatemoto and co-workers (1). It was initially implicated to play a role in the contraction of smooth muscle tissues, with the additional capability of modulating hyperglycemia (1). Further research revealed that galanin is extremely diverse in its biological actions having been shown to be involved in the regulation of feeding behaviors, neuronal hyperexcitability, pain pathways, and anxiety (2).

It has been shown that the N-terminal fragment of the peptide, Gal (1-16), binds with comparable low nanomolar affinity to that of the full-length peptide (3, 4). Moreover, Crawley and others have reported that central administration of the Gal (1-16) fragment was sufficient to elicit similar agonist activity to that exhibited by the full-length peptide (4,5). Unlike the N-terminal fragment, the C-terminal portion of galanin, Gal (17-29), exhibits no such behavior suggesting that the biological activity of galanin is contained within the sequence of the first sixteen amino acid residues (3, 6). Alanine-positional scanning experiments later identified residues within the bioactive fragment responsible for the effective binding and agonistic activities of Gal (1-16) as Trp2, Asn5, and Tyr9, in addition to the N-terminal amine. Mutations to these residues resulted in drastic differences in ligand binding affinity for galanin receptors (3). Using available structure-activity data, researchers have set out to develop both small molecule and

peptide-derived GalR agonists with the aim of developing compounds capable of treating various neurological disorders.

Galanin exerts its biological actions by activating one of three G protein coupled receptor targets (GalR1, GalR2, or GalR3) (4, 7). GalR3 has been identified and cloned; however, the precise function of this receptor unclear at the present time, it is not expected to play a role in epilepsy. Studies have shown that the receptor subtypes are located centrally (brain and spinal chord), peripherally (peripheral neurons such as dorsal root ganglion), and in the gut tissues. As mentioned previously, galanin plays an important role in the neuroendocrine system activation of the GalR-subtypes and signals the release of certain hormones for the modulation of feeding behaviors. However, more relevant to our work, is the ability of this peptide to control neuronal excitability from which neurological disorders such as neuropathic pain and epilepsy originate (2, 8). Ito and coworkers proposed that galanin inhibits neuronal excitability via hyperpolarization of the cell membrane by increasing K^+ conductance and decreasing Ca^{2+} conductance (9). Previous studies have shown that GalR1, GalR2, as well as galanin itself, can be found at elevated levels in the hippocampus of the brain (4). The presence of galanin and its respective receptors in this region are of significance because damage to the hippocampus has been implicated in epileptogenesis (10). In support of this idea, GalR1 knock-out studies in mice showed an increase in frequency and severity of pilocarpine-induced seizures (11). Furthermore, Mazarati and others have previously shown that direct intracerebroventricular (i.c.v.) injection of galanin (1-29) into the hippocampus inhibited seizure activity in pertussis-toxin (PTX) treated rats (11).

2.2.2 Current Approaches to Targeting Gal-receptors: Small

Molecule Versus Peptide-based Galanin Analogs

Two small molecule GalR agonists of particular interest are galmic and galnon. These compounds exhibited increased resistance to serum degradation and were shown active in animal models of epilepsy (*12, 13*). Though small molecule GalR agonists, such as galmic and galnon, have shown promise as antiepileptic drugs, receptor binding affinities were significantly lower than those exhibited by peptide-based galanin agonists (μM versus nM) (*14*). Furthermore, galnon was shown to act on numerous GPCRs aside from Gal-receptors (i.e., off target effects) (*15*). Numerous peptide-derived GalR agonists have also been previously reported in the literature (*16*). However, these analogs lacked either the metabolic-stability or BBB-permeability necessary for further development as systemically-bioavailable treatments for neurological disorders (*17*). As such, there is still an unmet need for peptide-based compounds that are systemically-bioavailable.

2.2.3 The Lipidization-Cationization Strategy

In order to create systemically-active peptide-based agonists of GalR1 or GalR2, metabolic stability and BBB-permeability must be improved. As mentioned in the previous chapter, numerous strategies have been employed to overcome the inherent shortcomings of peptide-based drugs. However, current approaches have met with limited success. We showed that the combination of lipidization and cationization applied to the bioactive fragments of endogenous neuropeptides resulted in peptide analogs possessing improved metabolic stabilities, increased logD values that also

possessed potent anticonvulsant properties in the 6 Hz pharmacoresistant model of epilepsy. This strategy has been studied extensively through our development of galanin analogs possessing the lipidization-cationization motifs (17-20). The following section will highlight our findings with respect to this approach. Specifically, this chapter will place special emphasis on my individual role in studying how these modifications influence physicochemical properties such as serum stability and *n*-octanol/water partitioning coefficients (logD).

2.3 General Methods and Materials

A complete description of methods and materials relevant to this chapter can be found in the attached manuscripts (17-20).

2.4 Results and Discussion

Results presented in this section are a compilation of data, published and unpublished, from the attached manuscripts (17-20). Special emphasis will be placed on the relationships between galanin analog structure and physicochemical attributes such as metabolic stability and partitioning coefficient (logD). To date, over 120 analogs of galanin have been designed and synthesized. A number of these compounds have been further examined to determine which structural properties translate into metabolically-stable, systemically-bioavailable anticonvulsant galanin analogs.

2.4.1 Relationship Between Structure and Metabolic Stability

of Galanin Analogs

It was observed from the in vitro serum stability data that the modifications made to the galanin active fragment (i.e., lipidization-cationization motifs) significantly improved the $t_{1/2}$ -values for the analogs. This becomes apparent through comparison of the $t_{1/2}$ -values for each of the modified analogs to that of Gal (1-16) (Table 2.1).

By plotting the $t_{1/2}$ -values, several important observations could be made with regard to structure-stability relationships (Figure 2.1). First, addition of either the lipidization or cationization motifs, individually, had an immediate effect on serum half-lives. Introduction of a oligo-lysine motif in the Gal-K(4) analog increased the half-life to approximately 4.7 h. This is consistent with previous work on endomorphin I and II which showed that increased cationic character resulted in increased resistance to proteolytic degradation (21, 22). It was hypothesized that this increase may arise from limited protease accessibility to sensitive N- or C-terminal regions (21). Furthermore, conjugation of a lipoamino acid motif appears to be the major contributor for improved metabolic stability. Coupling of N^ε-palmitoyl-L-lysine to the C-terminus of Gal (1-15) in the Gal-LAA analog exhibited serum stability of over 15 h.

Second, examination of the fatty acid motif revealed direct correlation between the length of the fatty acid and $t_{1/2}$ values (19). Through synthesis of a series of analogs in which the length of the fatty acid varied from C₈ to C₁₈, it was shown that chain lengths longer than C₁₀ and shorter than C₁₈ yielded $t_{1/2}$ values greater than 8 h. It was hypothesized that the observed increase in serum stability may result from i) limitation of proteases that would typically degrade the unmodified peptide and/or ii) through

Table 2.1 Summary of in vitro serum stability data for galanin analogs.

| | Galanin Analog | Sequence | t_{1/2} (h) |
|----|--------------------------|--|----------------------------|
| 1 | Gal (1-16) | GWTLNSAGYLLGPHAV | 0.13 |
| 2 | Gal-B2-C ₈ | (Sar)WTLNSAGYLLGPKK(Lys-octanoyl)K | 3.1 |
| 3 | Gal-K(4) | (Sar)WTLNSAGYLLGPKKKK | 4.7 |
| 4 | Gal-B8 | (Sar)WTLNSAGYLLGPRR(Kp)R | 4.8 |
| 5 | Gal-B2-C ₁₀ | (Sar)WTLNSAGYLLGPKK(Lys-decanoyl)K | 5.5 |
| 6 | Gal-B11 | (Sar)WTLNSAGYLLGKK(Kp)K | 5.6 |
| 7 | Gal-B2-C ₁₈ | (Sar)WTLNSAGYLLGPKK(Lys-stearoyl)K | 7.2 |
| 8 | Gal-B3 | (Sar)WTLNSAGYLLGPK(Kp)KK | 8.6 |
| 9 | Gal-B2-C ₁₄ | (Sar)WTLNSAGYLLGPKK(Lys-myristoyl)K | 8.6 |
| 10 | Gal-B10 | (Sar)WTLNSAGYLLKKKK(Kp)K | 8.7 |
| 11 | [N-Me,des-Sar] Gal-B2 | (N-Methyl-Trp)TLNSAGYLLGPKK(Kp)K | 9.0 |
| 12 | Gal-B2 | (Sar)WTLNSAGYLLGPKK(Kp)K | 9.4 |
| 13 | Gal-B5 | WTLNSAGYLLGPKK(Kp)K | 10 |
| 14 | Gal-B1 | (Sar)WTLNSAGYLLGPKKK(Kp) | 10.3 |
| 15 | Gal-B2-C ₁₂ | (Sar)WTLNSAGYLLGPKK(Lys-lauroyl)K | 11.5 |
| 16 | Gal-B12 | (Sar)WTLNSAGYLLKK(Kp)K | 12.0 |
| 17 | Gal-B2-MPEG ₄ | (Sar)WTLNSAGYLLGPKK(Lys-MPEG ₄)K | 15.0 |
| 18 | Gal-B6 | GWTLNSAGYLLGPKK(Kp)K | > 15 |
| 19 | Gal-LAA | (Sar)WTLNSAGYLLGPHA(Kp) | > 15 |
| 20 | Gal-B4 | (Sar)WTLNSAGYLLGP(Kp)KKK | > 15 |
| 21 | Gal-B9 | (Sar)WTLNSAGYLLGP(D-K)(D-K)(Kp)(D-K) | > 15 |

Table summarizes galanin analogs, amino acid sequences and calculated serum half-lives (t_{1/2}) for compounds studied in an in vitro serum stability assay. Analogs were incubated in the presence of 25% rat blood serum, 0.1 M Tris-HCl, pH 7.4 and nH₂O at 37 °C for 8 h. At discrete time points (0, 0.5, 1, 2, 4, and 8 h) reactions were quenched, precipitated, and supernatants analyzed by analytical HPLC. Degradation was determined as the disappearance of the native peptide with respect to time. The t_{1/2}-values were obtained from the average of at least three independent time-course experiments. Colors represent relative half-lives for each of the analogs (Black: 0-4 h, Purple: 4-8 h, Blue: 8-12 h, and Green: t_{1/2} ≥ 15 h).

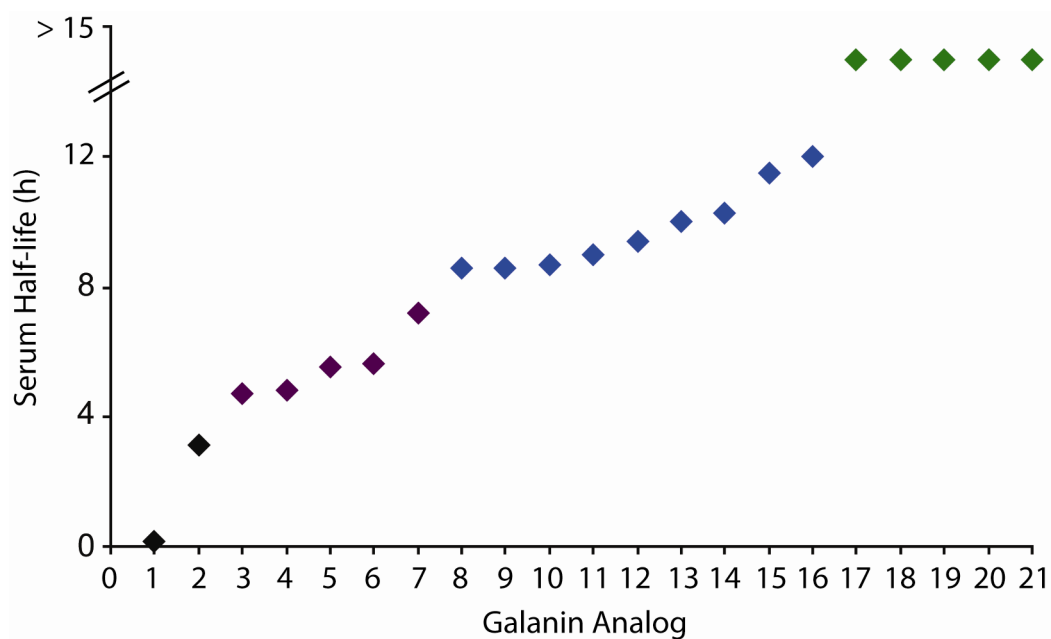


Figure 2.1 Serum stability of modified galanin analogs. Each point represents the average of at least three independent time course experiments. Analogs were divided into four groups based on calculated $t_{1/2}$ values: Black (0-4 h), Purple (4-8 h), Blue (8-12 h), and Green (> 15 h). For identity of galanin analogs, refer to table 1.

increased stability by binding of the lipidized peptide to fatty acid binding sites on serum albumin (19). Interestingly, it was also observed that above C₁₄, t_{1/2}-values began to decrease with the extension of the fatty acid motif with each additional ethylene group (Gal-B2-C₁₆ and Gal-B2-C₁₈); suggesting an optimal fatty acid chain length with respect to serum stability. These results were consistent to those of van de Waterbeemd et al who suggested that increased lipophilicity, beyond a certain threshold, may result in increased metabolic liability (23).

Third, it was shown that maximal metabolic stability could be attained through i) “shifting” of the lipoamino acid towards the N-terminus (Gal-LAA and Gal-B4), ii) conjugation of polymers such as monodispersed PEG₄ (Gal-B2-MPEG₄), and iii) incorporation of peptidase-resistant _D-amino acids (Gal-B9). It was observed that direct conjugation of the lipoamino acid to the C-terminus of the galanin active fragment resulted in t_{1/2}-values greater than 15 h. It is thought that the fatty acid tail may act to prevent endopeptidase access to the peptide backbone. However, in these analogs, we also observed a loss in pharmacological activity, resulting from steric interference of the bulky modification with respect to receptor binding (18). Polymer-mediated transport using polyethylene glycols has been employed for delivery of numerous biomolecules (24). In the context of the lipidization-cationization strategy, the MPEG₄ modification was shown to have a dramatic effect on the serum stability of the galanin analog Gal-B2-MPEG₄. Similar to the internally truncated peptides, this analog exhibited improved stability, but was significantly less active in the 6 Hz model of epilepsy. Finally, modification of the cationization motif, by incorporation of _D-Lys, yielded the largest increase in t_{1/2} (Gal-B9). As many proteases are not active on _D-amino acids, this strategy

remains one of the most promising options for increasing peptide stability. However, as suggested by Youngblood, the development of peptide libraries containing D-amino acids may be limited by the relatively high cost of these amino acid residues (25).

2.4.2 Relationship Between Structure and Partitioning Coefficient

(logD) of Galanin Analogs

The next physicochemical property explored was that of lipophilicity. Octanol/water partitioning (logD) is currently one of the most employed methods for description of compound lipophilicity. The values obtained from these experiments are often used to describe the potential for a compound to penetrate biological membranes such as the BBB. LogD values were assessed either by the shake-flask method or by determination of the capacity factor (k') using HPLC retention times (17-19). A linear relationship exists between experimental logD values and HPLC retention times (23) (Figure 2.2). A summary of the HPLC retention times and logD values calculated by either of these two methods is summarized in Table 2.2.

Plotting the data obtained for each of the analogs provided important information regarding the effects of the lipidization-cationization strategy on logD values (Figure 2.3). The Gal (1-16) fragment by itself was modestly hydrophobic without further modification (logD = 0.7). When an oligo-Lys motif was added to the C-terminus (Gal-K(4)), the additional positive charge resulted in a shift in HPLC retention time,

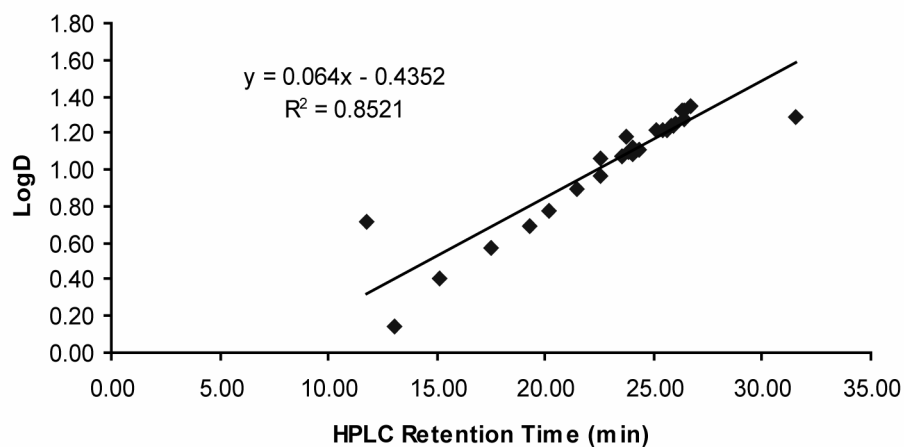


Figure 2.2 Correlation between HPLC retention times and logD. Each point represents the average of three logD experiments for the analogs listed in Table 2.2. LogD values of Gal (1-16), Gal-K(4), Gal-B2, and Gal-LAA were determined by the shake-flask method. These values were plotted against retention time to create a standard curve by which the logD of remaining analogs could be determined using HPLC retention times (18).

Table 2.2 Summary of the relative lipophilicities of galanin analogs.

| | Galanin Analog | Sequence | Retention Time (min) | LogD |
|----|--------------------------|---|-----------------------------|-------------|
| 1 | Gal-K(4) | (Sar)WTLNSAGYLLGPKKKK | 15.13 ± 0.42 | 0.40 ± 0.05 |
| 2 | Gal-B2-MPEG ₄ | (Sar)WTLNSAGYLLGPKK(Lys-MPEG ₄)K | 17.57 ± 0.01 | 0.57 ± 0.00 |
| 3 | Gal (1-16) | GWTLNSAGYLLGPHAV | 19.32 ± 0.37 | 0.69 ± 0.02 |
| 4 | Gal-B2-C ₈ | (Sar)WTLNSAGYLLGPKK(Lys-octanoyl)K | 20.13 ± 0.05 | 0.78 ± 0.01 |
| 5 | Gal-B2-C ₁₀ | (Sar)WTLNSAGYLLGPKK(Lys-decanoyl)K | 21.49 ± 0.05 | 0.90 ± 0.01 |
| 6 | Gal-B6 | GWTLNSAGYLLGPKK(K _p)K | 22.53 ± 0.42 | 0.96 ± 0.24 |
| 7 | Gal-B2-C ₁₂ | (Sar)WTLNSAGYLLGPKK(Lys-lauroyl)K | 22.51 ± 0.03 | 1.06 ± 0.01 |
| 8 | Gal-B10 | (Sar)WTLNSAGYLLKKKK(K _p)K | 24.00 ± 0.13 | 1.08 ± 0.02 |
| 9 | Gal-B2-C ₁₄ | (Sar)WTLNSAGYLLGPKK(Lys-myristoyl)K | 23.76 ± 0.03 | 1.18 ± 0.01 |
| 10 | Gal-B9 | (Sar)WTLNSAGYLLGP(D-K)(D-K)(K _p)(D-K) | 25.44 ± 0.12 | 1.21 ± 0.02 |
| 11 | Gal-B5 | WTLNSAGYLLGPKK(K _p)K | 25.62 ± 0.10 | 1.22 ± 0.02 |
| 12 | Gal-B11 | (Sar)WTLNSAGYLLGKK(K _p)K | 25.67 ± 0.14 | 1.23 ± 0.02 |
| 13 | Gal-B2 | (Sar)WTLNSAGYLLGPKK(K _p)K | 25.84 ± 0.10 | 1.24 ± 0.02 |
| 14 | Gal-B4 | (Sar)WTLNSAGYLLGP(K _p)KKK | 25.88 ± 0.14 | 1.24 ± 0.02 |
| 15 | Gal-B12 | (Sar)WTLNSAGYLLKK(K _p)K | 25.82 ± 0.10 | 1.24 ± 0.02 |
| 16 | Gal-B3 | (Sar)WTLNSAGYLLGP(K _p)KK | 25.96 ± 0.29 | 1.25 ± 0.03 |
| 17 | Gal-B1 | (Sar)WTLNSAGYLLGPKKK(K _p) | 25.99 ± 0.16 | 1.25 ± 0.03 |
| 18 | Gal-B8 | (Sar)WTLNSAGYLLGPRR(K _p)R | 26.26 ± 0.09 | 1.28 ± 0.02 |
| 19 | [N-Me,des-Sar] Gal-B2 | (N-Methyl-Trp)TLNSAGYLLGPKK(K _p)K | 31.5 ± 0.01 | 1.29 ± 0.01 |
| 20 | Gal-B2-C ₁₈ | (Sar)WTLNSAGYLLGPKK(Lys-stearoyl)K | 26.73 ± 0.18 | 1.35 ± 0.02 |
| 21 | Gal-LAA | (Sar)WTLNSAGYLLGPHA(K _p) | 28.31 ± 0.04 | 1.45 ± 0.02 |

Table summarizes galanin analogs, amino acid sequences HPLC retention times, and calculated logD values. Values were calculated using either the shake-flask method or by HPLC capacity factor (k'). Colors represent the range of logD values for each of the analogs (Black: 0-1.0, Purple: 1.0-1.25, Blue: 1.25-1.5). Data were collected as the average of three independent experiments. All samples were analyzed by analytical HPLC over a linear gradient ranging from 20-100% solvent B (90% acetonitrile, 0.1% trifluoroacetic acid) in 40 min.

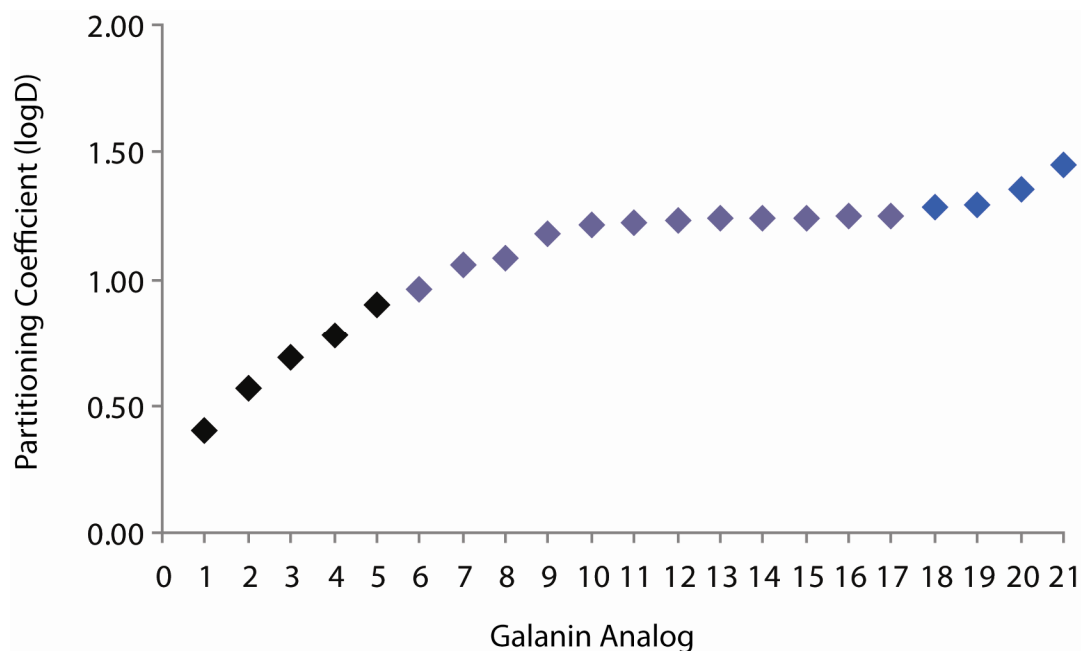


Figure 2.3 Effects of the lipidization-cationization strategy on logD values. Data represent the average logD values obtained from three independent experiments. Individually, lipidization and cationization had dramatic effects on logD. Increased cationization resulted in analogs with logD values lower than that of the galanin active fragments (logD Gal-(K)4 = 0.4); whereas, lipidization of the active fragment dramatically increased logD (logD Gal-LAA = 1.45). The majority of analogs containing lipidization-cationization motifs had logD values of about 1.24. Analogs were divided into three groups based on logD values: Black: 0-1.0, Purple: 1.0-1.25, Blue: 1.25-1.5.

reflected by a lower logD of 0.4. This is due to the increased number of basic residues, which exhibit a positive charge at physiological pH. Likewise, conjugation of the Lys-PEG₄ decreased the logD value, presumably by the same means. Similar to serum stability data, there was good correlation between the length of the fatty acid motif and increased logD values where $C_8 < C_{10} \ll C_{18}$ (19). As mentioned in the introductory chapter, logD values in ranging from 1-3 are ideal for good CNS penetration; the C₈ and C₁₀ fatty acids fall just short of this range, but did exhibit some anticonvulsant activity in the 6 Hz mouse model of epilepsy (19, 23). When the lipoamino acid was coupled directly to the bioactive fragment (Gal-LAA), a dramatic shift in retention time was observed (logD = 1.45). This would suggest that the presence of the lipoamino acid is the key determinant for increased logD. Combination of the lipidization and cationization strategies resulted in a number of galanin analogs with logD values at or near 1.24. The largest logD values were observed in the Gal-B2-C₁₈ and Gal-LAA analogs, suggesting that increased chain length or a decrease in charge results in increased lipophilicity.

In addition to increased serum half-lives conferred by the lipidization-cationization motifs, it was also concluded that these modifications influenced the lipophilicity of galanin analogs. Through modification of the galanin active fragment, we were able to generate compounds with increased logD (0.69 for Gal (1-16) compared to ≥ 1.24 for modified analogs). Most peptide-based drugs do not cross the BBB because of i) overall hydrophilic character of the peptide and ii) the absence of specific peptide transport systems on the BBB membrane. (23, 24). By coupling of lipophilic motifs, such as fatty acids, the balance is shifted towards making the compounds more hydrophobic and therefore increases the rates of passive diffusion across the BBB (24).

It is the conclusion of this study, that attachment of the fatty acid to the ϵ -amine of one of the Lys-residues within the lipidization-cationization motif sufficiently improved logD values for increased penetration into the BBB. Neither the position of the LAA, central truncation of the bioactive fragment, nor the composition of the cationization motifs had a significant effect on logD; the major determinant of logD is likely the length of the fatty acid.

2.5 Publications

The following subsections will include publications relevant to the galanin project. All manuscripts lend support to the main goal of this project which is to develop metabolically-stable, systemically-bioavailable galanin analogs that possess potent anticonvulsant activity. Furthermore, results from the in vitro serum stability and logD assays are further described. Section 2.4.1 focuses on the application of lipidization-cationization motifs to GAL (1-16). Design, synthesis, and both physicochemical and pharmacological characterization are described. LogD and serum stability data from a number of galanin analogs will be described in this chapter. Section 2.4.2 describes the synthesis and characterization of Gal-B2 analogs containing alternative lipidization motifs conjugated to the ϵ -amine of Lys-16. The pharmacological consequences of these modifications in addition to their effect on serum stability and logD values are illustrated in this subsection. Section 2.4.3 is an in-depth look at the pharmacological properties of the Gal-B2 (NAX-5055) analog. Finally, Section 2.4.4 will describe efforts in developing subtype-selective Gal-B2 based analogs through a strategy of “atom shaving” of the N-terminus. Using the Gal-B2 analog, we showed that removal of atoms from the

N-terminus yielded metabolically stable, systemically bioavailable galanin analogs that exhibited preference for the GalR2 subtype.

2.5.1 Design, Synthesis, and Characterization of High-Affinity,
Systemically-Active Galanin Analogues with Potent
Anticonvulsant Activities

Manuscript Reproduced with Permission From:

Bulaj, G., Green, B. R., Lee, H.-K., Robertson, C. R., White, K., Zhang, L., Sochanska, M., Flynn, S. P., Scholl, E. A., Pruess, T. H., Smith, M. D., and White, H. S. (2008) Design, synthesis, and characterization of high-affinity, systemically-active galanin analogues with potent anticonvulsant activities, *J. Med. Chem.* 51, 8038-8047.

© 2008 American Chemical Society

Design, Synthesis, and Characterization of High-Affinity, Systemically-Active Galanin Analogues with Potent Anticonvulsant Activities

Grzegorz Bulaj,^{*,†} Brad R. Green,[†] Hee-Kyoung Lee,[†] Charles R. Robertson,[†] Karen White,[†] Liuyin Zhang,[†] Marianna Sochanska,[†] Sean P. Flynn,[‡] Erika Adkins Scholl,[‡] Timothy H. Pruess,[‡] Misty D. Smith,[‡] and H. Steve White[‡]

Department of Medicinal Chemistry, Department of Pharmacology and Toxicology, College of Pharmacy, University of Utah, Salt Lake City, Utah 84108

Received September 2, 2008

Galanin is an endogenous neuropeptide that modulates seizures in the brain. Because this neuropeptide does not penetrate the blood–brain barrier, we designed truncated galanin analogues in which nonessential amino acid residues were replaced by cationic and/or lipoamino acid residues. The analogues prevented seizures in the 6 Hz mouse model of epilepsy following intraperitoneal administration. The most active analogue, Gal-B2 (NAX 5055), contained the -Lys-Lys-Lys(palmitoyl)-Lys-NH₂ motif and exhibited high affinity for galanin receptors ($K_i = 3.5$ nM and 51.5 nM for GalR1 and GalR2, respectively), $\log D = 1.24$, minimal helical conformation and improved metabolic stability. Structure–activity-relationship analysis suggested that cationization combined with position-specific lipidization was critical for improving the systemic activity of the analogues. Because the anticonvulsant activity of galanin is mediated by the receptors located in hippocampus and other limbic brain structures, our data suggest that these analogues penetrate into the brain. Gal-B2 may lead to development of first-in-class antiepileptic drugs.

Introduction

Anticonvulsant neuropeptides are potent modulators of neuronal excitability.^{1,2} This class of peptides include galanin,³ neuropeptide Y (NPY),^{4,5} somatostatin,⁶ or dynorphin A,⁷ when endogenously expressed or delivered directly into the central nervous system (CNS), these peptides not only can suppress seizures in animal models of epilepsy but they also mediate antinociceptive effects. Furthermore, there is a growing body of evidence that some anticonvulsant neuropeptides may have disease-modifying properties, such as slowing, halting, or perhaps even preventing development of epileptic seizures.^{8–10} Therefore, the anticonvulsant neuropeptides provide an opportunity to develop disease-modifying therapeutics for epilepsy.^{6,8,11,12} If these peptides could be specifically targeted into the CNS, they may become first-in-class cures for many neurological diseases.

Galanin is an example of such a promising anticonvulsant peptide that exhibits disease-modification properties.^{8,13,14} The acute administration of galanin receptor agonists or virus-mediated overexpression of galanin in the hippocampus has been found to inhibit limbic status epilepticus, pentylenetetrazol, and picrotoxin seizures in rats and mice.^{13,15–19} Furthermore, the seizure threshold of galanin overexpressing transgenic animals is increased in status epilepticus and kindling models.^{14,20,21} In

vitro, galanin inhibits glutamate release from the hippocampus.^{20,22}

Galanin elicits multiple effects in the brain via three galanin receptors belonging to the G protein-coupled receptors (GPCRs).^{23–25} Galanin receptor subtype 1 (GalR1) is present in many brain areas but displays the highest expression in the hippocampus.²⁶ The galanin receptor subtype 2 (GalR2) is expressed in the hypothalamus, the hippocampus, the amygdala, piriform cortex, basal forebrain (medial septum/diagonal band), the cerebellum, and the brainstem. Galanin receptor subtype 3 (GalR3) is most abundant in the hypothalamus but is absent from the hippocampus. Results from studies with the GalR1 knockout mice and rats treated with GalR2 peptide nucleic acid antisense suggests that galanin exerts its anticonvulsant effect through an action at both GalR1 and GalR2.^{27,28} Furthermore, GalR2 is thought to play an important role in the neuroprotective effects of galanin in hippocampal neurons.^{17,27,29,30} Results from a study conducted in a model of rapid kindling suggest that hippocampal GalR1 and GalR2 exert antiepileptogenic effects although via different signaling pathways.⁸ Therefore, on the basis of the current literature, systemically active galanin receptor agonists that penetrate into the hippocampus might offer promising novel therapeutics that not only control epileptic seizures, but could also modify the progression of epilepsy.

Previous attempts to generate systemically active galanin agonists provided two compounds, galnon and galmic (Figure 1A, Table 1).^{16,19,31} Galnon became a useful pharmacological tool to study the effects of galanin receptors in the CNS.^{21,32,33} However, subsequent studies revealed that, at a concentration of 10 μ M, both galnon and galmic interacted with a variety of nongalanin receptors including 5-HT-1A, 1B receptors, D2 dopamine receptors, ghrelin and melanocortin receptors, NPY receptors (galnon only), or μ -opioid receptors (galmic only), suggesting that some of the pharmacological properties of galnon or galmic might be mediated by nongalanin receptors.³⁴ Thus, despite these previous efforts, there is a continuous need for systemically active and selective galanin receptor ligands. Improved penetration of peptides into the CNS was successfully

* To whom correspondence should be addressed. Phone: (801) 581-4629. Fax: (801)581-7087. E-mail: bulaj@pharm.utah.edu. Address: Department of Medicinal Chemistry, College of Pharmacy, University of Utah, 421 Wakara Way, Suite 360, Salt Lake City, Utah 84108.

[†] Department of Medicinal Chemistry, College of Pharmacy, University of Utah.

[‡] Department of Pharmacology and Toxicology, College of Pharmacy, University of Utah.

^a Abbreviations: AEDs, antiepileptic drugs; AUC, area under the curve; BBB, blood–brain barrier; CD, circular dichroism; CMC, critical micelle concentration; CNS, central nervous system; Gal-B2, lead galanin compound described in this work; GalR1, galanin receptors subtype 1; GalR2, galanin receptors subtype 2; GPCRs, G-protein coupled receptors; ip, intraperitoneally; LAA, lipoamino acid; NPY, neuropeptide Y; PBS, phosphate buffered saline; SDS, sodium dodecyl sulfate; TFE, 2,2,2-trifluoroethanol; TPE, time to peak effect.

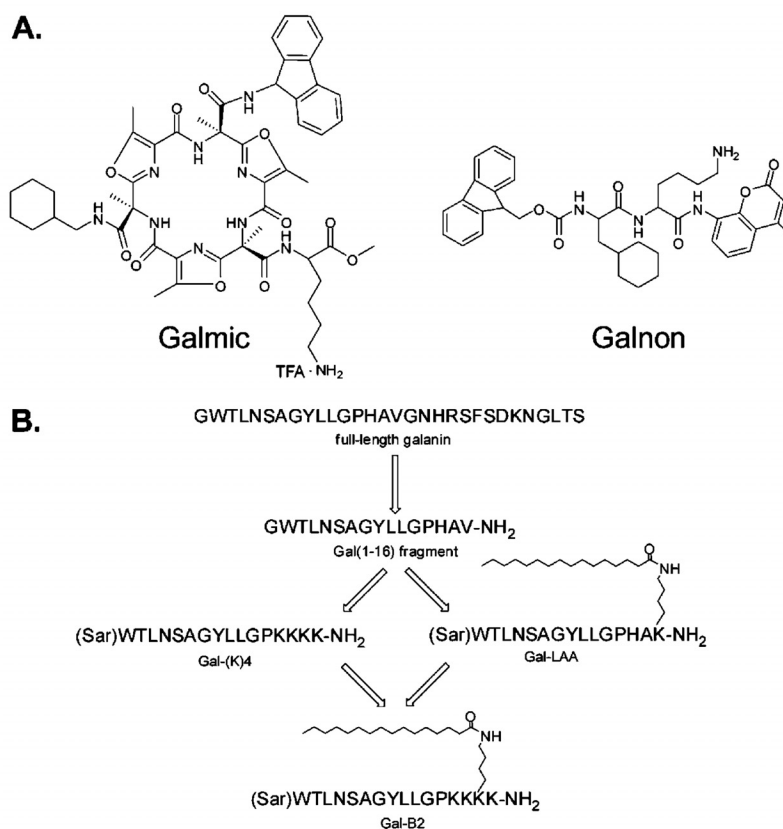


Figure 1. Developing systemically active galanin receptor ligands. (A) structures of two galanin agonists, galmic and galnon, discovered through combinatorial approaches. (B) A rational design of systemically active galanin analogues described in this work.

Table 1. Selected Galanin-Based Ligands and Their Affinities to the Galanin Receptors^a

| ligand | affinity ^a , K_d [nM] | | |
|---|------------------------------------|---------|--------|
| | hGalR1 | hGalR2 | hGalR3 |
| agonists | | | |
| hGAL(1–29) | 0.4 | 2.3 | 69.0 |
| pGAL(1–16) | 3.2 | 5.0 | 315.0 |
| GAL(2–11) | 879 | 1.8 | n.d. |
| agonists that cross blood–brain barrier | | | |
| galnon | 12000 | 24000 | n.d. |
| galmic | 34000 | >100000 | n.d. |
| antagonists | | | |
| M35 | 0.1 | 2 | 15 |
| M15 (galantide) | 0.3 | 1 | 40 |

^a K_d values are taken from the ref 25.

achieved by introducing such chemical modifications as polyamines (cationization), lipids, or glycosyl groups.^{35–37} In this research, we investigated how selected chemical modifications may improve CNS bioavailability of galanin. Here, we report that the combination of C-terminal cationization/lipidization to the Gal(1–13) core provided metabolically stable and high-affinity galanin analogues that exert potent anticonvulsant activity following systemic administration.

Results

Design Strategy. Galanin is a 29–30 amino acid long peptide (Figure 1B),³⁸ where the first N-terminal 14 residues are highly conserved within different animal species.³⁹ The N-terminal core

fragment comprises critical residues: Gly1, Trp2, Asn5, Tyr9, and Gly12, and it was previously shown to maintain high affinity toward galanin receptors.^{40,41} Indeed, the truncated Gal(1–16)-NH₂ analogue is a low nanomolar agonist for both GalR1 and GalR2, slightly preferring GalR1. Alanine-walk analogues of Gal(1–16) indicated that individual replacements of amino acid residues within the (1–12) fragment affected binding properties to both galanin receptors, with GalR2 being more sensitive.^{42,43} All analogues of Gal(1–13) with the ϵ -amino group of Lys14 conjugated to different groups varying in size retained high affinity, suggesting that the C-terminal portion of the truncated analogues may be amenable to the introduction of bulky modifications.⁴⁴ Additional SAR information utilized in our design was that the N-methylation of Gly1 did not affect receptor binding properties, whereas it improved metabolic stability of the analogue containing the N-terminal sarcosine residue.⁴⁵

To develop systemically active galanin analogues, we first applied two common strategies: lipidization and cationization (Figure 1B). The introduction of a lipoamino acid residue at the C-terminus of the [Gly1Sar]Gal(1–16)-NH₂ could serve two functions: (1) to improve penetration of the analogue across the membranes by increasing lipophilicity and (2) to increase the metabolic stability, as was observed in other peptides.^{46–49} The Lys-palmitoyl (Lys-P) residue was introduced at the C-terminus of the [Gly1Sar]Gal(1–16)-NH₂ analogue (analogue Gal-LAA). We also tested how the presence of positively charged residues at the C-terminus of [Gly1Sar]Gal(1–16)-NH₂ may improve anticonvulsant activity. Because the N-terminal

Table 2. Sequences, Mass Spectrometry Data, HPLC Retention Times and logD Values for the Galanin analogues^a

| analogue | structure | mass spec data (calc/exp) | HPLC retention time ^b | logD ^c |
|-----------|--|---------------------------|----------------------------------|--------------------|
| Gal(1–16) | GWTLNSAGYLLGPHAV-NH ₂ | 1653.86/1654.67 | 19.32 ± 0.37 | 0.69 ± 0.02 |
| Gal-LAA | (Sar)WTLNSAGYLLGPH(A(Lys-P) | 1936.30/1936.32 | 28.31 ± 0.04 | 1.45 ± 0.02 |
| Gal-(K)4 | (Sar)WTLNSAGYLLGPKKKK | 1873.09/1873.14 | 15.13 ± 0.42 | 0.34 ± 0.02 |
| Gal-B1 | (Sar)WTLNSAGYLLGPKKK(Lys-P) | 2112.60/2112.33 | 25.99 ± 0.16 | 1.25 ± 0.02 |
| Gal-B2 | (Sar)WTLNSAGYLLGPKKK(Lys-P)K | 2112.60/2112.33 | 25.84 ± 0.10 | 1.24 ± 0.02 |
| Gal-B3 | (Sar)WTLNSAGYLLGPK(Lys-P)KK | 2112.60/2112.26 | 25.96 ± 0.29 | 1.25 ± 0.03 |
| Gal-B4 | (Sar)WTLNSAGYLLGPK(Lys-P)KKK | 2112.60/2112.29 | 25.88 ± 0.14 | 1.24 ± 0.02 |
| Gal-B5 | WTLNSAGYLLGPKKK(Lys-P)K | 2040.46/2040.13 | 25.62 ± 0.10 | 1.22 ± 0.02 |
| Gal-B6 | GWTLNSAGYLLGPKK(Lys-P)K | 2098.60/2098.18 | 22.53 ± 3.20 | 0.96 ± 0.24 |
| Gal-B7 | (Ahx)WTLNSAGYLLGPKK(Lys-P)K | 2154.70/2154.44 | 25.80 ± 0.12 | 1.24 ± 0.02 |
| Gal-B8 | (Sar)WTLNSAGYLLGPKRR(Lys-P)R | 2195.51/2195.43 | 26.36 ± 0.09 | 1.28 ± 0.02 |
| Gal-B9 | (Sar)WTLNSAGYLLGPK _p K _p K(Lys-P) _p K | 2112.60/2112.33 | 25.44 ± 0.12 | 1.21 ± 0.02 |
| Gal-B10 | (Sar)WTLNSAGYLLK _p KKK(Lys-P)K | 2213.61/2213.29 | 24.00 ± 0.13 | 1.08 ± 0.02 |
| Gal-B11 | (Sar)WTLNSAGYLLGKK(Lys-P)K | 2015.50/2015.30 | 25.67 ± 0.14 | 1.23 ± 0.02 |
| Gal-B12 | (Sar)WTLNSAGYLLKK(Lys-P)K | 1957.42/1957.18 | 25.82 ± 0.10 | 1.24 ± 0.02 |

^aLys-P is Lysine-palmitoyl, Sar is sarcosine, Ahx is 6-aminohexanoic acid. ^bLinear gradient of H₂O/acetonitrile. ^cCalculated values based on HPLC retention times, as shown in Supplementing Information Table S1 and Figure S2.

galanin fragment is relatively hydrophobic and it lacks positively charged residues (known to improve penetration of peptides across biological membranes), several Lys residues were added to the C-terminus of the analogue (Gal-(K)4). The overall design strategy is summarized in Figure 1B. These two analogues were chemically synthesized and screened by the Anticonvulsant Screening Program at the NIH. Our initial screening results indicated that these two analogues failed to effectively protect mice from limbic seizures induced by 6 Hz corneal stimulation, although the observed activity of the analogue Gal-(K)4 provided a hint that cationization might in fact be an effective strategy to improve systemic bioavailability. However, because of apparent motor impairment toxicity of Gal-(K)4, we discontinued exploring increasing or replacing the positively charged residues at the C-terminus.

Next, we tested whether combining cationization and lipidization could be more effective in improving systemic activity of the analogues, as compared to each of the modifications alone. Therefore, a series of four analogues (Gal-B1, Gal-B2, Gal-B3, and Gal-B4) was designed, chemically synthesized, and screened; these analogues contained a Lys-palmitoyl residue in combinations with three Lys residues. Once we discovered that the combined presence of lipoamino acid at the position 16 and cationization was important for improving systemic activity of Gal-B2, subsequent subsets of SAR analogues were designed to address several questions: (1) Does the number and type of positively charged residues play a role in systemic bioavailability? (2) Does a further truncation of galanin analogues affect systemic bioavailability? (3) And is the N-terminal methylation important? Structures of the galanin analogues described in this work are summarized in Table 2.

Synthesis and Physicochemical Characterization of the Galanin Analogues. Galanin analogues were synthesized on a solid support using automated peptide synthesizer and the Fmoc chemistry. After removal of the peptides from the resin, the analogues were purified using reversed-phase HPLC separations on a diphenyl preparative column. The peptides were quantified by measuring UV absorbance at 280 nm, aliquoted, and dried in a speed vac. Mass spectrometry analysis confirmed the chemical identity of all analogues. HPLC retention times are summarized in Table 2. The purity of all analogues is summarized in Supporting Information Figure S1 and Table S1, and the HPLC trace of the lead analogue, Gal-B2, showing 98.8% purity, is provided in Supporting Information Figure S2.

To characterize the lipophilicity of the analogues, we determined their water/octanol partitioning coefficients (logD) using previously established methods.^{50,51} First, the shake-flask

method was employed for the selected analogues to determine logD between *n*-octanol and aqueous phase (Supporting Information Table S1). The capacity factor (*k'*) for the analogues were calculated by the formula $k' = (t_r - t_0)/t_0$, where *t_r* was the retention time of the test peptide and *t₀* is the solvent front. From the linear correlation (Supporting Information Figure S3), the capacity factors and subsequent logD's were determined for all the analogues.

As summarized in Table 2, unmodified Gal(1–16) analogue was found to have logD = 0.69. Presence of the N-terminal methyl and the C-terminal Lys-palmitoyl residue significantly increased logD to 1.45 (analogue Gal-LAA). Conversely, cationization by four C-terminal lysine residues, analogue Gal-(K)4, increased hydrophilicity, with accompanied shift in the logD to 0.34. For analogues containing Sar1, Lys-palmitoyl, and three Lys residues, logD was around 1.2. Conversion of the N-terminal glycine to sarcosine seen in analogue Gal-B2, reduced the positive charge, effectively increasing lipophilicity to a logD from 0.96 to 1.24 (comparing analogues Gal-B6 and Gal-B2). The shortening of the peptide did not affect logD but replacing Gly12-Pro13 with two Lys residues decreased logD from 1.25 to 1.08. Taken together, most galanin analogues in this series had a CNS-favorable logD greater or equal to 1.0.

Because of the amphipathic character of the galanin analogues, we selected a representative analogue, Gal-B2, containing Lys-palmitoyl and three Lys residues to determine the critical micelle concentration (CMC). We employed a fluorescence-based method in 96-well microtiter plates. The surfactants, sodium dodecyl sulfate (SDS), and polyoxyethylene (20) sorbitan monolaurate, were used as controls. On the basis of changes in the fluorescence of fluorescein as a function of peptide concentration (Figure 2A), the CMC of Gal-B2 was calculated as 3.65 μM. This value is higher as compared to the reported CMC for human galanin 0.4 μM.⁵² CMC value for polyoxyethylene (20) sorbitan monolaurate was 0.02 mM, whereas for SDS it was 0.43 mM (Supporting Information Figure S4), comparable to those previously reported.⁵³

Structural Characterization of the Galanin Analogues. Normally unstructured galanin acquires α-helical conformation in complex with its receptor, as well as in 50% TFE.^{54–56} As illustrated in Figure 2B, a presence of Lys-palmitoyl residue at the C-terminus would result in possible additional interactions with other hydrophobic residues that could favor helical conformation. To better understand structural consequences of introducing the lipoamino acid and cationization into the galanin analogues, their conformational properties were studied using circular dichroism (CD). The CD spectra were acquired in

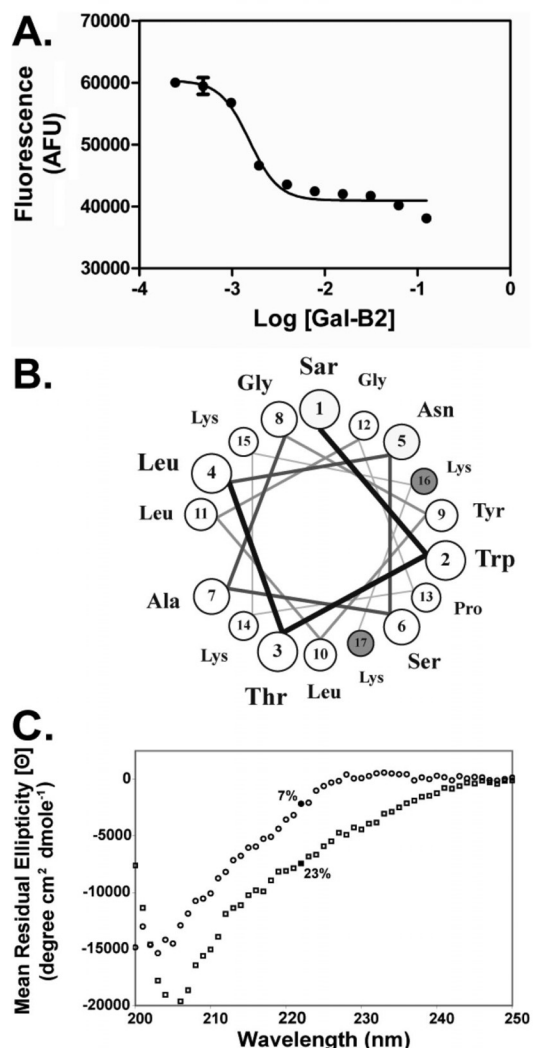


Figure 2. Characterization of the Gal-B2 analogue. (A) Determination of the critical micelle concentration using the fluorescence-based method. (B) Wheel representation of the Gal-B2 helical structure. (C) CD spectra of the Gal-B2 analogue in PBS (circles) and 50% TFE/PBS (squares).

aqueous 150 mM NaF phosphate buffer, pH 7.4 in the absence or presence of 50% (v/v) 2,2,2-trifluoroethanol (TFE). Figure 2C shows representative CD spectra and Table 3 summarizes amount of calculated α -helical structure in the galanin analogues. Conformation of Gal(1–16) in buffer was similar to published results for human galanin.⁵⁷ In the absence of TFE, Gal(1–16) gave a spectrum typical of random coil, with Θ_{222} showing $\sim 1\%$ helical structure. In 50% TFE, helical structure was stabilized and Gal(1–16) was calculated to have 22% helical structure, which coincides with literature results. For Gal(1–16), this equates to one helical turn (in TFE), however small distortions of the carbonyl chromophore from regular helical geometries in short peptides impair proper CD measurements and these values are considered to be the lower limit.

Some galanin analogues containing lipoamino acid showed increased tendency to form helical structure in aqueous solution (Table 3). The increase was generally dependent on the position

Table 3. Summary of the CD Spectrometry and the in Vitro Serum Stability Analyses

| analogue | % α -helix (in water) | % α -helix (in 50% TFE) | half-life in 25% rat serum |
|-----------|------------------------------|--------------------------------|----------------------------|
| Gal(1–16) | 1 | 22 | 28 min |
| Gal-LAA | 0 | 13 | >10 h |
| Gal-(K)4 | 0 | 14 | 4.6 h |
| Gal-B1 | 31 | 16 | >10 h |
| Gal-B2 | 7 | 23 | 9.4 h |
| Gal-B3 | 2 | 18 | 8.6 h |
| Gal-B4 | | 20 | >10 h |
| Gal-B5 | 6 | 17 | >10 h |
| Gal-B6 | 4 | 16 | >10 h |
| Gal-B7 | 4 | 19 | >10 h |
| Gal-B8 | 3 | 16 | 4.8 h |
| Gal-B9 | 0 | 1 | >10 h |
| Gal-B10 | 10 | 42 | 8.7 h |
| Gal-B11 | 10 | 36 | 5.6 h |
| Gal-B12 | 20 | 40 | >10 h |

of the Lys-palmitoyl residue. For example, the analogue Gal-B1 with the very terminal Lys-palmitoyl residue contained over 30% α -helicity, suggesting that the palmitoyl moiety may interact with specific side chains to stabilize the conformation (Figure 2B). Interestingly, this effect was diminished in the presence of 50% TFE. The Gly12-Pro13 fragment significantly affected the conformation of the analogues: their replacement or removal dramatically stabilized the helical conformation. Upon addition of TFE, the α -helical structure was further induced in most of the analogues. Interestingly, Gal-B1, that contained 31% α -helical conformation, was destabilized. The percentage of helical structure of analogue Gal-B2 was correlated to the position of Lys-palmitoyl residue. An α -helical wheel projection, shown in Figure 2B, shows that the lipoamino acid may stabilize the conformation through possible interactions with Tyr9, which is centered about a hydrophobic core (Ser6-Ala7-Gly8-Tyr9-Leu10-Leu11) where the helix resides.

Metabolic Stability of Galanin Analogues. To assess effects of the chemical modifications on the metabolic stability of the galanin analogues, their resistance to proteolytic degradation was determined in 25% rat serum incubated at 37 °C. Quantification of the analogues was determined by HPLC assay (Supporting Information Figure S5), and the recovery of the analogues at the initial time ($t = 0$ min) was higher than 80%. Representative time-courses for disappearance of the galanin analogues are illustrated in Figure 3 and calculated half-life are summarized in Table 3. Unmodified galanin analogue Gal(1–16) was very unstable with $t_{1/2} = 7.8$ min. All analogues exhibited significantly improved metabolic stability, with nearly half of them having $t_{1/2} > 10$ h.

Receptor Binding Studies. Affinities of the galanin analogues against human hGalR1 and hGalR2 were determined using time-resolved fluorescence based competitive binding assay. The assay was essentially performed in the same manner, as previously described.⁵⁸ Representative binding curves for Gal(1–16) and Gal-B2 analogues are shown in Figure 4; K_i values are summarized in Table 4. Consistent with the literature data, Gal(1–16) exhibited low nanomolar affinities toward both subtypes, with about 20-fold preference toward GalR1 subtype. The presence of lipoamino acid decreased the affinity of the analogues for both GalR1 and GalR2, but the effects were dependent on the sequence position of Lys-palmitoyl. The C-terminal cationization did not affect binding constants. The central truncations of Gal-B2 resulted in a decrease in the receptor affinities. The most potent, yet “nonselective” analogue was Gal-B7, displaying K_i values of 21.5 and 51 nM toward

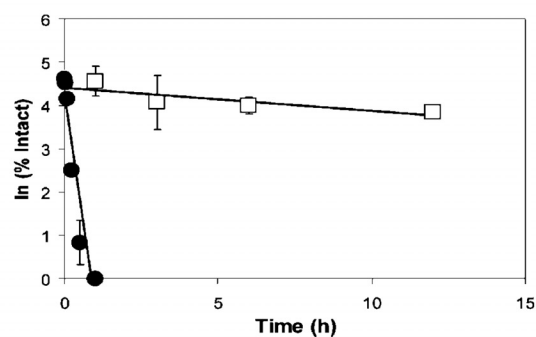


Figure 3. In vitro serum stability assay. Determination of the in vitro metabolic stability of the unmodified Gal(1–16) (closed circles) and the Gal-B2 analogue (open squares). Time-course of the disappearance of the intact peptides in the presence of 25% rat serum incubated at 37 °C is shown. The analogues were quantified by HPLC as shown in Supporting Information Figure S5. Half-lives for the Gal(1–16) and Gal-B2 analogues were calculated as 7.8 min and 9.4 h, respectively.

GalR1 and GalR2, respectively. In summary, most analogues exhibited nanomolar affinity toward the galanin receptors, and the presence of the C-terminal –Lys-Lys-Lys(palmitoyl)-Lys-NH₂ motif did not significantly affect binding affinities toward the galanin receptors.

Anticonvulsant Screening. Because all designed analogues maintained high affinities toward galanin receptors, their anticonvulsant activities were determined in the animal screening assay using the 6 Hz (32 mA) seizure model. The 6 Hz seizure test is a robust screening assay employed by the NIH-sponsored Anticonvulsant Screening Program to evaluate antiepileptic drug candidates. This acute seizure test is a model of pharmacoresistant epilepsy that displays a unique pharmacological profile. Moreover, seizures evoked by 6 Hz stimulation, unlike acute seizures evoked by maximal electroshock and/or pentylenetetrazol are blocked by levetiracetam. Prior to the anticonvulsant screening following systemic administration, we demonstrated that the Gal(1–16) fragment was very potent in suppressing seizures in this model of pharmacoresistant epilepsy following intracerebroventricular (icv) injection. ED₅₀ was determined as 1.7 nmole (95% CI = 0.8 – 4.7). For the screening, each galanin analogue was administered intraperitoneally (ip) to 5 groups of mice at an identical dose of 4 mg/kg. At 15, 30, 60, 120, and 240 min after the drug administration, mice were challenged with a 6 Hz corneal stimulation. Mice not displaying characteristic limbic seizures were considered protected. Table 4 summarizes the results from this in vivo screening assay, and Figure 5 illustrates the area under the curve (AUC) for the time course of the anticonvulsant activities of the analogues.

As shown in Table 4, neither Gal(1–16) nor the lipoamino acid containing analogue, Gal-LAA, produced any anticonvulsant activity following ip administration. In contrast, Gal-(K)4 exhibited some degree of protection against seizures with a time to peak effect (TPE) of 30 min. Strikingly, one out of four analogues containing combined lipoamino acid and Lys residues was very active in this test, providing 100% protection against seizures from 30 min to 2 h following drug administration. As mentioned earlier, Gal-B2 was selected as a lead compound to further advance the SAR analysis. The analogues with the modifications at the N-terminus (Gal-B5, Gal-B6, and Gal-B7) all displayed pronounced antiepileptic activity. The presence of additional Lys residues or replacing Lys with Arg or D-Lys did not significantly modify the anticonvulsant activity, although

the D-Lys containing analogue was, as predicted, longer-lasting when compared to Gal-B2. Removal of Pro13 significantly decreased anticonvulsant activity, an effect consistent with changing the relative position of Lys-palmitoyl, as observed in the analogue Gal-B3. The GalR2-preferring analogue, Gal-B5, was less active as compared to GalR1-preferring Gal-B2 (both analogues are identical except Gal-B5 lacks N-terminal sarcosine). The most active analogue, Gal-B2, yielded an ED₅₀ of 0.8 mg/kg (95% CI = 0.43 – 1.56) determined at the time-to-peak effect (TPE) of 1 h. Even at the highest efficacious doses tested, no behavioral toxicity was observed. The rotarod test was employed to evaluate the effect of higher doses of Gal-B2 on motor function. In this study, the median toxic dose, or TD₅₀, was determined to be 21 mg/kg (Figure 6). Gal-B2 exhibits the protective index (PI = TD₅₀/ED₅₀) above 25.

Discussion

This work describes our ongoing research efforts on developing systemically active galanin analogues. To the best of our knowledge, this is the first report that describes applying chemical modifications to galanin to improve its CNS activity. Previous attempts to produce systemically active galanin analogues, such as galnon or galmic, included combinatorial libraries based on peptidomimetic scaffolds.^{16,19,31,59} Chemical modifications, such as glycosylation, lipidization, or cationization, have been extensively studied for opioid peptides, neurotensin or somatostatin, but were never a subject of a rational design using galanin.⁶⁰ On the basis of available SAR data, we designed a series of truncated galanin analogues in which the N-terminal Gly1 was replaced by sarcosine, and the C-terminal residues were replaced by a combination of lipoamino acid and Lys residues. These modifications did not significantly affect binding affinity toward galanin receptors but dramatically improved systemic bioavailability, as determined by high anticonvulsant potency following systemic administration. There are two major outcomes of this research: (1) combining chemical modifications improves bioavailability of peptides, and (2) the Gal-B2 analogue provides a new pharmacological tool to study the role of galanin receptors in the nervous system.

Chemical modifications such as lipidization or cationization are commonly used to improve bioavailability of peptides.^{37,61,62} Lipoamino acids have been introduced to a number of neuropeptide analogues including somatostatin,^{46,63} conotoxins,⁴⁷ or opioid peptides.⁶⁴ A reversible lipidization strategy was successfully applied to improve bioavailability of opioid peptides⁶⁵ or octreotide.⁴⁹ Furthermore, increased lipophilicity of peptides has been well-established factor to improve their BBB penetration.⁶⁶ However, lipidization of the [Gly1Sar]Gal(1–16)-NH₂ analogue did not improve its systemic bioactivity despite significantly increasing its logD value and the in vitro metabolic stability. Although introduction of the lysine-palmitoyl moiety noticeably decreased the affinities toward both GalR1 and GalR2, a lack of the antiepileptic activity of Gal-LAA could not be easily accounted for by a 1–2 order of magnitude decrease in the receptor affinities (analogues Gal-B10 and Gal-B12 had comparable affinities to that of Gal-LAA, but both analogues were significantly more active than Gal-LAA following systemic administration, as shown in Table 4). Thus, the presence of a lipoamino acid alone did not improve systemic bioavailability. Similarly, cationization is well-known to improve both penetration across biological membranes^{67,68} and penetration into the CNS via adsorptive-mediated endocytosis.^{69,70} Indeed, introduction of four Lys residues (analogue Gal-(K)4) resulted in an increase of the anticonvulsant activity following

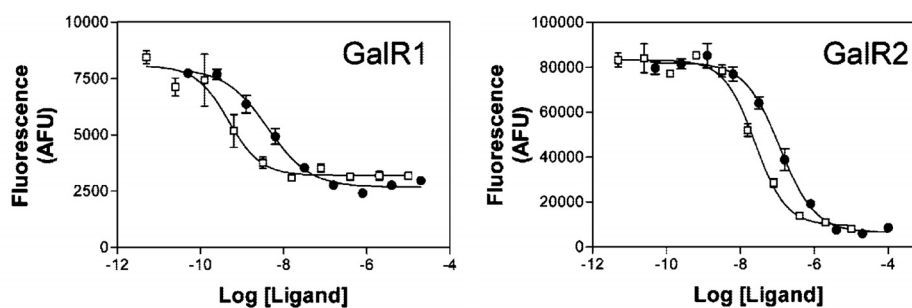


Figure 4. Galanin receptor binding studies. A representative graph from competitive receptor binding studies for GalR1 (left) and GalR2 (right). Binding assay was performed with GalR1 and GalR2 membrane preparations for Gal-B2 (closed circle) and Gal(1–16) (open square). Each data point represents the average of four assay points. Europium-labeled galanin was used as a ligand for the assay. K_i values for the analogues are summarized in Table 4.

Table 4. In Vitro and in Vivo Pharmacological Properties of the Galanin Analogues

| analogue | in vitro assay (receptor binding) | | in vivo assay (anticonvulsant activity) | | | | | AUC ^a |
|-----------|-----------------------------------|------------------|---|-----|-----|------|------|------------------|
| | GalR1 K_i [nM] | GalR2 K_i [nM] | 6 Hz, 32 mA, 4 mg/kg | | | | | |
| | | | 15' | 30' | 60' | 120' | 240' | |
| Gal(1–16) | 0.5 ± 0.2 | 13.0 ± 5.4 | 0/4 | 0/4 | 0/4 | 0/4 | 0/4 | 0 |
| Gal-LAA | 85.0 ± 58.0 | 160.0 ± 9.9 | 0/4 | 0/4 | 0/4 | 0/4 | 0/4 | 0 |
| Gal-(K)4 | 0.4 ± 0.1 | 24.0 ± 9.9 | 0/4 | 3/4 | 1/3 | 0/3 | 0/4 | 3186 |
| Gal-B1 | 1.9 ± 0.6 | 22.0 ± 9.2 | 1/4 | 1/4 | 2/4 | 0/4 | 0/4 | 3000 |
| Gal-B2 | 3.5 ± 1.0 | 51.5 ± 34.4 | 3/4 | 4/4 | 4/4 | 4/4 | 0/4 | 16313 |
| Gal-B3 | 6.0 ± 1.4 | 28.0 ± 4.9 | 1/4 | 3/4 | 0/4 | 0/4 | 0/4 | 1875 |
| Gal-B4 | 25.5 ± 6.4 | 108.0 ± 15.6 | 0/4 | 1/4 | 1/4 | 0/4 | 1/4 | 3188 |
| Gal-B5 | 387.0 ± 123.0 | 48.0 ± 11.3 | 2/4 | 1/4 | 2/4 | 2/4 | 0/4 | 8250 |
| Gal-B6 | 5.3 ± 3.0 | 22.5 ± 3.5 | 1/4 | 3/4 | 3/4 | 0/4 | 0/4 | 5250 |
| Gal-B7 | 21.5 ± 12.0 | 51.0 ± 11.3 | 4/4 | 3/4 | 3/4 | 1/4 | 1/4 | 9563 |
| Gal-B8 | 3.3 ± 0.3 | 65.5 ± 0.7 | 2/4 | 3/4 | 4/4 | 3/4 | 0/4 | 13313 |
| Gal-B9 | 0.9 ± 0.2 | 15.0 ± 8.5 | 2/4 | 3/4 | 4/4 | 2/4 | 3/4 | 15563 |
| Gal-B10 | 41.5 ± 12.0 | 214.5 ± 24.7 | 2/4 | 2/4 | 3/4 | 3/3 | 2/3 | 17871 |
| Gal-B11 | 25.5 ± 4.9 | 75.0 ± 10.6 | 1/4 | 2/4 | 2/4 | 0/4 | 0/4 | 3563 |
| Gal-B12 | 306.5 ± 12.0 | 1,323.5 ± 27.6 | 1/4 | 4/4 | 4/4 | 1/4 | 0/4 | 9188 |

^a area under the curve values summarize the anticonvulsant time–response curves. The percent of animals protected at each time-point was plotted against time, and the AUC values were calculated as described in the Methods Section.

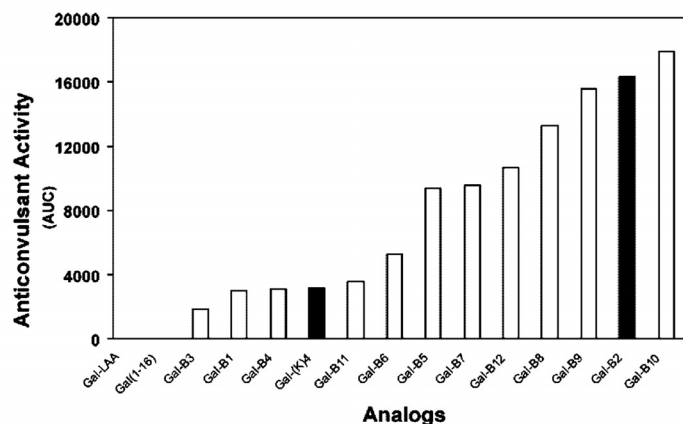


Figure 5. Anticonvulsant screening of the galanin analogues. Bar graphs represent area under the curve values for each of the analogue calculated from a time–response study for a single bolus dose of 4 mg/kg (ip).

systemic administration. However, the relatively modest anti-epileptic activity with a slow onset and a short duration of action was accompanied by an apparent toxic effect thereby precluding further attempts to optimize this scaffold. To our surprise, the combination of lipoamino acid and lipidization appeared superior in producing very active antiepileptic compounds that voided behavioral neurotoxicity at the efficacious doses.

By combining lipidization and cationization, we have synthesized a number of galanin analogues that are highly active anticonvulsants following systemic administration. Importantly, the combined chemical modifications did not affect affinity toward galanin receptors. In contrast, the modifications increased lipophilicity, metabolic stability, and in some instances, an amount of α -helical structure in aqueous solution and in 50%

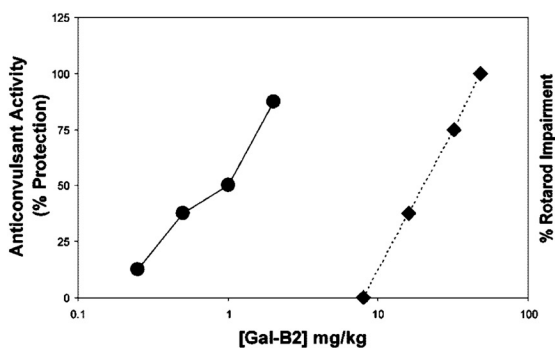


Figure 6. Separation of the potency and toxicity of the Gal-B2 analogue in the 6 Hz model (32 mA) of pharmacoresistant epilepsy in mice. Bolus injections of Gal-B2 were administered intraperitoneally, and the dose–response data were generated for the 1 h time point (time-to-peak effect). On the basis of these results, ED₅₀ and TD₅₀ were calculated as 0.8 and 21 mg/kg, respectively, yielding the protective index (PI) of 26.

TFE. It is well-known logD and metabolic stability are two important factors that should be considered when developing systemically active peptide analogues that target the CNS. The optimal range of logD for CNS drugs is between 1.5 and 2.7,⁷¹ thus the Gal-B2 analogues display a favorable logD value. The increased lipophilic character of the analogues was not reflected in lower water solubility, in fact, the Gal-B2 analogue could be easily dissolved in aqueous solutions (water, phosphate buffered saline (PBS)) at concentrations as high as 10–20 mg/mL. The amphipathic properties of the combined cationization/lipidization were also reflected by their ability to form micelles at a CMC value of 3.65 μ M. The presence of the lipoamino acid/cationization moieties not only increased lipophilic and amphipathic properties of the galanin analogues studied here, but they also improved their metabolic stability, as determined by extended half-life in the *in vitro* serum stability test. Our structure–stability relationship data suggest that each of the modifications (cationization and lipidization) played a significant role to the increased resistance to a proteolytic degradation; this effect might be in part accounted for by increased binding to serum albumin. For example, acetylation of insulin with fatty acids is known to increase their binding properties to serum albumin,^{72,73} and similarly cationic peptides can also bind to albumin.^{74,75} It is, therefore, conceivable that the increased protein binding may extend half-lives of the galanin analogues in serum solutions, allowing a better penetration into the brain.

The mechanism of penetration of the analogues into the brain remains unclear and can be only speculated at this time. Furthermore, a major limitation of this work is the lack of sensitive bioanalytical methods to reliably determine the brain levels of the Gal-B2 (although this is a work in progress). Apparently, the efficacious levels of the analogues reach the limbic brain structures and the galanin receptors responsible for suppressing seizures.^{8,76} Our current hypothesis is that a passive diffusion (lipidization) and an adsorptive-mediated endocytosis (cationization) may both contribute to the improved penetration across the BBB.³⁷ Given the number of the transport mechanisms that exist at the BBB,⁶¹ we cannot rule out additional mechanisms. Recently, Nelson and co-workers showed that the “–(Lys-myristoyl)-Lys-Lys-Lys-NH₂” motif was able to transport a fluorescently labeled peptide into living cells,⁷⁷ suggesting that such cationization/lipidization modifications are capable of transporting a cargo similarly to the cell-penetrating peptides.⁷⁸

A cell-permeable analogue of galanin, namely transportan, has been described;⁷⁹ however, it is not known whether this galanin analogue exhibits the anticonvulsant activity following systemic administration. Transportan was, however, effective in delivering peptide-nucleic acids to the nervous system.⁸⁰ A role of helical conformation in improving systemic bioavailability of galanin analogues is less apparent, although many antimicrobial peptides that penetrate membranes have helical conformations.⁸¹ Differences between the amount of the helical structure and the anticonvulsant activity of two analogues: Gal-B2 (very active, 7% helix in buffer) and Gal-B1 (poor anticonvulsant, 31% helix in buffer) suggest that there is no such relationship (these two analogues exhibit comparable logD values, metabolic stabilities, and receptor binding properties). Our current studies are focused on quantifying the brain penetration by the Gal-B2 analogue, as well as the mechanism of transport of the analogues across the cell-based biological membranes.

Perhaps the most important discovery described in this work is the finding that the Gal-B2 analogue exhibits potent antiepileptic activity following systemic administration. This compound has nanomolar affinity toward both GalR1 and GalR2 receptors. In this respect, it displays a selectivity profile comparable to that of Gal(1–16). The Gal-B2 analogue is a useful pharmacological tool to study a role of galanin receptors in the nervous system, including the CNS. Moreover, because galanin also produces analgesic effects,^{82–84} the systemically active galanin analogues are likely to provide new pain therapeutics as well. Indeed, the Gal-B2 analogue appeared very active in several animal pain models (E. Adkins Scholl, et al., manuscript in preparation).

Methods

Chemical Synthesis. All analogues were synthesized in an automated peptide synthesizer using Rink Amide resin (25 or 50 μ mole scales) and standard Fmoc-based coupling protocols. Fmoc-Lys(Palmitoyl)-OH was obtained from Chem-Impex International Inc. The peptide analogues were removed from the resin by a 3 h treatment with the reagent K (90/5/2.5/7.5/5 by volume; trifluoroacetic acid/water/ethanedithiol/phenol/thioanisole) and then precipitated out in cold methyl-*tert*-butyl ether. Crude peptides were purified by reversed-phase HPLC using preparative HPLC column (Vydac diphenyl, 219TP1011522) and eluted with a linear gradient of acetonitrile (0.1% TFA). The flow rate was 10 mL/min, and the elution was monitored by UV detection at 220 nm. The purities of peptides were determined by analytical reversed-phase HPLC separations (Vydac diphenyl column): buffer A (0.1% TFA in water) and buffer B (0.1% TFA, v/v, in 90% aqueous acetonitrile) were used to produce a linear gradient from 20 to 100% of buffer B over 40 min. The flow rate was 1 mL/min, and the elution was monitored by measuring absorbance at 220 nm. Purified analogues were quantified by measuring UV absorbance at 279.8 nm (molar absorbance coefficient $\epsilon = 7000$). The molecular masses of peptides were determined by MALDI-TOF MS at the University of Utah Core Facility.

Partitioning Coefficient, logD. Shake-Flask Method. Water saturated *n*-octanol was made by shaking equal volumes of *n*-octanol and water for 24 h at room temperature. Lyophilized peptides (0.4 mg) were reconstituted in 1 mL of PBS, pH 7.4, for 20 min; peptides with low aqueous solubility were reconstituted in 1 mL water saturated octanol. To the peptide solutions, 1 mL of water saturated octanol was added (1 mL PBS to peptides in organic phase), and the biphasic solution was placed on a rotary mixer for 24 h at room temperature. The samples were allowed to settle for 30 min, and the organic phase was removed (950 μ L) without disturbing the meniscus. The aqueous layer was sonicated in a bath sonicator for 5–10 s. Peptide concentration in a 50 μ L aliquot of the aqueous phase was quantified by HPLC. By mass balance, the concentration of peptide in the organic phase was determined to

be total peptide concentration minus the aqueous peptide concentration. For each analogue, four independent sample preparations and logD measurements were carried out. LogD was calculated:

$$\text{logD} = \log \left(\frac{[\text{octanol}]_{\text{peptide}}}{[\text{aqueous}]_{\text{peptide}}} \right)$$

HPLC Capacity Factor (k') Method. For the logD determination, the HPLC buffers were buffer A (1 L H₂O + 1 mL TFA) and buffer B (900 mL acetonitrile + 100 mL H₂O + 1 mL TFA). A 5.0 μg standard (run in triplicate) was injected onto a Vydac diphenyl column using a linear gradient starting at 80/20 buffer A:buffer B and ending at 10/90 buffer A:Buffer B in 15 min before immediate return to initial conditions. The retention times are the average of 3 runs. The capacity factors (k') of the peptides were calculated using the formula below; t_0 is the solvent front, t_r is the retention time of the peptide. The logD's obtained from the shake-flask method were plotted against their peptides respective k' values giving a linear plot. LogD's for all other peptides were calculated of this standard curve.

$$k' = \frac{t_r - t_0}{t_0}$$

Determination of Critical Micelle Concentration. CMC was determined by measuring changes in fluorescence of fluorescein as a function of peptide concentration. The Gal-B2, sodium dodecyl sulfate or polyoxyethylene (20) sorbitan monolaurate were dissolved in PBS and serial dilutions were prepared in the Costar 96-well clear plate. Next, 60 μL of 50 nM fluorescein in PBS solution was added to every well containing 200 μL of the test compound. The plate was subjected to a gentle shaking for 24 h, followed by recording the fluorescence at 485/535 nm using VICTOR³ spectrofluorometer. The data were analyzed using GraphPad Prism and the sigmoidal dose-response (variable slope) equation.

Conformational Studies. α -Helical conformation of each analogue was studied using circular dichroism. Lyophilized peptides (0.1 mg) were reconstituted in 1.0 mL of NaF/phosphate buffer (50 mg KH₂PO₄, 54 mg Na₂HPO₄, 1.55 g NaF, 250 mL H₂O, pH 7.4 with Na₂HPO₄) or in 0.5 mL NaF/phosphate buffer and 0.5 mL 2,2,2-trifluoroethanol. After 1 h of reconstitution, 250 μL of peptide solution were loaded into a 0.1 cm quartz cuvette and placed into an Aviv 62DS CD spectropolarimeter, at room temperature. Scans were collected from 250 to 200 nm every 1.0 nm with 1 s dwell time. Data were averaged from 5 scans and processed by eq 1, where M_r is molecular weight, c is concentration (mg/mL), d is path length (cm), and n is the number of peptide bonds. Percent helical content are calculated using eqs 2 and 3.

$$[\Theta] = \frac{\theta \times 100 \times M_r}{c \times d \times n} \quad (1)$$

$$[\Theta_{\text{max}}] = -39500 \left[1 - \left(\frac{2.57}{n} \right) \right] \quad (2)$$

$$\% \alpha \text{ helix} = \frac{[\Theta_{222}]}{[\Theta_{\text{max}}]} \times 100\% \quad (3)$$

Metabolic Stability Assay. Peptide stability was assessed in a rat serum assay. One mL of 25% rat serum was incubated at 37 °C for 10 min prior to addition of the analogues. Reactions were prepared by adding each analogue, dissolved in nanopure H₂O, to a solution containing 25% rat blood serum and 0.1 M Tris-HCl, pH 7.5 to a final peptide concentration of 20 μM . At appropriate time intervals (ranging up to 8 h), 200 μL aliquots were withdrawn and added to 100 μL "quenching solution" (15% trichloroacetic acid in 40% isopropanol). Isopropanol (40%, aqueous solution) was added to quenching mixture (this step improved recovery of the Gal-B2 and other analogues). Upon precipitation with the quenching mixture, the samples were incubated at -20 °C for 15 min and centrifuged at 12000 rpm. The supernatant was analyzed using HPLC separation with an YMC ODS-A 5 μm 120 Å column

(Waters, cat. no.: AA12S052503WT). In cases where analogue peaks overlapped with peaks observed in the "serum-only" control samples, the gradient was optimized by changing the composition of the mobile phases, column temperature, or HPLC column (for example C₈ rather than diphenyl column). Recovery of the analogues was assessed by spiking "serum-only" control samples after the trichloroacetic acid precipitation with known amounts of the analogue. Metabolic stability was assessed by monitoring the disappearance of the analogues over a period of 8 h. This was accomplished by comparison the area under the curve for the peak corresponding to the intact analogue at each time point. Half-life, $t_{1/2}$, for each analogue was calculated using the average of three independent experiments for each time point. Results were plotted on a log-scale plot using the Kaleidagraph software. Linear curve-fit analysis was used to fit the time-course of the degradation of the analogues according to the following formula: $t_{1/2} \text{ (h)} = \ln(50 - b)/(m)$, where " m " represents the slope of the line and " b " is the y-intercept.

Receptor Binding Assay. The fluorescence-based assay with europium-labeled galanin was employed to determine binding affinities for GalR1 and GalR2 receptors. Competitive binding assay was performed on AcroWell filter plates using receptor membrane preparations and Eu-galanin (Perkin-Elmer), and the samples were tested in quadruplicate. Both GalR1 (expressed in HEK-293 EBNA) and GalR2 (expressed in CHO-K1) membrane preparations were purchased from Perkin-Elmer. Binding assay was carried out with 6 μg of membrane protein (1.4 pmol/mg protein) and 2 nM of Eu-galanin in a volume of 100 μL of the binding buffer (50 mM Tris-HCl pH 7.5, 5 mM MgCl₂, 25 μM EDTA, and 0.2% BSA). Samples were incubated at room temperature for 90 min, followed by washing four times with wash buffer (50 mM Tris-HCl pH 7.5 and 5 mM MgCl₂) using a vacuum manifold. Enhancement solution (200 μL) was added, and the plates were incubated at room temperature for 30 min. The plates were read on a VICTOR³ spectrofluorometer using a standard time-resolved fluorescence measurement for europium-based compounds (excitation at 340 nm, delay for 400 μs , and emission at 615 nm). Competition binding curves were analyzed using GraphPad Prism software. The sigmoidal dose-response (variable slope) equation for nonlinear regression analysis was used to calculate the EC₅₀, and K_i values were calculated using the formula: $K_i = \text{EC}_{50}/(1 + [\text{Eu-Gal}]/K_d)$, where K_d (4.3 nM) was provided by Perkin-Elmer.

Anticonvulsant Activity. Each galanin analogue was administered intraperitoneally to five groups of CF-1 mice ($n = 4$ mice) at a dose of 4 mg/kg. At various times (i.e., 15, 30, 60, 120, and 240 min) after ip administration, mice were challenged with a 6 Hz corneal stimulation (32 mA for 3 s delivered via corneal electrodes). Mice not displaying a characteristic limbic seizure (jaw chomping, vibrissae twitching, forelimb clonus, Straub tail) were considered protected. The percent of animals protected at each time-point was plotted against time, and the AUC values were calculated with GraphPad Prism software suite using the trapezium rule and the formula below:

$$\sum \left(\frac{\% \text{protected}}{2} \right) \times \Delta \text{time}$$

Acknowledgment. This work was supported in part by the Epilepsy Therapy Grants Program from the Epilepsy Research Foundation, the University of Utah Startup Funds, and the University of Utah Research Foundation. Pharmacology of Gal-B2 was presented at the IX EILAT Conference on New Antiepileptic Drugs. We thank the Anticonvulsant Screening Program (ASP) at the NIH/NINDS, and in particular the ASP Director, James Stables, and his dedicated ASP staff for their support with screening galanin analogues. Invaluable support and help with data analysis, preparation of figures, and laboratory management efforts from Dan McDougale is also greatly appreciated. We thank Professors Andrey Mazarati and Tony Yaksh for numerous discussions on the pharmacology of

galanin. We are also indebted to Professor Bob Schackmann and Scott Endicott from the DNA/Peptide Synthesis Core Facility at the University of Utah for their help with the peptide synthesis. G.B. and H.S.W. are scientific cofounders of NeuroAdjuvants, Inc.

Supporting Information Available: Tables S1 and S2 summarize properties of the galanin analogues related to logD and purity, as determined by HPLC. Figures S1–S5 show: the HPLC traces of the galanin analogues, integrated HPLC trace for the lead compound, Gal-B2, the plot with a linear correlation between the capacity factor and logD, fluorescence-based determination of CMC values for control compounds, polyoxyethylene (20) sorbitan monolaurate (Polysorbate 20) and sodium dodecyl sulfate, and HPLC traces for Gal-B2 from the in vitro serum stability experiments. This material is available free of charge via the Internet at <http://pubs.acs.org>.

References

- Hokfelt, T.; Broberger, C.; Xu, Z. Q.; Sergeev, V.; Ubink, R.; Diez, M. Neuropeptides—an overview. *Neuropharmacology* **2000**, *39*, 1337–1356.
- Baraban, S. C.; Tallent, M. K. Interneuron Diversity series: Interneuron neuropeptides—endogenous regulators of neuronal excitability. *Trends Neurosci.* **2004**, *27*, 135–142.
- Lerner, J. T.; Sankar, R.; Mazarati, A. M. Galanin and epilepsy. *Cell. Mol. Life Sci.* **2008**, *65*, 1864–1871.
- Baraban, S. C. Neuropeptide Y and epilepsy: recent progress, prospects and controversies. *Neuropeptides* **2004**, *38*, 261–265.
- Vezzani, A.; Sperk, G.; Colmers, W. F. Neuropeptide Y: emerging evidence for a functional role in seizure modulation. *Trends Neurosci.* **1999**, *22*, 25–30.
- Vezzani, A.; Hoyer, D. Brain somatostatin: a candidate inhibitory role in seizures and epileptogenesis. *Eur. J. Neurosci.* **1999**, *11*, 3767–3776.
- Solbrig, M. V.; Koob, G. F. Epilepsy, CNS viral injury and dynorphin. *Trends Pharmacol. Sci.* **2004**, *25*, 98–104.
- Mazarati, A.; Lundstrom, L.; Sollenberg, U.; Shin, D.; Langel, U.; Sankar, R. Regulation of kindling epileptogenesis by hippocampal galanin type 1 and type 2 receptors: The effects of subtype-selective agonists and the role of G-protein-mediated signaling. *J. Pharmacol. Exp. Ther.* **2006**, *318*, 700–708.
- Tallent, M. K.; Qiu, C. Somatostatin: An endogenous antiepileptic. *Mol. Cell. Endocrinol.* **2008**, *286*, 96–103.
- Richichi, C.; Lin, E. J.; Stefanin, D.; Colella, D.; Ravizza, T.; Grignaschi, G.; Veglianesi, P.; Sperk, G.; During, M. J.; Vezzani, A. Anticonvulsant and antiepileptogenic effects mediated by adeno-associated virus vector neuropeptide Y expression in the rat hippocampus. *J. Neurosci.* **2004**, *24*, 3051–3059.
- Noe, F.; Nissinen, J.; Pitkanen, A.; Gobbi, M.; Sperk, G.; During, M.; Vezzani, A. Gene therapy in epilepsy: the focus on NPY. *Peptides* **2007**, *28*, 377–383.
- Noe, F.; Pool, A. H.; Nissinen, J.; Gobbi, M.; Bland, R.; Rizzi, M.; Balducci, C.; Ferraguti, F.; Sperk, G.; During, M. J.; Pitkanen, A.; Vezzani, A. Neuropeptide Y gene therapy decreases chronic spontaneous seizures in a rat model of temporal lobe epilepsy. *Brain* **2008**, *131*, 1506–1515.
- Mazarati, A. M.; Halasz, E.; Telegdy, G. Anticonvulsive effects of galanin administered into the central nervous system upon the picrotoxin-kindled seizure syndrome in rats. *Brain Res.* **1992**, *589*, 164–166.
- Kokaia, M.; Holmberg, K.; Nanobashvili, A.; Xu, Z. Q.; Kokaia, Z.; Lendahl, U.; Hilke, S.; Theodorsson, E.; Kahl, U.; Bartfai, T.; Lindvall, O.; Hokfelt, T. Suppressed kindling epileptogenesis in mice with ectopic overexpression of galanin. *Proc. Natl. Acad. Sci. U.S.A.* **2001**, *98*, 14006–14011.
- Mazarati, A. M.; Liu, H.; Soomets, U.; Sankar, R.; Shin, D.; Katsumori, H.; Langel, U.; Wasterlain, C. G. Galanin modulation of seizures and seizure modulation of hippocampal galanin in animal models of status epilepticus. *J. Neurosci.* **1998**, *18*, 10070–10077.
- Saar, K.; Mazarati, A. M.; Mahlapuu, R.; Hallnemo, G.; Soomets, U.; Kilk, K.; Hellberg, S.; Pooga, M.; Tolf, B. R.; Shi, T. S.; Hokfelt, T.; Wasterlain, C.; Bartfai, T.; Langel, U. Anticonvulsant activity of a nonpeptide galanin receptor agonist. *Proc. Natl. Acad. Sci. U.S.A.* **2002**, *99*, 7136–7141.
- Haberman, R. P.; Samulski, R. J.; McCown, T. J. Attenuation of seizures and neuronal death by adeno-associated virus vector galanin expression and secretion. *Nat. Med.* **2003**, *9*, 1076–1080.
- Lin, E. J.; Richichi, C.; Young, D.; Baer, K.; Vezzani, A.; During, M. J. Recombinant AAV-mediated expression of galanin in rat hippocampus suppresses seizure development. *Eur. J. Neurosci.* **2003**, *18*, 2087–2092.
- Bartfai, T.; Lu, X.; Badie-Mahdavi, H.; Barr, A. M.; Mazarati, A.; Hua, X. Y.; Yaksh, T.; Haberhauer, G.; Ceide, S. C.; Trembleau, L.; Somogyi, L.; Krock, L.; Rebek, J., Jr. Galmic, a nonpeptide galanin receptor agonist, affects behaviors in seizure, pain, and forced-swim tests. *Proc. Natl. Acad. Sci. U.S.A.* **2004**, *101*, 10470–10475.
- Mazarati, A. M.; Hohmann, J. G.; Bacon, A.; Liu, H.; Sankar, R.; Steiner, R. A.; Wynick, D.; Wasterlain, C. G. Modulation of hippocampal excitability and seizures by galanin. *J. Neurosci.* **2000**, *20*, 6276–6281.
- Schlifke, I.; Kuteeva, E.; Hokfelt, T.; Kokaia, M. Galanin expressed in the excitatory fibers attenuates synaptic strength and generalized seizures in the piriform cortex of mice. *Exp. Neurol.* **2006**, *200*, 398–406.
- Zini, S.; Roisin, M. P.; Langel, U.; Bartfai, T.; Ben-Ari, Y. Galanin reduces release of endogenous excitatory amino acids in the rat hippocampus. *Eur. J. Pharmacol.* **1993**, *245*, 1–7.
- Hokfelt, T.; Xu, Z. Q.; Shi, T. J.; Holmberg, K.; Zhang, X. Galanin in ascending systems. Focus on coexistence with 5-hydroxytryptamine and noradrenaline. *Ann. N.Y. Acad. Sci.* **1998**, *863*, 252–263.
- Branchek, T. A.; Smith, K. E.; Gerald, C.; Walker, M. W. Galanin receptor subtypes. *Trends Pharmacol. Sci.* **2000**, *21*, 109–117.
- Lundstrom, L.; Elmquist, A.; Bartfai, T.; Langel, U. Galanin and its receptors in neurological disorders. *Neuromol. Med.* **2005**, *7*, 157–180.
- Burgevin, M. C.; Loquet, I.; Quarteronet, D.; Habert-Ortoli, E. Cloning, pharmacological characterization, and anatomical distribution of a rat cDNA encoding for a galanin receptor. *J. Mol. Neurosci.* **1995**, *6*, 33–41.
- Mazarati, A.; Lu, X.; Kilk, K.; Langel, U.; Wasterlain, C.; Bartfai, T. Galanin type 2 receptors regulate neuronal survival, susceptibility to seizures and seizure-induced neurogenesis in the dentate gyrus. *Eur. J. Neurosci.* **2004**, *19*, 3235–3244.
- Mazarati, A.; Lu, X.; Shinmei, S.; Badie-Mahdavi, H.; Bartfai, T. Patterns of seizures, hippocampal injury and neurogenesis in three models of status epilepticus in galanin receptor type 1 (GalR1) knockout mice. *Neuroscience* **2004**, *128*, 431–441.
- Pirondi, S.; Fernandez, M.; Schmidt, R.; Hokfelt, T.; Giardino, L.; Calza, L. The galanin-R2 agonist AR-M1896 reduces glutamate toxicity in primary neural hippocampal cells. *J. Neurochem.* **2005**, *95*, 821–833.
- Hwang, I. K.; Yoo, K. Y.; Kim, D. S.; Do, S. G.; Oh, Y. S.; Kang, T. C.; Han, B. H.; Kim, J. S.; Won, M. H. Expression and changes of galanin in neurons and microglia in the hippocampus after transient forebrain ischemia in gerbils. *Brain Res.* **2004**, *1023*, 193–199.
- Ceide, S. C.; Trembleau, L.; Haberhauer, G.; Somogyi, L.; Lu, X.; Bartfai, T.; Rebek, J., Jr. Synthesis of galmic: a nonpeptide galanin receptor agonist. *Proc. Natl. Acad. Sci. U.S.A.* **2004**, *101*, 16727–16732.
- Lu, X.; Barr, A. M.; Kinney, J. W.; Sanna, P.; Conti, B.; Behrens, M. M.; Bartfai, T. A role for galanin in antidepressant actions with a focus on the dorsal raphe nucleus. *Proc. Natl. Acad. Sci. U.S.A.* **2005**, *102*, 874–879.
- Badie-Mahdavi, H.; Behrens, M. M.; Rebek, J.; Bartfai, T. Effect of galanin on induction of long-term potentiation in dentate gyrus of C57BL/6 mice. *Neuropeptides* **2005**, *39*, 249–251.
- Lu, X.; Lundstrom, L.; Langel, U.; Bartfai, T. Galanin receptor ligands. *Neuropeptides* **2005**, *39*, 143–146.
- Poduslo, J. F.; Curran, G. L. Glycation increases the permeability of proteins across the blood–nerve and blood–brain barriers. *Brain Res. Mol. Brain Res.* **1994**, *23*, 157–162.
- Poduslo, J. F.; Curran, G. L. Polyamine modification increases the permeability of proteins at the blood–nerve and blood–brain barriers. *J. Neurochem.* **1996**, *66*, 1599–1609.
- Witt, K. A.; Gillespie, T. J.; Huber, J. D.; Egleton, R. D.; Davis, T. P. Peptide drug modifications to enhance bioavailability and blood–brain barrier permeability. *Peptides* **2001**, *22*, 2329–2343.
- Tatemoto, K.; Rokaeus, A.; Jornvall, H.; McDonald, T. J.; Mutt, V. Galanin—a novel biologically active peptide from porcine intestine. *FEBS Lett.* **1983**, *164*, 124–128.
- Langel, U.; Bartfai, T. Chemistry and molecular biology of galanin receptor ligands. *Ann. N.Y. Acad. Sci.* **1998**, *863*, 86–93.
- Land, T.; Langel, U.; Low, M.; Berthold, M.; Uden, A.; Bartfai, T. Linear and cyclic N-terminal galanin fragments and analogs as ligands at the hypothalamic galanin receptor. *Int. J. Pept. Protein Res.* **1991**, *38*, 267–272.
- Fisone, G.; Berthold, M.; Bedecs, K.; Uden, A.; Bartfai, T.; Bertorelli, R.; Consolo, S.; Crawley, J.; Martin, B.; Nilsson, S.; et al. N-terminal galanin-(1–16) fragment is an agonist at the hippocampal galanin receptor. *Proc. Natl. Acad. Sci. U.S.A.* **1989**, *86*, 9588–9591.

- (42) Carpenter, K. A.; Schmidt, R.; Yue, S. Y.; Hodzic, L.; Pou, C.; Payza, K.; Godbout, C.; Brown, W.; Roberts, E. The glycine residue in cyclic lactam analogues of galanin(1–16)-NH₂ is important for stabilizing an N-terminal helix. *Biochemistry* **1999**, *38*, 15295–15304.
- (43) Jureus, A.; Langel, U.; Bartfai, T. L-Ala-substituted rat galanin analogs distinguish between hypothalamic and jejunal galanin receptor subtypes. *J. Pept. Res.* **1997**, *49*, 195–200.
- (44) Pooga, M.; Jureus, A.; Razaeei, K.; Hasanvan, H.; Saar, K.; Kask, K.; Kjellen, P.; Land, T.; Halonen, J.; Mäoorg, U.; Uri, A.; Solyom, S.; Bartfai, T.; Langel, U. Novel galanin receptor ligands. *J. Pept. Res.* **1998**, *51*, 65–74.
- (45) Rivera Baeza, C.; Kask, K.; Langel, U.; Bartfai, T.; Uden, A. Analogs of galanin (1–16) modified in positions 1–3 as ligands to rat hypothalamic galanin receptors. *Acta Chem. Scand.* **1994**, *48*, 434–438.
- (46) Dasgupta, P.; Singh, A.; Mukherjee, R. N-terminal acylation of somatostatin analog with long chain fatty acids enhances its stability and antiproliferative activity in human breast adenocarcinoma cells. *Biol. Pharm. Bull.* **2002**, *25*, 29–36.
- (47) Blanchfield, J. T.; Dutton, J. L.; Hogg, R. C.; Gallagher, O. P.; Craik, D. J.; Jones, A.; Adams, D. J.; Lewis, R. J.; Alewood, P. F.; Toth, I. Synthesis, structure elucidation, in vitro biological activity, toxicity, and Caco-2 cell permeability of lipophilic analogues of α -conotoxin MII. *J. Med. Chem.* **2003**, *46*, 1266–1272.
- (48) Blanchfield, J. T.; Lew, R. A.; Smith, A. I.; Toth, I. The stability of lipidic analogues of GnRH in plasma and kidney preparations: the stereoselective release of the parent peptide. *Bioorg. Med. Chem. Lett.* **2005**, *15*, 1609–1612.
- (49) Yuan, L.; Wang, J.; Shen, W. C. Reversible lipidization prolongs the pharmacological effect, plasma duration, and liver retention of octreotide. *Pharm. Res.* **2005**, *22*, 220–227.
- (50) Wang, J.; Wu, D.; Shen, W. C. Structure–activity relationship of reversibly lipidized peptides: studies of fatty acid–desmopressin conjugates. *Pharm. Res.* **2002**, *19*, 609–614.
- (51) van de Waterbeemd, H.; Lennernas, H.; Artursson, P. *Drug Bioavailability: Estimation of Solubility, Permeability, Adsorption and Bioavailability*; Wiley-VCH Verlag GmbH & Co: Germany, 2003.
- (52) Dagar, S.; Onyuksel, H.; Akhter, S.; Krishnadas, A.; Rubinstein, I. Human galanin expresses amphipathic properties that modulate its vasoreactivity in vivo. *Peptides* **2003**, *24*, 1373–1380.
- (53) Cai, L. F.; Gochin, M. Colloidal aggregate detection by rapid fluorescence measurement of liquid surface curvature changes in multiwell plates. *J. Biomol. Screening* **2007**, *12*, 966–971.
- (54) Dyson, H. J.; Rance, M.; Houghten, R. A.; Wright, P. E.; Lerner, R. A. Folding of immunogenic peptide fragments of proteins in water solution. II. The nascent helix. *J. Mol. Biol.* **1988**, *201*, 201–217.
- (55) Dyson, H. J.; Merutka, G.; Waltho, J. P.; Lerner, R. A.; Wright, P. E. Folding of peptide fragments comprising the complete sequence of proteins. Models for initiation of protein folding. I. Myohemerythrin. *J. Mol. Biol.* **1992**, *226*, 795–817.
- (56) Shin, H. C.; Merutka, G.; Waltho, J. P.; Wright, P. E.; Dyson, H. J. Peptide models of protein folding initiation sites. 2. The G-H turn region of myoglobin acts as a helix stop signal. *Biochemistry* **1993**, *32*, 6348–6355.
- (57) Morris, M. B.; Ralston, G. B.; Biden, T. J.; Browne, C. L.; King, G. F.; Iismaa, T. P. Structural and biochemical studies of human galanin: NMR evidence for nascent helical structures in aqueous solution. *Biochemistry* **1995**, *34*, 4538–4545.
- (58) Valenzano, K. J.; Miller, W.; Kravitz, J. N.; Samama, P.; Fitzpatrick, D.; Seeley, K. Development of a fluorescent ligand-binding assay using the AcroWell filter plate. *J. Biomol. Screening* **2000**, *5*, 455–461.
- (59) Sollenberg, U.; Bartfai, T.; Langel, U. Galnon—a low-molecular-weight ligand of the galanin receptors. *Neuropeptides* **2005**, *39*, 161–163.
- (60) Boules, M.; Fredrickson, P.; Richelson, E. Bioactive analogs of neurotensin: Focus on CNS effects. *Peptides* **2006**, *27*, 2523–2533.
- (61) Egleton, R. D.; Davis, T. P. Bioavailability and transport of peptides and peptide drugs into the brain. *Peptides* **1997**, *18*, 1431–1439.
- (62) Egleton, R. D.; Davis, T. P. Development of neuropeptide drugs that cross the blood–brain barrier. *NeuroRx* **2005**, *2*, 44–53.
- (63) Dasgupta, P.; Mukherjee, R. Lipophilization of somatostatin analog RC-160 with long chain fatty acid improves its antiproliferative and antiangiogenic activity in vitro. *Br. J. Pharmacol.* **2000**, *129*, 101–109.
- (64) Uchiyama, T.; Kotani, A.; Tatsumi, H.; Kishida, T.; Okamoto, A.; Okada, N.; Murakami, M.; Fujita, T.; Fujiwara, Y.; Kiso, Y.; Muranishi, S.; Yamamoto, A. Development of novel lipophilic derivatives of DADLE (leucine enkephalin analogue): intestinal permeability characteristics of DADLE derivatives in rats. *Pharm. Res.* **2000**, *17*, 1461–1467.
- (65) Wang, J.; Hogenkamp, D. J.; Tran, M.; Li, W. Y.; Yoshimura, R. F.; Johnstone, T. B.; Shen, W. C.; Gee, K. W. Reversible lipidization for the oral delivery of leu-enkephalin. *J. Drug Targeting* **2006**, *14*, 127–136.
- (66) Banks, W. A.; Kastin, A. J. Peptides and the blood–brain barrier: lipophilicity as a predictor of permeability. *Brain Res. Bull.* **1985**, *15*, 287–292.
- (67) Fuchs, S. M.; Raines, R. T. Internalization of cationic peptides: the road less (or more?) traveled. *Cell. Mol. Life Sci.* **2006**, *63*, 1819–1822.
- (68) Drin, G.; Cottin, S.; Blanc, E.; Rees, A. R.; Tamsamani, J. Studies on the internalization mechanism of cationic cell-penetrating peptides. *J. Biol. Chem.* **2003**, *278*, 31192–31201.
- (69) Tamai, I.; Sai, Y.; Kobayashi, H.; Kamata, M.; Wakamiya, T.; Tsuji, A. Structure–internalization relationship for adsorptive-mediated endocytosis of basic peptides at the blood–brain barrier. *J. Pharmacol. Exp. Ther.* **1997**, *280*, 410–415.
- (70) Drin, G.; Rousselle, C.; Scherrmann, J. M.; Rees, A. R.; Tamsamani, J. Peptide delivery to the brain via adsorptive-mediated endocytosis: advances with SynB vectors. *AAPS PharmSci* **2002**, *4*, E26.
- (71) Pajouhesh, H.; Lenz, G. R. Medicinal chemical properties of successful central nervous system drugs. *NeuroRx* **2005**, *2*, 541–553.
- (72) Kurtzhals, P.; Havelund, S.; Jonassen, I.; Kiehr, B.; Larsen, U. D.; Ribel, U.; Markussen, J. Albumin binding of insulins acylated with fatty acids: characterization of the ligand-protein interaction and correlation between binding affinity and timing of the insulin effect in vivo. *Biochem. J.* **1995**, *312* (Pt 3), 725–731.
- (73) Havelund, S.; Plum, A.; Ribel, U.; Jonassen, I.; Volund, A.; Markussen, J.; Kurtzhals, P. The mechanism of protraction of insulin detemir, a long-acting, acylated analog of human insulin. *Pharm. Res.* **2004**, *21*, 1498–1504.
- (74) Menezes, Y.; Khatchadourian, C. Peptides bound to albumin. *Life Sci* **1986**, *39*, 1751–1753.
- (75) Svenson, J.; Brandsdal, B. O.; Stensen, W.; Svendsen, J. S. Albumin binding of short cationic antimicrobial micropeptides and its influence on the in vitro bactericidal effect. *J. Med. Chem.* **2007**, *50*, 3334–3349.
- (76) Mazarati, A. M. Galanin and galanin receptors in epilepsy. *Neuropeptides* **2004**, *38*, 331–343.
- (77) Nelson, A. R.; Borland, L.; Allbritton, N. L.; Sims, C. E. Myristoyl-based transport of peptides into living cells. *Biochemistry* **2007**, *46*, 14771–14781.
- (78) Zorko, M.; Langel, U. Cell-penetrating peptides: mechanism and kinetics of cargo delivery. *Adv. Drug Delivery Rev.* **2005**, *57*, 529–545.
- (79) Pooga, M.; Hallbrink, M.; Zorko, M.; Langel, U. Cell penetration by transportan. *FASEB J.* **1998**, *12*, 67–77.
- (80) Pooga, M.; Soomets, U.; Hallbrink, M.; Valkna, A.; Saar, K.; Razaeei, K.; Kahl, U.; Hao, J. X.; Xu, X. J.; Wiesenfeld-Hallin, Z.; Hokfelt, T.; Bartfai, T.; Langel, U. Cell penetrating PNA constructs regulate galanin receptor levels and modify pain transmission in vivo. *Nat. Biotechnol.* **1998**, *16*, 857–861.
- (81) Tossi, A.; Sandri, L.; Giangaspero, A. Amphipathic, α -helical antimicrobial peptides. *Biopolymers* **2000**, *55*, 4–30.
- (82) Hua, X. Y.; Hayes, C. S.; Hofer, A.; Fitzsimmons, B.; Kilk, K.; Langel, U.; Bartfai, T.; Yaksh, T. L. Galanin acts at GalR1 receptors in spinal antinociception: synergy with morphine and AP-5. *J. Pharmacol. Exp. Ther.* **2004**, *308*, 574–582.
- (83) Hua, X. Y.; Salgado, K. F.; Gu, G.; Fitzsimmons, B.; Kondo, I.; Bartfai, T.; Yaksh, T. L. Mechanisms of antinociception of spinal galanin: how does galanin inhibit spinal sensitization. *Neuropeptides* **2005**, *39*, 211–216.
- (84) Liu, H. X.; Brumovsky, P.; Schmidt, R.; Brown, W.; Payza, K.; Hodzic, L.; Pou, C.; Godbout, C.; Hokfelt, T. Receptor subtype-specific pronociceptive and analgesic actions of galanin in the spinal cord: selective actions via GalR1 and GalR2 receptors. *Proc. Natl. Acad. Sci. U.S.A.* **2001**, *98*, 9960–9964.

JM801088X

2.5.2 Structural Requirements for a Lipoamino Acid in Modulating
the Anticonvulsant Activities of Systemically Active
Galanin Analogues

Manuscript Reproduced with Permission From:

Zhang, L., Robertson, C. R., Green, B. R., Pruess, T. H., White, H. S., and Bulaj, G.
(2009) Structural requirements for a lipoamino acid in modulating the anticonvulsant
activities of systemically active galanin analogues, *J. Med. Chem.* 52, 1310-1316.

© 2009 American Chemical Society

Structural Requirements for a Lipoamino Acid in Modulating the Anticonvulsant Activities of Systemically Active Galanin Analogues

Liuyin Zhang,[†] Charles R. Robertson,[†] Brad R. Green,[†] Timothy H. Pruess,[‡] H. Steve White,[‡] and Grzegorz Bulaj^{*,†}

Department of Medicinal Chemistry and Department of Pharmacology and Toxicology, College of Pharmacy, University of Utah, Salt Lake City, Utah, 84108

Received November 5, 2008

Introduction of lipoamino acid (LAA), Lys-palmitoyl, and cationization into a series of galanin analogues yielded systemically active anticonvulsant compounds. To study the relationship between the LAA structure and anticonvulsant activity, orthogonally protected LAAs were synthesized in which the Lys side chain was coupled to fatty acids varying in length from C₈ to C₁₈ or was coupled to a monodispersed polyethylene glycol, MPEG₄. Galanin receptor affinity, serum stability, lipophilicity (log *D*), and activity in the 6 Hz mouse model of epilepsy of each of the newly synthesized analogues were determined following systemic administration. The presence of various LAAs or Lys(MPEG₄) did not affect the receptor binding properties of the modified peptides, but their anticonvulsant activities varied substantially and were generally correlated with their lipophilicity. Our results suggest that varying the length or polarity of the LAA residue adjacent to positively charged amino acid residues may effectively modulate the antiepileptic activity of the galanin analogues.

Introduction

When delivered directly into the brain, many neuropeptides, including galanin, neuropeptide Y, somatostatin, neurotensin, or opioid peptides can modulate excitatory or inhibitory circuits and suppress seizures and/or pain sensation.^{1–4} Despite a considerable interest in generating blood–brain barrier (BBB^a) permeable analogues of neuropeptides, only a few successful examples have been reported to date.^{4–12} To improve central nervous system (CNS) bioavailability of neuroactive peptides, various strategies have been explored, including lipidization, cationization, and glycosylation.^{13–15} Banks and Kastin showed that the lipophilicity of peptides improved their permeability through the BBB.¹⁶ Despite the finding that only small amounts of the peptides entered the brain, the authors noted a direct correlation between the log *D* values and the blood-to-brain ratio. Reversible lipidization of opioid peptides also improved centrally mediated analgesic effects.¹⁷ It is also important to note that oral bioavailability of the somatostatin analogue TT-232 was achieved by coupling various LAAs to either N- or C-terminal components of the analogue.¹⁸ Although lipophilicity has been acknowledged to play an important role in structure–bioavailability relationships,^{16,19} very few examples are available where lipidization of neuropeptides has been found to improve their activity in the brain.^{17,20,21} As pointed out in a review by Witt et al.,¹³ “lipidization of peptides may increase plasma

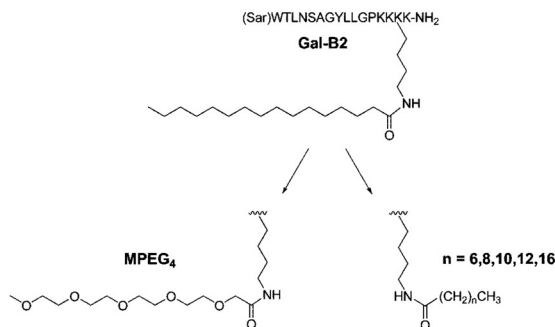


Figure 1. Structures of Gal-B2 and LAAs used in this SAR study. Note that MPEG₄ has an identical number of atoms as the C₁₆ (palmitoyl) but is significantly less lipophilic.

protein binding, systemic elimination, and intracellular sequestration, thus hampering their efficient penetration into the CNS.” Indeed, when just the lipidization strategy was applied to galanin, the truncated galanin analogue containing a Lys-palmitoyl residue was inactive as an anticonvulsant, despite displaying high affinity toward galanin receptors and a high log *D*.²²

In contrast, lipidization appeared very effective in improving the CNS bioavailability of the truncated galanin analogues when the Lys(palmitoyl) residue was introduced in concert with cationization.²² The most active analogue, Gal-B2, contained the C-terminal “-Lys-Lys-Lys(palmitoyl)-Lys-NH₂” motif (Figure 1). The combined lipidization and cationization resulted in very potent antiepileptic compounds; e.g., the anticonvulsant ED₅₀ of Gal-B2 was found to be 0.8 mg/kg when tested intraperitoneally (ip) in the 6 Hz pharmacoresistant model of epilepsy. Since galanin suppresses seizures by activating GalR1 and GalR2 located in the hippocampus and other limbic structures, our data suggest that the combination of cationization and lipidization is effective in improving the BBB penetration of Gal-B2 without negatively affecting receptor affinity. Furthermore, our results suggest that the sequence position of LAAs

* To whom correspondence should be addressed. Address: Department of Medicinal Chemistry, College of Pharmacy, University of Utah, 421 Wakara Way, Suite 360, Salt Lake City, Utah 84108. Phone: (801) 581-4629. Fax: (801) 581-7087. E-mail: bulaj@pharm.utah.edu.

[†] Department of Medicinal Chemistry.

[‡] Department of Pharmacology and Toxicology.

^a Abbreviations: AUC, area under the curve; BBB, blood–brain barrier; CD, circular dichroism; CNS, central nervous system; DCC, *N,N'*-dicyclohexylcarbodiimide; DIPEA, *N,N*-diisopropylethylamine; Fmoc, *N*-(9-fluorenyl)methoxycarbonyl; GalR1, galanin receptors subtype 1; GalR2, galanin receptors subtype 2; GPCRs, G-protein-coupled receptors; ip, intraperitoneally; LAA, lipoamino acid; MPEG₄, monodispersed polyethylene glycol PEG₄; PyBop, (benzotriazol-1-yloxy)tripyrrolidinophosphonium hexafluorophosphate; SAR, structure–activity relationship; SPPS, solid phase peptide synthesis; TFA, trifluoroacetic acid; TFE, 2,2,2-trifluoroethanol.

Table 1. Structures of LAAs Used for SPSS of the Systemically Active Galanin Analogues

| LAA | Name | Structure |
|-----|------------------------|-----------|
| 1 | Fmoc-Lys(octanoyl)-OH | |
| 2 | Fmoc-Lys(decenoyl)-OH | |
| 3 | Fmoc-Lys(lauroyl)-OH | |
| 4 | Fmoc-Lys(myristoyl)-OH | |
| 5 | Fmoc-Lys(stearoyl)-OH | |
| 6 | Fmoc-Lys(MPEG4)-OH | |

is important for the systemic activity of Gal-B2, suggesting that the lipidization/cationization motif was not simply producing the additive effect by combining hydrophobicity and positive charges.

In order to define the structural requirements of the LAA residue for improving the anticonvulsant activity of Gal-B2, we synthesized a series of LAAs in which the Lys side chain was either coupled to fatty acids, varying in length from C₈ to C₁₈, or to a monodispersed PEG₄ (MPEG₄). These LAAs were used to replace the Lys-palmitoyl residue in position 16 of Gal-B2 (Figure 1). The binding affinity, octanol/water partitioning coefficient, and ability to suppress seizures in the *in vivo* 6 Hz model of epilepsy was determined following *ip* administration. Our findings suggest that the length and polarity of the LAAs are important for maintaining antiepileptic activity of the galanin analogues.

Results

Design and Chemical Synthesis. To study the role of Lys-palmitoyl, residue 16, in the activity of Gal-B2, we designed a series of analogues where we systematically changed the length of the fatty acid or replaced the palmitoyl motif with a MPEG₄ (Figure 1). The length of the LAAs varied from C₈ to C₁₈ by two carbon atom increments (Table 1). The MPEG₄-containing Gal-B2 analogue was designed to dissect the lipophilic contribution of the Lys-palmitoyl residue, since MPEG₄ is significantly more polar than C₁₆ despite having an identical number of atoms. To synthesize these new structure–activity relationship (SAR) analogues of Gal-B2, we applied a direct coupling of the orthogonally protected *N*^ε-lipolysine intermediates (*N*^ε-palmitoyl-*N*^ε-Fmoc-lysine is commercially available). For the synthesis of *N*^ε-octanoyl **1** (C₈), -decenoyl **2** (C₁₀), -lauryl **3** (C₁₂), -myristoyl **4** (C₁₄), and -stearoyl **5** (C₁₈) substituted *N*^ε-Fmoc-lysine, a convenient method was applied using Na₂CO₃ as a coupling reagent with a corresponding acid halide in dioxane/water solvent system (Scheme 1). Synthesis of Fmoc-Lys-(MPEG₄)-OH **6** was achieved by coupling Fmoc-Lys-OH with perfluorophenol activated MPEG₄-acetic acid **7**. Compound **7** was synthesized from the substitution reaction of MPEG₄-OH with ethyl bromoacetate followed by ester hydrolysis (Scheme 2). The modified amino acids were purified by flash chromatography and used for solid-phase peptide synthesis (SPSS).

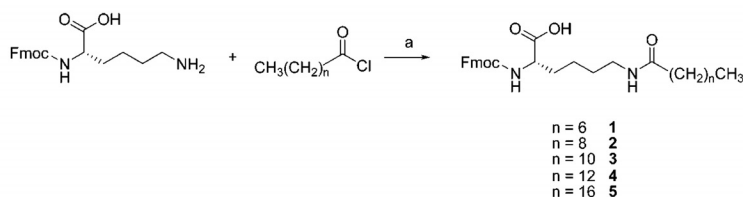
The SPSS was carried out using an automated peptide synthesizer at 25 μmol scale on preloaded Fmoc-Lys(Boc)-Rink amide AM resin. The 5-fold Fmoc-amino acids/PyBop/DIPEA (1:1:2) were used in peptide synthesis. A 2-fold of the Fmoc protected LAAs or MPEG₄-lysine was used in manual coupling synthesis. The synthesized peptides were cleaved from the resin

using reagent K (trifluoroacetic acid (TFA)/water/thioanisole/phenol/ethanedithiol, 90/5/5/7.5/2.5 v/v), followed by precipitation and washing with ice cold methyl *tert*-butyl ether (MTBE). Crude peptides were purified by preparative reversed-phase HPLC using a diphenyl column with a linear gradient of water/acetonitrile (both buffered with 0.1% TFA). The purities of peptides were greater than 95% by analytical HPLC analyses (Supporting Information Figure S1 and Table S1). Purified analogues were quantified by UV absorbance ($\lambda = 279.8$ nm, $\epsilon = 7000$ cm⁻¹ M⁻¹), and their monoisotopic mass was confirmed by MALDI-TOF mass spectrometry (Table 2).

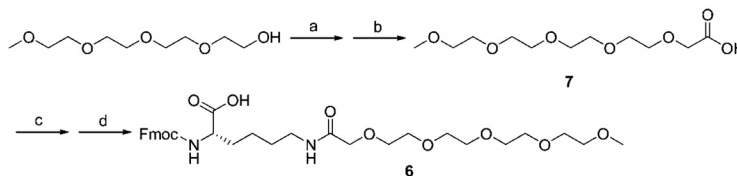
Physicochemical and Structural Properties. To determine the lipophilicity of the analogues, log *D* values were calculated using the combination of the HPLC retention times and the log *D* determined from the classical shake-flask method, as previously described.²² Calculations of log *D* values are provided in Supporting Information Table S2. For the LAA containing analogues, the log *D* values ranged from 0.78 for Gal-B2-C₈ to 1.35 for Gal-B2-C₁₈. As shown in Figure 2, the log *D* values linearly correlated with the carbon chain length of the LAA (linear fit yielded $R^2 = 0.98$). Since the log *D* values increased 4-fold by replacing one Lys residue with Lys-stearoyl (compare log *D* of Gal-(K)4 (0.34)²² with that of Gal-B2-C₁₈ (1.35)) and almost doubled by changing the LAA from C₈ to C₁₈, these results emphasize the effectiveness of the LAAs to increase the lipophilicity of short peptides. The analogue with the MPEG₄-amino acid isostere had approximately 2-fold lower log *D* (0.57), compared to the Lys-palmitoyl residue (1.24).

Gal-B2 is largely unstructured in water but contains 23% α -helical content in the presence of 50% trifluoroethanol (TFE).²² In our previous work,²² we hypothesized that the presence of LAA could stabilize the helical conformation of the systemically active galanin analogues by hydrophobic interactions with Tyr9 and/or Trp2. To test this hypothesis, the conformational properties of the Gal-B2 analogues were investigated by circular dichroism (CD). In the presence of 5 mM potassium phosphate containing 150 mM NaF (pH 7.5), the helical content varied among the analogues from 1% to 7% (only Gal-B2-C₈ had 15%). The helical content in 50% TFE increased for most analogues compared to that determined in “buffer only” conditions (Table 2). No apparent correlations were observed between the length of the LAA and percentage of helical content in the analogues.

Metabolic Stability. To investigate how the length of the LAA residue might affect resistance of the galanin analogues to proteolytic degradation, we employed the *in vitro* metabolic stability assay. The half-life of the analogues was determined in buffered 25% rat blood serum incubated at 37 °C. The amount of each analogue remaining after an appropriate time interval was quantified by HPLC, and the time-course of disappearance of the analogues is shown in Figure 3A. Calculated half-lives for the analogues are summarized in Figure 3B. All analogues exhibited pronounced resistance to proteolytic degradation (for comparison, the unmodified Gal(1–16) analogue had 7.8 min half-time under these conditions).²² Interestingly, the galanin analogues containing the shortest or the longest aliphatic chain were the least stable whereas the analogue containing C₁₄ had the longest half-life of 12 h (Figure 3B). This correlation suggested a rather complex mechanism by which the LAAs might increase the stability of galanin analogues in plasma. We hypothesized that the metabolic stability of the galanin analogues might be correlated with their serum albumin binding properties (e.g., binding properties of long-chain carboxylic acids to albumin are dependent on aliphatic chain length).²³ However,

Scheme 1. Synthesis of the Fmoc-Protected LAAs^a

^a Reagents and conditions: (a) Na_2CO_3 , $\text{H}_2\text{O}/\text{dioxane}$, room temp, overnight, 64–87%.

Scheme 2. Synthesis of Fmoc-Lys(MPEG₄)-OH^a

^a Reagents and conditions: (a) NaH , 0 °C, 1 h; ethyl bromoacetate, 50 °C, 16 h; (b) 1 M $\text{LiOH}/\text{CH}_3\text{OH}$, 6 h, 59% (from two steps); (c) perfluorophenol, DCC, overnight; (d) Fmoc-L-lysine, DIPEA, 0 °C, 60% (from two steps).

Table 2. Structure and Properties of the Galanin Analogues^a

| analog | structure | HPLC retention time ^b | α -helix ^c (%) | MS (MALDI, MH^+) calcd/found |
|-----------------------------------|--|----------------------------------|----------------------------------|--|
| Gal-(K) ₄ ^d | (Sar)WTLNSAGYLLGPKKKK | 15.13±0.42 | 14 | 1873.09/1873.14 |
| Gal-B2-C ₈ | (Sar)WTLNSAGYLLGPKK(Lys-octanoyl)K | 20.13±0.17 | 9 | 2001.21/2001.17 |
| Gal-B2-C ₁₀ | (Sar)WTLNSAGYLLGPKK(Lys-decanoyl)K | 21.49±0.05 | 6 | 2029.24/2029.45 |
| Gal-B2-C ₁₂ | (Sar)WTLNSAGYLLGPKK(Lys-lauroyl)K | 22.51±0.03 | 16 | 2057.28/2057.26 |
| Gal-B2-C ₁₄ | (Sar)WTLNSAGYLLGPKK(Lys-myristoyl)K | 23.76±0.18 | 16 | 2085.31/2085.33 |
| Gal-B2 ^d | (Sar)WTLNSAGYLLGPKK(Lys-palmitoyl)K | 25.84±0.10 | 23 | 2112.31/2112.33 |
| Gal-B2-C ₁₈ | (Sar)WTLNSAGYLLGPKK(Lys-stearoyl)K | 26.73±0.18 | 5 | 2141.33/2141.48 |
| Gal-B2-MPEG ₄ | (Sar)WTLNSAGYLLGPKK(Lys-MPEG ₄)K | 17.52±0.03 | 18 | 2123.23/2123.29 |

^a All analogues are amidated at the C-terminus. ^b A linear gradient of water/90% acetonitrile (buffered with 0.1% TFA) on a Vydac diphenyl column, starting from 20% acetonitrile to 100% acetonitrile in 40 min. ^c Determined in the presence of 50% v/v 2,2,2-trifluoroethanol. ^d Data from ref 22.

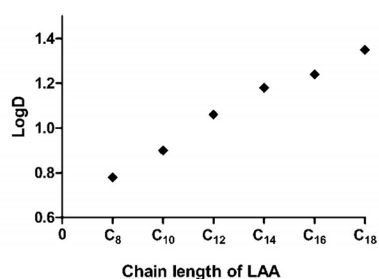


Figure 2. Relationships between the aliphatic chain length of the LAAs in Gal-B2 analogues and the octanol/water partition coefficient ($\log D$). Linear fit yielded $R^2 = 0.9839$, $P < 0.0001$.

our efforts in determining the protein binding properties of Gal-B2 by microdialysis failed because of possible micelle formation.²² The Gal-B2-MPEG₄ analogue exhibited a very long half-life (12.4 ± 0.65 h), suggesting that the extended amino acid residue might provide steric hindrance for access of proteinases.

In Vitro and in Vivo Pharmacology. Since two galanin receptors, GalR1 and GalR2, are known to be involved in controlling seizures in the brain,^{24,25} we investigated the interactions of the galanin analogues with both receptor subtypes using a competitive binding assay. As described in our previous work, K_i values were determined using a time-resolved fluorescence binding assay with a europium-labeled galanin.²² The GPCR membrane preparations used in the assay were commercially available (Perkin-Elmer or Millipore) and were derived from recombinant human GalR1 or GalR2 gene sequences. As

shown in Table 3, when compared to each other, none of the analogues studied here exhibited significantly different affinities toward either receptor subtype. This suggested that the relatively large LAA moiety did not affect the affinity of the analogues toward the galanin receptors. All analogues maintained several-fold preference in binding to GalR1 subtype, compared to GalR2, similar to that of unmodified Gal(1–16).²²

The anticonvulsant activity of the analogues was studied in the 6 Hz (32 mA) model of pharmacoresistant epilepsy following ip administration of a bolus dose of 4 mg/kg. The analogues were evaluated for their ability to suppress seizures at various times (0.25–4 h) after peptide administration. The time–response curves were then integrated to provide a qualitative measurement of efficacy, i.e., area under the curve (AUC) values (Table 3, Figure 4). The analogues differed significantly in their ability to protect mice from seizures. On the basis of the AUC values, the most active galanin analogues contained Gal-B2-C₁₆ and Gal-B2-C₁₈, whereas the least active analogues included C₈ and C₁₀. Interestingly, the Lys-MPEG₄-containing analogue was also active as an anticonvulsant, albeit significantly less when compared to Gal-B2.

Discussion

To study the structural requirements for the LAA residue 16 in mediating the antiepileptic activity of the systemically active galanin analogues,²² we synthesized and characterized a new series of analogues that differed in their length/polarity of the fatty acid moiety coupled to the Lys16 residue. The major finding of this work was that the six galanin analogues (despite

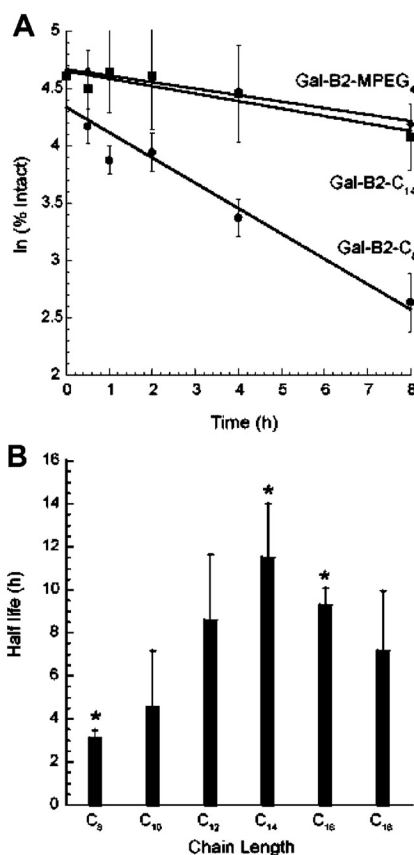


Figure 3. (A) In vitro serum stability assay for the galanin analogues. Representative plots showing a time-course of degradation for C₈- (●), C₁₄- (■), and MPEG₄- (◆)-containing galanin analogues in the presence of 25% rat serum at 37 °C. Degradation of analogues was monitored by analytical HPLC. Data points were obtained at 0, 0.5, 1, 2, 4, and 8 h from the average of at least three independent experiments. (B) Relationships between the length of the LAAs and the in vitro metabolic stability of the galanin analogues. The half-lives were determined by incubating the peptides in 25% diluted rat serum at 37 °C. The concentrations of the remaining analogues were determined by HPLC. Data were obtained from at least three independent experiments. ANOVA single factor analysis yielded a *P*-value of 0.004 for C₈-, C₁₄-, and C₁₆-containing species (*).

having comparable affinities toward the galanin receptors and differing in the length of the fatty acid from C₈ to C₁₈) exhibited pronounced differences in their anticonvulsant activities following ip administration. The analogues containing shorter fatty acids were less active compared to those with longer chains. These results suggest that the increased lipophilicity provided by the longer fatty acids is an important factor in improving the anticonvulsant activity of galanin analogues following systemic administration. Further work will be required to determine whether the resulting compounds are agonists, partial agonists, or antagonists. Interestingly, both Gal-B2 and Gal-B2-C₈ showed comparable analgesic activities in a mouse pain assay following ip administration (E. Adkins-Scholl, H. S. White, G. Bulaj, unpublished results), suggesting that systemically active galanin analogues varying in the length of a LAA may control seizures or pain via galanin receptors in the CNS or peripheral nerves, respectively.^{26–28} Our previous data indicated that the position of the LAA residue appeared to be

important for the anticonvulsant activity of Gal-B2,²² thus implying that lipophilicity alone (which would be expected to increase passive diffusion) is not the sole important factor for improving seizure suppression by this analogue. Although the “-Lys-Lys-Lys(palmitoyl)-Lys-NH₂” motif appeared to be the most effective in increasing the anticonvulsant activity of the galanin analogues following ip administration, clearly, more SAR studies, or perhaps even a combinatorial approach, will be needed to further improve the potency of the Gal-B2 related analogues.²²

Introduction of the LAA to the galanin analogues significantly improved their in vitro metabolic stability; this effect may be, at least in part, accounted for by steric effects of the long side chain in position 16 of the analogues. This finding is not surprising in light of previous reports with lipopeptides, in which prolonged in vitro and/or in vivo half-lives were observed,²⁹ including gonadotropin-releasing hormone analogues,³⁰ glucagon-like peptide 1 analogues,³¹ insulin,³² and octreotide.²⁰ The metabolic stability of lipopeptides may also be affected by their interactions with fatty acid binding sites in serum albumin.³² As shown in Figure 3B, the longest serum half-lives were observed for Gal-B2-C₁₄ and Gal-B2-C₁₆ whereas the shortest were observed for Gal-B2-C₈. Interestingly, the C₈ (octanoic acid) moiety binds with 11-fold higher affinity to human serum albumin compared to the C₁₄ (myristic acid).²³

Another aspect of this work is our less conventional approach of using orthogonally protected LAAs and MPEG₄-amino acids as building blocks for SPPS. Introduction of LAA into peptides have been reported using three distinct strategies: (1) on-resin fatty acid acylation of *N*^α-amino acids^{33,34} or *N*^ε-lysine,³⁵ (2) esterification of fatty acids,³⁶ and (3) conjugation at the C-terminus of peptide.^{18,37} Our strategy of using the Fmoc protected LAAs directly coupled during the solid-phase peptide synthesis offers apparent advantages in applications such as routine synthesis of lipopeptide analogues for SAR studies or synthesis of peptide-based combinatorial libraries directed toward optimization of the chain length of the LAAs in the cationic/lipidic motif.

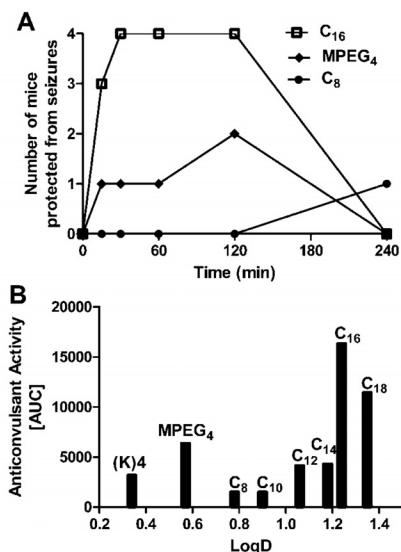
To what extent the systemically active galanin analogues may have improved the BBB permeability remains unanswered. However, since some of the modified galanin analogues possess pronounced antiepileptic activity believed to be mediated by the galanin receptors located in the limbic system and, thus, behind the blood–brain barrier, these data suggest that sufficient quantities of the analogues must penetrate into the brain. As we have suggested previously,²² lipidization may improve CNS bioavailability of Gal-B2 via a combination of adsorptive-mediated endocytosis and passive diffusion.^{38,39} More mechanistic studies assessing the mechanism of transport of galanin analogues across the cell-based models of BBB are underway. Regardless of the mechanism by which these analogues penetrate into the brain, our data suggest that changing the length and/or polarity of the LAA residue in the context of cationization may offer a useful strategy to modulate CNS bioavailability of galanin analogues. In summary, we believe that the variations in lipidization and cationization appear to provide a useful strategy for modulating CNS bioavailability of not only the galanin analogues described here but perhaps even other neuropeptides.

Experimental Section

General Synthetic Procedures. Reagent chemicals were obtained from Aldrich Chemical Corporation and were used without prior purification. Reactions were performed under N₂ atmosphere,

Table 3. In Vitro and in Vivo Pharmacological Properties of the Galanin Analogues

| analogue | in vitro assay (receptor binding), K_i (nM) | | in vivo assay (anticonvulsant activity) (6 Hz, 32 mA, 4 mg/kg) | | | | |
|--------------------------|---|-----------|--|--------|-----|-----|-----|
| | GalR1 | GalR2 | 15 min | 30 min | 1 h | 2 h | 4 h |
| Gal-(K) ^a | 0.4±0.1 | 24.0±9.9 | 0/4 | 3/4 | 1/3 | 0/3 | 0/4 |
| Gal-B2-C ₈ | 0.7±0.1 | 14.9±0.6 | 0/4 | 0/4 | 0/4 | 0/4 | 1/4 |
| Gal-B2-C ₁₀ | 1.3±0.7 | 14.4±0.6 | 2/4 | 2/4 | 0/4 | 0/4 | 0/4 |
| Gal-B2-C ₁₂ | 1.4±0.4 | 16.1±8.5 | 1/4 | 3/4 | 2/4 | 0/4 | 0/4 |
| Gal-B2-C ₁₄ | 2.6±0.1 | 18.2±1.6 | 2/4 | 3/4 | 2/4 | 0/4 | 0/4 |
| Gal-B2 ^a | 3.5±1.0 | 51.5±34.4 | 3/4 | 4/4 | 4/4 | 4/4 | 0/4 |
| Gal-B2-C ₁₈ | 4.0±2.0 | 15.0±1.0 | 4/4 | 3/4 | 4/4 | 2/4 | 0/4 |
| Gal-B2-MPEG ₄ | 0.5±0.1 | 20.5±6.5 | 1/4 | 1/4 | 1/4 | 2/4 | 0/4 |

^aData from ref 22.**Figure 4.** Anticonvulsant activity of the galanin analogues. The analogues were administered ip as a bolus dose of 4 mg/kg; (A) time–response studies ranging from 15 min to 4 h were used to calculate area under the curve values (AUC); (B) relationships between log *D* and the anticonvulsant activity (AUC values) of the galanin analogues in the 6 Hz model of epilepsy.

unless otherwise indicated. Chromatography refers to flash chromatography on silica gel (Whatman 230–400 mesh ASTM silica gel). Analytical thin layer chromatography was performed using EMD Aluminium TLC silica gel 60 PF254. Preparative HPLC was performed on a Waters 600 pump system equipped with a Waters 2487 dual wavelength detector ($\lambda_1 = 220$ nm, $\lambda_2 = 280$ nm) and a preparative Vydac diphenyl column (219TP101522). Analytical HPLC used an analytical Vydac diphenyl column (219TP54). The HPLC mobile phases are buffer A, 100% water (0.1% TFA), and buffer B, 90% acetonitrile (0.1% TFA). Metabolic stability used a Waters Alliance 2695 system equipped with an autosampler, dual wavelength detector, and a Waters YMC ODS-A diphenyl column (AA125052503WT). NMR spectra were recorded at 400 MHz (¹H), 101 MHz (¹³C) at 25 °C. Proton and carbon chemical shifts are given in ppm relative to TMS internal standard. MALDI-TOF MS was conducted at the University of Utah Core Facility. CD spectra were obtained on an Aviv 62DS CD spectropolarimeter at room temperature. Optical rotations were measured on a Perkin-Elmer polarimeter (model 343) using a 1 mL capacity quartz cell with a 10 cm path length.

Fmoc-Lys(octanoyl)-OH (1). Fmoc-L-lysine (0.737 g, 2.0 mmol) was added to dioxane (10 mL), and then a solution of Na₂CO₃ (0.636 g, 6.0 mmol) in H₂O (12.6 mL) was added dropwise at 0 °C. After 5 min, a solution of octanoyl chloride (0.325 g, 2.0 mmol) in dioxane (10 mL) was added to the mixture. The solution was allowed to warm to room temperature and stirred overnight.

The solvents were extracted with CH₂Cl₂ (250 mL), washed with saturated NaHCO₃ (20 mL), 1 M HCl (2 mL), and brine (20 mL), dried over Na₂SO₄, and concentrated. Flash chromatography (CH₂Cl₂/CH₃OH, 6:1) gave a white amorphous solid **1** (0.86 g, 87%). TLC $R_f = 0.29$ (CH₂Cl₂/CH₃OH, 10:1). $[\alpha]_D^{20} +10.2^\circ$ (c 1, CHCl₃). ¹H NMR (CDCl₃): δ (ppm) 7.68 (d, $J = 7.6$ Hz, 2H), 7.53 (m, 2H), 7.32 (m, 2H), 7.23 (m, 2H), 5.67 (m, 1H), 4.29 (m, 2H), 4.13 (m, 1H), 3.19 (m, 2H), 2.10 (tm, 2H), 1.84–1.17 (m, 16H), 0.78 (m, 3H). ¹³C NMR (CDCl₃): δ (ppm) 174.40, 143.95, 141.40, 127.90, 127.29, 125.39, 120.12, 67.15, 47.30, 39.42, 36.84, 31.94, 29.52, 29.27, 26.07, 22.84, 14.31. HRMS (MALDI) (m/z) (MNa⁺): found 517.2673. Calcd for C₂₉H₃₈N₂O₅Na 517.2678.

Fmoc-Lys(decanoyl)-OH (2). Compound **2** was submitted to the same procedure described above for the preparation of **1** and gave a white amorphous solid (yield, 78%). TLC $R_f = 0.40$ (CH₂Cl₂/CH₃OH, 8:1). $[\alpha]_D^{20} +12.0^\circ$ (c 1, CHCl₃). ¹H NMR (CDCl₃): δ (ppm) 7.67 (d, $J = 7.6$ Hz, 2H), 7.52 (m, 2H), 7.30 (m, 2H), 7.21 (m, 2H), 5.78 (d, $J = 7.6$ Hz, 1H), 4.27 (m, 2H), 4.12 (m, 1H), 3.17 (m, 1H), 2.10 (tm, 2H), 1.83–1.14 (m, 20H), 0.78 (t, $J = 7.2$ Hz, 3H). ¹³C NMR (CDCl₃): δ (ppm) 174.69, 156.64, 144.14, 143.91, 141.45, 127.94, 127.31, 125.38, 120.17, 98.99, 67.27, 66.36, 61.17, 54.04, 47.31, 39.41, 36.87, 32.26, 32.09, 29.72, 29.60, 29.53, 29.04, 26.08, 22.90, 22.54, 14.36. HRMS (MALDI) (m/z) (MNa⁺): found 545.2978. Calcd for C₃₁H₄₂N₂O₅Na 545.2991.

Fmoc-Lys(lauroyl)-OH (3). Compound **3** was submitted to the same procedure described above for the preparation of **1** and gave a white solid (yield, 64%), mp 126.0–128.0 °C. TLC $R_f = 0.76$ (CH₂Cl₂/CH₃OH, 4:1). $[\alpha]_D^{20} +14.3^\circ$ (c 1, CHCl₃). ¹H NMR (CDCl₃): δ (ppm) 7.67 (d, $J = 7.6$ Hz, 2H), 7.52 (m, 2H), 7.30 (m, 2H), 7.21 (m, 2H), 5.82–5.77 (m, 2H), 4.26–4.39 (m, 2H), 4.12 (t, $J = 7.2$ Hz, 1H), 3.17 (m, 2H), 2.09 (m, 2H), 1.83–1.35 (m, 6H), 1.48 (m, 17H), 0.79 (t, $J = 7.2$ Hz, 3H). ¹³C NMR (CDCl₃): δ (ppm) 175.11, 174.81, 156.56, 143.93, 141.49, 127.93, 127.31, 125.38, 120.18, 67.32, 53.76, 47.34, 39.36, 36.94, 32.13, 29.84, 29.72, 29.56, 29.14, 26.03, 22.91, 22.34, 14.35. HRMS (MALDI) (m/z) (MNa⁺): found 573.3299. Calcd for C₃₃H₄₆N₂O₅Na 573.3304.

Fmoc-Lys(myristoyl)-OH (4). Compound **4** was submitted to the same procedure described above for the preparation of **1** and gave a white solid (yield, 64%), mp 132.0–134.0 °C. TLC $R_f = 0.81$ (CH₂Cl₂/CH₃OH, 3:1). $[\alpha]_D^{20} +13.4^\circ$ (c 1, CHCl₃). ¹H NMR (CDCl₃): δ (ppm) 7.73 (d, $J = 7.6$ Hz, 2H), 7.59 (m, 2H), 7.37 (m, 2H), 7.27 (m, 2H), 5.97 (br, 1H), 5.79 (d, $J = 7.6$ Hz, 1H), 4.41–4.33 (m, 2H), 4.18 (t, $J = 7.6$ Hz, 1H), 3.23 (m, 2H), 2.15 (m, 2H), 1.89–1.41 (m, 6H), 1.21 (m, 22H), 0.87 (t, $J = 6.8$ Hz, 3H). ¹³C NMR (CDCl₃): δ (ppm) 175.27, 174.86, 156.58, 144.11, 143.92, 141.48, 127.94, 127.32, 125.39, 120.18, 67.37, 53.78, 47.33, 39.39, 36.91, 32.16, 29.93, 29.89, 29.75, 29.59, 29.53, 29.08, 26.06, 22.93, 22.40, 14.36. HRMS (MALDI) (m/z) (MNa⁺): found 601.3623. Calcd for C₃₅H₅₀N₂O₅Na 601.3617.

Fmoc-Lys(stearoyl)-OH (5). Compound **5** was submitted to the same procedure described above for the preparation of **1** and gave a white solid (yield, 68%), mp 133.0–135.0 °C. TLC $R_f = 0.62$ (CH₂Cl₂/CH₃OH, 5:1). $[\alpha]_D^{20} +11.8^\circ$ (c 1, CHCl₃). ¹H NMR (CDCl₃): δ (ppm) 7.68 (d, $J = 7.6$ Hz, 2H), 7.52 (m, 2H), 7.31 (m, 2H), 7.22 (m, 2H), 5.73 (d, $J = 7.2$ Hz, 1H), 4.28 (m, 2H), 4.12 (m, 1H), 3.19 (m, 2H), 2.09 (m, 2H), 1.84–1.18 (m, 37H), 0.80 (m, 3H). ¹³C NMR (CDCl₃): δ (ppm) 175.27, 174.69, 156.54,

144.13, 143.94, 141.41, 127.94, 127.31, 125.40, 120.19, 67.32, 53.75, 47.35, 39.29, 36.97, 32.15, 29.93, 29.58, 29.10, 29.19, 26.03, 22.92, 22.33, 14.35. HRMS (MALDI) (m/z) (MNa^+): found 657.4240. Calcd for $C_{39}H_{58}N_2O_5 Na$ 657.4243.

MPEG₄-acetic Acid (7). To a solution of MPEG₄-OH (2.20 g, 10.6 mmol) in THF (20 mL) was added NaH (60%, 0.635 g, 15.9 mmol) at 0 °C. The solution was stirred for 1 h at room temperature, and then ethyl bromoacetate (1.4 mL, 12.6 mmol) was added dropwise. After 16 h at 50 °C, the solution was concentrated in vacuo. The residue was hydrolyzed with 1 M LiOH (8 mL) and CH_3OH (8 mL) for 6 h at room temperature. The solution was acidified with 1 M HCl to pH 1, and then the solvents were removed under reduced pressure. The residue was purified by chromatography (CH_2Cl_2/CH_3OH , 10:1) to afford **7** (1.66 g, 59%) as a colorless oil. TLC R_f = 0.15 (CH_2Cl_2/CH_3OH , 4:1). ¹H NMR ($CDCl_3$): δ (ppm) 9.10 (br, 1H), 4.03 (s, 2H), 73.57–3.44 (m, 16H), 3.25 (s, 3H). ¹³C NMR ($CDCl_3$): δ (ppm) 172.94, 71.93, 71.09, 70.64, 70.58, 70.55, 70.51, 70.45, 68.61, 61.61, 59.02. HRMS (MALDI) (m/z) (MNa^+): found 289.1248. Calcd for $C_{11}H_{22}O_7Na$ 289.1263.

Fmoc-Lys(MPEG₄)-OH (6). To a solution of MPEG₄-acetic acid **7** (0.266 g, 1.0 mmol) and perfluorophenol (0.202 g, 1.1 mmol) in CH_2Cl_2 (5 mL) was added DCC (0.247 g, 1.2 mmol) at room temperature. After being stirred overnight, the mixture was diluted with acetone (50 mL) and filtered. The residue was dried in vacuo to give the activated ester, which was used directly in the next step. The crude oil in DMF (5 mL) was added to a solution of Fmoc-L-lysine (0.442 g, 1.2 mmol) and DIPEA (0.7 mL, 4 mmol) in DMF (10 mL) at 0 °C. The solution was stirred overnight at room temperature and then poured into brine (50 mL), extracted with CH_2Cl_2 (150 mL), and washed with 1 M HCl, brine, dried, and purified by flash chromatography (CH_2Cl_2/CH_3OH , 5:1) to afford an amorphous solid **6** (0.37 g, 60%). TLC R_f = 0.21 (CH_2Cl_2/CH_3OH , 5:1). $[\alpha]_D^{20} +19.5^\circ$ (c 3, $CHCl_3$). ¹H NMR ($CDCl_3$): δ (ppm) 7.67 (d, J = 7.2 Hz, 2H), 7.52 (m, 2H), 7.29 (m, 2H), 7.21 (m, 2H), 5.78 (d, J = 6.8 Hz, 1H), 4.29 (d, J = 6.8 Hz, 2H), 4.11 (m, 1H), 3.91 (s, 2H), 3.54–3.52 (m, 14H), 3.45–3.43 (m, 2H), 3.27 (s, 3H), 1.81–1.18 (m, 6H). ¹³C NMR ($CDCl_3$): δ (ppm) 171.04, 156.36, 144.18, 144.03, 141.48, 127.90, 127.30, 125.39, 120.15, 72.07, 71.09, 70.69, 70.61, 70.27, 67.05, 59.15, 53.92, 47.38, 38.54, 31.78, 29.91, 29.00, 22.27. HRMS (MALDI) (m/z) (MNa^+): found 639.2917. Calcd for $C_{32}H_{44}N_2O_{10}Na$ 639.2893.

Peptide Synthesis. All galanin analogues were synthesized on a Symphony peptide synthesizer (Protein Technologies Inc.) using Fmoc-based coupling protocols as previously described.²² Cleaved peptides were purified by reversed-phase HPLC using preparative HPLC column (Vydac diphenyl, 219TP1011522) and eluted with a linear gradient of acetonitrile (0.1% TFA). The flow rate was 10 mL/min, and the elution was monitored by UV detection at 220 and 280 nm. Buffer A (0.1% TFA in water) and buffer B (0.1% TFA, *v/v*, in 90% aqueous acetonitrile) were used to produce a linear gradient from 20% to 100% of buffer B over 40 min. Purified analogues were quantified by measuring UV absorbance at 279.8 nm (molar absorbance coefficient ϵ = 7000 $cm^{-1} M^{-1}$).

Partitioning Coefficient, log *D*. The log *D* values were determined on the basis of calculated capacity factors derived from HPLC retention times as previously described.²² The log *D* for five galanin analogues were determined using conventional shake-flask methods, using 400 μg of peptide reconstituted in 1 mL of phosphate buffered saline. The aqueous peptide solution was shaken with an equal volume of water-saturated octanol for 24 h. Concentration of the aqueous layer was determined by HPLC. Retention times for the analogues were determined on a linear gradient of 20–100% buffer B in 40 min, with immediate return to initial conditions and a 20 min re-equilibration. A linear correlation between log *D* and HPLC retention times gave calculated log *D* values.

Circular Dichroism. α -Helical conformation of each analogue was studied using CD as previously described.²² Peptides were reconstituted in NaF buffer to a concentration of 0.1 mg/mL.

The peptides were scanned from 250 to 200 nm, with a 1 nm step size and 1.0 s dwell time. Data were averaged from five scans.

Metabolic Stability Assay. Peptide stability was assessed in a buffered 25% rat blood serum assay as previously described.²² To 200 μL of buffered serum, 2.5 μg of peptide was added and the solution was incubated at 37 °C. Reactions were quenched at select time points upon the addition of “quenching solution” (15% trichloroacetic acid in 40% isopropanol), and the remaining amount of intact peptide was determined by HPLC.

Pharmacological Characterization. Galanin receptor binding assay and the anticonvulsant screening were carried out as previously described in detail.²² Briefly, the competitive binding assay was performed using human GalR1 and GalR2 receptor membrane preparations and europium-labeled galanin (Perkin-Elmer). Samples were incubated at room temperature for 90 min, followed by four washings with wash buffer (50 mM Tris-HCl, pH 7.5, and 5 mM $MgCl_2$) using a vacuum manifold. Enhancement solution (200 μL) was added, and the plates were incubated at room temperature for 30 min. The plates were read on a VICTOR³ spectrofluorometer. Competition binding curves were analyzed using GraphPad Prism software, using a nonlinear regression, sigmoidal dose–response (variable slope) curve with no constraints or weights, seen below:

$$y = \text{Bottom} + \frac{\text{Top} - \text{Bottom}}{1 + 10^{(\alpha - \log EC_{50})}}; \quad EC_{50} = 10^{\left[\log K_1 \left(1 + \frac{[Eu\text{-galanin}]}{K_d} \right) \right]}$$

Top and Bottom are the plateaus on the y-axis. With this model, we hold the K_1 and concentration of europium-labeled galanin constant (4.3 and 2 nM, respectively) and assume one binding site with reversible binding at equilibrium. Anticonvulsant efficacy was assessed following ip administration to five groups of CF-1 mice (n = 4 mice) at a dose of 4 mg/kg. At various times (i.e., 0.25, 0.5, 1, 2, and 4 h) after administration, mice were challenged with a 6 Hz corneal stimulation (32 mA, 3 s, 6 Hz). Mice not displaying a characteristic limbic seizure were considered protected. The percent of animals protected at each time point was plotted against time, and the AUC values were calculated with GraphPad Prism.

Acknowledgment. This work was supported in part by the Epilepsy Therapy Grants Program from the Epilepsy Research Foundation, the University of Utah Startup Funds, and the NIH Grant R21 NS059669. We thank the Anticonvulsant Screening Program (ASP) Project Officer James Stables and his group at the NIH/NINDS for their support with screening galanin analogues. Technical assistance of Dan McDougale is greatly appreciated. GB and HSW are scientific cofounders of Neuro-Adjvants, Inc.

Supporting Information Available: Tables S1 and S2 listing the purity and log *D* calculations, respectively, and Figure S1 showing the HPLC chromatograms of the galanin analogues. This material is available free of charge via the Internet at <http://pubs.acs.org>.

References

- (1) Tallent, M. K.; Qiu, C. Somatostatin: an endogenous antiepileptic. *Mol. Cell. Endocrinol.* **2008**, *286*, 96–103.
- (2) Lerner, J. T.; Sankar, R.; Mazarati, A. M. Galanin and epilepsy. *Cell. Mol. Life Sci.* **2008**, *65*, 1864–1871.
- (3) Vezzani, A.; Sperk, G.; Colmers, W. F. Neuropeptide Y: emerging evidence for a functional role in seizure modulation. *Trends Neurosci.* **1999**, *22*, 25–30.
- (4) Boules, M.; Fredrickson, P.; Richelson, E. Bioactive analogs of neurotensin: focus on CNS effects. *Peptides* **2006**, *27*, 2523–2533.
- (5) Polt, R.; Dhanasekaran, M.; Keyari, C. M. Glycosylated neuropeptides: a new vista for neuropsychopharmacology. *Med. Res. Rev.* **2005**, *25*, 557–585.
- (6) Rousselle, C.; Clair, P.; Smirnova, M.; Kolesnikov, Y.; Pasternak, G. W.; Gac-Breton, S.; Rees, A. R.; Scherrmann, J. M.; Tamsamani, J. Improved brain uptake and pharmacological activity of dalargin using a peptide-vector-mediated strategy. *J. Pharmacol. Exp. Ther.* **2003**, *306*, 371–376.

- (7) Prokai-Tatrai, K.; Prokai, L.; Bodor, N. Brain-targeted delivery of a leucine-enkephalin analogue by retrometabolic design. *J. Med. Chem.* **1996**, *39*, 4775–4782.
- (8) Elmagbari, N. O.; Egleton, R. D.; Palian, M. M.; Lowery, J. J.; Schmid, W. R.; Davis, P.; Navratilova, E.; Dhanasekaran, M.; Keyari, C. M.; Yamamura, H. I.; Porreca, F.; Hruby, V. J.; Polt, R.; Bilsky, E. J. Antinociceptive structure–activity studies with enkephalin-based opioid glycopeptides. *J. Pharmacol. Exp. Ther.* **2004**, *311*, 290–297.
- (9) Egleton, R. D.; Mitchell, S. A.; Huber, J. D.; Janders, J.; Stropova, D.; Polt, R.; Yamamura, H. I.; Hruby, V. J.; Davis, T. P. Improved bioavailability to the brain of glycosylated Met-enkephalin analogs. *Brain Res.* **2000**, *881*, 37–46.
- (10) Banks, W. A.; Schally, A. V.; Barrera, C. M.; Fasold, M. B.; Durham, D. A.; Csernus, V. J.; Groot, K.; Kastin, A. J. Permeability of the murine blood–brain barrier to some octapeptide analogs of somatostatin. *Proc. Natl. Acad. Sci. U.S.A.* **1990**, *87*, 6762–6766.
- (11) Kokko, K. P.; Hadden, M. K.; Price, K. L.; Orwig, K. S.; See, R. E.; Dix, T. A. In vivo behavioral effects of stable, receptor-selective neurotensin[8–13] analogues that cross the blood–brain barrier. *Neuropharmacology* **2005**, *48*, 417–425.
- (12) Banks, W. A.; Wustrow, D. J.; Cody, W. L.; Davis, M. D.; Kastin, A. J. Permeability of the blood–brain barrier to the neurotensin8–13 analog NT1. *Brain Res.* **1995**, *695*, 59–63.
- (13) Witt, K. A.; Gillespie, T. J.; Huber, J. D.; Egleton, R. D.; Davis, T. P. Peptide drug modifications to enhance bioavailability and blood–brain barrier permeability. *Peptides* **2001**, *22*, 2329–2343.
- (14) Egleton, R. D.; Davis, T. P. Development of neuropeptide drugs that cross the blood–brain barrier. *NeuroRx* **2005**, *2*, 44–53.
- (15) Banks, W. A. Delivery of peptides to the brain: emphasis on therapeutic development. *Biopolymers* **2008**, *90*, 589–594.
- (16) Banks, W. A.; Kastin, A. J. Peptides and the blood–brain barrier: lipophilicity as a predictor of permeability. *Brain Res. Bull.* **1985**, *15*, 287–292.
- (17) Wang, J.; Hogenkamp, D. J.; Tran, M.; Li, W. Y.; Yoshimura, R. F.; Johnstone, T. B.; Shen, W. C.; Gee, K. W. Reversible lipidization for the oral delivery of leu-enkephalin. *J. Drug Targeting* **2006**, *14*, 127–136.
- (18) Toth, I.; Malkinson, J. P.; Flinn, N. S.; Drouillard, B.; Horvath, A.; Erchegyi, J.; Idei, M.; Venetianer, A.; Artursson, P.; Lazorova, L.; Szende, B.; Keri, G. Novel lipoamino acid- and liposaccharide-based system for peptide delivery: application for oral administration of tumor-selective somatostatin analogues. *J. Med. Chem.* **1999**, *42*, 4010–4013.
- (19) Hitchcock, S. A.; Pennington, L. D. Structure–brain exposure relationships. *J. Med. Chem.* **2006**, *49*, 7559–7583.
- (20) Yuan, L.; Wang, J.; Shen, W. C. Reversible lipidization prolongs the pharmacological effect, plasma duration, and liver retention of octreotide. *Pharm. Res.* **2005**, *22*, 220–227.
- (21) Weber, S. J.; Abbruscato, T. J.; Brownson, E. A.; Lipkowski, A. W.; Polt, R.; Misicka, A.; Haaseth, R. C.; Bartosz, H.; Hruby, V. J.; Davis, T. P. Assessment of an in vitro blood–brain barrier model using several [Met5]enkephalin opioid analogs. *J. Pharmacol. Exp. Ther.* **1993**, *266*, 1649–1655.
- (22) Bulaj, G.; Green, B. R.; Lee, H. K.; Robertson, C. R.; White, K.; Zhang, L.; Sochanska, M.; Flynn, S. P.; Scholl, E. A.; Pruess, T. H.; Smith, M. D.; White, H. S. Design, synthesis, and characterization of high-affinity, systemically-active galanin analogues with potent anticonvulsant activities. *J. Med. Chem.* **2008**, *51*, 8038–8047.
- (23) Kragh-Hansen, U.; Watanabe, H.; Nakajou, K.; Iwao, Y.; Otagiri, M. Chain length-dependent binding of fatty acid anions to human serum albumin studied by site-directed mutagenesis. *J. Mol. Biol.* **2006**, *363*, 702–712.
- (24) Mazarati, A.; Lundstrom, L.; Sollenberg, U.; Shin, D.; Langel, U.; Sankar, R. Regulation of kindling epileptogenesis by hippocampal galanin type 1 and type 2 receptors: the effects of subtype-selective agonists and the role of G-protein-mediated signaling. *J. Pharmacol. Exp. Ther.* **2006**, *318*, 700–708.
- (25) Mazarati, A. M. Galanin and galanin receptors in epilepsy. *Neuropeptides* **2004**, *38*, 331–343.
- (26) Liu, H. X.; Hokfelt, T. The participation of galanin in pain processing at the spinal level. *Trends Pharmacol. Sci.* **2002**, *23*, 468–474.
- (27) Flatters, S. J.; Fox, A. J.; Dickenson, A. H. In vivo and in vitro effects of peripheral galanin on nociceptive transmission in naive and neuropathic states. *Neuroscience* **2003**, *116*, 1005–1012.
- (28) Wynick, D.; Thompson, S. W.; McMahon, S. B. The role of galanin as a multi-functional neuropeptide in the nervous system. *Curr. Opin. Pharmacol.* **2001**, *1*, 73–77.
- (29) Toth, I. A novel chemical approach to drug delivery: lipidic amino acid conjugates. *J. Drug Targeting* **1994**, *2*, 217–239.
- (30) Blanchfield, J. T.; Lew, R. A.; Smith, A. I.; Toth, I. The stability of lipidic analogues of GnRH in plasma and kidney preparations: the stereoselective release of the parent peptide. *Bioorg. Med. Chem. Lett.* **2005**, *15*, 1609–1612.
- (31) Knudsen, L. B.; Nielsen, P. F.; Huusfeldt, P. O.; Johansen, N. L.; Madsen, K.; Pedersen, F. Z.; Thogersen, H.; Wilken, M.; Agerso, H. Potent derivatives of glucagon-like peptide-1 with pharmacokinetic properties suitable for once daily administration. *J. Med. Chem.* **2000**, *43*, 1664–1669.
- (32) Havelund, S.; Plum, A.; Ribel, U.; Jonassen, I.; Volund, A.; Markussen, J.; Kurtzhals, P. The mechanism of protraction of insulin detemir, a long-acting, acylated analog of human insulin. *Pharm. Res.* **2004**, *21*, 1498–1504.
- (33) Oh, H. S.; Kim, S.; Cho, H.; Lee, K. H. Development of novel lipid–peptide hybrid compounds with antibacterial activity from natural cationic antibacterial peptides. *Bioorg. Med. Chem. Lett.* **2004**, *14*, 1109–1113.
- (34) Rivett, D. E.; Hewish, D.; Kirkpatrick, A.; Werkmeister, J. Inhibition of membrane-active peptides by fatty acid–peptide hybrids. *J. Protein Chem.* **1999**, *18*, 291–295.
- (35) Chicharro, C.; Granata, C.; Lozano, R.; Andreu, D.; Rivas, L. N-Terminal fatty acid substitution increases the leishmanicidal activity of CA(1–7)M(2–9), a cecropin–melittin hybrid peptide. *Antimicrob. Agents Chemother.* **2001**, *45*, 2441–2449.
- (36) Pignatello, R.; Puglisi, G. Lipophilicity evaluation by RP-HPLC of two homologous series of methotrexate derivatives. *Pharm. Acta Helv.* **2000**, *74*, 405–410.
- (37) Horvath, A.; Olive, C.; Wong, A.; Clair, T.; Yarwood, P.; Good, M.; Toth, I. Lipoamino acid-based adjuvant carrier system: enhanced immunogenicity of group A streptococcal peptide epitopes. *J. Med. Chem.* **2002**, *45*, 1387–1390.
- (38) Tamai, I.; Sai, Y.; Kobayashi, H.; Kamata, M.; Wakamiya, T.; Tsuji, A. Structure–internalization relationship for adsorptive-mediated endocytosis of basic peptides at the blood–brain barrier. *J. Pharmacol. Exp. Ther.* **1997**, *280*, 410–415.
- (39) Drin, G.; Cottin, S.; Blanc, E.; Rees, A. R.; Tamsamani, J. Studies on the internalization mechanism of cationic cell-penetrating peptides. *J. Biol. Chem.* **2003**, *278*, 31192–31201.

JM801397W

2.5.3 Developing Novel Antiepileptic Drugs: Characterization
of NAX 5055, a Systemically-Active Galanin Analog, in
Epilepsy Models

Manuscript Reproduced with Permission From:

White, H. S., Scholl, E. A., Klein, B. D., Flynn, S. P., Pruess, T. H., Green, B. R., Zhang, L., and Bulaj, G.. (2009) Developing novel antiepileptic drugs: Characterization of NAX 5055, a systemically-active galanin analog, in epilepsy models, *Neurotherapeutics* 6, 372-380.

© 2009 Elsevier

Developing Novel Antiepileptic Drugs: Characterization of NAX 5055, a Systemically-Active Galanin Analog, in Epilepsy Models

H. Steve White,* Erika A. Scholl,‡ Brian D. Klein,‡ Sean P. Flynn,* Timothy H. Pruess,*
Brad R. Green,† Liuyin Zhang,† and Grzegorz Bulaj†

*Department of Pharmacology and Toxicology, †Department of Medicinal Chemistry, College of Pharmacy, University of Utah, Salt Lake City, Utah 84108, ‡NeuroAdjuvants, Inc., Salt Lake City, Utah, 84108

Summary: The endogenous neuropeptide galanin and its associated receptors galanin receptor 1 and galanin receptor 2 are highly localized in brain limbic structures and play an important role in the control of seizures in animal epilepsy models. As such, galanin receptors provide an attractive target for the development of novel anticonvulsant drugs. Our efforts to engineer galanin analogs that can penetrate the blood-brain-barrier and suppress seizures, yielded NAX 5055 (Gal-B2), a systemically-active analog that maintains low nanomolar affinity for galanin receptors and displays a potent anticonvulsant activity. In this report, we show that NAX 5055 is active in three models of epilepsy: 1) the Frings audiogenic seizure-susceptible mouse, 2) the mouse corneal kindling model of partial epilepsy, and 3) the 6 Hz model of pharmacoresistant

epilepsy. NAX 5055 was not active in the traditional maximal electroshock and subcutaneous pentylenetetrazol seizure models. Unlike most antiepileptic drugs, NAX 5055 showed high potency in the 6 Hz model of epilepsy across all three different stimulation currents; i.e., 22, 32 and 44 mA, suggesting a potential use in the treatment of pharmacoresistant epilepsy. Furthermore, NAX 5055 was found to be biologically active after intravenous, intraperitoneal, and subcutaneous administration, and efficacy was associated with a linear pharmacokinetic profile. The results of the present investigation suggest that NAX 5055 is a first-in-class neurotherapeutic for the treatment of epilepsy in patients refractory to currently approved antiepileptic drugs. **Key Words:** Neuropeptide, anticonvulsant drug, audiogenic seizures, 6 Hz seizure, corneal kindled mouse.

INTRODUCTION

It is estimated that there are 50 to 60 million people with epilepsy worldwide. Epilepsy affects approximately 3 million people in the United States alone. Each year, 125,000 new cases are diagnosed. Unfortunately, only 70% of patients are effectively treated with currently available antiepileptic drugs (AEDs). For a substantial number of patients with epilepsy, the currently available therapies are often not effective in controlling their symptoms. As such, there is a substantial need for more effective therapies.

Neuropeptides are potent modulators of neuronal excitability.^{1,2} Under ambient conditions, peptides are “silent” and exert little effect on normal neurotransmission. However, under conditions of excessively high neuronal

firing (i.e., epileptic seizures), neuropeptides are released and exert a modulatory effect on neurotransmission. Unlike small molecule neurotransmitters, neuropeptides are released distal to the synaptic cleft and their action is limited by diffusion and enzymatic degradation, instead of being eliminated by reuptake or rapid degradation. Unlike classical neurotransmitters, the action of neuropeptides is slow, sustained, and can extend beyond the synaptic region.³ One such neuropeptide is galanin and it has been implicated in such diverse behaviors as sleep, feeding, reproduction, nociception, and cognition. Galanin is found along with many neurotransmitters, including glutamate, gamma-aminobutyric acid (GABA), acetylcholine, norepinephrine, serotonin, dopamine and histamine, suggesting it has many roles in the brain.^{4,5} Galanin, which can be found both centrally and peripherally, is highly expressed along with the galanin receptor 1 (GalR1) in the hippocampus, a plastic structure highly susceptible to seizure activity.

Address correspondence and reprint requests to: H. Steve White, Ph.D., Anticonvulsant Drug Development Program, Department of Pharmacology and Toxicology, 417 Wakara Way, Suite 3211, Salt Lake City, Utah 84108. E-mail: swhite@hsc.utah.edu.

There have been numerous studies linking galanin to seizure activity. Expression levels of galanin and its receptors change in response to, or as a result of, seizures.⁶ For example, galanin levels and galanin receptor 2 (GalR2) are decreased after status epilepticus. Since the work of Mazarati and coworkers,⁷ there has been increasing evidence that galanin is a potent anticonvulsant peptide. Previous investigations have demonstrated that galanin and galanin agonists, when delivered directly to the brain, possess anticonvulsant properties.^{8,9} Moreover, the acute administration of galanin receptor agonists or virus-mediated overexpression of galanin in the hippocampus has been found to inhibit limbic status epilepticus, pentylenetetrazol-induced, and picrotoxin-induced seizures in rats and mice.^{7,8,10} Furthermore, several reports have suggested that centrally administered galanin may modify the damage associated with limbic seizures and delay or prevent the development of epilepsy (i.e., disease modifying). Kokaia et al.¹¹ reported delayed kindling in galanin peptide overexpressing mice. Furthermore, results from studies with GalR1 knockout mice and rats treated with antisense GalR2 oligonucleotides suggests that galanin exerts its anticonvulsant effect through an action at both GalR1 and GalR2.^{12,13}

Previous attempts to pharmacologically target the galanin system have been plagued by the finding that peptides are generally not metabolically stable and do not readily penetrate the blood-brain-barrier (BBB). Two galanin-based agonists, i.e., galmic and galnon, that possess anticonvulsant activity have been reported in the literature.^{14,15} However, these compounds show little receptor subtype specificity (2- to 3-fold difference in affinity for GalR1 and GalR2), and they have a 10,000- to 100,000-fold lower affinity for galanin receptors relative to the native peptide (FIG. 1). Furthermore, significant off-target activities have been described for both galmic and galnon.¹⁶

In the present investigation we describe the anticonvulsant actions and pharmacological profile of the novel BBB permeable galanin analog NAX 5055 (Gal-B2) which is bioavailable, metabolically stable, and retains nanomolar affinity and selectivity for galanin receptors.¹⁷ Previously published results from our laboratory have described in detail the physicochemical properties of this and other galanin analogs. Here we describe the activity of NAX 5055 in various animal seizure and epilepsy models, and we discuss its pharmacokinetic profile and systemic bioavailability. In addition, our results demonstrate that the anticonvulsant activity of this modified peptide is specific for the intact structure of NAX 5055.

MATERIALS AND METHODS

Peptide synthesis

NAX 5055 and two galanin analogs (a truncated and a scrambled peptide) were chemically synthesized using identical methods as previously described.¹⁷ Briefly, the

peptides were assembled on solid support using the Fmoc protocol and an automated peptide synthesizer. The analogs were cleaved from the resin by a treatment with reagent K and purified using reverse-phase high performance liquid chromatography (HPLC) separations. Chemical identities of the analogs were confirmed by mass spectroscopy analyses.

Animals and test substances

Male albino CF-1 mice (18 to 25 g; Charles River, Portage, MI) and male and female Frings audiogenic seizure (AGS)-susceptible mice (20 to 30 g; obtained from an in-house colony at the University of Utah) were used as experimental animals. All animals were allowed free access to both food (LabDiet, Richmond, IN) and water except when they were removed from their cages for the experimental procedure. All mice were housed, fed, and handled in a manner consistent with the recommendations in the National Research Council Publication, "Guide for the Care and Use of Laboratory Animals." No insecticides capable of altering hepatic drug metabolism enzymes were used in the animal facilities. Except for corneal kindling studies, animals were used once. All animals were euthanized in accordance with the Institute of Laboratory Resources policies on the humane care of laboratory animals.

NAX 5055 was administered in 0.9% saline intravenously (i.v.), intraperitoneally (i.p.), subcutaneously (s.c.), or orally (p.o.) in a volume of 0.01 mL/g body weight.

Anticonvulsant tests

The anticonvulsant activity of NAX 5055 was established by both electrical and chemical tests. The electrical tests used were the maximal electroshock seizure, the 6 Hz psychomotor seizure, and the corneal kindled mouse.¹⁸⁻²⁰ The chemical tests included the s.c. pentylenetetrazol (PTZ) seizure.¹⁸

Maximal electroshock and 6 Hz tests. For the maximal electroshock and 6 Hz tests, a drop of anesthetic/electrolyte solution (0.5% tetracaine hydrochloride in 0.9% saline) was applied to the eyes of each animal prior to placement of the corneal electrodes. The electrical stimulus in the maximal electroshock test was 50 mA, 60 Hz delivered for 0.2 sec by an apparatus similar to that originally described by Woodbury and Davenport.²¹ Elimination of the hind leg tonic extensor component of the seizure was used as the endpoint.

The ability of the test substance to prevent seizures induced by 6 Hz corneal stimulation (6 Hz, 0.2 msec rectangular pulse width, 3 sec duration) was evaluated at convulsive currents (CC) of 22, 32, and 44 mA. The current was delivered with a Grass S48 stimulator (Grass Technologies, West Warwick, RI). Six Hz seizures are characterized by a minimal clonic phase that is followed by stereotyped automatic behaviors, originally described as being similar to the aura of human patients

Table 1. Anticonvulsant Profile of NAX 5055

| Seizure Model | ED ₅₀ (mg/kg i.p.) | Protective Index* |
|-------------------------|----------------------------------|----------------------|
| Corneal kindling | 0.65 | ~30 |
| Audiogenic seizures | 3.2 | ~7 |
| Maximal electroshock | Inactive at 20 mg/kg | <1 |
| Pentylenetetrazol, s.c. | 25% at 20 mg/kg | <1 |

s.c. = subcutaneous injection.

*Toxic dose 50 (21 mg/kg)/ED₅₀.

with partial seizures.^{19,22} Animals not displaying this behavior were considered protected.

Corneal kindling. NAX 5055 was evaluated for its ability to block the fully expressed corneal kindled seizure. Individual mice were corneal kindled according to the procedures established by Matagne and Klitgaard.²³ Briefly, each mouse received a twice daily corneal stimulation of 3 mA for 3 s Monday through Friday. Prior to each of the stimulations, a drop of 0.5% tetracaine was applied to the cornea of each mouse. The kindling procedure was continued until each mouse displayed at least

five consecutive secondarily generalized seizures (i.e., stage 4 to 5 seizures according to the Racine scale).²⁴ On the day of the experiment, fully kindled mice were treated i.p. with NAX 5055. One h after NAX 5055 administration, the mice were challenged with the same current stimulus used to kindle them (i.e., 3 mA for 3 sec). Mice not displaying a prototypical seizure were considered protected.

Pentylenetetrazol (PTZ)-induced seizures. NAX 5055 was evaluated for its ability to block a minimal 3-s episode of a clonic seizure induced by 85 mg/kg PTZ (dissolved in 0.9% saline) administered s.c. into a loose fold on the back of the neck. Animals were observed for at least 30 min for the presence or absence of a seizure.

Audiogenic seizures. NAX 5055 was tested for its ability to block AGS in the Frings AGS-susceptible mouse after i.p. administration. At the previously determined time-to-peak effect (TPE), individual male and female Frings mice were placed into a plastic cylinder (diameter, 15 cm; height, 18 cm) fitted with an audio transducer (Model AS-ZC; FET Research and Development, Salt Lake City, UT) and exposed to a sound stim-

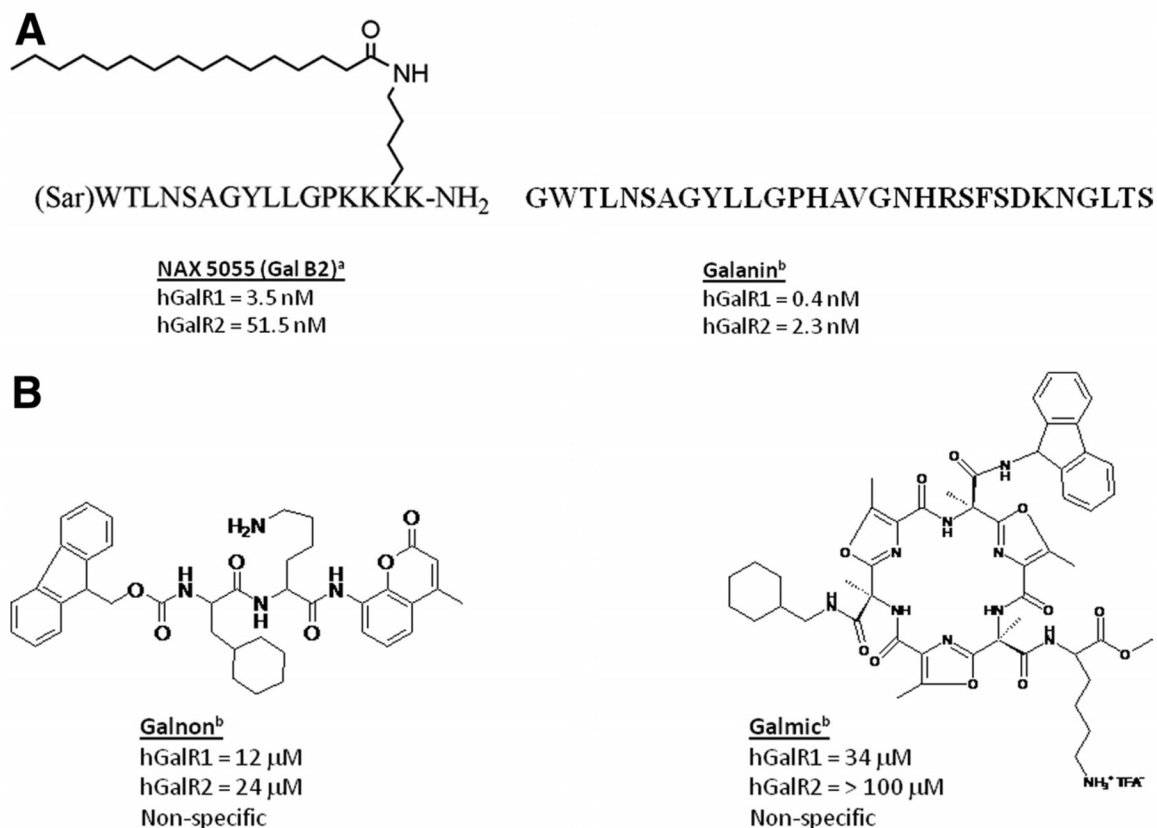


FIG. 1. Structures of selected galanin ligands and their affinities to the human (h)-galanin receptor 1 and h-galanin receptor 2 receptors. A: The peptides NAX 5055 (Gal B2) and galanin. B: Two small molecule galanin agonists (galnon and galmic). ^aPreviously reported Ki

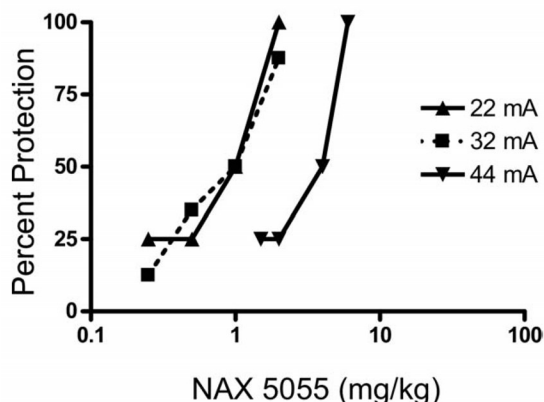


FIG. 2. NAX 5055 maintains potent anticonvulsant activity in the mouse 6 Hz seizure model with increasing stimulation intensities (22 mA, 32 mA, and 44 mA). Bolus injections of NAX 5055 were administered intraperitoneally and dose-response data were generated at the 1 h time point (time-to-peak effect). Based on these results, ED_{50} values were calculated as 0.7 mg/kg for 22 mA, 0.8 mA for 32 mA, and 2.9 mg/kg for 44 mA stimulations.

ulus of 110 decibels (11 KHz) delivered for 20 s. A sound-induced AGS is characterized by wild running followed by loss of righting reflex with forelimb and hind limb tonic extension. Mice not displaying hind limb tonic extension were considered protected.

Minimal toxicity tests

Minimal toxicity was identified in mice by the rotarod procedure.²⁵ When a mouse is placed on a 1-inch knurled rod that rotates at a speed of 6 rpm, the animal can maintain its equilibrium for long periods of time. Mice were considered toxic if they fell off this rotating rod three times during a 1-min period. In addition, individual mice were observed for the presence or absence of ataxia, abnormal gait, somnolence, and other signs of acute toxicity. Also, the effect of NAX 5055 on core body temperature was evaluated at various times after i.p. administration of 4 mg/kg.

Determination of median effective dose (ED_{50}) or toxic dose (TD_{50})

All quantitative *in vivo* anticonvulsant/toxicity studies were conducted at the time-to-peak effect after i.v., i.p., s.c., and p.o. administration. Groups of at least eight mice were tested with various doses of NAX 5055 until at least two points were established between the limits of 100% protection or maximal toxicity and 0% protection or minimal toxicity. The dose of NAX 5055 required to produce the desired endpoint in 50% of animals (ED_{50}) or toxic dose 50 and the 95% confidence intervals were then calculated by a computer program based on the method described by Finney.²⁶

Pharmacokinetics

To determine the plasma levels of NAX 5055, trunk blood was collected at appropriate time points into hep-

arin-coated tubes and centrifuged for 3 min at 5,000 rpm. Plasma samples were then collected, immediately frozen on dry ice and stored in a -80°C freezer. Prior to the liquid chromatography/mass spectrometry (LC/MS) analysis, 50 μL of plasma samples were transferred to 96-well plates, diluted with 50 μL of 5% formic acid in water, mixed by vortexing for 1 min, followed by the addition of 600 μL acetonitrile. Diluted samples were mixed by vortexing for 1 min, centrifuged at 3,000 rpm for 3 min, and the resulting supernatant was transferred to a clean 96-well plate. Samples were dried under nitrogen in the Turbovap, and then reconstituted with 300 μL of 0.1% formic acid in 20% acetonitrile in aqueous solution. To produce the standard curve, the plasma samples from untreated mice were spiked with known amounts of NAX 5055. Samples were separated by reversed-phase HPLC (Shimadzu SCL-10A controller with LC-10AD pump; Shimadzu Scientific Instruments, Columbia, MD), using a C_{18} column (Varian Metasil, AQ C18, 50×2 mm; Varian, Inc, Palo Alto, CA), a linear gradient of acetonitrile in 0.2% formic acid and a flow rate of 0.5 mL/min. The separations were monitored by electrospray ionization mass spectrometry (API 5000) in the positive ion ionization mode. The standard curve was linear within the range of 12.5 ng/mL to 20,000 ng/mL.

RESULTS

Anticonvulsant profile

The results obtained with NAX 5055 in a battery of well-established anticonvulsant tests are summarized in

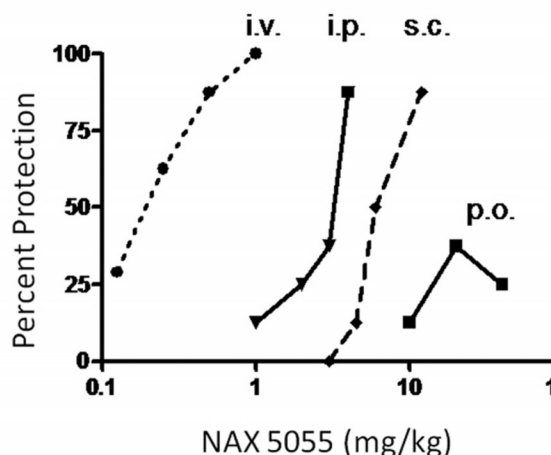


FIG. 3. Bioavailability of NAX 5055 after several routes of systemic administration. NAX 5055 was administered intravenously (i.v.), intraperitoneally (i.p.), subcutaneously (s.c.), and orally (p.o.) in CF-1 mice. Dose-response data were generated at the following time points for each route of administration 1 h (i.v., i.p., and s.c.) and 2 hr (p.o.).

Table 2. Comparative Anticonvulsant Activity of NAX 5055 and Several Control Analogs (e.g. Gal[1-16], "Scrambled" and "Truncated") in the 6 Hz (32 mA) Model of Epilepsy in CF-1 Mice

| Analog | Structure | Dose (4 mg/kg, i.p.) | | | | |
|--------------------|----------------------------------|----------------------|-----|-----|------|------|
| | | 15' | 30' | 60' | 120' | 240' |
| Galanin (1-16)* | GWTLNSAGYLLGPHAV-NH ₂ | 0/4 | 0/4 | 0/4 | 0/4 | 0/4 |
| NAX 5055* | (Sar)WTLNSAGYLLGPKK(Lys-P)K | 3/4 | 4/4 | 4/4 | 4/4 | 0/4 |
| NAX 5055 scrambled | (Sar)YTLLSAGWLLGPKK(Lys-P)K | 0/4 | 0/4 | 0/4 | 0/4 | 0/4 |
| NAX 5055 truncated | Ac-YLLGPKK(Lys-P)K | 0/4 | 0/4 | 0/4 | 0/4 | 1/4 |

Values shown represent a number of mice protected from seizures in groups of four mice per time point. Note that Trp2, Asn5, and Tyr9 are critical residues for binding to the galanin receptors. Any modifications or replacement of these amino acid residues results in a loss of the affinity to the galanin receptors.^{42,43} Sar = sarcosine; Lys-P = lipo-amino acid; Lysine = palmitoyl.

*Values reported previously from Bulaj et al.¹⁷ 2008.

Table 1 and FIGS. 2 and 3. The anticonvulsant activity of NAX 5055 was initially defined in the Frings AGS-susceptible mouse model of reflex epilepsy after i.p. administration of 4 mg/kg. At various times after i.p. administration, each mouse was placed into a cylindrical test chamber fitted with an audio transducer and challenged with a high-intensity sound stimulus. The results obtained from this study demonstrate that NAX 5055 displays a time-dependent anticonvulsant effect with a time-to-peak effect of 1 h. The ED₅₀ for protection against sound-induced seizures was determined to be 3.2 mg/kg, i.p. (Table 1).

After i.p. administration, NAX 5055 was found to be highly potent against acute psychomotor seizures induced by 6 Hz corneal stimulation, regardless of the stimulus intensity used (FIG. 2). For example, ED₅₀s determined at the i.p. time-to-peak effect against 6 Hz seizures induced at 22, 32, and 44 mA were 0.7, 0.8, and 2.9 mg/kg, respectively.

NAX 5055 was also extremely potent against the fully expressed secondarily generalized seizure in the mouse corneal kindling model of partial seizures (ED₅₀: 0.65 mg/kg; Table 1). In this test, NAX 5055 reduced the seizure severity from an average Racine score of 5 to < 1 at the highest dose evaluated (i.e., 6 mg/kg, i.p.).

In an effort to determine the relative bioavailability of NAX 5055, it was administered by i.v., i.p., s.c., and p.o. routes in the 32 mA 6 Hz seizure model. The rank order of potency was i.v. > i.p. > s.c. > p.o. (FIG. 3). When compared with the i.p. route, NAX 5055 was approximately 7 times more potent after i.v. administration and approximately 3-fold less potent after s.c. administration (ED₅₀s: 0.25, 1.8, and 7.8 mg/kg, respectively). NAX 5055 was not fully efficacious after p.o. administration. As shown in FIG. 3, a maximum of 37.5% protection was observed at a dose of 20 mg/kg, p.o. Moreover, increasing the dose to 40 mg/kg, p.o. resulted in a slightly lower level of protection (25%).

In contrast to the modified galanin-based analog NAX 5055, the unmodified native peptide galanin (1-16) was inactive at a dose of 4 mg/kg, i.p. when tested at a current

intensity of 32 mA (Table 2). Previously we have demonstrated that the native peptide fragment was active when it was administered directly to the brain via intracerebroventricular administration.¹⁷ Two NAX 5055 analogs, scrambled and truncated, were also inactive in this model when tested across time at a dose of 4 mg/kg, i.p. (Table 2). These two analogs had critical residues for the galanin receptor binding either exchanged (NAX 5055 scrambled) or removed (NAX 5055 truncated). Collectively, these results suggest that anticonvulsant activity of NAX 5055 is dependent on penetration of the BBB and selectivity for the target GalR1 receptor.

Pharmacokinetics

To assess the pharmacokinetic profile of NAX 5055, plasma levels of the galanin analog were determined in mice at different time points after bolus i.p. administration. As illustrated in FIG. 4A, detectable plasma levels of NAX 5055 were observed after 15 min post-drug administration (2 mg/kg) and peaked at 1 hour. Based on a time course of disappearance of NAX 5055, the half-life was estimated to be 120 minutes. As shown in FIG. 4B, the time-dependent protection against seizures in the 32 mA 6 Hz model was correlated with NAX 5055 plasma levels. In addition, NAX 5055 displayed linear pharmacokinetics between 0.1 mg/kg to 4 mg/kg. Full protection of animals from seizures was obtained with plasma levels of 4,500 ng/mL.

DISCUSSION

The goal of the present study was to extend the pharmacological profile of NAX 5055 in epilepsy models. We previously showed that NAX 5055 was active in the 32 mA 6 Hz model of refractory epilepsy.¹⁷ The present study demonstrated that NAX 5055 retained its potency in the 6 Hz test across all stimulation intensities (22 mA to 44 mA). The ED₅₀ value at each stimulation intensity was well below the dose producing motor impairment in mice. These results are in contrast with those for several other marketed AEDs which show a significant loss of

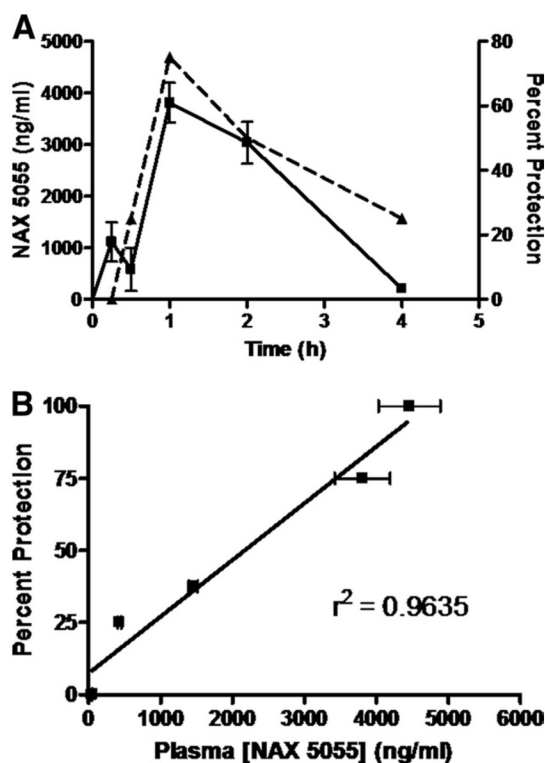


FIG. 4. Pharmacokinetic analysis of NAX 5055 in CF-1 mice. A: time-dependent changes of NAX 5055 (solid line) after a bolus intraperitoneal administration of 2 mg/kg dose. Dash line represents a time response of NAX 5055 at the same dose in protecting mice from seizures in the 6 Hz (32 mA) seizure model. B: A linear correlation between plasma levels of NAX 5055 and percent of seizure protection at doses 0.1, 0.25, 0.5, 2, and 4 mg/kg. Plasma levels were determined at 1 h after the administration of NAX 5055.

potency or become inactive in the 6 Hz test at higher stimulation intensities (Table 3). In addition to the 6 Hz model, NAX 5055 was found to be a potent blocker of secondarily generalized seizures in the corneal kindled mouse. NAX 5055 was also effective in controlling sound-induced motor seizures in Frings audiogenic mice. However, NAX 5055 was not active in the mouse maximal electroshock test and was only minimally active in the s.c. PTZ at high dose. We previously showed that NAX 5055 binds the GalR1 and GalR2 receptors,¹⁷ and the antiepileptic effects for NAX 5055 observed in this study do not appear to be mediated by the chemical modifications to the analog. Neither the scrambled nor truncated peptides showed antiepileptic activity when evaluated in the 6 Hz test.

These study results revealed that NAX 5055 was active after several routes of systemic administration (i.v., i.p., s.c. and p.o.) and possesses predictable pharmacokinetic properties. It was most potent with i.v. administration and only weakly active after oral administration.

One hour after i.p. administration there was a linear correlation between antiepileptic activity and measured plasma concentration. The time-course of activity in the 6 Hz test also tracked closely with measured plasma levels of the compound. Behavioral activity was apparent at 15 minutes with measurable plasma levels and declined after 2 hours, which is near the half-time for measured plasma levels.

Galanin and its receptors have been validated as antiepileptic therapeutic targets using genetic and pharmacological tools.^{27–29} Galanin immunoreactivity in the hippocampus is highest in the dentate gyrus, which receives excitatory innervations from the entorhinal cortex. The entorhinal cortex-dentate gyrus fiber tract is also known as the perforant pathway, which can be stimulated to evoke seizure activity.³⁰ The Gal-R1 and Gal-R2 subtypes are both expressed in the hippocampus and are believed to contribute to different components of seizure generation and epileptogenesis.³¹ There is obviously great therapeutic potential in the targeting of these two receptors. Compounds active at the galanin receptors that also penetrate the BBB have been previously synthesized. Galnon and galmic are nonpeptide small molecules, and both can be administered systemically to inhibit seizures in animal models of PTZ-stimulated and perforant path-stimulated seizures.^{32,33} However, these compounds have had limited value due to low binding affinity and the lack of receptor subtype discrimination. Our efforts have instead been directed toward making a galanin peptide analog that not only can penetrate the BBB and remain metabolically stable, but can also retain nanomolar affinity. We have shown that by using a combination of lipidization and cationization on the galanin backbone, these goals can be achieved.¹⁷ Furthermore, we have been able to engineer GalR1 or GalR2 selectivity into these galanin analogs. In this article we demonstrate the functionality of one compound, NAX 5055, in halting the seizure activity in particular forms of evoked seizures.

As previously summarized, NAX 5055 is not active in the maximal electroshock and subcutaneous PTZ tests. In this regard, the anticonvulsant profile of NAX 5055 is very much like that of the SV2a modulator levetiracetam, which is also inactive in these two acute seizure models.^{34,35} It is also important to note that NAX 5055, unlike the two previously described small molecule galanin agonists (galnon and galmic), is not effective against PTZ-induced seizures. This apparent discrepancy in anticonvulsant profile is likely due to the low μ M affinity of galnon and galmic for galanin receptors and their reported off-target actions. For example, at 10 μ M, both galnon and galmic interact with a variety of nongalanin receptors, including 5-HT-1A and 5-HT-1B receptors, D2 dopamine receptors, ghrelin and melanocortin receptors, NPY receptors (galnon only), or μ -opioid re-

Table 3. Anticonvulsant Profile of NAX 5055 Compared with Other Antiepileptic Drugs in the 6 Hz Model

| AED | ED ₅₀ , mg/kg, i.p. (95% confidence interval) | | |
|----------------------------|--|----------------------------|---------------------------|
| | Stimulation Intensity | | |
| | 22 mA | 32 mA | 44 mA |
| NAX 5055 | 0.7 (0.4–1.2) PI* = 30 | 0.8 (0.4–1.6) PI = 26.3 | 2.9 (1.9–4.3) PI = 7.2 |
| Valproic acid [†] | 41.5 (16.1–68.8) PI = 11.6 | 126 (94.5–152) PI = 3.8 | 310 (258–335) PI = 1.6 |
| Levetiracetam [†] | 4.6 (1.1–8.7) PI > 217 | 19.4 (9.9–36.0) PI > 51 | 1089 (787–2650) PI ≥ 1 |
| Ethosuximide [†] | 86.9 (37.8–156) PI = 3.7 | 167 (114–223) PI = 1.9 | >600 PI < 0.6 |
| Phenytoin [†] | 9.4 (4.7–14.9) PI = 4.6 | >60 PI < 0.7 | >60 PI < 0.7 |
| Lamotrigine [†] | 4.4 (2.2–6.6) PI = 6.8 | >60 PI < 0.5 | >60 PI < 0.5 |
| Lacosamide [‡] | — | 9.9 (7.7–12.8) PI = 2.7 | — |

AED = antiepileptic drug; i.p. = intraperitoneal injection; PI = protective index.

*Toxic dose 50 value for motor impairment/ED₅₀ value.

[†]Barton et al., 2001.¹⁹

[‡]Stöhr et al., 2007.⁴⁴

ceptors (galmic only). Activities at one or more of these nongalanergic targets likely contribute to their efficacy in the PTZ test. Thus, the primary limitation of these first generation galanin agonists is that they are both nonselective, low affinity molecules that can interact with other pharmacological targets.¹⁶ In this respect, high affinity and receptor selectivity of NAX 5055 for galanin receptors provides two distinct advantages in comparison with currently available galanin agonists for dissecting the role of galanin receptors in epilepsy and other CNS disorders.

In the present investigation, NAX 5055 was uniquely active in the 6 Hz psychomotor seizure test. Interestingly, the pharmacological profile of the 6 Hz model is somewhat dependent on the intensity of the stimulation (Table 3). For example, a convulsive current (CC) of 22 mA is sufficient to induce a prototypical seizure in 97% of the population tested (i.e., the CC₉₇), the 6 Hz seizure test is relatively nondiscriminating (that is, the large majority of AEDs evaluated (phenytoin, lamotrigine, ethosuximide, levetiracetam, and valproic acid) and are effective in blocking the acute seizure. As the current intensity is increased to a level that is 1.5 times the CC₉₇ (32 mA), several of the AEDs lose their ability to protect against a 6 Hz seizure. At a current equivalent to two times the CC₉₇ (i.e., 44 mA), only valproic acid and levetiracetam retained their ability to block 6 Hz seizures; albeit, the potency of both drugs at two times the CC₉₇ was markedly reduced. Given the pharmacological profile of this model, it has evolved as a unique model for differentiating the potential anticonvulsant compounds that might be useful for the treatment of refractory partial

epilepsy. In this regard, the results obtained in this study suggest that NAX 5055 may provide some advantages over other available AEDs. Among the various AEDs that have been evaluated in the 6 Hz model, NAX 5055 is extremely potent after i.p. administration (Table 3). Moreover, it retained excellent efficacy at all three stimulus currents evaluated. Unlike the sodium channel blockers phenytoin, carbamazepine, and lamotrigine, the SV2A modulator levetiracetam and the broad-spectrum AED valproic acid, the potency of NAX 5055 was largely retained as the stimulus intensity was increased from 22 to 44 mA. It is also of interest to note that among the various AEDs evaluated in this model, NAX 5055 was the most potent at all three stimulus intensities.

NAX 5055 was also shown to be highly efficacious and potent in a rodent model believed to mimic temporal lobe epilepsy, the most common type of epilepsy in adult humans.^{36,37} The pharmacology of the corneal kindled mouse model is very consistent with that observed in more traditional electrical kindling models, such as the hippocampal kindled rat (Rowley et al., manuscript in preparation). For example, lamotrigine, carbamazepine, and valproic acid are all active in this model at doses of 9.9, 33, and 121 mg/kg, i.p. Phenytoin is not active at doses that produce marked motor impairment (i.e., > 50 mg/kg, i.p.). NAX 5055 decreased the seizure severity in a dose-dependent manner at doses well below those that produced behavioral toxicity (ED₅₀; 0.65 mg/kg, i.p.). Thus, NAX 5055 is at least one order of magnitude more potent in this model than several of the established AEDs. It is also important to note that activity of NAX 5055 in the corneal kindled mouse is an activity that it

shares with the SV2A modulator levetiracetam.²⁰ This finding further supports the potential therapeutic use of galanin-based therapeutics for the symptomatic treatment of partial epilepsy.

Because galanin plays a role in pleiotropic neurological functions, including seizure control, epileptogenesis, antinociception, neuroprotection, and neurotrophic activities, NAX 5055 represents a drug prototype that may have broad clinical applications. First, the potent antiepileptic activity of NAX 5055 in the pharmacoresistant model of epilepsy makes this class of analogs drug candidates for treatment of refractory seizures. As a potential first-in-class therapeutic, NAX 5055 or its analogs will have to be carefully evaluated for their long-term toxicity, safety, and tolerance before entering the clinical development stage. Antiepileptogenic and neuroprotective actions of galanin may also be retained in NAX 5055, but more studies are needed to evaluate these beneficial aspects of galanin-based antiepileptic therapy. Second, GalR1 and GalR2 selective agonists also display anxiolytic activity, thus applications of NAX 5055 may extend to controlling anxiety and modulating mood disorders.³⁸ Third, the potential of NAX 5055 as an analgesic is also apparent: numerous studies have demonstrated a role of galanin in neuropathic pain.^{39–41} Our results indeed suggest that NAX 5055 is an effective analgesic in various animal pain models (Adkins-Scholl et al, manuscript in preparation). Given the broad spectrum bioavailability of NAX 5055, various routes of administration (ranging from subcutaneous depo-formulations to a rapid intranasal delivery) may facilitate multiple clinical applications. Current efforts of our research group are focused on selecting optimal therapeutic indications for NAX 5055 analogs to enter clinical development.

Disclosure

G. B. and H. S. W. are scientific co-founders of NeuroAdjuvants, Inc.

Acknowledgments: This work was supported in part by the Epilepsy Therapy Grants Program from the Epilepsy Research Foundation, the University of Utah Startup Funds, the University of Utah Research Foundation, and NIH grant R21 NS059669 (GB and HSW). We thank the Anticonvulsant Screening Program (ASP) Project Officer, James Stables, and his group at the National Institutes of Health, National Institute of Neurological Disorders and Stroke for their support of the galanin project. We also thank Dan McDougale for his help with purification of the galanin analogs.

REFERENCES

- Baraban SC, Tallent MK. Interneuron diversity series: interneuronal neuropeptides—endogenous regulators of neuronal excitability. *Trends Neurosci* 2004;27:135–142.
- Hökfelt T, Broberger C, Xu ZQ, Sergeev V, Ubink R, Diez M. Neuropeptides—an overview. *Neuropharmacology* 2000;39:1337–1356.
- Waxham N. Neuropeptides and nitric oxide. In: Byrne JH, ed. *Neuroscience Online*, 2007. Available at: <http://neuroscience.uth.tmc.edu>. Accessed July 15, 2007.
- Gundlach AL, Jungnickel R-F. Galanin and GALP systems in brain - molecular pharmacology, anatomy, and putative roles in physiology and pathology. In: Kastin AJ, ed. *Handbook of biologically active peptides*. Amsterdam: Elsevier, 2006:753–761.
- Hawes JJ, Picciotto MR. Characterization of GalR1, GalR2, and GalR3 immunoreactivity in catecholaminergic nuclei of the mouse brain. *J Comp Neurol* 2004;479:410–423.
- Gorter JA, van Vliet EA, Aronica E, et al. Potential new antiepileptogenic targets indicated by microarray analysis in a rat model for temporal lobe epilepsy. *J Neurosci* 2006;26:11083–11110.
- Mazarati AM, Halaszi E, Telegdy G. Anticonvulsive effects of galanin administered into the central nervous system upon the picrotoxin-kindled seizure syndrome in rats. *Brain Res* 1992;589:164–166.
- Gu XL, Sun YG, Yu LC. Involvement of galanin in nociceptive regulation in the arcuate nucleus of hypothalamus in rats with mononeuropathy. *Behav Brain Res* 2007;179:331–335.
- Kanter-Schlifke I, Toft Sørensen A, Ledri M, Kuteeva E, Hökfelt T, Kokaia M. Galanin gene transfer curtails generalized seizures in kindled rats without altering hippocampal synaptic plasticity. *Neuroscience* 2007;150:984–992.
- Wynick D, Bacon A. Targeted disruption of galanin: new insights from knock-out studies. *Neuropeptides* 2002;36:132–144.
- Kokaia M, Holmberg K, Nanobashvili A, et al. Suppressed kindling epileptogenesis in mice with ectopic overexpression of galanin. *Proc Natl Acad Sci U S A* 2001;98:14006–14011.
- Liu HX, Brumovsky P, Schmidt R, et al. Receptor subtype-specific pronociceptive and analgesic actions of galanin in the spinal cord: selective actions via GalR1 and GalR2 receptors. *Proc Natl Acad Sci U S A* 2001;98:9960–9964.
- Mahoney SA, Hosking R, Farrant S, et al. The second galanin receptor GalR2 plays a key role in neurite outgrowth from adult sensory neurons. *J Neurosci* 2003;23:416–421.
- Branchek TA, Smith KE, Gerald C, Walker MW. Galanin receptor subtypes. *Trends Pharmacol Sci* 2000;21:109–117.
- Lundstrom L, Elmquist A, Bartfai T, Langel U. Galanin and its receptors in neurological disorders. *Neuromolecular Med* 2005;7:157–180.
- Lu X, Lundstrom L, Langel U, Bartfai T. Galanin receptor ligands. *Neuropeptides* 2005;39:143–146.
- Bulaj G, Green BR, Lee H-K, et al. Design, synthesis and characterization of high-affinity, systemically-active galanin analogs with potent anticonvulsant activities. *J Med Chem* 2008;51:8038–8047.
- White HS, Watson WP, Hansen SL, et al. First demonstration of a functional role for central nervous system betaine/[gamma]-aminobutyric acid transporter (mGAT2) based on synergistic anticonvulsant action among inhibitors of mGAT1 and mGAT2. *J Pharmacol Exp Ther* 2005;312:866–874.
- Barton ME, Klein BD, Wolf HH, White HS. Pharmacological characterization of the 6 Hz psychomotor seizure model of partial epilepsy. *Epilepsy Res* 2001;47:217–227.
- Matagne A, Klitgaard H. Validation of corneally kindled mice: a sensitive screening model for partial epilepsy in man. *Epilepsy Res* 1998;31:59–71.
- Woodbury LA, Davenport VD. Design and use of a new electroshock seizure apparatus, and analysis of factors altering seizure threshold and pattern. *Arch Int Pharmacodyn Ther* 1952;92:97–104.
- Brown WC, Schiffman DO, Swinyard EA, Goodman LS. Comparative assay of antiepileptic drugs by “psychomotor” seizure test and minimal electroshock threshold test. *J Pharmacol Exp Ther* 1953;107:273–283.
- Matagne A, Klitgaard H. Validation of corneally kindled mice: a sensitive screening model for partial epilepsy in man. *Epilepsy Res Suppl* 1998;31:59–71.
- Racine RJ. Modification of seizure activity by electrical stimulation. II. Motor seizure. *Electroencephalogr Clin Neurophysiol* 1972;32:281–294.
- Dunham MS, Miya TA. A note on a simple apparatus for detecting neurological deficit in rats and mice. *J Amer Pharm Ass Sci Ed* 1957;46:208–209.

26. Finney DJ. Probit Analysis, 3rd ed. London: Cambridge University Press, 1971.
27. Lang R, Gundlach AL, Kofler B. The galanin peptide family: receptor pharmacology, pleiotropic biological actions, and implications in health and disease. *Pharmacol Ther* 2007;115:177–207.
28. Lerner JT, Sankar R, Mazarati AM. Galanin and epilepsy. *Cell Mol Life Sci* 2008;65:1864–1871.
29. Mitsukawa K, Lu X, Bartfai T. Galanin, galanin receptors and drug targets. *Cell Mol Life Sci* 2008;65:1796–1805.
30. Heinemann U, Schmitz D, Eder C, Gloveli T. Properties of entorhinal cortex projection cells to the hippocampal formation. *Ann N Y Acad Sci* 2000;911:112–126.
31. Mazarati A, Lundstrom L, Sollenberg U, Shin D, Langel U, Sankar R. Regulation of kindling epileptogenesis by hippocampal galanin type 1 and type 2 receptors: The effects of subtype-selective agonists and the role of G-protein-mediated signaling. *J Pharmacol Exp Ther* 2006;318:700–708.
32. Bartfai T, Lu X, Badie-Mahdavi H, et al. Galmic, a nonpeptide galanin receptor agonist, affects behaviors in seizure, pain, and forced-swim tests. *Proc Natl Acad Sci U S A* 2004;101:10470–10475.
33. Saar K, Mazarati AM, Mahlapuu R, et al. Anticonvulsant activity of a nonpeptide galanin receptor agonist. *Proc Natl Acad Sci U S A* 2002;99:7136–7141.
34. Klitgaard H, Matagne A, Gobert J, Wulfert E. Evidence for a unique profile of levetiracetam in rodent models of seizures and epilepsy. *Eur J Pharmacol* 1998;353:191–206.
35. Loscher W, Honack D. Profile of ucb L059, a novel anticonvulsant drug, in models of partial and generalized epilepsy in mice and rats. *Eur J Pharmacol* 1993;232:147–158.
36. Loscher W. Animal models of epilepsy for the development of anti-epileptogenic and disease-modifying drugs. A comparison of the pharmacology of kindling and post-status epilepticus models of temporal lobe epilepsy. *Epilepsy Res* 2002;50:105–123.
37. Stables JP, Bertram EH, White HS, et al. Models for epilepsy and epileptogenesis: report from the NIH workshop, Bethesda, Maryland. *Epilepsia* 2002;43:1410–1420.
38. Wrenn CC, Holmes A. The role of galanin in modulating stress-related neural pathways. *Drug news & perspectives* 2006;19:461–467.
39. Hygge-Blakeman K, Brumovsky P, Hao JX, et al. Galanin overexpression decreases the development of neuropathic pain-like behaviors in mice after partial sciatic nerve injury. *Brain research* 2004;1025:152–158.
40. Liu H, Hokfelt T. Effect of intrathecal galanin and its putative antagonist M35 on pain behavior in a neuropathic pain model. *Brain research* 2000;886:67–72.
41. Wiesenfeld-Hallin Z, Xu XJ, Langel U, Bedecs K, Hokfelt T, Bartfai T. Galanin-mediated control of pain: enhanced role after nerve injury. *Proceedings of the National Academy of Sciences of the United States of America* 1992;89:3334–3337.
42. Fisone G, Berthold M, Bedecs K, et al. N-terminal galanin-(1-16) fragment is an agonist at the hippocampal galanin receptor. *Proceedings of the National Academy of Sciences of the United States of America* 1989;86:9588–9591.
43. Land T, Langel U, Low M, Berthold M, Uden A, Bartfai T. Linear and cyclic N-terminal galanin fragments and analogs as ligands at the hypothalamic galanin receptor. *International journal of peptide and protein research* 1991;38:267–272.
44. Stohr T, Kupferberg HJ, Stables JP, et al. Lacosamide, a novel anti-convulsant drug, shows efficacy with a wide safety margin in rodent models for epilepsy. *Epilepsy research* 2007;74:147–154.

2.5.4. Engineering Galanin Analogues That Discriminate
Between GalR1 and GalR2 Receptor Subtypes and
Exhibit Anticonvulsant Activity Following
Systemic Delivery

Manuscript Reproduced with Permission From:

Robertson, C. R., Scholl, E. A., Pruess, T. H., Green, B. R., White, H. S., and Bulaj, G.
(2010) Engineering galanin analogues that discriminate between GalR1 and GalR2
subtypes and exhibit anticonvulsant activity following systemic delivery, *J. Med. Chem.*
53, 1871-1875.

© 2010 American Chemical Society

Engineering Galanin Analogues That Discriminate between GalR1 and GalR2 Receptor Subtypes and Exhibit Anticonvulsant Activity following Systemic Delivery

Charles R. Robertson,[‡] Erika Adkins Scholl,^{||} Timothy H. Pruess,^{||} Brad R. Green,[‡] H. Steve White,^{||} and Grzegorz Bulaj^{*‡}

[‡]Department of Medicinal Chemistry and ^{||}Department of Pharmacology and Toxicology, College of Pharmacy, University of Utah, 421 Wakara Way, Salt Lake City, Utah 84108

Received December 11, 2009

Galanin modulates seizures in the brain through two galanin receptor subtypes, GalR1 and GalR2. To generate systemically active galanin receptor ligands that discriminate between GalR1 and GalR2, the GalR1-preferring analogue Gal-B2 (or NAX 5055) was rationally redesigned to yield GalR2-preferring analogues. Systematic truncations of the N-terminal backbone led to [*N*-Me,des-Sar]Gal-B2, containing *N*-methyltryptophan. This analogue exhibited 18-fold preference in binding toward GalR2, maintained agonist activity, and exhibited potent anticonvulsant activity in mice following intraperitoneal administration.

Introduction

The endogenous neuropeptide galanin has been shown to modulate hyperexcitability in the brain through two associated galanin receptor subtypes, GalR1^a and GalR2.^{1–3} Systemically active agonists of galanin receptors include galmic, galnon, and Gal-B2.^{4,5} Galmic and galnon (entries 8 and 9, Table 1) are the only nonpeptidic compounds claimed to be subtype-selective and systemically active galanin receptor agonists, but these two compounds display relatively low binding affinity compared to their peptide counterparts and have been shown to bind nonspecifically to several off-target GPCRs.^{4,6} Gal-B2 is a 17-residue galanin analogue containing a lipoamino acid and several Lys residues at the C-terminus (entry 7, Table 1).^{5,7} A combination of lipidization and cationization turned out to be the most effective strategy to improve penetration of the galanin analogues across the blood–brain barrier (BBB). Gal-B2 was found to have potent anticonvulsant activity in the 6 Hz corneal stimulation mouse model for epilepsy with an ED₅₀ of 0.8 mg/kg after ip administration.⁵ Gal-B2 was also found to be active in other seizure and epilepsy models.⁸ The chemical modifications applied to galanin analogues enhanced their in vitro stability in rat serum (serum half-life of Gal-B2 increased from 7 min to 9.4 h). Gal-B2 maintained low nanomolar affinity for GalR1 and GalR2 receptors; i.e., 3.5 and 51.5 nM, respectively. Thus, Gal-B2 displayed a ~15-fold preference for GalR1 over GalR2.

To engineer GalR2 preferring analogues, N-terminal modifications of galanin have been reported in the literature.^{9,10} First, the des-Gly analogues (Table 1, entries 10 and 11) were found to possess decreased affinity for GalR1 while

maintaining a GalR2 binding preference, providing a significant clue for generating GalR2 selective agonists. In support of the des-Gly hypothesis, the Gal(2–11) fragment was found to be a potent GalR2 selective agonist.⁹ Further characterization using alanine displacement studies on the Gal(1–13) fragment showed that Gly1, Trp2, Tyr9, and Gly12 are important for high affinity binding to galanin receptors;¹¹ however, an Ala-walk on Gal(2–11) fragments showed that residues Trp2, Asn5, Gly8, and Tyr9 are necessary for high affinity binding toward GalR2.¹² A second strategy for improving GalR2 over GalR1 affinity was to use D-tryptophan at position 2 of human galanin (Table 1, entry 12).¹⁰ This inversion of stereochemistry led to a significant loss of binding to both receptors, though the analogue did have a slight preference toward GalR2.

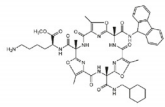
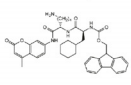
Site directed mutagenesis and molecular modeling of human GalR1 were performed to identify the key residues needed for high affinity binding toward galanin.^{10,13} The major interactions were found to be His264 and His267 toward Trp2, Phe292 toward Try9, and Phe115 toward Gly1. Currently, GalR2 has not been characterized in this way, and thus, the research community is still uncertain as to what structural features define receptor subtype selectivity. Since modeling studies are not predictive, more SAR studies are needed to better understand how galanin discriminates between receptor subtypes. Here, we report the results of a SAR study with the N-terminal part of the Gal-B2 analogue that suggest a strategy for developing GalR2 preferring systemically active galanin analogues.

The rational design of GalR2 preferring galanin analogues was achieved using a new approach, a backbone atom shaving technique, as illustrated in Figure 1. It is known in the literature that removal of the N-terminal Gly residue results in GalR2-preferring agonist activity, yet very little explanation is given as to why this pharmacophore has preference for GalR2 over GalR1.⁹ The backbone atom shaving allowed for identification of key groups at the N-terminus of Gal-B2 that were necessary for discriminating affinities toward GalR1

*To whom correspondence should be addressed. Phone: (801) 581-4629. Fax: (801) 581-7087. E-mail: bulaj@pharm.utah.edu.

^aAbbreviations: BBB, blood–brain barrier; Kp, lysine–palmitoyl; Sar, sarcosine; GalR1, galanin receptor subtype 1; GalR2, galanin receptor subtype 2; GalR3, galanin receptor subtype 3; GPCR, G-protein-coupled receptor; ip, intraperitoneal.

Table 1. Summary of Galanin Receptor Agonists, Their Structures, and Respective Binding Affinities^c

| entry | ligand | structure | K _i in nM | | ref. | |
|--------|--------|-------------|---|------------------|-----------------------|--------|
| | | | hGalR1 | hGalR2 | | |
| hGalR1 | 1 | Galanin | GWTLSAGYLLGPHAVGNHRSPDKNGLTS-CONH ₂ | 0.03 | 0.9 | 14, 15 |
| | 2 | C7 | GWTLSAGYLLGPrPKPQwFwLL-CONH ₂ ^a | 0.08 | 0.6 | 14, 16 |
| | 3 | M15 | GWTLSAGYLLGPPQFFGLM-CONH ₂ | 0.03 | 1.1 | 14, 16 |
| | 4 | M32 | GWTLSAGYLLGPRHYINLITRQRY-CONH ₂ | 0.30 | 1.4 | 14, 16 |
| | 5 | M35 | GWTLSAGYLLGPPGFSPFR-CONH ₂ | 0.01 | 1.8 | 14, 15 |
| | 6 | M40 | GWTLSAGYLLGPPALALA-CONH ₂ | 0.10 | 1.5 | 14, 15 |
| | 7 | GalB2 | (Sar)WTLNSAGYLLGPKK(Kp)K-CONH ₂ ^b | 3.50 | 52 | 5 |
| | 8 | Galmic |  | 34,200 | >100,000 ^c | 4 |
| | 9 | Galnon |  | 11,700 | 34,100 ^c | 4 |
| hGalR2 | 10 | Gal(2-30) | WTLNSAGYLLGPHAVGNHRSPDKNGLTS-CONH ₂ | 51 ^d | 9.8 ^d | 10 |
| | 11 | Gal(2-11) | WTLNSAGYLL-CONH ₂ | 870 ^d | 1.74 ^d | 9 |
| | 12 | [D-Trp2]Gal | GwTLNSAGYLLGPHAVGNHRSPDKNGLTS-CONH ₂ ^a | 545 ^d | 218 ^d | 10 |

^a Lower case letters denote D-amino acids. ^b Sar = sarcosine (*N*-methylglycine). Kp = lysine-palmitoyl. ^c Data taken from rat GalR2. ^d Derived from IC₅₀ values using the Cheng-Prusoff equation.¹⁷ ^e All analogues are C-terminal amides.

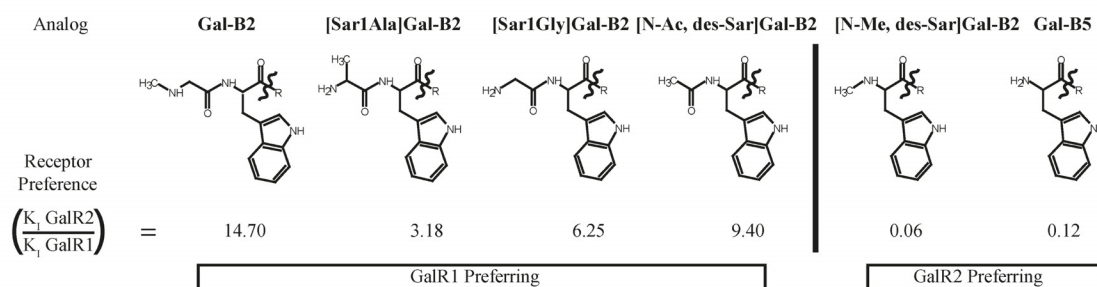


Figure 1. Structures of the N-terminus and GalR2/GalR1 receptor preference for galanin analogues. Analogues generated using the backbone “atom shaving” technique. All analogues maintain the Gal(2–13) pharmacophore and have the C-terminal KK(Lys-palmitoyl)K motif [R = TLNSAGYLLGPKK(Lys-palmitoyl)K-CONH₂].

or/and GalR2 receptors. Starting with the full length Gal-B2 analogue that contains a N-terminal sarcosine, we shaved atoms by successively altering the N-terminus with derivatives introduced during solid phase peptide synthesis. All of our analogues maintain the galanin(2–13) core with the oligo-lysine C-terminus, where the penultimate lysine is conjugated with palmitic acid (KK[Lys-palmitoyl]K) and the amidated C-terminus. The C-terminal derivatives included sarcosine (Gal-B2), alanine ([Sar1Ala]Gal-B2), glycine ([Sar1Gly]Gal-B2), *N*-acetyltryptophan ([*N*-Ac,des-Sar]Gal-B2), *N*-methyltryptophan ([*N*-Me,des-Sar]Gal-B2), and tryptophan (Gal-B5).⁵

Results and Discussion

The galanin analogues were synthesized using Fmoc-based solid phase peptide synthesis and purified by preparative

RP-HPLC, as described previously.^{5,7} Peptide masses were confirmed by MALDI-TOF MS, and the peptides were initially characterized by their HPLC retention times (Supporting Information Table S2), which were then used to calculate log *D*, as described elsewhere.⁵ All analogues studied here, Table 2, exhibited similar log *D* ranging from 1.22 to 1.30, suggesting that small structural changes at the N-terminus did not significantly alter their physicochemical profiles. Since previously characterized analogue Gal-B2 had log *D* = 1.24, all new analogues were expected to have CNS bioavailability comparable to that of this GalR1-preferring analogue.

To test the hypothesis that atom shaving in the Gal-B2 analogue will result in GalR2-preferring analogues, we determined affinities of the analogues toward human GalR1 and GalR2. Galanin receptor membrane preparations were purchased from Millipore or Perkin-Elmer. The receptor binding

Table 2. Peptide Sequences, Calculated log *D*, and Their Stability in Rat Serum Described in This Work^a

| analogue | structure | calcd log <i>D</i> | rat serum stability, <i>t</i> _{1/2} (h) |
|-------------------------------|--|--------------------|--|
| Gal-B2 | (Sar)WTLNSAGYLLGPKK(K _p)K | 1.24 ± 0.02 | 9.4 |
| [Sar1Ala]Gal-B2 | AWTLNSAGYLLGPKK(K _p)K | 1.28 ± 0.01 | nd |
| [Sar1Gly]Gal-B2 | GWTLNSAGYLLGPKK(K _p)K | 1.30 ± 0.04 | > 10 |
| [<i>N</i> -Ac,des-Sar]Gal-B2 | (<i>N</i> -Ac-Trp)TLNSAGYLLGPKK(K _p)K | 1.28 ± 0.02 | nd |
| [<i>N</i> -Me,des-Sar]Gal-B2 | (<i>N</i> -Me-Trp)TLNSAGYLLGPKK(K _p)K | 1.29 ± 0.01 | 9.0 |
| Gal-B5 | WTLNSAGYLLGPKK(K _p)K | 1.22 ± 0.02 | 10.0 |

^aK_p is palmitoylation of N^ε of lysine. Calculated log *D* was determined from HPLC retention times. Serum stability was determined by incubation of peptide in 25% rat serum at 37° C.

studies were carried out using time-resolved fluorescent competitive binding assay with Eu³⁺ labeled galanin as the competitor (see Supporting Information).⁵ The representative binding curves are shown in Figure 2, and the calculated *K*₁ values are summarized in Table 3. All the analogues maintained relatively high affinities toward hGalR2. However, as the N-terminus was truncated from the (*N*-acetyl)Trp analogue to the (*N*-methyl)Trp, a significant loss in hGalR1 binding affinity was observed. Analogue [*N*-Me,des-Sar]Gal-B2 had a *K*₁ of 364 nM for hGalR1 and 20 nM for hGalR2, which was an 18-fold preference for hGalR2. Further removal of methyl group from the N-terminus (Gal-B5) reduced the binding toward GalR2 by 2-fold. When the binding affinities of [*N*-Me,des-Sar]Gal-B2 and Gal-B5 are compared to Gal-B2 (Figure 2 and Table 3), it is apparent that the first two analogues are GalR2-preferring, with [*N*-Me,des-Sar]Gal-B2 having a greater preference toward this subtype.

Analogue [*N*-Me,des-Sar]Gal-B2 was selected to further characterize its properties in greater detail. To demonstrate that analogue [*N*-Me,des-Sar]Gal-B2 is a galanin receptor agonist, a calcium mobilization assay (GPCRProfiler Screening, Millipore, St. Charles, MO) was carried out using CHO-K1 cells overexpressing galanin receptors. The receptor activation was normalized to known galanin receptor agonists: Gal(1–30) for GalR1 and Gal(2–29) for GalR2. As shown in Figure 3A, [*N*-Me,des-Sar]Gal-B2 activated GalR2 receptors with an apparent preference toward GalR2 at the concentration tested (1.25 μM). This finding supports the binding data that showed a preference of [*N*-Me,des-Sar]Gal-B2 for hGalR2 over hGalR1.

Although seizures are controlled by GalR1 and GalR2 galanin receptor subtypes, we cannot exclude the possibility that the systemically active galanin analogues studied here also interact with the third galanin receptor subtype, GalR3. It is known from the literature that truncated galanin analogue Gal(2–11) maintains GalR2 binding and has moderate GalR3 receptor binding, with a 12-fold preference for toward GalR2 above GalR3.¹⁸ We acknowledge that more experimentation is needed to verify that [*N*-Me,des-Sar]Gal-B2 will have similar binding profiles toward GalR3 as Gal(2–11).

We have previously shown that the combination of cationization and lipidization improved stability in rat serum of our galanin analogues (including Gal-B2) and thereby contributed to increased systemic bioavailability.⁷ The analogues described herein were also found to be metabolically stable when incubated in 25% rat serum at 37° C. For [*N*-Me,des-Sar]Gal-B2, the half-life was determined to be > 10 h, compared to 9.4 h for Gal-B2 (see Supporting Information Table S2). It is noteworthy that having an N-terminal modification such as methylation or acetylation did not affect the in vitro serum stability of the galanin analogues.

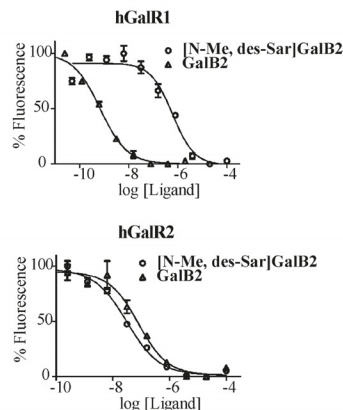


Figure 2. Representative binding curves for analogues Gal-B2 (triangles) and [*N*-Me,des-Sar]Gal-B2 (circles) against hGalR1 (top) and hGalR2 (bottom). Each binding assay was performed in triplicate to generate one 10-point binding curve. Binding affinities are reported as the average of three independent binding curves. Binding affinities (*K*₁) for Gal-B2 are 3.5 nM hGalR1 and 52 nM hGalR2. For [*N*-Me,des-Sar]Gal-B2, they are 364 nM hGalR1 and 20 nM hGalR2.

To evaluate the anticonvulsant activity of the galanin analogues, they were administered intraperitoneally (ip) to CF-1 mice at a dose of 4 mg/kg, as described previously.^{5,19} The mice were then challenged with a 6 Hz corneal stimulation (32 mA for 3 s delivered via corneal electrodes) 15, 30, 60, 120, and 240 min after ip administration. Mice not displaying any characteristic limbic seizure activity (jaw chomping, vibrissae twitching, forelimb clonus, or Straub tail) were considered protected; protection is graded as all or none.¹⁹ All studied analogues exhibited anticonvulsant activity, with maximal protection persisting up to 2 h after administration. Figure 3B shows the dose-dependent response of analogue [*N*-Me,des-Sar]Gal-B2, where subjects were challenged 1 h after dosing. The calculated ED₅₀ of analogue [*N*-Me,des-Sar]Gal-B2 was 0.77 mg/kg (see Supporting Information). This value is comparable to an ED₅₀ of 0.8 mg/kg for Gal-B2, suggesting that at the doses tested, GalR1- and GalR2-preferring analogues exhibit similar levels of anticonvulsant activity. Currently, we are uncertain of the level of BBB penetration; however, anticonvulsant activity is considered a good surrogate measurement of CNS bioavailability.

Conclusions

Developing a GalR2 subtype-selective receptor agonist will provide not only an important pharmacological tool for understanding the SAR of galanin but also insight into their

Table 3. In Vivo Pharmacology and in Vitro Receptor Binding Results^a

| analogue | primary screening at 4 mg/kg (6 Hz, 32 mA) | primary screening (AUC) | GalR1 <i>K_i</i> (nM) | GalR2 <i>K_i</i> (nM) |
|----------------------|--|-------------------------------|------------------------------------|------------------------------------|
| Gal-B2 | 3/4, 4/4, 4/4, 4/4, 0/4 | 16313 | 3.5 ± 1.0 | 51.5 ± 34.4 |
| [Sar1Ala]Gal-B2 | 4/4, 4/4, 4/4, 1/4, 0/4 | 9750 | 11.0 ± 6.0 | 35.0 ± 8.0 |
| [Sar1Gly]Gal-B2 | 1/4, 3/4, 3/4, 0/4, 0/3 | 5250 | 2.8 ± 0.9 | 17.5 ± 4.0 |
| [N-Ac,des-Sar]Gal-B2 | nd | nd | 1.7 ± 0.8 | 15.9 ± 3.3 |
| [N-Me,des-Sar]Gal-B2 | 0/4, 3/4, 3/4, 1/4, 0/3 | 7313 | 364.5 ± 58.4 | 20.2 ± 2.1 |
| Gal-B5 | 2/4, 1/4, 2/4, 2/4, 0/3 | 9375 | 387.0 ± 123.0 | 48.0 ± 11.3 |

^a Antiepileptic activity was assessed after CF-1 mice were treated ip with analogues and challenged with corneal stimulation at 15, 30, 60, 120, and 240 min. The number of mice protected out of the sample group is presented; integrated area under the curve (AUC) is shown for each analogue. Competitive receptor binding was performed on receptor membrane preps (Millipore or Perkin Elmer) against Eu-labeled galanin in a time-resolved fluorescence-based assay.

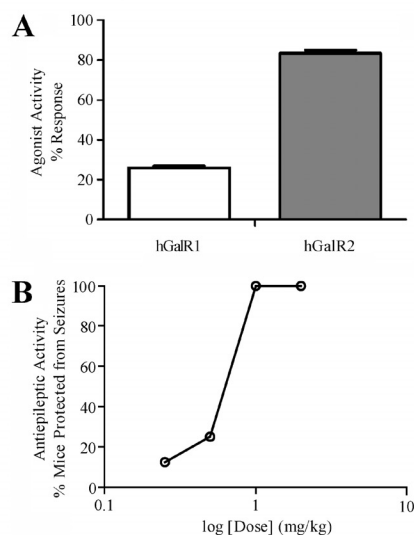


Figure 3. (A) Agonist activity of analogues determined by calcium mobilization assay (Millipore). The % response is normalized to galanin receptor agonists: Gal(1–30) for hGalR1 and Gal(2–29) for hGalR2. At 1.25 μ M ligand concentration, analogue [N-Me,des-Sar]Gal-B2 preferentially activates hGalR2 over hGalR1, to 83% ± 3.8% and 26% ± 1.9%, respectively ($n = 4$, $p < 0.01$). (B) Dose-response curve for analogue [N-Me,des-Sar]Gal-B2. CF-1 mice ($n = 8$) were treated with the analogue and challenged with 6 Hz (32 mA) corneal stimulation 1 h after ip administration. The % animals protected is [(number of mice protected)/(number of mice tested)] × 100.

therapeutic potential as anticonvulsants and analgesics. Generation of Gal(2–11) advanced our knowledge of the galanin signaling; however, this peptide is limited in its use because of its low bioavailability. Here, we describe galanin analogues that discriminate between receptor subtypes GalR1 and GalR2 and are systemically active, which can be used as an even greater pharmacological tool for investigating galanergic signaling.

The backbone atom shaving approach used to determine the individual contributions of individual atoms in the backbone toward the galanin receptors is a unique feature of this study. Focus is normally devoted toward side chain interactions with receptor binding and is often probed via peptide-Ala walks. Our method showed that with the loss of the carbonyl functional group from analogue [N-Ac,des-Sar]Gal-B2 to [N-Me,des-Sar]Gal-B2, the analogues lost affinity toward the GalR1 receptor but maintained affinity toward GalR2. With this development we find that independent

N-terminal or C-terminal modifications are critical for independent engineering of subtype preference or bioavailability, respectively.⁵

During the preparation of this manuscript, Runesson independently published compelling results reinforcing N-terminal modifications of galanin-like peptides for generating GalR2 agonists.¹⁸ What is unique about our results is the functional readout of anticonvulsant activity obtained by administering the modified analogue [N-Me,des-Sar]Gal-B2 in vivo, after ip administration to CF-1 mice. When taken together with the in vitro receptor binding data, enhanced rat serum stability, and favorable log *D*, we illustrate the generation of systemically active galanin analogues that discriminate between receptor subtypes.

Experimental Section

Peptide Synthesis. All analogues were synthesized using Fmoc-based solid-phase synthesis. The peptide analogues were removed from the resin by a 2.5 h treatment with reagent K (82.5% TFA, 5% *n*H₂O, 5% ethanedithiol, 2.5% thioanisole v/v, 75 mg/mL phenol). After precipitation with ice cold MTBE, a diphenyl preparative HPLC column was used to purify large quantities of the analogues. The HPLC buffers were buffer A (1 L of H₂O + 1 mL of TFA) and buffer B (900 mL of acetonitrile + 100 mL of H₂O + 1 mL of TFA). Elution of the analogues from the column was carried out over a linear gradient from 20% to 90% buffer B over 30 min. Purified analogues were quantified by measuring UV absorbance at 279.8 nm ($\epsilon = 7000 \text{ M}^{-1} \text{ cm}^{-1}$). Purity of all analogues was found to be >95% by analytical HPLC running a linear gradient of 20% buffer B to 100% buffer B in 40 min (Table S2). Calculated masses were confirmed by MALDI mass spectrometry analysis at the University of Utah core facility.

log *D*. HPLC Capacity Factor (*k'*) Method.⁵ The HPLC buffers were buffer A (1 L of H₂O + 1 mL of TFA) and buffer B (900 mL of acetonitrile + 100 mL of H₂O + 1 mL of TFA). A 5.0 μ g standard (run in triplicate) was injected onto a Vydac diphenyl column using a linear gradient starting at 80/20 buffer A/buffer B and ending at 10/90 buffer A/buffer B in 15 min before immediate return to initial conditions. The retention times are the average of three runs. The capacity factors (*k'*) of the peptides were calculated using the following formula:

$$k' = \frac{t_r - t_o}{t_o}$$

t_o is the solvent front, and t_r is the retention time of the peptide. The log *D* values obtained from the shake-flask method were plotted against their peptides respective *k'* values, giving a linear plot. The log *D* values for all other peptides were calculated using this standard curve.

Stability in Rat Serum. An amount of 1 mL of 25% rat serum was incubated at 37 °C for 10 min prior to addition of the

analogue. Reactions were prepared by adding each analogue, dissolved in $n\text{H}_2\text{O}$ to a solution containing 25% rat serum and 0.1 M Tris-HCl, pH 7.5, to a final peptide concentration of 20 μM . At appropriate time intervals (up to 8 h), 200 μL aliquots were withdrawn and added to 100 μL of "quenching solution" (15% trichloroacetic acid in 40% isopropanol). The 40% isopropanol was added to the quenching mixture, as it was noted to improve recovery of the Gal-B2 analogue. Upon precipitation with the quenching mixture, the samples were incubated at $-20\text{ }^\circ\text{C}$ for 15 min and centrifuged at 12000 rpm to separate serum proteins. The supernatant was analyzed using HPLC separation with an YMC ODS-A 5 μm , 120 Å column (AA12S052503WT). In cases where analogue peaks overlapped with peaks observed in the "serum-only" control samples, the gradient was optimized by changing the composition of the mobile phases, column temperature, or HPLC column (for example, diphenyl or C8). Recovery of the analogues was assessed by spiking "serum-only" control samples after the TCA precipitation with known amounts of the analogue. Metabolic stability was assessed by monitoring the disappearance of the analogues over 8 h. This was accomplished by comparison of the area under the curve for the peak corresponding to the intact peptide at each time point. These values were then used to calculate half-lives for each analogue.

Anticonvulsant Activity. Each galanin analogue was administered intraperitoneally to five groups of CF-1 mice ($n = 4$ mice) at a dose of 4 mg/kg. At various times (i.e., 15, 30, 60, 120, and 240 min) after ip administration, mice were challenged with a 6 Hz corneal stimulation (32 mA for 3 s delivered via corneal electrodes). Mice not displaying a characteristic limbic seizure (e.g., jaw chomping, vibrissae twitching, forelimb clonus, Straub tail, graded as all or none, were considered protected. The percent of animals protected at each time point was plotted against time, and the area under the curve (AUC) for the time-response study was calculated for each analogue.

Receptor Binding. Competitive binding assays were performed in 96-well format on AcroWell filter plates (Perkin-Elmer) using receptor membrane preparations, purchased from Millipore or Perkin-Elmer (hGalR1 and hGalR2) and Eu galanin (Perkin-Elmer), using the DELFIA assay buffers (Perkin-Elmer). The samples were performed in quadruplicate. Binding assay was carried out with 6 μg of receptor membrane preparations (1.4 pmol/mg protein) and 2 nM Eu galanin in a volume of 100 μL of the DELFIA L*R binding buffer (50 mM Tris-HCl, pH 7.5, 5 mM MgCl_2 , 25 μM EDTA, and 0.2% BSA). Samples were incubated at room temperature for 90 min, followed by washing (4 \times) with 200 μL of DELFIA wash buffer (50 mM Tris-HCl, pH 7.5, and 5 mM MgCl_2). DELFIA enhancement solution (200 μL) was added, and the plates were incubated at room temperature for 30 min. The plates were read on a VICTOR³ spectrofluorometer using a standard Eu-TRF measurement (excitation at 340 nm, delay for 400 μs , and emission at 615 nm for 400 μs). Competition curves were analyzed with GraphPad Prism software using the sigmoidal dose-response (variable slope) equation for nonlinear regression analysis.

Acknowledgment. The authors thank Karen White and Daniel R. McDougale for their technical assistance. We also thank Professor Bob Shackmann and Scott Endicott from the DNA/Peptide Synthesis Core Facility at the University of Utah. This work was funded by the University of Utah startup funds, the Epilepsy Research Foundation, and NIH Grant R21 NS059669. Conflict of interest disclosure: G.B. and H.S.W. are scientific cofounders of NeuroAdjvants, Inc.

Supporting Information Available: Physicochemical characterization, MALDI MS results, peptide purity, and HPLC

retention times. This material is available free of charge via the Internet at <http://pubs.acs.org>.

References

- Mazarati, A.; Lundström, L.; Sollenberg, U.; Shin, D.; Langel, U.; Sankar, R. Regulation of kindling epileptogenesis by hippocampal galanin type 1 and type 2 receptors: the effects of subtype-selective agonists and the role of G-protein-mediated signaling. *J. Pharmacol. Exp. Ther.* **2006**, *318*, 700–708.
- Mitsukawa, K.; Lu, X.; Bartfai, T. Galanin, galanin receptors and drug targets. *Cell. Mol. Life Sci.* **2008**, *65*, 1796–1805.
- Xu, X. J.; Hökfelt, T.; Wiesenfeld-Hallin, Z. Galanin and spinal pain mechanisms: Where do we stand in 2008? *Cell. Mol. Life Sci.* **2008**, *65*, 1813–1819.
- Bartfai, T.; Xiaoying, L.; Badie-Mahdavi, H.; Barr, A. M.; Mazarati, A.; Hua, X.-Y.; Yaksh, T.; Haberhauer, G.; Ceide, S. C.; Trembleau, L.; Somogyi, L.; Kröck, L.; Rebek, J. Galmic, a nonpeptide galanin receptor agonist, affects behaviors in seizure, pain, and forced-swim tests. *Proc. Natl. Acad. Sci. U.S.A.* **2004**, *101*, 10470–10475.
- Bulaj, G.; Green, B. R.; Lee, H.-K.; Robertson, C. R.; White, K.; Zhang, L.; Sochanski, M.; Flynn, S.; Scholl, E. A.; Pruess, T.; Smith, M. D.; White, H. S. Design, synthesis and characterization of high-affinity, systemically-active galanin analogues with potent anticonvulsant activity. *J. Med. Chem.* **2008**, *51*, 8038–8047.
- Saar, K.; Mazarati, A.; Mahlapuu, R.; Hallnemo, G.; Soomets, U.; Kilk, K.; Hellberg, S.; Pooga, M.; Tolf, B.-R.; Shi, T. S.; Hökfelt, T.; Wasterlain, C.; Bartfai, T.; Langel, U. Anticonvulsant activity of a nonpeptide galanin receptor agonist. *Proc. Natl. Acad. Sci. U.S.A.* **2002**, *99*, 7136–7141.
- Zhang, L.; Robertson, C. R.; Green, B. R.; Pruess, T. H.; White, H. S.; Bulaj, G. Structural requirements for a lipooamino acid in modulating the anticonvulsant activities of systemically active galanin analogues. *J. Med. Chem.* **2009**, *52*, 1310–1316.
- White, H. S.; Scholl, E. A.; Klein, B. D.; Flynn, S. P.; Pruess, T. H.; Green, B. R.; Zhang, L.; Bulaj, G. Developing novel antiepileptic drugs: characterization of NAX 5055, a systemically-active galanin analog, in epilepsy models. *Neurotherapeutics* **2009**, *6*, 372–380.
- Liu, H. X.; Brumovsky, P.; Schmidt, R.; Brown, W.; Payza, K.; Hodzic, L.; Pou, C.; Godbout, C.; Hökfelt, T. Receptor subtype-specific pronociceptive and analgesic actions of galanin in the spinal cord: selective actions via GalR1 and GalR2 receptors. *Proc. Natl. Acad. Sci. U.S.A.* **2001**, *98*, 9960–9964.
- Church, W. B.; Jones, K. A.; Kuiper, D. A.; Shine, J.; Iismaa, T. P. Molecular modelling and site-directed mutagenesis of human GALR1 galanin receptor defines determinants of receptor subtype specificity. *Protein Eng.* **2002**, *15*, 313–323.
- Land, T.; Langel, U.; Löw, M.; Berthold, M.; Undén, A.; Bartfai, T. Linear and cyclic N-terminal galanin fragments and analogs as ligands at the hypothalamic galanin receptor. *Int. J. Pept. Protein Res.* **1991**, *38*, 267–272.
- Lundström, L.; Lu, X.; Langel, U.; Bartfai, T. Important pharmacophores for binding to galanin receptor 2. *Neuropeptides* **2005**, *39*, 169–171.
- Berthold, M.; Kahl, U.; Jurèus, A.; Kask, K.; Nordvall, G.; Langel, U.; Bartfai, T. Mutagenesis and ligand modification studies on galanin binding to its GTP-binding-protein-coupled receptor GalR1. *Eur. J. Biochem.* **1997**, *249*, 601–606.
- Fitzgerald, L. W.; Patterson, J. P.; Conklin, D. S.; Horlick, R.; Largent, B. L. Pharmacological and biochemical characterization of a recombinant human galanin GalR1 receptor: agonist character of chimeric galanin peptides. *J. Pharmacol. Exp. Ther.* **1998**, *287*, 448–456.
- Bloomquist, B. T.; Beauchamp, M. R.; Zhelmin, L.; Brown, S.-E.; Gore-Willse, A. R.; Gregor, P.; Cornfield, L. J. Cloning and expression of the human galanin receptor GalR2. *Biochem. Biophys. Res. Commun.* **1998**, *243*, 474–479.
- Borowsky, B.; Walker, M. W.; Huang, L.-Y.; Jones, K. A.; Smith, K. E.; Bard, J.; Brancheck, T. A.; Gerald, C. Cloning and characterization of the human galanin GALR2 receptor. *Peptides* **1998**, *19*, 1771–1781.
- Cer, R. Z.; Mudunuri, U.; Stephens, R.; Lebeda, F. J. IC₅₀-to-K_i: a Web-based tool for converting IC₅₀ to K_i values for inhibitors of enzyme activity and ligand binding. *Nucleic Acids Res.* **2009**, *37*, W441–445.
- Runeson, J.; Saar, I.; Lundström, L.; Järv, J.; Langel, U. A novel GalR2-specific peptide agonist. *Neuropeptides* **2009**, *43*, 187–192.
- Barton, M. E.; Klein, B. D.; Wolf, H. H.; White, H. S. Pharmacological characterization of the 6 Hz psychomotor seizure model of partial epilepsy. *Epilepsy Res.* **2001**, *47*, 217–227.

2.6 Conclusions

The compounds described in this section constitute our efforts to elucidate how lipidization and cationization motifs influence the physicochemical and pharmacological properties of galanin analogs such as metabolic stability and logD. Though modest improvements to logD and serum stability were observed by implementation of either the lipidization or cationization motifs, individually, it was the combination of these two strategies that yielded the most promising results. Furthermore, only by combining the two strategies were the potent anticonvulsant effects observed. Our results showed that the key determinant for improved physicochemical properties was the presence, and chemical structure, of the attached fatty acid. Follow-up experiments have focused on further modification of Gal-B2 through incorporation of alternative lipidization motifs (i.e. unsaturated fatty acids), conformational constraint (via lactamization), and others. Aside from galanin a number of endogenous neuropeptides have also been implicated as having important neuromodulatory roles in pain pathways and in seizure control. The following chapters will explore the potential for application of the lipidization-cationization strategy described here for the development of systemically-active analogs of neurotensin (NT), neuropeptide Y (NPY), neuropeptide W (NPW), and other endogenous neuropeptides.

2.7 References

1. Tatemoto, K., Rökaeus, Å., Jörnvall, H., McDonald, T. J., and Mutt, V. (1983) Galanin - a novel biologically active peptide from porcine intestine, *FEBS Lett.* *164*, 124-128.
2. Mazarati, A., Langel, Ü., and Bartfai, T. (2001) Galanin: An endogenous anticonvulsant?, *Neuroscientist* *7*, 506-517.
3. Land, T., Langel, Ü., Löw, M., Berthold, M., Undén, A., and Bartfai, T. (1991) Linear and cyclic N-terminal galanin fragments and analogs as ligands at the hypothalamic galanin receptor, *Int. J. Pept. Protein Res.* *38*, 267-372.
4. Lang, R., Gundlach, A. L., and Kofler, B. (2007) The galanin peptide family: Receptor pharmacology, pleiotropic biological actions, and implications in health and disease, *Pharmacol. Ther.* *115*, 177-207.
5. Crawley, J. N., Austin, M. C., Fiske, S. M., Martin, B., Consolo, S., Berthold, M., Langel, Ü., Fisone, G., and Bartfai, T. (1990) Activity of centrally administered galanin fragments in stimulation of feeding behavior and on galanin receptor binding in the rat hypothalamus, *J. Neurosci.* *10*, 3695-3700.
6. Fisone, G., Berthold, M., Bedecs, K., Undén, A., Bartfai, T., Bertorelli, R., Consolo, S., Crawley, J., Martin, B., Nilsson, S., and Hökfelt, T. (1989) N-terminal galanin-(1-16) fragment is an agonist at the hippocampal galanin receptor, *Proc. Natl. Acad. Sci.* *86*, 9588-9591.
7. Langel, U., and Bartfai, T. (1998) Chemistry and molecular biology of galanin receptor ligands, *Ann. N.Y. Acad. Sci.* *863*, 86-93.
8. Wynick, D., Thompson, S. W., and McMahon, S. B. (2001) The role of galanin as a multi-functional neuropeptide in the nervous system, *Curr. Opin. Pharmacol.* *1*, 73-77.
9. Ito, M. (2009) Functional roles of neuropeptides in cerebellar circuits, *Neuroscience* *162*, 666-672.
10. Gamss, R. P., Slasky, S. E., Bello, J. A., Miller, T. S., and Shinner, S. (2009) Prevalence of hippocampal malrotation in a population without seizures, *AJNR Am. J. Neuroradiol.* *30*, 1571-1573.
11. Mazarati, A., and Lu, X. (2005) Regulation of limbic status epilepticus by hippocampal galanin type 1 and type 2 receptors, *Neuropeptides* *39*, 277-280.

12. Ceide, S. C., Trembleau, L., Haberhauer, G., Somogyi, L., Lu, X., Bartfai, T., and J. Rebeck, J. (2004) Synthesis of galmic: A nonpeptide galanin receptor agonist, *Proc. Natl. Acad. Sci. 101*, 16727-16732.
13. Saar, K., Mazarati, A. M., Mahlapuu, R., Hallnemo, G., Soomets, U., Kilk, K., Hellberg, S., Pooga, M., Tolf, B.-R., Shi, T. S., Hökfelt, T., Wasterlain, C., Bartfai, T., and Langel, Ü. (2002) Anticonvulsant activity of a nonpeptide galanin receptor agonist, *Proc. Natl. Acad. Sci. 99*, 7136-7141.
14. Bartfai, T., Lu, X., Badie-Mahdavi, H., Barr, A. M., Mazarati, A., Hua, X.-Y., Yaksh, T., Haberhauer, G., Ceide, S. C., Trembleau, L., and Somogyi, L. (2004) Galmic, a nonpeptide galanin receptor agonist, affects behaviors in seizure, pain, and forced-swim tests, *Proc. Natl. Acad. Sci. 101*, 10470-10475.
15. Florén, A., Sollenberg, U., Lundström, L., Zorko, M., Stojan, J., Budihna, M., Wheatly, M., Martin, N. P., Kilk, K., Mazarati, A., Bartfai, T., Lindgren, M., and Langel, Ü. (2005) Multiple interaction sites of galanin trigger its biological effects, *Neuropeptides 39*, 547-558.
16. Lu, X., Lundström, L., Langel, U., and Bartfai, T. (2005) Galanin receptor ligands, *Neuropeptides 39*, 143-146.
17. Robertson, C. R., Scholl, E. A., Pruess, T. H., Green, B. R., White, H. S., and Bulaj, G. (2010) Engineering galanin analogues that discriminate between GalR1 and GalR2 receptor subtypes and exhibit anticonvulsant activity following systemic delivery, *J. Med. Chem. 53*, 1871-1875.
18. Bulaj, G., Green, B. R., Lee, H. K., Robertson, C. R., White, K., Zhang, L., Sochanska, M., Flynn, S. P., Scholl, E. A., Pruess, T. H., Smith, M. D., and White, H. S. (2008) Design, synthesis, and characterization of high-affinity, systemically-active galanin analogues with potent anticonvulsant activities, *J. Med. Chem. 51*, 8038-8047.
19. Zhang, L., Robertson, C. R., Green, B. R., Pruess, T. H., White, H. S., and Bulaj, G. (2009) Structural requirements for a lipoamino acid in modulating the anticonvulsant activities of systemically active galanin analogues, *J. Med. Chem. 52*, 1310-1316.
20. White, H. S., Scholl, E. A., Klein, B. D., Flynn, S. P., Pruess, T. H., Green, B. R., Zhang, L., and Bulaj, G. (2009) Developing novel antiepileptic drugs: characterization of NAX 5055, a systemically-active galanin analog, in epilepsy models, *Neurotherapeutics 6*, 372-380.
21. Hau, V. S., Huber, J. D., Campos, C. R., Lipkowski, A. W., Misicka, A., and Davis, T. P. (2002) Effect of guanidino modification and proline substitution on

- the in vitro stability and blood-brain barrier permeability of endomorphin II, *J. Pharm. Sci.* *91*, 2140-2149.
22. Liu, H.-M., Liu, X.-F., Yao, J.-L., Wang, C.-L., Yu, Y., and Wang, R. (2006) Utilization of combined chemical modifications to enhance the blood-brain barrier permeability and pharmacological activity of endomorphin-1, *J. Pharmacol. Exp. Ther.* *319*, 308-316.
 23. van de Waterbeemd, H., Lennernäs, H., and Artursson, R. (2003) *Drug Bioavailability: Estimation of Solubility, Permeability, Absorption and Bioavailability*, Wiley, VCH, Weinheim.
 24. Taylor, M. D., and Amidon, G. L. (1995) *Peptide-Based Drug Design: Controlling transport and metabolism*, American Chemical Society, Washington D. C.
 25. Youngblood, D. S., Hatlevig, S. A., Hassinger, J. N., Iverson, P. L., and Moulton, H. M. (2007) Stability of cell-penetrating peptide - Morpholino oligomer conjugates in human serum and in cells, *Bioconjugate Chem.* *18*, 50-60.

CHAPTER 3

INTRODUCTION OF LIPIDIZATION-CATIONIZATION MOTIFS AFFORDS SYSTEMICALLY BIOAVAILABLE NEUROPEPTIDE Y AND NEUROTENSIN ANALOGS WITH ANTICONVULSANT ACTIVITIES

Manuscript Reproduced with permission from:

Green, B. R., White, K. L., McDougle, D. R., Zhang, L., Klein, B., Scholl, E. A., Pruess, T. H., White, H. S., and Bulaj, G. (2010) Introduction of lipidization-cationization motifs affords systemically bioavailable neuropeptide Y and neurotensin analogs with anticonvulsant activities, *J. Pept. Sci.* 16, 486-495.

© 2010 Wiley-Blackwell Publishing Ltd.

Introduction of lipidization – cationization motifs affords systemically bioavailable neuropeptide Y and neurotensin analogs with anticonvulsant activities

Brad R. Green,^a Karen L. White,^a Daniel R. McDougale,^a Liuyin Zhang,^a Brian Klein,^b Erika A. Scholl,^c Timothy H. Pruess,^c H. Steve White^c and Grzegorz Bulaj^{a*}

The neuropeptides galanin (GAL), neuropeptide Y (NPY) or neurotensin (NT) exhibit anticonvulsant activities mediated by their respective receptors in the brain. To transform these peptides into potential neurotherapeutics, their systemic bioavailability and metabolic stability must be improved. Our recent studies with GAL analogs suggested that an introduction of lipoamino acids in the context of oligo-Lys residues (lipidization–cationization motif) significantly increases their penetration into the brain, yielding potent antiepileptic compounds. Here, we describe an extension of this strategy to NPY and NT. Rationally designed analogs of NPY and NT containing the lipidization–cationization motif were chemically synthesized and their physicochemical and pharmacological properties were characterized. The analogs NPY-BBB2 and NT-BBB1 exhibited increased serum stability, possessed $\log D > 1.1$, retained high affinities toward their native receptors and produced potent antiseizure activities in animal models of epilepsy following intraperitoneal administration. Our results suggest that the combination of lipidization and cationization may be an effective strategy for improving systemic bioavailability and metabolic stability of various neuroactive peptides. Copyright © 2010 European Peptide Society and John Wiley & Sons, Ltd.

Keywords: NPY; neurotensin; chemical modifications; bioavailability; epilepsy; blood–brain barrier

Introduction

Several endogenous neuropeptides, such as NPY (YPSKPDNPGEDAPAEDMARYYSALRHYINLITRQRY-NH₂), NT (ZLYENKPRRPYL), and GAL (GWTLSAGYLLGPHAVGNHRSFSDKNGLT-S-NH₂), possess both antiepileptic and antinociceptive properties mediated by their respective receptors in the CNS [1–3]. These neuropeptides show promise as potential first-in-class therapeutics for the treatment of epilepsy and/or pain. However, the lack of CNS bioavailability and marginal metabolic stability has slowed their preclinical and clinical development. The difficulty of delivering peptides, proteins, and other drugs across the BBB has long been challenged using a variety of strategies [4–6]. BBB-permeable analogs of NPY, NT, or GAL could provide useful pharmacological tools that could also validate their native receptors as drug targets in humans.

NPY is a 36-amino acid anticonvulsant peptide that is an endogenous ligand for five receptor subtypes (Y1–Y5) [7]. Among the five subtypes, the Y2 receptor was previously identified as the potential molecular target for the treatment of epilepsy, as it is implicated in modulating the neural excitability in the hippocampus [1,8]. Furthermore, over-expression of NPY in the rat brain using an adeno-associated virus has shown therapeutic promise as a treatment for epilepsy and is poised to enter clinical trials [9,10]. The NPY-based gene therapy strategy underscores the lack of systemically active NPY analogs that penetrate the

BBB. Such analogs would provide lead compounds for developing NPY-based pharmacological therapies.

SAR studies of NPY identified critical amino acid residues for interactions with subtypes of NPY receptors [11,12]. Results from alanine-scan and truncated analog studies suggested that the C-terminal fragment of NPY was necessary for high affinity binding to Y2 receptors [13–15]. α -Helical character of the C-terminal fragment of NPY was found necessary for Y2-binding [11,16]. Replacement of naturally occurring amino acid residues with L-alanine perturbed helix formation and resulted in peptides with decreased binding affinities [11]. Based on the receptor selectivity of the C-terminal decapeptide and the stabilizing effects

* Correspondence to: Grzegorz Bulaj, Department of Medicinal Chemistry, College of Pharmacy, University of Utah, 421 Wakara Way Suite 360, Salt Lake City, UT 84108, USA. E-mail: bulaj@pharm.utah.edu

^a Department of Medicinal Chemistry, College of Pharmacy, University of Utah, Salt Lake City, UT 84108, USA

^b Neuro Adjuvants, Inc., Salt Lake City, UT 84108, USA

^c Department of Pharmacology and Toxicology, College of Pharmacy, University of Utah, Salt Lake City, UT 84108, USA

Abbreviations used: BBB, blood–brain barrier; GAL, galanin; K_p, N^ε-palmitoyl-L-lysine; NPFF, neuropeptide FF; nH₂O, nanopure water; NT, neurotensin; NTR-1, neurotensin receptor subtype 1; Y2, neuropeptide Y receptor subtype 2; Z, pyroglutamic acid.

of *N*-terminal amino acids, the Beck-Sickinger group designed a series of centrally truncated NPY analogs. These analogs were compared for their binding affinities for both Y1 and Y2 receptor subtypes; analogs possessing the C-terminal fragment NPY (25–36) could readily discriminate between receptor subtypes with low nanomolar affinities for Y2 [11,12,16]. Taken together, it is possible to develop reduced-size peptide analogs that are potent agonists for the Y2 receptor.

NT mediates a number of physiological responses in the CNS [17,18]. This 13-residue peptide has been widely studied for its antinociceptive properties, shown to be mediated through two receptor subtypes, NTR-1 and NTR-2 [19,20]. More recently, Lee and coworkers demonstrated the ability of NT and its glycosylated analogs to suppress epileptic seizures in the brain with remarkable potency (for NT, $ED_{50} = 0.001$ nmol in the 6 Hz mouse model of epilepsy, intracerebroventricular injection) [2]. SAR studies have revealed that the C-terminal portion of the peptide, NT (8–13), is sufficient for receptor activation [21,22]. There have been many attempts to generate metabolically stable, BBB-permeable analogs of NT, including peptide minimization, cyclization, backbone modification, and amino acid substitution [18,23,24]. Work by our group has recently shown that conjugated polyamine motifs could be coupled to the NT active fragment, resulting in an analog with improved CNS bioavailability [25]. The polyamine-containing NT analog possessed subnanomolar binding affinity ($K_i = 0.25$ nM) and low nanomolar agonist potency toward NTR-1 ($EC_{50} = 1.4$ nM) [25]. Based on the large body of evidence, NT is not only a good model to study novel modifications for improving CNS bioavailability, but this neuropeptide also offers an attractive template for designing future drugs for pain, psychiatric diseases, and even perhaps for epilepsy.

Our recent research with the anticonvulsant neuropeptide, GAL, showed that combining lipidization (by addition of Lys-palmitoyl, (K_p)) and cationization (through incorporation of three Lys residues) significantly improved CNS bioavailability of the resulting GAL analogs. The modified GAL analogs exhibited potent antiepileptic activity that was also accompanied by increased log *D* values and improved metabolic stability [26–28]. Lipidization of peptides is known to improve BBB-penetration of peptides [6,29]. Similarly, increased cationic character of the peptides has been previously shown to improve their delivery across biological membranes, including the BBB [30,31]. Despite its effectiveness in generating systemically active GAL analogs with antiepileptic activity, the lipidization–cationization strategy has not been evaluated on any other anticonvulsant neuropeptides.

To test the hypothesis that the combination of lipidization and cationization could improve systemic activity of structurally diverse anticonvulsant neuropeptides, this chemical modification strategy was applied to NPY and NT. Herein we report the design, chemical synthesis, and characterization of several BBB-penetrating analogs of both NPY and NT. Our results suggest that the lipidization–cationization strategy might be more broadly applicable across diverse neuropeptides toward improving metabolic stability and CNS bioactivity.

Materials and Methods

Chemical Synthesis

Synthesis of all analogs was carried out on solid phase using pre-loaded Rink Amide (NPY) or Wang (NT) resins.

Syntheses were carried out at 100 μ mol scale using Fmoc-Tyr(*t*Bu)-Rink Amide-MBHA resin (subs. 0.41 meq/g) or Fmoc-Leu-Wang resin (subs. 0.57 meq/g). Three couplings (30, 30, and 40 min) were performed using 0.2 M PyBOP (benzotriazol-1-yl-oxytripyrrolidinophosphonium hexafluorophosphate), 0.4 M DIPEA (*N,N*-diisopropylethylamine), and 200 mM of the appropriate amino acid. Fmoc-protecting groups were removed prior to the addition of the next amino acid by 30-min treatment with 20% piperidine. Protected amino acids, including Fmoc-Lys(palmitoyl) and Fmoc-6-aminohexanoic acid, were obtained from Chem-Impex International. Peptides were cleaved from resin by treatment with reagent K (82.5% TFA, 5% water, 5% ethanedithiol, 2.5% thioanisole *v/v*, 75 mg/ml phenol) followed by vacuum filtration to separate peptide from resin, and finally precipitated with chilled methyl-*tert*-butyl ether. Crude peptides were then purified by preparative reversed-phase HPLC over a linear gradient of Buffer B (90% acetonitrile in 0.1% TFA) ranging from 5 to 95% in 45 min. Purities of HPLC separations were assessed by analytical reversed-phase HPLC using a linear gradient ranging from 5 to 95% Buffer B in 30 min. HPLC fractions with peptide purities greater than 95% were pooled and quantified by measuring UV absorbance at 274.6 nm. Molecular masses of all analogs were confirmed by MALDI-TOF MS.

Partitioning Coefficient, log *D*

As an *in vitro* measure of lipophilicity of the analogs, log *D* values were calculated using the shake-flask method. Water-saturated *n*-octanol was prepared by mixing equal volumes of *n*-octanol and water for 24 h at room temperature. Lyophilized peptides were then reconstituted in 1 ml phosphate-buffered saline (PBS), followed by addition of an equal volume of water-saturated *n*-octanol. Samples were then allowed to mix on a rotary mixer for 24 h. Aqueous phases were carefully removed and analyzed by analytical HPLC over a gradient of Buffer B ranging from 5 to 95% in 30 min. The amount of peptide in the aqueous phase was determined by HPLC using a standard curve constructed for each peptide. Log *D* values for each analog were then calculated using the following equation [26,32]:

$$\log D = \log \left(\frac{[\text{Peptide}]_{\text{Octanol}}}{[\text{Peptide}]_{\text{Aqueous}}} \right) \quad (1)$$

Serum Stability Assay

The stability of peptides in the presence of 25% rat blood serum was evaluated for each analog by incubation at 37 °C for 0 min, 30 min, 1 h, 2 h, and 4 h. Samples were prepared by adding 10 μ g linear peptide, resuspended in *n*H₂O, to pre-heated tubes containing 25% rat blood serum and 0.1 M Tris–HCl, pH 7.5 to yield a final peptide concentration of 20 μ M. At the appropriate time points, reactions were quenched by precipitation of serum proteins through addition of 100 μ l isopropanol/water/trichloroacetic acid (45%:40%:15% by volume). Samples were then incubated at –20 °C for 20 min, followed by centrifugation at 10 000 rpm for 3 min to remove serum proteins. Supernatants were then analyzed by analytical HPLC equipped with a Waters YMC ODS-A 5 μ m 120 Å column using a gradient ranging from 5 to 95% Buffer B in 45 min including a 15-min pre-equilibration. Metabolic stability was assessed by determining a time-course of the disappearance of an intact peptide. Half-lives ($t_{1/2}$) for each peptide were determined from at least three independent time-course experiments using

the equation below (where m is the slope of the line and b is the y -intercept [26]):

$$t_{1/2}(h) = \frac{[\ln(50) - b]}{m} \quad (2)$$

Circular Dichroism

The α -helical content of NPY analogs was determined by CD. A measured quantity of 0.1 mg peptide was reconstituted in 1.0 ml NaF/phosphate buffer (50 mg KH_2PO_4 , 54 mg Na_2HPO_4 , 1.55 g NaF, 250 ml H_2O , pH 7.4 with Na_2HPO_4) or in 0.5 ml NaF/phosphate buffer combined with 0.5 ml TFE. After 1 h, 250 μl of each sample was loaded into a 0.1-cm quartz cuvette and analyzed using an Aviv 410 CD spectropolarimeter set to 25 °C. Scans were collected over the range of 250–200 nm in 1.0 nm steps with 1 s dwell time. Data were averaged from three scans and processed using Eqn (3), where M_r is the molecular weight, c is concentration (mg/ml), d is path length (cm), and n is the number of peptide bonds. Percent helicity was determined using Eqns (4) and (5) [26,33]:

$$[\Theta] = \frac{\Theta \times 100 \times M_r}{c \times d \times n} \quad (3)$$

$$[\Theta]_{\max} = -39\,500 \left[1 - \left(\frac{2.57}{n} \right) \right] \quad (4)$$

$$\% \alpha\text{-helix} = \frac{[\Theta_{222}]}{[\Theta_{\max}]} \times 100 \quad (5)$$

CD spectra for NT analogs were not collected as it has been shown previously that this peptide lacks secondary structure in both aqueous and sodium dodecyl sulfate ($\text{C}_{12}\text{H}_{25}\text{OSO}_3\text{Na}$)-containing environments [34].

Receptor Binding

Determination of binding affinity (K_i) for NPY analogs was provided by the National Institute of Mental Health's Psychoactive Drug Screening Program (NIMH PDSP). Binding affinities for the NPY-Y2 subtype were obtained using a nonlinear regression of radioligand competition binding isotherms. K_i values were calculated from best fit IC_{50} values using the Cheng–Prusoff equation [35]. Competitive binding of NT analogs toward the NTR-1 receptor subtype was assessed using a fluorescence-based assay. The assays were conducted in quadruplicate in a 96-well format on AcroWell filter plates using NTR-1 membrane preparations and Eu-labeled NT (Perkin-Elmer). Samples were incubated at room temperature followed by repeated rinsing with wash buffer (50 mM Tris-HCl, pH 7.5, and 5 mM MgCl_2) using a vacuum manifold. Prior to analysis, samples were incubated in 200 μl enhancement solution for 30 min at room temperature. Plates were read using a Perkin-Elmer VICTOR³ spectrofluorometer. Competitive binding curves were generated by GraphPad Prism software using a nonlinear regression, sigmoidal dose–response (variable slope) curve with no weights or constraints [27].

Anticonvulsant Activity

The anticonvulsant activity of the analogs was studied in the 6 Hz (32 mA) model of pharmacoresistant epilepsy following a bolus i.p. administration of a dose of 4 mg/kg to five groups of CF-1 mice ($n = 4$). At discrete time points (15, 30, 60, 120, and 240 min) following the drug administration, mice were challenged with a 6 Hz corneal stimulation (32 mA for 3 s delivered via corneal electrodes). Mice which did not exhibit classical limbic seizure

behavior (i.e. jaw chomping, vibrissae twitching, forelimb clonus, or Straub tail) were classified as protected. In addition to the 6 Hz screening, dose–response studies were carried out for the NPY-BBB2 and NT-BBB1 analogs. Briefly, peptide analogs were administered i.p., and at 1 h (time-to-peak effect), mice were then challenged with a 32-mA corneal stimulation. Based on the numbers of protected animals at each dosage, ED_{50} values were determined for each peptide using Probit software.

Results

Design Strategy

The lipidization–cationization strategy, previously applied to the truncated GAL analogs such as Gal-B2 (NAX-5055), was applied to the bioactive fragments of NPY and NT. To design NPY-derived compounds, two key SAR results were taken into account: (i) the C-terminal fragment of NPY, NPY(25–36), retains the agonist activity toward the Y2 receptor and (ii) bulky substituents can be added to the N -terminus of NPY(25–36) [12,15,36]. As illustrated in Figure 1, the Y2-targeting analogs were based on previously characterized $[\text{Ahx}^{5-24}]$ NPY, which contains the C-terminal fragment (NPY 25–36) [12,36]. To introduce the lipidization–cationization motif, a positively charged core was created near the N -terminus by replacement of the Pro-Ser sequence with Lys-Lys, whereas, Lys4 in $[\text{Ahx}^{5-24}]$ NPY was replaced with a N^{ϵ} -palmitoyl-L-lysine (K_p)

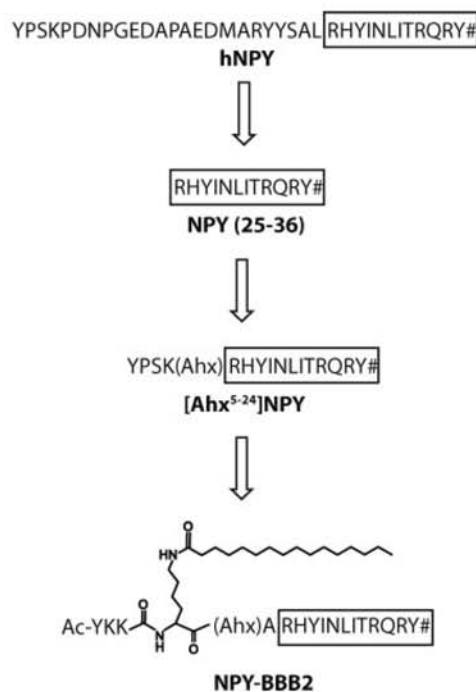


Figure 1. Rational design of systemically active NPY analogs with improved penetration across the BBB. Analogues were designed based on the Y2 receptor subtype selectivity of the NPY pharmacophore NPY (25–36) and the stabilizing effects of N -terminal residues observed in the previously described analog $[\text{Ahx}^{5-24}]$ NPY [12]. NPY-BBB2 combines the strategies of cationization and lipidization into centrally truncated NPY. (#) denotes C-terminal amidation of peptides, (Ahx) is 6-aminohexanoic acid.

Table 1. Summary of sequences, mass spectrometry data, HPLC retention times, and log *D* values for NT and NPY analogs^a

| Peptide analog | Structure | Molecular mass (calc/exp) | HPLC retention time ^b | Log <i>D</i> ^c |
|----------------|--|---------------------------|----------------------------------|---------------------------|
| NPY | | | | |
| NPY-BBB0 | Ac-(Ahx)ARHYINLITRQRY [#] | 1857.05/1856.81 | 16.8 ± 0.08 | -2.13 ± 0.68 |
| NPY-BBB1(K3) | Ac-YKKK(Ahx)RHYINLITRQRY [#] | 2333.36/2333.55 | 15.5 ± 0.01 | -1.38 ± 0.12 |
| NPY-BBB2(K3) | Ac-YKKK(Ahx)ARHYINLITRQRY [#] | 2404.4/2404.46 | 15.8 ± 0.07 | -1.11 ± 0.31 |
| NPY-BBB1 | Ac-YKK(K _p)(Ahx)RHYINLITRQRY [#] | 2571.59/2572.4 | 21.5 ± 0.03 | 2.82 ± 0.74 |
| NPY-BBB2 | Ac-YKK(K _p)(Ahx)ARHYINLITRQRY [#] | 2642.63/2642.7 | 21.8 ± 0.01 | 1.76 ± 0.01 |
| NT | | | | |
| NT-BBB0 | RRPYIL [^] | 816.5/816.5 | 14.0 ± 0.14 | -1.31 ± 0.35 |
| NT-BBB1(K4) | Ac-KKKKPYIL [^] | 1058.69/1058.70 | 13.1 ± 0.03 | 0.48 ± 0.01 |
| NT-BBB1 | Ac-K(K _p)KKPYIL [^] | 1296.91/1296.9 | 22.7 ± 0.01 | 1.19 ± 0.12 |

([#]) denotes an amidated C-terminus. (^) represents carboxylation at the C-terminus.
^a K_p is N^ε-palmitoyl-L-lysine, Ahx is 6-aminohexanoic acid.
^b Linear gradient of H₂O/acetonitrile.
^c Log *D* values calculated by the shake-flask method.

residue (Figure 1). No additional positively charged residues were introduced, as the presence of the Arg-His sequence provided additional positively charged residues located adjacent to the KKK_p(Ahx) motif (NPY-BBB1). Based on our previous SAR study with Gal-B2 [26], we designed an additional NPY analog, NPY-BBB2, in which the lipidization-cationization motif, 'KKK_p(Ahx)', was further separated from the active fragment by an additional Ala residue (Table 1, Figure 1). As the spacing between the active neuropeptide fragment and the lipidized-cationic motif was important for improving bioavailability of the GAL analogs, as determined by truncation of Gal-B2, we chose to insert an additional alanine into NPY-BBB1 (resulting in NPY-BBB2) rather than further truncate NPY-BBB1. In addition to the modified peptides, three additional NPY analogs were designed as controls (Table 1). All NPY-derived analogs were acetylated at the N-terminus and amidated at the C-terminus.

As summarized in Figure 2, a similar design strategy was applied to engineer NT analogs. The C-terminal hexapeptide sequences of NT (RRPYIL) and Contulakin-G (KKPYIL) (Contulakin-G is a venom-derived glycosylated conopeptide) are the active NT fragments that bind specifically to the NT receptors [37]. Noteworthy, the naturally occurring 'Lys-Lys' sequence in Contulakin-G provided part of the lipidization-cationization motif, whereas the lipoamino acid, Lys-palmitoyl, was introduced proximal to the Lys-Lys sequence. The position of Lys-palmitoyl was based on our previous finding that this position could accommodate a Lys-spermine residue without affecting receptor binding properties toward NTR-1 subtype of the NT receptors [25]. One additional Lys residue was added to the N-terminus, resulting in the KK_pKK motif. All NT analogs were acetylated at the N-terminus and contained a free carboxyl group at the C-terminus.

Chemical Synthesis

All analogs were synthesized on solid support using an automated peptide synthesizer and standard Fmoc protocols. Peptides were cleaved from resin by treatment with reagent K and were purified by preparative reversed-phase HPLC. Peptides were quantified by UV absorbance at 274.6 nm, aliquoted, and lyophilized. Masses of all compounds were confirmed by MALDI-TOF MS. Final yields of purified peptide analogs ranged between 2% for the modified peptides and 8% for the unmodified active fragments. Overall

yields were calculated from the averages of multiple syntheses with respect to the amount of resin used in each 100 μmole synthesis. Retention times were calculated from the average of three independent analyses of each analog and are summarized in Table 1.

The partitioning coefficient (log *D*) for each analog was determined using the shake-flask method. Calculated values for partitioning are summarized in Table 1. The unmodified active fragments NT-BBB0 and NPY-BBB0 were hydrophilic in nature indicated by negative log *D* values of -1.31 and -2.13, respectively. Cationization through conjugation of the oligo-Lys motif to the N-terminus of the bioactive fragments showed slight improvement in partitioning with values of 0.48 for NT-BBB1 (K4), -1.38 for NPY-BBB1(K3), and -1.11 for NPY-BBB2(K3). The analogs possessing the combination of cationization and lipidization showed dramatic improvement over both the peptide active fragments and the cationic analogs. NT-BBB1 had a log *D* of 1.19, NPY-BBB1 a log *D* of 2.82, and NPY-BBB2 a log *D* of 1.76 (Figure 3).

Structural Characterization of NT/NPY Analogs

To evaluate effects of the chemical modifications on helical content of the resulting NPY analogs, CD experiments were carried out (Figure 4). Recordings were performed in aqueous 150 mM NaF phosphate buffer, pH 7.4 both in the absence and in the presence of 50% (v/v) TFE. Helical content (θ₂₂₂) for full-length NPY in the presence of TFE was calculated as 21.4%. The NPY-BBB0 analog exhibited comparable helicity at 18.1%. Increased cationization of the active fragment in the BBB1(K3) and BBB2(K3) analogs disrupted the secondary structure and resulted in helical contents of 9.7 and 2.2%, respectively. For NPY analogs containing the lipoamino acid and oligo-Lys components, helicity was determined as 12.6 and 15.0% for BBB1 and BBB2, respectively (Figure 4). We did not characterize NT analogs using CD, as the previous work has shown NT lacks secondary structure [33,34].

Metabolic Stability of NT/NPY Analogs

To determine how the lipidization-cationization changed the *in vitro* metabolic stability of the NPY and NT analogs, the selected peptides were incubated in 25% rat blood serum at

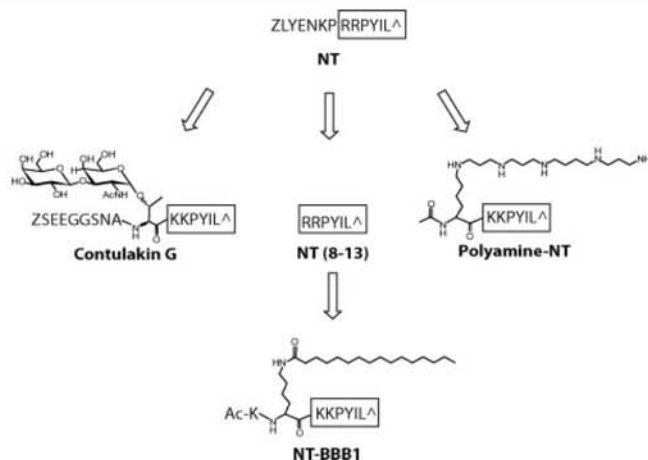


Figure 2. Rational design of systemically active NT-based analogs with improved penetration across the BBB. The Contulakin-G isolated from cone snail venom [37], the NT active fragment RRPYIL [21], and polyamine-NT [25] are all potent ligands for the NT receptor. In NT-BBB1, the lipomoino acid was introduced in the position proximal to the C-terminal active fragment. The cationization part was achieved by adding the N-terminal Lys residue to two already existing Lys residues that comprised the NT active fragment. (Z) denotes pyrroglutamic acid and (^) represents carboxylated C-terminus.

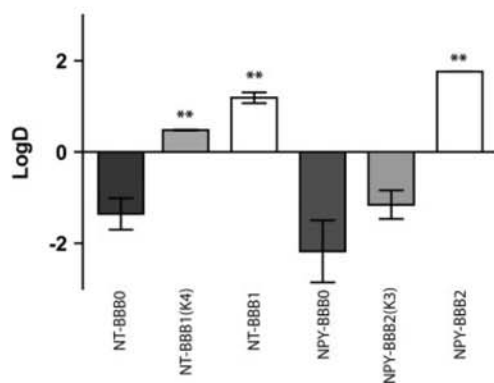


Figure 3. Summary of log *D* values of NT and NPY analogs. Log *D* values were obtained from the average of three independent experiments via the shake-flask method using a 50:50 ratio of *n*-octanol/PBS, pH 7.4 at 25 °C. The amount of peptide in the aqueous phase was determined by peak area using analytical HPLC over a gradient ranging from 5 to 95% Buffer B in 30 min. Results were obtained from the slopes of at least three independent experiments. Statistical comparisons between unmodified and modified analogs were performed using the two-tailed *t*-test function of GraphPad software. Statistical significance was noted as: (**) *P*-value < 0.01.

37 °C and degradation was monitored by HPLC. Aliquots were withdrawn after 30 min, 1 h, 2 h, and 4 h and quenched with TCA followed by HPLC separations [26,38]. The time courses of the disappearance of the intact peaks were plotted and half-lives were calculated.

As summarized in Figure 5, *in vitro* metabolic stability was significantly increased using the strategy described here. For unmodified NPY and NT analogs, the $t_{1/2}$ values were 40 and 4.7 min, whereas the NPY-BBB1, NPY-BBB2, and NT-BBB1 analogs had $t_{1/2}$ values of 3.2, 3.0, and 2.7 h, respectively. Noteworthy, the *in vitro* metabolic stability was also increased in the analogs containing only oligo-Lys motifs, such as NT-

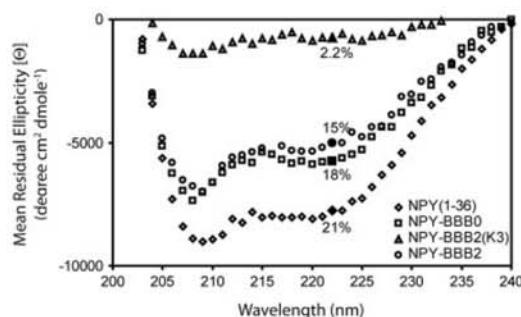


Figure 4. Helical properties of NPY-BBB2. CD spectra showing the relative α -helical content of NPY analogs: Full-length NPY (\diamond), NPY-BBB0 (\square), NPY-BBB2 (\circ), and NPY-BBB2(K3) (\triangle). Percent helicity was calculated at 222 nm and is noted by filled data points. Data were obtained in aqueous 150 mM NaF phosphate buffer, pH 7.4 both in the absence and in the presence of 50% (v/v) TFE.

BBB1(K4), NPY-BBB1(K3), and NPY-BBB2(K3). It was previously shown that short cationic peptides exhibit increased binding to serum albumin [39,40]. Furthermore, improved metabolic stability was observed for the GAL analogs: conjugation of the oligo-Lys motif to the GAL active fragment ($t_{1/2}$ = 28 min) increased $t_{1/2}$ by nearly tenfold ($t_{1/2}$ = 4.6 h) [26]. It is therefore possible that increased cationization of NPY, NT, and GAL analogs could result in extended $t_{1/2}$ values through increased peptide binding to albumin in serum-containing solutions.

Pharmacological Characterization

NPY and NT analogs were characterized both in the receptor binding assays and in a mouse model of epilepsy. Binding affinities were determined for the Y2 receptor through a competition assay against [¹²⁵I] Peptide YY, whereas for the NTR-1 receptor, a time-resolved fluorescence-based competitive binding assay

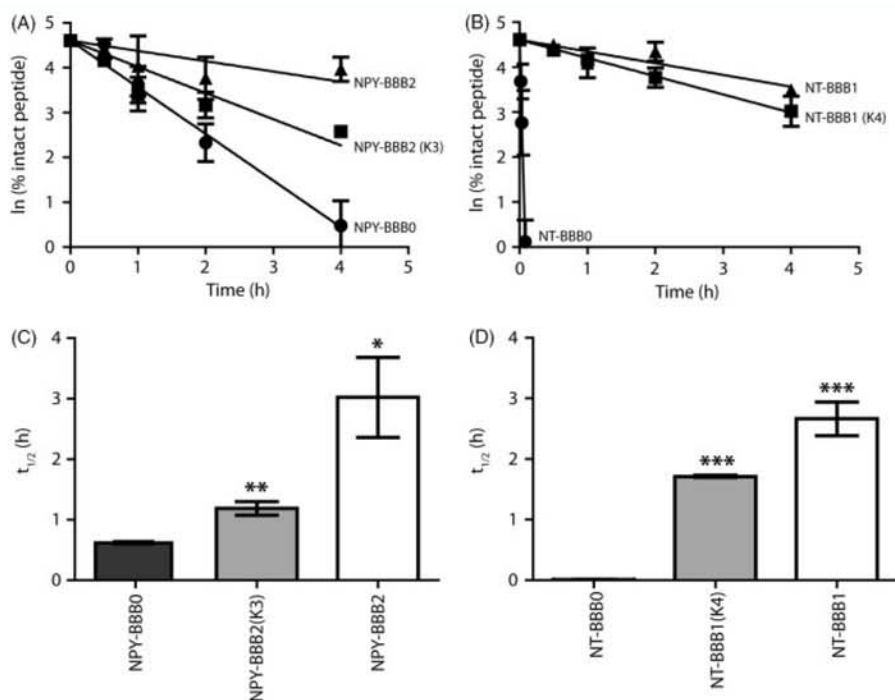


Figure 5. Metabolic stability of the NT and NPY analogs determined in the *in vitro* serum stability assay. (A) Time-course of disappearance of NPY-based analogs. (B) Time-course of disappearance of NT-based analogs. (C) Half-lives for NPY-BBB0, NPY-BBB2(K3), and NPY-BBB2 were calculated as 0.67, 1.2, and 3.0 h, respectively. (D) $t_{1/2}$ for NT-BBB0, NT-BBB1(K4), and NT-BBB1 were calculated as 0.01, 1.7, and 2.7 h, respectively. Results were obtained from the slopes of at least three independent experiments. Statistical comparisons of unmodified and modified analogs were performed using the two-tailed *t*-test function of GraphPad software. Statistical significance was noted as: (*) *P*-value <0.05, (**) *P*-value <0.01, and (***) *P*-value <0.0001.

was employed. The antiepileptic activity of the analogs was assessed in the 6 Hz model of epilepsy in mice following *i.p.* administration. All pharmacological data are summarized in Table 2.

All modified analogs exhibited low nanomolar affinities toward their target receptors (Table 2 and Figure 6), suggesting that the chemical modifications did not affect interactions with the target receptors. The K_i value for the unmodified NPY-BBB0 was determined as 60.6 nM. Noteworthy, NPY-BBB1(K3) and NPY-BBB1 actually exhibited tighter binding toward the Y2 receptor as compared to the active fragment by itself. For NT analogs, the addition of two Lys residues did not affect the affinity of the NT active fragment toward NTR-1; however, incorporation of the lipoamino acid decreased the affinity by 1 order of magnitude (K_i for NT-BBB1 was 4.0 nM).

Next, the analogs were characterized for their ability to suppress seizures in mice following systemic administration. The time-response curves were determined by measuring the number of mice protected from seizures (in groups of four mice) at the following time points: 15, 30, 60, 120, and 240 min. The unmodified and oligo-Lys containing analogs of NPY did not exhibit significant anticonvulsant activity at 4 mg/kg, *i.p.* (this dose was previously used for *in vivo* screening of anticonvulsant analogs of GAL). The dose of 4 mg/kg of NPY-BBB1 produced, at most, a very modest anticonvulsant activity at 30 and 60 min post-drug administration, whereas at the same dose, NPY-BBB2 yielded a significant anticonvulsant

effect with time-to-peak effect between 30 and 60 min. For NT analogs, the unmodified active fragment (NT-BBB0) lacked antiepileptic activity. The lipoamino acid containing NT-BBB1 was very active in the epilepsy test, producing a full protection from seizures at 60 min. The two most active analogs (NPY-BBB2 and NT-BBB1) were further evaluated in a dose-response study. Figure 6 illustrates the dose-response curves, and the calculated ED_{50} data are shown in Table 3. ED_{50} values for NT-BBB1 and NPY-BBB2 were calculated as 2.86 mg/kg (95% CI = 1.44–4.36 mg/kg) and 1.07 mg/kg (95% CI = 0.41–1.80 mg/kg), respectively.

Discussion

Our previous work on engineering systemic bioavailability in GAL analogs yielded very potent antiepileptic compounds [26–28,41]. In the present work, we successfully applied the same strategy, namely combining a lipoamino acid with several adjacent Lys residues (lipidization-cationization motif) to two other anticonvulsant neuropeptides, NPY and NT. The apparent similarities of physicochemical and pharmacological properties of all three analogs, GAL-B2, NPY-BBB2, and NT-BBB1, are summarized in Table 3. Two analogs described in this work, namely NPY-BBB2 and NT-BBB1, appeared as potent antiepileptic compounds following systemic delivery while exhibiting improved *in vitro* serum stability, suggesting that this strategy might be

Table 2. Pharmacological properties of NT and NPY analogs

| Peptide analog | Receptor binding assay | <i>In vivo</i> anticonvulsant activity 6 Hz, 32 mA, 4 mg/kg | | | | |
|----------------|------------------------|---|--------|--------|---------|---------|
| | K_i [nM] | 15 min | 30 min | 60 min | 120 min | 240 min |
| NPY | | | | | | |
| NPY-BBB0 | 60.6 ± 4.6 | | | n.d. | | |
| NPY-BBB1(K3) | 3.6 ± 0.4*** | 1/4 | 0/4 | 0/4 | 0/4 | 0/4 |
| NPY-BBB2(K3) | n.d. | 1/4 | 0/4 | 0/4 | 0/4 | 0/4 |
| NPY-BBB1 | 14.2 ± 0.7*** | 0/4 | 1/4 | 1/4 | 0/4 | 0/4 |
| NPY-BBB2 | 26.1 ± 1.7*** | 1/4 | 3/4 | 3/4 | 0/4 | 0/4 |
| NT | | | | | | |
| NT-BBB0 | 0.2 ± 0.1 | 0/4 | 0/4 | 0/4 | 0/4 | 0/4 |
| NT-BBB1(K4) | 0.5 ± 0.1* | 0/4 | 0/4 | 0/4 | 0/4 | 0/4 |
| NT-BBB1 | 4.0 ± 0.2*** | 3/4 | 2/4 | 4/4 | 3/4 | 1/4 |

K_i values were calculated as the average of three independent binding experiments. Statistical significance between unmodified and modified analogs, calculated using the two-tailed *t*-test function GraphPad software, was noted as: (*) *P*-value <0.05, (**) *P*-value <0.01, and (***) *P*-value <0.0001. 6 Hz data obtained from five independent groups of four mice each. Data represent the number of mice within each group that did not exhibit classical seizure activity at each time point.

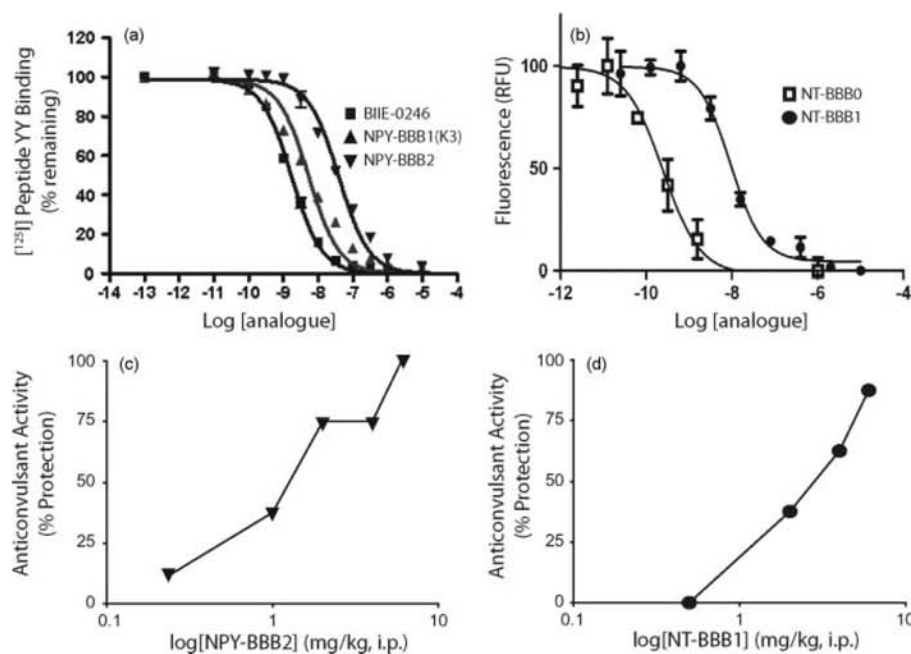


Figure 6. Pharmacological characterization of NPY and NT analogs. (A) NPY analogs were screened in a competitive binding assay against ¹²⁵I-labeled NPY. (A) The binding curves for NPY-BBB1 (K3) ($K_i = 3.6$ nM) and NPY-BBB2 ($K_i = 26$ nM) and the BIIE-0246 reference standard ($K_i = 1.2$ nM). (B) Binding affinities of NT analogs toward the NTR-1 receptor were determined using fluorescence-based competitive binding assay. Shown here are the binding curves for NT-BBB0 and NT-BBB1 ($K_i = 0.2$ and 4.0 nM, respectively). (C) Bolus injections of NPY-BBB2 and NT-BBB1 (shown in panel D) were administered i.p. and dose–response curves were generated at the 1 h time point. Based on the dose–response data, the calculated ED50 values for NPY-BBB2 and NT-BBB1 were calculated as 1.07 and 2.86 mg/kg, respectively, using Probit software.

more generally applicable to neuropeptides to improve their penetration across the BBB.

Lipidization–cationization was successfully applied to the KKPYL motif (NT-BBB0). The *N*-terminal addition of Lys and Lys-palmitoyl residues resulted in an increased log *D* value and improved half-life in the serum stability assay, whereas the receptor binding retained high nanomolar affinity. The improvements of

log *D* and metabolic stability were correlated with pronounced anticonvulsant activity in the 6 Hz mouse model of epilepsy after i.p. administration. Noteworthy, the lipidization–cationization alone did not produce antiseizure activity [28] suggesting that the anticonvulsant activities of the modified neuropeptides are mediated by their target receptors expressed in the brain. Although this work adds one more example of BBB-permeable NT-based analogs

Table 3. Summary of physicochemical and pharmacological properties of three lead anticonvulsant neuropeptides containing the lipidization–cationization motif

| Analog | Log <i>D</i> | <i>t</i> _{1/2} (h) | ED ₅₀ (mg/kg) ^a | <i>K</i> _i [nM] ^b |
|---------------------|--------------|-----------------------------|---------------------------------------|---|
| Gal-B2 ^a | 1.24 | 9.4 | 0.8 (0.4–1.6) | 3.5 |
| NPY-BBB2 | 1.76 | 3.0 | 1.1 (0.4–1.8) | 26.1 |
| NT-BBB1 | 1.19 | 2.7 | 2.9 (1.4–4.4) | 4.0 |

Partitioning coefficients were calculated using the shake-flask method of log *D* determination. All modified analogs were shown to possess increased lipophilicity compared to the unmodified peptides. Modified GAL, NPY, and NT analogs showed increased resistance to proteolytic degradation in an *in vitro* serum stability assay as evidenced by increased serum half-lives (*t*_{1/2}).

^a ED₅₀ values were calculated at a time-to-peak effect of 1 h.

^b *K*_i values for analogs were calculated against receptors implicated in seizure activity (i.e. hGalR1, hNTR-1, and hNPY-Y2, respectively).

(such as NT69L [42], JMW2012 [23], or KK13 [43]), it is the first report of the systemically active NT analog that has antiepileptic activity.

Systemically active NPY analogs were rationally designed based on Y2-selective analogs developed by the group of Beck-Sickinger [12]. NPY-BBB2 contained the lipidization–cationization motif and exhibited increased log *D*, improved metabolic stability and systemic bioavailability, while maintaining nanomolar affinity toward NPY-Y2 receptor. The C-terminal residues of NPY (NPY 25–36) are required for Y2 receptor subtype specificity [12,15] and NPY-BBB2 indeed maintained similar Y2-binding affinity to that described by Rist and colleagues for the Ac-NPY 25–36 analog (*K*_i = 26.1 nM vs 21 nM) [15]. We hypothesize that the anticonvulsant activity of NPY-BBB2 is mediated by targeting Y2 receptor subtypes expressed in hippocampus [1], but more *in vivo* pharmacological studies are needed to prove this hypothesis. In addition, we acknowledge that further receptor binding and functional studies are required to evaluate the subtype selectivity and agonist properties of NPY-BBB2. Without more detailed receptor studies, it is also difficult to reconcile the differences in anticonvulsant activity between NPY-BBB1 and NPY-BBB2. Our work encourages further engineering of systemically active NPY analogs not only as antiepileptic drugs, but also as analgesics and as drug leads for other indications. We are currently evaluating NPY analogs in analgesic models. It is

possible to modify NPY analogs toward subtype selectivity for Y1 receptor by either point mutations, such as Q34P [12] or lactamization [15]. Such modifications may result in peptide-based leads for regulating food uptake, blood pressure, or anxiety [12,44].

Our efforts to generate systemically active analogs of GAL, NPY, and NT peptide analogs with anticonvulsant properties encourages the extension of the lipidization–cationization strategy for delivery of other neuropeptides into the brain and/or spinal cord. Table 4 summarizes examples of neuropeptides that are attractive targets for improving their BBB-penetration. Available SAR results facilitate the rational design of such BBB-permeable analogs by choosing optimal positions outside the active fragments for the introduction of the lipidization–cationization motif. Typically, either the N- or C-terminus in a given neuropeptide has been observed to be most amenable for modification. Based on the previous SAR studies, N-terminal modifications of NPFF or bombesin with oligo-Lys and lipoamino acids may improve their systemic bioavailabilities [45,46], whereas these modifications may be more effective at the C-terminus of orphanin and ghrelin [47–49]. Although our strategy of improving bioavailability of anticonvulsant neuropeptides (GAL, NT, and NPY) described here and in our previous studies requires further validation, nonetheless it offers an attractive alternative to the challenging development of systemically bioavailable non-peptidic agonists that are receptor-specific and subtype-selective [50]. Such BBB-permeable analogs could not only be useful pharmacological tools but perhaps could even offer first-in-class compounds to validate therapeutic targets in human clinical trials.

Acknowledgements

This work was supported by the University of Utah Startup Funds and the NIH grant R21 NS059669. Receptor binding of NPY analogs was performed by the NIMH PDSP at the University of North Carolina at Chapel Hill. Gratitude is extended to Charles Robertson and Hee-Kyoung Lee for numerous conversations integral to this work. GB and HSW are scientific co-founders of NeuroAdjvants, Inc.

References

- 1 El Bahh B, Balosso S, Hamilton T, Herzog H, Beck-Sickinger AG, Sperk G, Gehlert DR, Vezzani A, Colmers WF. The anti-epileptic

Table 4. Selected examples of neuroactive peptides that may be modified with either N- or C-terminal lipidization–cationization motif for improved metabolic stability and bioavailability

| Peptide | Structure | Target receptor(s) | Potential application | Literature reference |
|----------|---|--|---|----------------------|
| NPFF | <u>FLFQPQR</u> [#] | Neuropeptide FF receptor (NPFFR1) agonist | Analgesia | 45 |
| Bombesin | <u>ZQLGNQWAVGHLM</u> [#] | Bombesin receptor subtype 3 (BRS-3) agonist | Regulation of food intake; anxiolytic drug | 46 |
| Orphanin | <u>EGGFTGARKSARKLANQ</u> [^] | Nociceptin (NOP) receptor agonist | Regulation of food intake; anxiolytic drug; nociception | 49 |
| Ghrelin | <u>GSS</u> [*] <u>FLSPEHQRVQRKESKPPAKLQPR</u> [^] | Growth hormone secretagog receptor (GHS-R) agonist | Metabolic disorders | 48 |

Selected neuroactive peptides that exert agonist activities through their respective receptors in the CNS. Underlined amino acid residues denote the biologically active fragment of each compound. Modified peptide analogs would retain this fragment while conjugating oligo-lysine and lipoamino acid motifs. (Z) represents pyroglutamic acid, (S*) denotes Ser(O-CO-C₇H₁₅) residue, (#) denotes an amidated C-terminus, and (^) represents carboxylation at the C-terminus.

- actions of neuropeptide Y in the hippocampus are mediated by Y₂ and not Y₅ receptors. *Eur. J. Neurosci.* 2005; **22**: 1417–1430.
- 2 Lee H-K, Zhang L, Smith MD, White HS, Bulaj G. Glycosylated neurotensin analogues exhibit sub-picomolar anticonvulsant potency in a pharmacoresistant model of epilepsy. *Chem. Med. Chem.* 2009; **4**: 400–405.
 - 3 Mazarati AM. Galanin and galanin receptors in epilepsy. *Neuropeptides* 2004; **38**: 331–343.
 - 4 Brasnjevic I, Steinbusch HWM, Schmitz C, Martinez-Martinez P. Delivery of peptide and protein drugs over the blood–brain barrier. *Prog. Neurobiol.* 2009; **87**: 212–251.
 - 5 van de Waterbeemd H, Lennernas H, Artursson P. *Drug Bioavailability: Estimation of Solubility, Permeability, Adsorption and Bioavailability*. Wiley-VCH: Weinheim, 2003.
 - 6 Egleton RD, Davis TP. Bioavailability and transport of peptides and peptide drugs into the brain. *Peptides* 1997; **18**: 1431–1439.
 - 7 Cabrele C, Beck-Sickinger AG. Molecular characterization of the ligand–receptor interaction of the neuropeptide Y family. *J. Pept. Sci.* 2000; **6**: 97–122.
 - 8 Parker SL, Balasubramaniam A, Neuropeptide Y. Y₂ receptor in health and disease. *Br. J. Pharmacol.* 2008; **153**: 420–431.
 - 9 Foti S, Haberman RP, Samulski RJ, McCown TJ. Adeno-associated virus-mediated expression and constitutive secretion of NPY or NPY13–36 suppresses activity in vivo. *Gene Ther.* 2007; **14**: 1534–1536.
 - 10 Noe F, Frasca A, Balducci C, Carli M, Sperk G, Ferraguti F, Pitkanen A, Bland R, Fitzsimons H, During M, Vezzani A. Neuropeptide Y. overexpression using recombinant adeno-associated viral vectors. *Neurotherapeutics* 2009; **6**: 300–306.
 - 11 Beck-Sickinger AG, Wieland HA, Wittneben H, Willim K-D, Rudolf K, Jung G. Complete L-alanine scan of neuropeptide Y reveals ligands binding to Y₁ and Y₂ receptors with distinguished conformations. *Eur. J. Biochem.* 1994; **225**: 947–957.
 - 12 Beck-Sickinger AG, Jung G. Structure–activity relationships of neuropeptide Y analogues with respect to Y₁ and Y₂ receptors. *Biopolymers* 1995; **37**: 123–142.
 - 13 Krstenansky JL, Owen TJ, Buck SH, Hagaman KA, McLean LR. Centrally truncated and stabilized porcine neuropeptide Y analogs: design, synthesis, and mouse brain receptor binding. *Proc. Natl. Acad. Sci.* 1989; **86**: 4377–4381.
 - 14 Rist B, Wieland HA, Willim K-D, Beck-Sickinger AG. A rational approach for the development of reduced-size analogues of neuropeptide Y with high affinity to the Y₁ receptor. *J. Pept. Sci.* 1995; **1**: 341–348.
 - 15 Rist B, Zerbe O, Ingenhoven N, Scapozza L, Peers C, Vaughan PFT, McDonald RL, Wieland HA, Beck-Sickinger AG. Modified, cyclic dodecapeptide analog of neuropeptide Y is the smallest full agonist at the human Y₂ receptor. *FEBS* 1996; **394**: 169–173.
 - 16 Cox HM, Krstenansky JL. The effects of selective amino acid substitution upon neuropeptide Y antisecretory potency in rat jejunum mucosa. *Peptides* 1991; **12**: 323–327.
 - 17 Cáceda R, Kinkead B, Nemeroff CB. Neurotensin: role in psychiatric and neurologic diseases. *Peptides* 2006; **27**: 2385–2404.
 - 18 Boules M, Fredrickson P, Richelson E. Bioactive analogs of neurotensin: focus on CNS effects. *Peptides* 2006; **27**: 2523–2533.
 - 19 Dobner PR. Neurotensin and pain modulation. *Peptides* 2006; **27**: 2405–2414.
 - 20 Fürst S. Transmitters involved in antinociception in the spinal chord. *Brain Res. Bull.* 1999; **48**: 129–141.
 - 21 Henry JA, Horwell DC, Meecham KG, Rees DC. A structure–affinity study of the amino acid side-chains of neurotensin: N and C terminal deletions and Ala-scan. *Bioorg. Med. Chem. Lett.* 1993; **3**: 949–952.
 - 22 Tyler-McMahon BM, Boules M, Richelson E. Neurotensin: peptide for the next millennium. *Regul. Pept.* 2000; **93**: 125–136.
 - 23 Bredeloux P, Cavelier F, Dubuc I, Vivet B, Costentin J, Martinez J. Synthesis and biological effects of c(Lys-Lys-Pro-Tyr-Ile-Leu-Lys-Pro-Tyr-Ile-Leu) (JMV2012), a new analogue of neurotensin that crosses the blood–brain barrier. *J. Med. Chem.* 2008; **51**: 1610–1616.
 - 24 Kokko KP, Hadden MK, Orwig KS, Mazella J, Dix TA. In vitro analysis of stable, receptor-selective neurotensin [8–13] analogs. *J. Med. Chem.* 2003; **46**: 4141–4148.
 - 25 Zhang L, Lee H-K, Pruess TH, White HS, Bulaj G. Synthesis and applications of polyamine amino acid residues: improving the bioactivity of an analgesic neuropeptide, neurotensin. *J. Med. Chem.* 2009; **52**: 1514–1517.
 - 26 Bulaj G, Green BR, Lee H-K, Robertson CR, White K, Zhang L, Sochanska M, Flynn SP, Scholl EA, Pruess TH, Smith MD, White HS. Design, synthesis, and characterization of high-affinity, systemically-active galanin analogues with potent anticonvulsant activities. *J. Med. Chem.* 2008; **51**: 8038–8047.
 - 27 Zhang L, Robertson CR, Green BR, Pruess TH, White HS, Bulaj G. Structural requirements for a lipoo amino acid in modulating the anticonvulsant activities of systemically active galanin analogues. *J. Med. Chem.* 2009; **52**: 1310–1316.
 - 28 White HS, Scholl EA, Klein BD, Flynn SP, Pruess TH, Green BR, Zhang L, Bulaj G. Developing novel antiepileptic drugs: characterization of NAX 5055, a systemically-active galanin analog, in epilepsy models. *Neurotherapeutics* 2009; **6**: 372–380.
 - 29 Egleton RD, Davis TP. Development of neuropeptide drugs that cross the blood–brain barrier. *NeuroRx* 2005; **2**: 44–53.
 - 30 Fuchs SM, Raines RT. Internalization of cationic peptides: the road less (or more?) traveled. *Cell. Mol. Life Sci.* 2006; **63**: 1819–1822.
 - 31 Drin G, Cottin S, Blanc E, Rees AR, Temsamani J. Studies on the internalization mechanism of cationic cell-penetrating peptides. *J. Biol. Chem.* 2003; **278**: 31192–31201.
 - 32 Wang J, Wu D, Shen WC. Structure–activity relationship of reversibly lipidized peptides: studies of fatty acid-desmopressin conjugates. *Pharm. Res.* 2002; **19**: 609–614.
 - 33 Chen Y-H, Yang JT, Chau KH. Determination of the helix and beta form of proteins in aqueous solution by circular dichroism. *Biochemistry* 1974; **13**: 3350–3359.
 - 34 Wu C-SC, Ikeda K, Yang JT. Ordered conformation of polypeptides and proteins in acidic dodecylsulfate solution. *Biochemistry* 1981; **20**: 566–570.
 - 35 Cheng Y-C, Prusoff WH. Relationship between the inhibition constant (K_i) and the concentration of inhibitor which causes 50 percent inhibition (IC₅₀) of an enzymatic reaction. *Biochem. Pharmacol.* 1973; **22**: 3099–3108.
 - 36 Langer M, Bella RL, Garcia-Garayoa E, Beck-Sickinger AG. 99mTc-labeled neuropeptide Y analogues as potential tumor imaging agents. *Bioconjug. Chem.* 2001; **12**: 1028–1034.
 - 37 Craig AG, Norberg T, Griffin D, Hoeger C, Akhtar M, Schmidt K, Low W, Dykert J, Richelson E, Navarro V, Mazella J, Watkins M, Hillyard D, Imperial J, Cruz LJ, Olivera BM. Contulakin-G, an O-glycosylated invertebrate neurotensin. *J. Biol. Chem.* 1999; **274**: 13752–13759.
 - 38 Malakoutikhah M, Teixidó M, Giralte E. Toward and optimal blood–brain barrier shuttle by synthesis and evaluation of peptide libraries. *J. Med. Chem.* 2008; **51**: 4881–4889.
 - 39 Svenson J, Brandsdal B, Stensen W, Svendsen JS. Albumin binding of short cationic antimicrobial micropeptides and its influence on the in vitro bactericidal effect. *J. Med. Chem.* 2007; **50**: 3334–3339.
 - 40 Manezo Y, Khachatourian C. Peptides bound to albumin. *Life Sci.* 1986; **39**: 1751–1753.
 - 41 Robertson CR, Scholl EA, Pruess TH, Green BR, White HS, Bulaj G. Engineering galanin analogues that discriminate between GalR1 and GalR2 subtypes and exhibit anticonvulsant activity following systemic delivery. *J. Med. Chem.* 2010; **53**: 1871–1875.
 - 42 Tyler-McMahon BM, Stewart JA, Farinas F, McCormick DJ, Richelson E. Highly potent neurotensin analog that causes hypothermia and antinociception. *Eur. J. Pharmacol.* 2000; **390**: 107–111.
 - 43 Hadden MK, Orwig KS, Kokko KP, Mazella J, Dix TA. Design, synthesis, and evaluation of the antipsychotic potential of orally bioavailable neurotensin (8–13) analogues containing non-natural arginine and lysine residues. *Neuropharmacology* 2005; **49**: 1149–1159.
 - 44 MacNeil DS. NPY Y₁ and Y₅ receptor selective antagonists as anti-obesity drugs. *Curr. Top. Med. Chem.* 2007; **7**: 1721–1733.
 - 45 Gicquel S, Mazarguil H, Desprat C, Allard M, Devillers J-P, Simonet G, Zajac J-M. Structure–activity study of neuropeptide FF: contribution of N-terminal regions to affinity and activity. *J. Med. Chem.* 1994; **37**: 3477–3481.
 - 46 Mantey SA, Gonzalez N, Schumann M, Pradhan TK, Shen L, Coy DH, Jensen RT. Identification of bombesin receptor subtype-specific ligands: effect of N-methyl scanning, truncation, substitution, and evaluation of putative reported selective ligands. *J. Pharmacol. Exp. Ther.* 2006; **319**: 980–989.
 - 47 Guerrini R, Caló G, Lambert DG, Carrá G, Arduin M, Barnes TA, McDonald J, Rizzi D, Trapella C, Marzola E, Rowbotham DJ, Regoli D, Salvadori S. N- and C-terminal modifications of nociceptin/orphanin

- FQ generate highly potent NOP receptor ligands. *J. Med. Chem.* 2005; **48**: 1421–1427.
- 48 Matsumoto M, Hosada H, Kitajima Y, Morozumi N, Minamitake Y, Tanaka S, Matsuo H, Kojima M, Hayashi Y, Kanagawa K. Structure–activity relationship of ghrelin: pharmacological study of ghrelin peptides. *Biochem. Biophys. Res. Commun.* 2001; **287**: 142–146.
- 49 Reinscheid RK, Ardati A, Frederick J, Monsma J, Civelli O. Structure–activity relationship studies on the novel neuropeptide orphanin FQ. *J. Biol. Chem.* 1996; **271**: 14163–14168.
- 50 Hruby VJ. Designing peptide receptor agonists and antagonists. *Nat. Rev. Drug Discov.* 2002; **1**: 847–858.

CHAPTER 4

ANALGESIC NEUROPEPTIDE W SUPPRESSES SEIZURES IN THE BRAIN REVEALED BY RATIONAL REPOSITIONING AND PEPTIDE ENGINEERING

4.1 Abstract

Various neuropeptides play an important neuromodulatory role in controlling neuronal hyperexcitability that leads to pain or seizures. Based on overlapping inhibitory mechanisms, anticonvulsant compounds exhibit concurrent analgesic and antiepileptic activities. The recently deorphanized neuropeptide W (NPW), targets the G-protein coupled receptors NPBW₁ (GPR7) and NPBW₂ (GPR8). This peptide was previously shown to possess analgesic properties, in addition to controlling feeding and energy metabolism coupled to brain levels of leptin. Given the similar mechanistic origins of pain and seizure, we tested the hypothesis that the analgesic activity of NPW may lead to the discovery the antiepileptic activity of this peptide. Indeed, intracerebroventricular (i.c.v.) administration of NPW potently reduced seizures in the 6 Hz psychomotor seizure model in mice. Subsequently, we rationally designed, synthesized, and characterized metabolically-stable NPW analogs aimed to penetrate the blood-brain barrier (BBB). The NPW analogs containing backbone spacers, a lipoamino acid and oligo-Lys motifs demonstrated anticonvulsant activity following systemic (intraperitoneal) administration.

Our results provided proof of concept that the combination of the repositioning strategy and engineering BBB-penetrating neuropeptide analogs could provide new drug leads for the treatment of pain and/or epilepsy. Furthermore, our lead analog, NPW-B1, has a potential for studying the anorexic effects of NPW. We suggest that rational repositioning of biologics is an attractive tool for discovering new functions of already well characterized peptides and proteins.

4.2 Introduction

Neuropathic pain and epileptic seizures both result from an imbalance between excitation and inhibition of neuronal firing. This imbalance is typically caused by agonism of excitatory neurotransmission or by antagonism of inhibitory neurotransmission. The recent use of antiepileptic compounds for the treatment of pain (repositioning) is largely due to the compounds' ability to inhibit excessive firing in neurons through voltage and ligand-gated ion channel activities (1). It has been well documented that several anticonvulsant neuropeptides possess concurrent antiepileptic and analgesic activities (Table 4.1). For example, galanin (Gal), neuropeptide Y (NPY), and somatostatin (SOM) are well known for their abilities to control seizures in the brain (2-4) in addition to exerting analgesic activities (5-7). Past studies of neurotensin (NT) and enkephalin (Enk) widely focused on their analgesic activities; however these peptides were recently shown to also act as potent anticonvulsants (8-10). The mutual relationship between analgesic and anticonvulsant properties of neuropeptides suggests that repositioning may be an attractive approach to discover their new functions.

Recently, two highly homologous endogenous neuropeptides, neuropeptide W (NPW) and neuropeptide B (NPB), were identified as high affinity ligands for NPBW₁

Table 4.1 Examples of neuropeptides that possess both analgesic and antiepileptic activities in animal models of pain and epilepsy.

| Neuropeptide | Analgesic Activity | Antiseizure Activity |
|---------------------|---|---|
| Galanin | Model: formalin inflammatory pain assay (5) | Model: self-sustaining status epilepticus (31) |
| NPY | Model: hindpaw withdraw latency and Randall Selitto assay (6) | Model: electrical hippocampal stimulation and kainate seizure (3) |
| Somatostatin | Model: foot-pressure assay (7) | Model: quinolinic/kainic acid-induced seizure (4) |
| Neurotensin | Model: hot plate and writhing assays (39) | Model: 6 Hz partial psychomotor seizure (8) |
| Enkephalin | Model: radiant-heat tail flick assay (40) | Model: 6 Hz partial psychomotor seizure (9) |
| NPW/NPB | Model: partial sciatic nerve ligation assay (14) | Model: 6 Hz partial psychomotor seizure. This work |

(GPR7) and/or NPBW₂ (GPR8) receptors (Figure 4.1) (11). NPW binds to both NPBW₁ and NPBW₂ with low nanomolar affinity ($K_i = 0.14$ and 29 nM, respectively). Early studies showed that NPW played an important role in modulating feeding behaviors (11, 12). Subsequent studies revealed that intrathecal (i.t.) administration of this peptide suppressed inflammatory pain in the mouse formalin test.

NPW was also shown to be anti-allodynic in partial sciatic nerve ligation model (13-15). Of particular interest, Zaratin and coworkers reported increased expression of NPBW₁ receptor subtypes in myelin-forming Schwann cells in animal models of acute inflammatory and trauma-induced neuropathic pain suggesting a central role for this peptide as an analgesic (16). Price et al showed that direct injection of NPW-23 into the hypothalamus influenced the excitability of specific groups of neurons in rats (17, 18). In short, NPW has been shown to be a multifunctional endogenous ligand for NPBW₁ and NPBW₂ where it plays an important role in modulating pain pathways and feeding behaviors (19). In this work we tested the hypothesis that, based on its analgesic properties, NPW may also suppress seizures when delivered into the brain. The anticonvulsant properties of NPW were confirmed following i.c.v. injections, as well as by engineering metabolically-stable and BBB-penetrant NPW analogs using a design strategy previously applied to GAL, NPY and NT (10, 20, 21).

4.3 Materials and Methods

4.3.1 Intracerebroventricular (i.c.v.) Administration of NPW

The 6 Hz partial psychomotor seizure test was performed to assess the anticonvulsant potential of NPW as described previously (22, 23). Stock solutions of

human NPW WYKHVASPRYHTVGRAAGLLMGLRRSPYLW
human NPB WYKPAAGHSSYSVGRAAGLLSGLRRSPYA

Figure 4.1 Comparison of the primary amino acid structures of neuropeptide W and neuropeptide B. Boxed regions denote areas of sequence homology between the two peptides. These fragments have been previously found necessary for high affinity binding to the GPCR targets NPBW₁ and NPBW₂. C-Terminally truncated NPW (NPW-23) was previously shown to exhibit similar binding properties and effective doses, with respect to NPBW₁ and NPBW₂, to that of the 29 amino acid peptide NPW-29 (15).

human NPW-23 (purchased from American Peptide Company, Inc.) were prepared in 0.9% saline and were diluted to the required concentration prior to i.c.v. injections. The time to peak anticonvulsant effect (TPE) was first determined at 0.25, 0.5, 1, 2, and 4 h following i.c.v. injection at a concentration of 1 nmol/5 μ L (22, 23). The TPE was calculated as the time at which 50% of animals were considered protected from seizure. For i.c.v. administrations, the test solution was administered in a volume of 5 μ L, using a Hamilton syringe (size number 701), directly through the skull to a depth of 3 mm into a lateral ventricle of the brain. A current of 32 mA was administered via corneal electrodes for 3 s in order to elicit psychomotor seizure. Animals not displaying seizures were considered “protected” (22, 23). Finally, an ED₅₀, confidence interval, line slope, and standard error (S.E.M.) of the slope were calculated by Probit analysis. Results were reported to two decimal places (24)

4.3.2 Chemical Synthesis

Synthesis of NPW analogs was carried out using a Symphony automated peptide synthesizer (Protein Technologies, Inc). Syntheses were carried out at 100 μ mol scale using Fmoc-Leu Amide-AM resin (subs. 0.71 meq/g). Triple couplings of each amino acid (30, 30, and 40 min) were performed using 0.2 M PyBOP (benzotriazol-1-yl-oxytripyrrolidinophosphonium hexafluorophosphate), 0.4 M DIPEA (*N,N*-diisopropylethylamine), and 200 mM of each amino acid. Protected amino acids, including Fmoc-Lys(palmitoyl) and Fmoc-5-aminovaleric acid were obtained commercially from Chem-Impex International. Peptides were cleaved from resin by

treatment with reagent K (82.5% TFA, 5% water, 5% ethanedithiol, 2.5% thioanisole v/v, 75 mg/mL phenol) followed by vacuum filtration to separate peptide from resin, and finally precipitated with chilled methyl-*tert*-butyl ether. Crude peptides were then purified by preparative reversed-phase HPLC over a linear gradient of solvent B (90% acetonitrile in 0.1% TFA) ranging from 5 to 95% in 45 min. Solvent A was 0.1% TFA in water. Purities of separated fractions were assessed by analytical reversed-phase HPLC using a linear gradient ranging from 5 to 95% of solvent B in 30 min. HPLC fractions with peptide purities greater than 95% were pooled and quantified by measuring UV absorbance at 279.8 nm. Molecular masses of all analogs were confirmed by MALDI-TOF MS.

4.3.3 Partitioning Coefficient (logD)

4.3.3.1 Shake-flask method. For selected analogs, logD values were calculated experimentally using the shake-flask method, as previously described (20, 25). Briefly, water-saturated *n*-octanol was prepared by mixing equal volumes of *n*-octanol and water for 24 h at room temperature. Lyophilized peptides (0.1 mg) were then reconstituted in 1 mL phosphate-buffered saline (PBS), followed by addition of an equal volume of water-saturated *n*-octanol. Samples were then allowed to mix on a rotary mixer for 24 h. Following mixing, samples were then allowed to settle for 15 min. Aqueous phases were carefully removed and analyzed by analytical HPLC over a gradient of solvent B ranging from 5 to 95% in 30 min. The amount of peptide in the aqueous phase was determined by HPLC using a standard curve constructed for each peptide. LogD values for each analog were then calculated using the Equation 4.1(20, 26):

$$\log D = \log \left(\frac{[\text{Peptide}_{\text{Octanol}}]}{[\text{Peptide}_{\text{Aqueous}}]} \right) \quad (4.1)$$

4.3.3.2 HPLC capacity factor (k') method. For remaining NPW analogs, logD values were calculated by comparison to HPLC retention times with experimentally-determined samples. Briefly, 5 μg standards of each peptide were injected, in triplicate, onto a Vydac diphenyl HPLC column over a linear gradient ranging from 5-95% solvent B in 45 min. The average retention time for each peptide standard was then used to calculate capacity factors (k') using Equation 4.2 seen below. In this equation t_0 is the solvent front and t_r is the retention time of each peptide standard. LogD values obtained experimentally from the shake-flask method were then plotted against their respective k' values, yielding a linear plot. This plot was then used to determine the logD values for remaining analogs using this standard curve (20, 25).

$$k' = \frac{(t_r - t_0)}{t_0} \quad (4.2)$$

4.3.4 Serum Stability Assay

The stability of peptides in the presence of 25% rat blood serum was evaluated for each analog by incubation at 37 °C for 0 min, 30 min, 1 h, 2 h, 4 h, and 8 h. Samples were prepared by adding 10 μg of a peptide, resuspended in nH_2O , to pre-heated tubes containing 25% rat blood serum and 0.1 M Tris-HCl, pH 7.5. At the appropriate time points, reactions were quenched by precipitation of serum proteins through addition of 100 μL isopropanol / water / trichloroacetic acid (45%:40%:15% v/v/v). Samples were then incubated at -20 °C for 20 min followed by centrifugation at 10,000 rpm for 3 min to remove serum proteins. Supernatants were then removed and were analyzed by analytical HPLC equipped with a Waters YMC ODS-A 5 μm 120 Å column using a

gradient ranging from 5% to 95% solvent B in 45 min including a 15 min pre-equilibration step. Metabolic stability was assessed by the determining a time-course of the disappearance of an intact peptide. Half-lives ($t_{1/2}$) for each peptide were determined from at least three independent time-course experiments using Equation 4.3 (where m is the slope of the line and b is the y-intercept):

$$t_{1/2}(h) = \frac{[\ln(50) - b]}{m} \quad (4.3)$$

4.3.5 Anticonvulsant Activity

The anticonvulsant activity of the analogs was studied in the 6 Hz (32 mA) partial psychomotor model of pharmaco-resistant epilepsy following a bolus intraperitoneal (i.p.) administration of a dose of 4 mg/kg to adult male CF-1 mice ($n = 4$). For i.p. administrations, test substances were administered to mice in a volume of 0.01 mL/g of body weight. At 30 min post administration, mice were challenged with a 6 Hz corneal stimulation (32 mA for 3 s delivered via corneal electrodes). In adult, male CF-1 mice, the convulsive current required to evoke a partial seizure in 97% (CC97) of mice is 22 mA. The 32 mA current used in the present study represents 1.5 times the CC97 of adult male CF-1 mice will display a partial seizure. Mice which did not exhibit classical limbic seizure behavior were classified as protected (27). This model is useful for discriminating drugs such as levetiracetam, that lack sensitivity to traditional screening models like the maximal electroshock (MES) or the subcutaneous pentylentetrazol (scPTZ) models, but maintain their anticonvulsant activity as the current is increased to 32 mA (1.5 times CC97) and then 44 mA (2 times the CC97) (22, 28). Typically, the seizure phenotype is characterized by a minimal clonic phase that is followed by

stereotyped, automatic behaviors described originally as being similar to the aura of human patients with partial seizures. Animals not displaying this behavior were considered protected. In addition to the 6 Hz screening of all analogs at the 30 min time point, dose-response studies were carried out for hNPW-23 (i.c.v. administration only) and NPW-B1 (i.p. administration). Briefly, peptide analogs were administered and at 30 min, mice were challenged with a 32 mA corneal stimulation. Based on the numbers of protected animals at each dosage, ED₅₀ values were determined for each peptide using Probit software (24).

4.3.6 Rotorod Testing

The rotorod procedure was used to disclose minimal muscular or neurological impairment. Briefly, the mouse was placed on a rod that rotated at a speed of 6 rpm, in order for the animal to maintain its equilibrium for extended periods of time. The animal was considered motor impaired (toxic) if it fell off of the rotating rod three times during a one min observation period (29).

4.3.7 Animal Care

Adult male CF No. 1 albino mice (26-35 g), obtained from Charles River (Portage, Michigan), were utilized for behavioral testing in both the 6Hz test and the rotorod procedure. The animals were maintained on an adequate diet (Prolab RMH 3000) and allowed free access to food and water, except during the short time they were removed from their cage for testing. The animals were housed, fed, and handled in a manner consistent with IACUC approved protocol.

4.4 Results

4.4.1 Intracerebroventricular (i.c.v.) Administration of hNPW-23

To test the hypothesis that analgesic NPW can also suppress seizures, this peptide was evaluated in the 6 Hz (32 mA) psychomotor seizure test in mice. Neuropeptide W-23 was injected i.c.v. into adult, male CF-1 mice. Mice were tested at 0.01, 0.1, 1, 2, and 4 nmol concentrations (per 5 μ L injection volume), and were evaluated after 15 min post-drug administration. At these doses 2/8, 4/8, 5/8, 6/8, and 6/8 mice, respectively, were protected from the seizure activity. At each concentration, 1/8 mice displayed rotorod toxicity. The ED₅₀ value was calculated as 0.24 nmol with a 95% confidence interval of 0.003-1.2 nmol ($b = 0.52 \pm 0.22$).

Similarly, the effect of NPB-29 in the 6 Hz epilepsy model in adult, male CF-1 mice was also evaluated. The time of peak effect was determined to be 0.25 h following i.c.v. administration. Mice were tested at 0.1, 1.0, 1.5, and 2 nmol concentrations (per 5 μ L i.c.v. injection volume). At these doses, 1/8, 2/8, 4/8, and 6/8 mice were protected from seizure activity, respectively (Figure 4.2). Furthermore, at these doses 0/8, 3/8, 3/8, and 4/8 mice were found to display motor toxicity, respectively. The ED₅₀ was determined to be 1.5 nmol with a 95% confidence interval of 0.4-128 nmol ($b=1.2 \pm 0.56$). Notably, the ED₅₀ value determined for NPB-29 (1.5 nmol/5 μ L) was approximately six fold higher than that which was determined for NPW-23 in the 6 Hz partial psychomotor seizure test at 32mA. This is the first report on the antiepileptic activities of NPW and NPB.

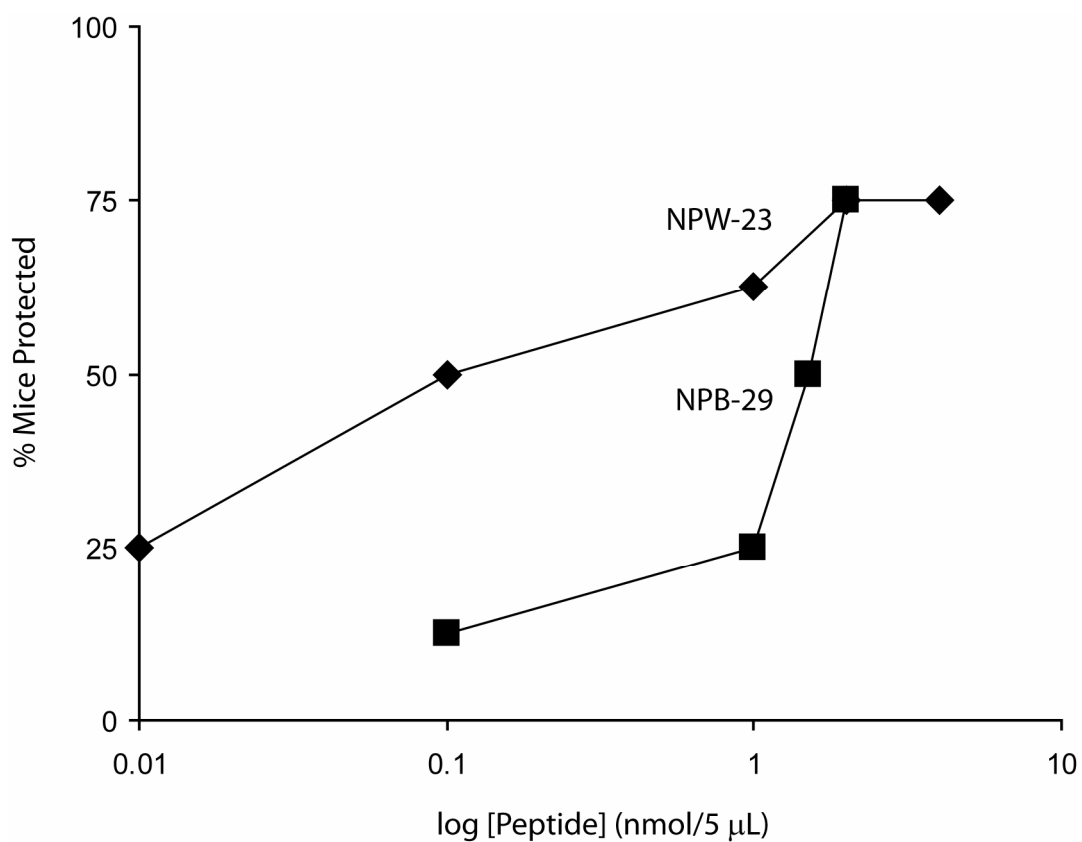


Figure 4.2 Summary of anticonvulsant activities of hNPW-23 and NPB-29 following i.c.v. administration. Peptides were injected i.c.v. into adult male CF-1 mice. Mice were tested at 0.01, 0.1, 1.0, 2 and 4 nmol/5 μL for hNPW-23 and 0.1, 1.0, 1.5, and 2 nmol/5 μL for NPB-29. Data represent the number of animals which did not exhibit classical seizure-type behaviors at 0.25 h post drug administration. ED₅₀ values were calculated at 0.24 nmol (95% CI = 0.003-1.2) and 1.5 nmol (95% CI = 0.4-128) for hNPW-23 and NPB-29, respectively.

4.4.2 Design of BBB-permeable Analogs of NPW

To design NPW-derived compounds that can penetrate BBB, we explored the lipidization-cationization strategy previously employed to engineer BBB-permeable analogs of GAL, NT and NPY (GAL-B2, NT-BBB1, and NPY-BBB2, respectively) (10, 20, 21, 30, 31). As illustrated in Figure 4.3, active fragments of these neuropeptides were used to introduce a lipoamino acid (Lysine-palmitoyl) in the context of several Lys residues, yielding the so called “lipidization-cationization” motif. These peptides potently suppressed seizures in mice following i.p. administration.

For NPW, the following previously published SAR results were considered towards designing BBB-permeable analogs: (i) the C-terminal fragment NPW¹⁴⁻²³ forms a distinct α -helix and is important for the activation of the NPBW₁ receptor, and (ii) the N-terminal tripeptide of NPW is integral in discriminating between the two receptor subtypes (32). Kanesaka and coworkers constructed centrally-truncated analogs of NPW in which non-essential amino acid residues were replaced by backbone spacer units (5-aminovaleric acid), resulting in potent and selective NPWB₁ agonists (12). The NPW analog containing three 5-aminovaleric acid units, namely NPW Ava-3 shown in Figure 4.4, exhibited similar NPBW₁ binding affinity to that of the full-length peptide (K_i (NPBW₁)= 0.40 nM versus 0.14 nM). As illustrated in Figure 4.4, the BBB-permeable analogs of NPW described here maintained the N-terminal “WYK” sequence and the C-terminal active fragment while replacing central, non-essential amino acid residues with varying combinations of oligo-Lys motifs, lipoamino acid, and the 5-Ava spacer. Based on our previous experience with BBB-permeable galanin analogs, the position of the Lys-palmitoyl and a number of Lys residues affected their in vivo activities in the epilepsy

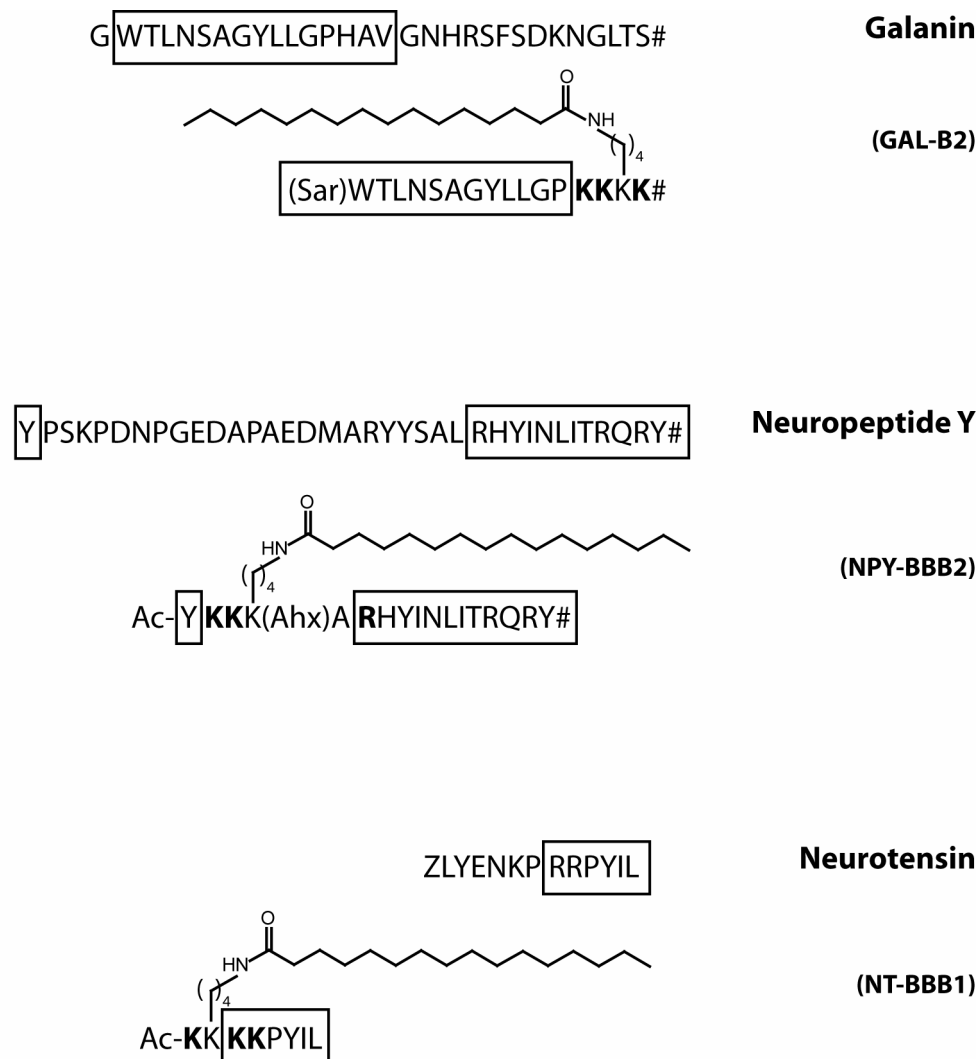


Figure 4.3 Examples of BBB-penetrating anticonvulsant neuropeptides modified by the lipidization-cationization motif. Full-length amino acid sequences for GAL, NPY and NT are shown with bioactive fragments marked by boxed sequences. Bolded regions denote areas of increased positive charge. (#) Represents C-terminal amidation. (Z) Represents a pyroglutamic acid residue (10, 20, 21, 31).

tests in mice (20).

4.4.3 Chemical Synthesis

All analogs were synthesized on solid support using an automated peptide synthesizer and standard Fmoc protocols. Peptides were cleaved from resin by treatment with reagent K and were purified by preparative reversed-phase HPLC. Peptides were quantified by measuring UV absorbance at 279.8 nm, then subsequently aliquoted and lyophilized by speedvac. Masses of all compounds were confirmed by MALDI-TOF MS. Retention times were calculated from the average of three independent HPLC separations for each analog and are summarized in Table 4.2.

4.4.4. Partitioning Coefficient (logD) Results

In our previous studies, we showed that application of the lipidization-cationization strategy greatly increased partitioning coefficient values (logD) for truncated analogs of galanin (logD GAL-B2 = 1.2), neuropeptide Y (logD NPY-BBB2 = 1.8), and neurotensin (logD NT-BBB1 = 1.2) when compared to those of the native peptides (10, 20). LogD-values for NPW analogs were determined using both the shake-flask and HPLC capacity factor methods. Calculated values for partitioning are summarized in Table 2. The unmodified peptide hNPW-23 was rather hydrophilic evidenced by a negative logD value of -0.13, whereas the modified analogs showed dramatic increase in their hydrophobicity over the full length peptide with logD values ranging from 1.6 to 1.8. NPW-B1 possessed a logD value of 1.7 (Table 4.2; Figure 4.5).

Table 4.2 Summary of sequences and physicochemical properties of neuropeptide W analogs

| Analog | ^aSequence | ^blogD | ^ct_{1/2} (h) |
|---------------|--|-------------------------|--|
| hNPW | WYKHAVSPRYHTVGRAAGLLMGL# | -0.13 ± 0.26 | 0.67 ± 0.05 |
| NPW-B1 | Ac-WYKK(K_p)K(Ava)GRAAGLLMGL# | 1.7 ± 0.14 | 3.6 ± 0.72 |
| NPW-B2 | Ac-WYK(K_p)KKK(Ava)GRAAGLLMGL# | 1.8 ± 0.01* | 3.7 ± 1.3 |
| NPW-B3 | Ac-WYKK(K_p)KK(Ava)GRAAGLLMGL# | 1.6 ± 0.01* | 1.5 ± 0.14 |
| NPW-B4 | Ac-WYKKK(K_p)K(Ava)GRAAGLLMGL# | 1.6 ± 0.01* | n.d. |
| NPW-B5 | Ac-WYKKKK(K_p)(Ava)GRAAGLLMGL# | 1.7 ± 0.15 | 1.9 ± 0.24 |
| NPW-B6 | Ac-WYKK(K_p)K(Ava)(Ava)GRAAGLLMGL# | 1.7 ± 0.01* | n.d. |
| NPW-B7 | Ac-WYKK(K_p)KK(Ava)(Ava)GRAAGLLMGL# | 1.5 ± 0.01* | n.d. |

^a(K_p) is N^ε-palmitoyl-L-lysine, (Ava) is 5-aminovaleric acid, (#) represents C-terminal amidation. ^bLogD values determined using the shake-flask method or based off of HPLC retention times. *Denotes logD values determined using capacity factor (k') which was calculated by average retention HPLC time. ^cHalf-life (t_{1/2}) values were determined using an in vitro serum stability assay. Peptides were incubated in 25% rat blood serum and degradation was monitored by analytical HPLC methods.

4.4.5 Metabolic Stability of NPW Analogs

Our previous results showed significant improvement in the in vitro half-life ($t_{1/2}$) values of modified analogs of galanin ($t_{1/2}$ GAL-B2 > 9 h), neuropeptide Y ($t_{1/2}$ NPY-BBB2 > 3 h), and neurotensin ($t_{1/2}$ NT-BBB1 > 2.7 h) in the rat serum stability assay (10, 20). To determine metabolic stability of NPW analogs, the peptides were incubated in 25% rat blood serum at 37 °C and their degradation was monitored by HPLC. Aliquots were withdrawn after 30 min, 1 h, 2 h, 4 h, and 8 h and quenched with TCA followed by HPLC separations (20). The time courses of the disappearance of the intact species were plotted and $t_{1/2}$ values were calculated. As summarized in Table 4.2 and Figure 4.6, in vitro metabolic stability was significantly increased. For the native peptide, the $t_{1/2}$ value was 0.67 h, whereas the NPW-B1 had $t_{1/2}$ of 3.6 h. Half-lives for the other selected NPW analogs were also increased, ranging from 1.5 – 3.7 h (Table 4.2; Figure 4.6).

4.4.6. Antiseizure activity

The antiepileptic activity of the analogs was evaluated in the 6 Hz model of epilepsy in mice following a bolus i.p. injection of 4 mg/kg. Protection from seizures was tested after 30 min post drug administration. As shown in Table 4.3, the unmodified NPW had no apparent antiepileptic activity, whereas NPW-B1, B2, B3, B5, and B7 analogs exhibited 50% protection of the animals tested. NPW-B6 exhibited 75% protection (3/4 mice protected at 30 min), but was associated with concurrent motor impairment.

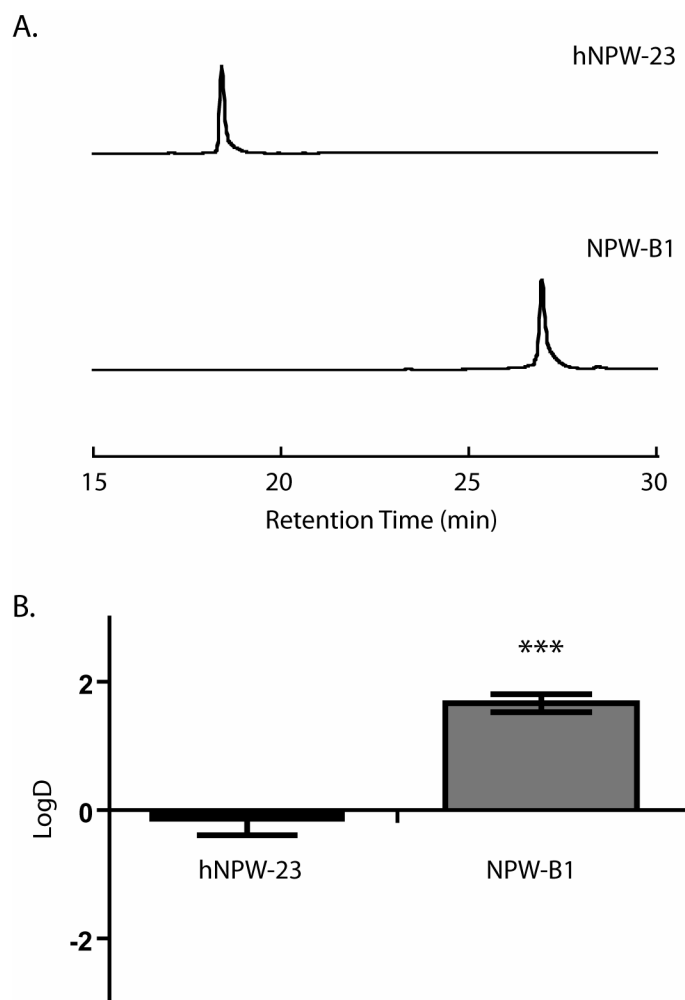


Figure 4.5 Comparison of the relative hydrophobicities of hNPW-23 and NPW-B1. (A) HPLC traces showing the relative hydrophobicities of hNPW-23 versus NPW-B1. Conjugation of poly-Lys and Lys-P motifs resulted in analogs that were much more hydrophobic in nature. Samples were analyzed by analytical HPLC over a linear gradient ranging from 5% to 95% Buffer B in 45 min. All modified analogs exhibited similar shifts in retention times to that of NPW-B1. (B) Comparison of experimentally determined logD values for hNPW-23 and NPW-B1. Values were calculated from the average of three independent experiments via the shake-flask method using a 50:50 ratio of n-octanol/PBS, pH 7.4. The amount of peptide in the aqueous phase was determined by the peak area using analytical HPLC over a gradient ranging from 5 to 95% solvent B in 45 min. LogD for the native peptide was calculated as -0.13; whereas, NPW-B1 had a logD value of 1.7. Statistical comparison between the full-length and modified peptide was performed using the two-tailed t-test function of GraphPad software. Statistical significance was noted as: (***) P-value < 0.001

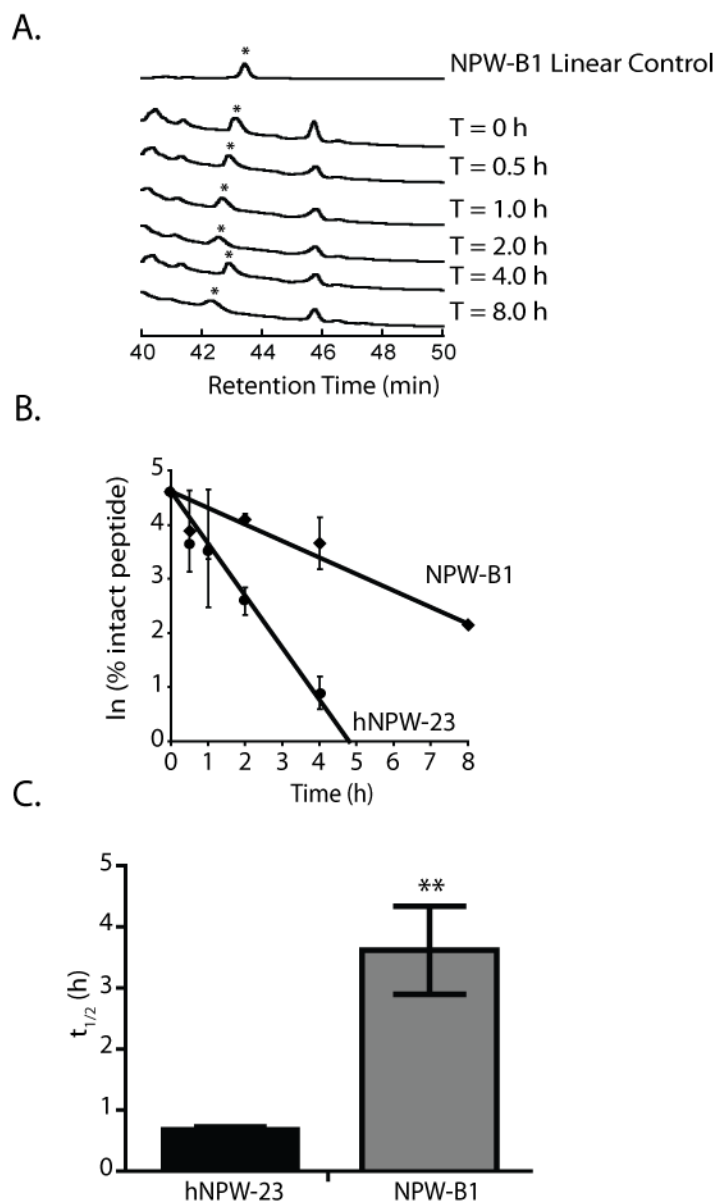


Figure 4.6 Comparison of metabolic stabilities of full-length hNPW-23 versus NPW-B1. (A) Representative time course showing the degradation of NPW-B1 in the presence of 25% rat blood serum. (B) Time-course experiments showing the time-dependence of the disappearance on the intact peptide between 0 and 8 h. Plot compares the degradation of hNPW-23 to that of NPW-B1. Using the slope of the fitted line, half-lives ($t_{1/2}$) were calculated as 0.67 and 3.6 h, respectively. (C) Comparison of the calculated half-lives ($t_{1/2}$) of hNPW-23 and NPW-B1 in the serum stability assay. Results were obtained from the average slopes of three independent time-course experiments. Statistical comparison was performed using the two-tailed t-test function. (**) P-value < 0.01.

Table 4.3. Summary of in vivo anticonvulsant activity for modified NPW analogs in the 6 Hz (32 mA) model of pharmacoresistant epilepsy.

| Analog | In vivo activity (4 mg/kg, i.p.) | |
|--------|----------------------------------|----------------|
| | mice protected at 30 min | Motor Toxicity |
| hNPW | 0/4 | 0/4 |
| NPW-B1 | 2/4 | 0/4 |
| NPW-B2 | 2/4 | 0/4 |
| NPW-B3 | 2/4 | 0/4 |
| NPW-B4 | 1/4 | 1/4 |
| NPW-B5 | 2/4 | 0/4 |
| NPW-B6 | 3/4 | 4/4 |
| NPW-B7 | 2/4 | 0/4 |

6 Hz data were obtained from groups of four CF1 mice. Data represent the number of mice within each group that did not exhibit classical seizure activity at the 30 min time point following i.p. administration of 4 mg/kg. Motor toxicity values were determined using a rotarod motor impairment test (29).

To carry out dose response studies, NPW-B1 was selected. Figure 4.7 illustrates the dose-response curve for the analog and the calculated ED₅₀ data are summarized in Table 4.3. ED₅₀ values, following i.p. administration, for NPW-B1 were calculated as 4.9 mg/kg (95% CI = 2.9-12.2).

4.5 Discussion

Through the strategy of neuropeptide repositioning, this work describes the discovery of the anticonvulsant properties of NPW. Recent studies have shown a high level of expression of NPW and NPW-receptors in the hippocampus and amygdala of both rodents and humans, suggesting an important role for this peptide in the CNS (13, 16, 33). The peptides described in this work likely mediate their anticonvulsant activities through activation of the NPBW₁ receptor as it has been previously shown that rodent models do not possess the NPBW₂ subtype (34). However, without detailed pharmacological studies, we cannot definitively exclude the possibility of off-target interactions with other GPCRs (noteworthy, the lipidization-cationization motifs applied here did not exhibit antiepileptic activities) (31). It has been previously reported that activation of NPBW₁ modulates hyperexcitability of neurons in the CNS (33). Price and coworkers previously reported that application of NPW to neurons in the paraventricular nucleus of the hypothalamus resulted in a large population of hyperpolarized neurons (57%) with smaller mixed populations of depolarized and unchanged neurons (18). We hypothesize that the observed anticonvulsant effects exerted by hNPW-23, and the modified NPW-analogs, resulted from activation of the NPBW₁ receptor which may result in hyperpolarization of the cell membrane. Hyperpolarization of the membrane would then result in decreased excitatory behavior of the neuron, thus modulating seizure

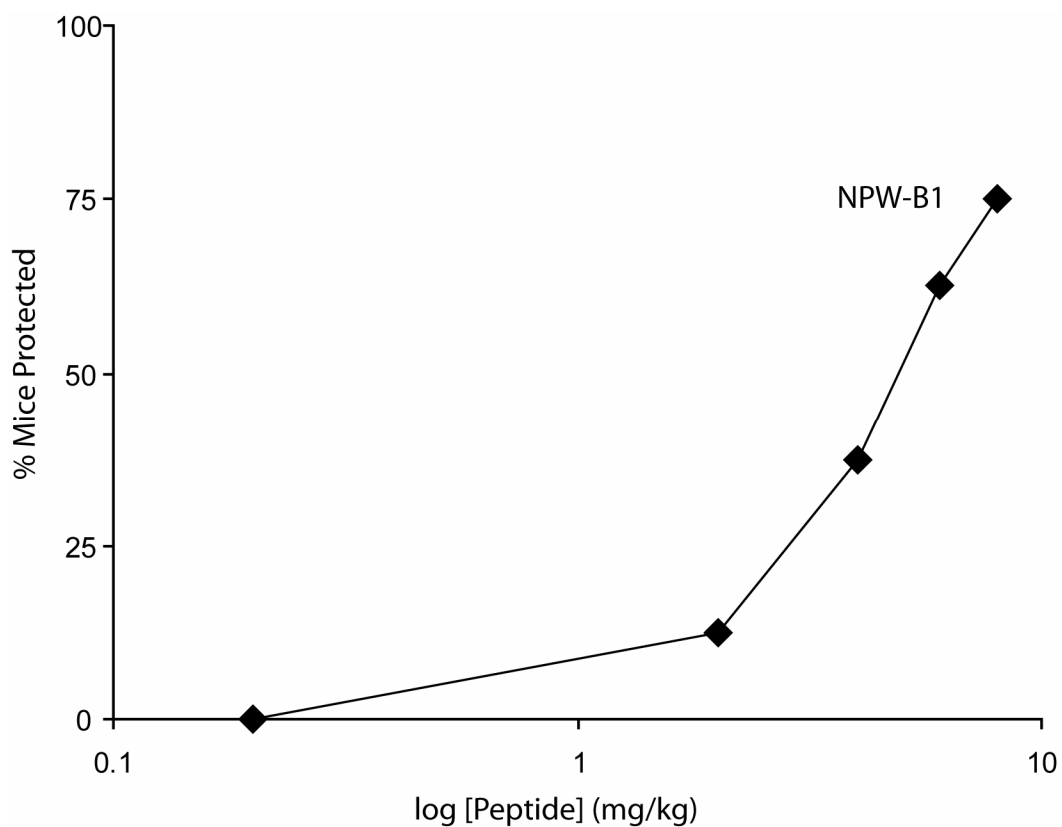


Figure 4.7 Dose-response curve for NPW-B1. Mice were injected with 0.2, 2, 4, 6, and 8 mg/kg NPW-B1. Peptide was administered i.p. into groups of eight adult male CF-1 mice ($n = 4$ for 0.2 and 8 mg/kg doses). Data represent the percentage of animals which did not exhibit classical seizure-type behaviors at 30 min post administration (TPE). ED_{50} for this analog was calculated as 4.9 mg/kg (95% CI = 2.9 – 12.2) using Probit software (24).

activity (1, 17). This hypothesis remains to be tested and it is acknowledged that further studies into the precise mechanism by which NPW inhibits neuronal hyperexcitability need to be conducted.

This work further extends the strategy of lipidization-cationization to improve CNS bioavailability of neuropeptides. Upon i.p. administration, hNPW-23 did not exhibit anticonvulsant activity suggesting that the native peptide does not reach its target in the brain. In the design of systemically-active NPW analogs, two structural elements were taken into account. First, a positional scanning of the lipoamino acid relative to the C-terminal active fragments of NPW was explored (NPW-B1 through NPW-B5). All analogs exhibited similar anticonvulsant activities, suggesting that the positioning of the lipoamino acid is not crucial to the analogs' anticonvulsant effects. This is in contrast to our previous works which reported that placement of Lys-palmitoyl directly affected the biological activity of GAL analogs (20). Second, the spacing between the N-terminal and C-terminal active fragments was examined through coupling of additional 5-Ava spacers (NPW-B6 and NPW-B7). Interestingly, NPW-B6 produced the most protection in the screening assay (3/4 mice protected at the 30 min time-point), but this analog also exhibited the highest levels of motor impairment (4/4 mice affected) in the rotarod test. In our previous work, we observed that insertion of an additional Ala-residue into modified NPY analogs resulted in pronounced changes in anticonvulsant activities when compared NPY-BBB1 with NPY-BBB2 (10). In light of these differences, it does not go unnoticed that further optimization of NPW analogs should be undertaken as a part of the lead optimization studies. It is conceivable that through the addition/deletion of 5-Ava

spacer units or introduction of other backbone spacers (9, 35), future NPW analogs may be designed that possess potent antiepileptic activity without exhibiting motor toxicity.

BBB permeable analogs of NPW exhibited similar physicochemical and pharmacological properties to those previously observed in the modified GAL, NPY, and NT analogs (10, 20). The insertion of Lys and Lys-palmitoyl residues to centrally-truncated NPW resulted in increased logD and improved half-life in the rat serum stability assay. The improvements to logD and metabolic stability were correlated with pronounced anticonvulsant activity in the 6 Hz mouse model of pharmaco-resistant epilepsy following i.p. administration. The anticonvulsant activity of the systemically-active NPW analogs is likely to be mediated by their native receptors in the brain. We show in our previous work, that the combination of the lipidization and cationization did not affect affinities of the GAL, NPY or NT to their respective native receptors (10, 20, 21, 30). Thus, based on SAR results for centrally-truncated NPW analogs (12), NPW-B1 to B7 are expected to retain similar affinities towards NPBW₁ receptors. We acknowledge here that more pharmacological studies are needed, both in vitro and in vivo, to dissect the exact mechanism of seizure control by BBB-permeable analogs of NPW.

The lipidization-cationization strategy sets out to overcome the issues of metabolic instability and poor bioavailability of neuropeptides. The development of systemically-active NPW analogs further increases the number of anticonvulsant neuropeptides that can be explored as CNS-acting neurotherapeutics. As alluded to earlier, NPW has garnered recent interest because of its ability to regulate feeding behaviors and influence metabolic function (36-38). It was previously reported that

NPW accomplishes these roles through activation of NPW-receptors in the hypothalamus. It has been hypothesized that NPW acts through a compensatory mechanism to regulate energy homeostasis when leptin levels in the brain are decreased (37). Therefore, the modified NPW analogs described here may be useful pharmacological compounds towards the development of therapies for metabolic illnesses leading to obesity. In summary, the combination of rational repositioning and peptide engineering has provided new tools to study a role of NPW in the brain.

4.6 Acknowledgements

This work was supported by the NIH grant R21 NS059669. Gratitude is extended to Charles Robertson and for critical review and numerous conversations integral to this work. Conflict of Interest Disclosure: GB and HSW are scientific co-founders of NeuroAdjuvants, Inc.

4.7 References

1. Todorovic, S. M., Rastogi, A. J., and Jevtovic-Todorovic, V. (2003) Potent analgesic effects of anticonvulsants on peripheral thermal nociception in rats, *Br. J. Pharmacol.* *140*, 255-260.
2. Mazarati, A. M., and Wasterlain, C. G. (2002) Anticonvulsant effects of four neuropeptides in the rat hippocampus during self-sustaining status epilepticus, *Neurosci. Lett.* *331*, 123-127.
3. Woldbye, D. P. D., and Kokaia, M. (2004) Neuropeptide Y and seizures: Effects of exogenously applied ligands, *Neuropeptides* *38*, 253-260.
4. Vezzani, A., Serafini, R., Stasi, M. A., Viganò, G., Rizzi, M., and Samanin, R. (1991) A peptidase-resistant cyclic octapeptide analog of somatostatin (SMS 201-995) modulates seizures induced by quinolinic and kainic acids differently in the rat hippocampus, *Neuropharmacology* *30*, 345-352.
5. Hua, X.-Y., Hayes, C. S., Hofer, A., Fitzsimmons, B., Kilk, K., Langel, Ü., Bartfai, T., and Yaksh, T. L. (2004) Galanin acts at GalR1 receptors in spinal antinociception: Synergy with morphine and AP-5, *J. Pharmacol. Exp. Ther.* *308*, 574-582.
6. Wang, J.-Z., Lundeberg, T., and Yu, L.-C. (2000) Antinociceptive effects induced by intra-periaqueductal grey administration of neuropeptide Y in rats, *Brain Res.* *859*, 361-363.
7. Tashev, R., Belcheva, S., Milenov, K., and Belcheva, I. (2001) Antinociceptive effect of somatostatin microinjected into caudate putamen, *Peptides* *22*, 1079-1083.
8. Lee, H.-K., Zhang, L., Smith, M. D., White, H. S., and Bulaj, G. (2009) Glycosylated neurotensin analogs exhibit sub-picomolar anticonvulsant potency in a pharmacoresistant model of epilepsy, *ChemMedChem* *4*, 400-405.
9. Lee, H.-K., Smith, M. D., Smith, B. J., Grussendorf, J., Xu, L., Gillies, R. J., White, H. S., and Bulaj, G. (2009) Anticonvulsant Met-enkephalin analogs containing backbone spacers reveal alternative non-opioid signaling in the brain, *ACS Chem. Biol.* *4*, 659-671.
10. Green, B. R., White, K. L., McDougale, D. R., Zhang, L., Klein, B., Scholl, E. A., Pruess, T. H., White, H. S., and Bulaj, G. (2010) Introduction of lipidization-cationization motifs affords systemically bioavailable neuropeptide Y and neurotensin analogs with anticonvulsant activities, *J. Pept. Sci.* *16*, 486-495.
11. Shimomura, Y., Harada, M., Goto, M., Sugo, T., Matsumoto, Y., Abe, M., Watanabe, T., Asami, T., Kitada, C., Mori, M., Onda, H., and Fujino, M. (2002)

- Identification of neuropeptide W as the endogenous for orphan G-protein-coupled receptors GPR7 and GPR8, *J. Biol. Chem.* 277, 35826-35832.
12. Kanesaka, M., Matsuda, M., Hirano, A., Tanaka, K., Kanatani, A., and Tokita, S. (2007) Development of a potent and selective GPR7 (NPBW₁) agonist: a systematic structure-activity study of neuropeptide B, *J. Pept. Sci.* 13, 379-385.
 13. Kelly, M. A., Beuckmann, C. T., Williams, S. C., Sinton, C. M., Motoike, T., Richardson, J. A., Hammer, R. E., Garry, M. G., and Yanagisawa, M. (2005) Neuropeptide B-deficient mice demonstrate hyperalgesia in response to inflammatory pain, *Proc. Natl. Acad. Sci.* 102, 9942-9947.
 14. Yamamoto, T., Saito, O., Shono, K., and Tanabe, S. (2006) Effects of intrathecal and i.c.v. administration of neuropeptide W-23 and neuropeptide B on the mechanical allodynia induced by partial sciatic nerve ligation in rats, *Neuroscience* 137, 265-273.
 15. Yamamoto, T., Saito, O., Shono, K., and Tanabe, S. (2005) Anti-hyperalgesic effects of intrathecally administered neuropeptide W-23, and neuropeptide B, in tests of inflammatory pain in rats, *Brain Res.* 1045, 97-106.
 16. Zaratin, P. F., Quattrini, A., Previtali, S. C., Comi, G., Hervieu, G., and Schneideler, M. A. (2005) Schwann cell overexpression of the GPR7 receptor in inflammatory and painful neuropathies, *Mol. Cell. Neurosci.* 28, 55-63.
 17. Price, C. J., Samson, W. K., and Ferguson, A. V. (2008) Neuropeptide W influences the excitability of neurons in the rat hypothalamic arcuate nucleus, *Neuroendocrinology* 88, 88-94.
 18. Price, C. J., Samson, W. K., and Ferguson, A. V. (2009) Neuropeptide W has cell phenotype-specific effects on the excitability of different subpopulations of paraventricular nucleus neurones, *J. Endocrinol.* 21, 850-857.
 19. Singh, G., and Davenport, A. P. (2006) Neuropeptide B and W: Neurotransmitters in an emerging G-protein-coupled receptor system, *Br. J. Pharmacol.* 148, 1033-1041.
 20. Bulaj, G., Green, B. R., Lee, H.-K., Robertson, C. R., White, K., Zhang, L., Sochanska, M., Flynn, S. P., Scholl, E. A., Pruess, T. H., Smith, M. D., and White, H. S. (2008) Design, synthesis, and characterization of high-affinity, systemically-active galanin analogs with potent anticonvulsant activities, *J. Med. Chem.* 51, 8038-8047.
 21. Zhang, L., Robertson, C. R., Green, B. R., Pruess, T. H., White, H. S., and Bulaj, G. (2009) Structural requirements for a lipoamino acid in modulating the

- anticonvulsant activities of systemically active galanin analogs, *J. Med. Chem.* 52, 1310-1316.
22. Barton, M. E., Klein, B. D., Wolf, H. H., and White, H. S. (2001) Pharmacological characterization of the 6 Hz psychomotor seizure model of partial epilepsy, *Epilepsy Res.* 47, 217-227.
 23. Barton, M. E., Peters, S. C., and Shannon, H. E. (2003) Comparison of the effect of glutamate receptor modulators in the 6 Hz and maximal electroshock seizure models, *Epilepsy Res.* 56, 17-26.
 24. Finney, D. J. (1971) *Probit Analysis*, 3rd ed., Cambridge Univ. Press, London.
 25. van de Waterbeemd, H., Lennernas, H., and Artursson, P. (2003) *Drug bioavailability: Estimation of solubility, permeability, adsorption, and bioavailability*, Wiley-VCH, Weinheim.
 26. Wang, J., Wu, D., and Shen, W. C. (2002) Structure-activity relationship of reversible lipidized peptides: studies of fatty acid-desmopressin conjugates, *Pharm. Res.* 19, 609-614.
 27. Toman, J. E. P., Swinyard, E. A., and Goodman, L. S. (1946) Properties of maximal seizures and their alteration by anticonvulsant drugs and other agents, *J. Neurophysiol.* 9, 231-240.
 28. White, H. S., Smith-Yockman, M. D., Srivastava, A. K., and Wilcox, K. S. (2006) Therapeutic assays for the identification and characterization of antiepileptic and antiepileptogenic drugs, in *Models of Seizure and Epilepsy* (Pitkanen, A., Schwartzkroin, P. A., and Moshe, S. L., Eds.), pp 539-549, Elsevier, Oxford.
 29. Dunham, M. S., and Miya, T. A. (1957) A note on a simple apparatus for detecting neurological deficit in rats and mice, *J. Amer. Pharm. Ass. Sci. Ed.* 46, 208-209.
 30. Robertson, C. R., Scholl, E. A., Pruess, T. H., Green, B. R., White, H. S., and Bulaj, G. (2010) Engineering galanin analogs that discriminate between GalR1 and GalR2 subtypes and exhibit anticonvulsant following systemic delivery, *J. Med. Chem.* 53, 1871-1875.
 31. White, H. S., Scholl, E. A., Klein B. D., Flynn, S. P., Pruess, T. H., Green, B. R., Zhang, L., and Bulaj, G. (2009) Developing novel antiepileptic drugs: Characterization of NAX 5055, a systemically-active galanin analog, in epilepsy models, *Neurotherapeutics* 6, 372-380.
 32. Lucyk, S., Miskolzie, M., and Kotovych, G. (2005) NMR conformational analyses on (des-bromo) neuropeptide B [1-23] and neuropeptide W [1-23]: The

- importance of α -helices, a cation-p interaction and a B-turn, *J. Biomolec. Struct. Dyn.* *23*, 77-90.
33. Takenoya, F., Yagi, M., Kageyama, H., Shiba, K., Endo, K., Nonaka, N., Date, Y., Nakazato, M., and Shioda, S. (2010) Distribution of neuropeptide W in the rat brain, *Neuropeptides* *44*, 99-106.
 34. Lee, D. K., Nguyen, T., Porter, C. A., Cheng, R., George, S. R., and O'Dowd, B. F. (1999) Two related G protein-coupled receptors: the distribution of GPR7 in rat brain and the absence of GPR8 in rodents, *Brain Res.* *71*, 96-103.
 35. Green, B. R., Catlin, P., Zhang, M. M., Fiedler, B., Bayudan, W., Morrison, A., Norton, R. S., Smith, B. J., Yoshikami, D., Olivera, B. M., and Bulaj, G. (2007) Conotoxins containing nonnatural backbone spacers: Cladistic-based design, chemical synthesis, and improved analgesic activity, *Chem. Biol.* *14*, 399-407.
 36. Takenoya, F., Kageyama, H., Shiba, K., Date, Y., Nakazato, M., and Shioda, S. (2010) Neuropeptide W: A key player in the homeostatic regulation of feeding and energy metabolism?, *Ann. N.Y. Acad. Sci.* *1200*, 162-169.
 37. Date, Y., Mondal, M. S., Kageyama, H., Ghamari-Langroudi, M., Takenoya, F., Yamaguchi, H., Shimomura, Y., Mori, M., Murakami, N., Shioda, S., Cone, R. D., and Nakazato, M. (2010) Neuropeptide W: An anorectic peptide regulated by leptin and metabolic state, *Endocrinology* *151*, 2200-2210.
 38. Beck, B., Bossenmeyer-Pourié, C., and Pourié, G. (2010, In Press) Association of neuropeptide W, but not obestatin, with energy intake and endocrine status in Zucker rats. A new player in long-term stress-feeding interactions, *Appetite*.
 39. Clineschmidt, B. V., Martin, G. E., and Veber, D. F. (1982) Antinocisponsive effects of neurotensin and neurotensin-related peptides, *Ann. N.Y. Acad. Sci.* *400*, 283-306.
 40. Inturrisi, C. E., Umans, J. G., Wolff, D., Stern, A. S., Lewis, R. V., Stein, S., and Udenfriend, S. (1980) Analgesic activity of the naturally occurring heptapeptide [Met]enkephalin-Arg⁶-Phe⁷, *Proc. Natl. Acad. Sci.* *77*, 5512-5514.

CHAPTER 5

INTRODUCTION OF LIPIDIZATION-CATIONIZATION MOTIFS INTO CYCLIC PEPTIDES: DESIGN, SYNTHESIS AND OXIDATION OF SOMATOSTATIN AND ERYTHROPOIETIN

5.1 Abstract

Anticonvulsant neuropeptides play an important role in controlling neuronal excitability that leads to pain or seizures. Based on overlapping inhibitory mechanisms, many anticonvulsant compounds have been found to exhibit both analgesic and antiepileptic activities. An analgesic neuropeptide W (NPW) targets recently deorphanized G-protein coupled receptors. Here, we tested the hypothesis that the analgesic activity of NPW may lead to the discovery of its antiepileptic properties. Indeed, direct administration of NPW into the brain potently reduced seizures in mice. To confirm this discovery, we rationally designed, synthesized and characterized NPW analogs that exhibited anticonvulsant activities following systemic administration. Our results suggest that the combination of neuropeptide repositioning and engineering NPW analogs that penetrate the blood-brain barrier could provide new drug leads, not only for

the treatment of epilepsy and pain, but also for studying effects of this peptide on regulating feeding and energy metabolism coupled to brain levels of leptin.

5.2 Introduction

5.2.1 Application of the Lipidization-cationization Strategy

to Conformationally-constrained Cyclic Peptides

Previous efforts have focused on conjugation of the lipidization-cationization motifs to the N- or C-termini of unstructured, linear peptides (GAL, NT, NPY, and NPW). These efforts revealed that this strategy was effective independent of the primary amino acid sequence or the point of attachment of the modification (N- or C-termini). This chapter will discuss the application of such modifications to short, conformationally-constrained cyclic peptides containing a single disulfide bridge. Formation of the disulfide bridge confers a level of rigidity to cyclic peptides. Cyclic peptides comprise a large and varied class of naturally-occurring and synthetically-derived compounds. Many of these peptides exhibit increased metabolic stability, receptor specificity, and increased biological activity (*1*). Five general topologies exist within cyclic peptides (Figure 5.1).

This chapter will focus on the modification of two peptides, somatostatin and erythropoietin mimetic peptide (EMP), that contain side-chain to side-chain cyclization through the formation of a single disulfide bridge. Emphasis will be placed on cyclic peptides that are conformationally-constrained through side-chain to side-chain cyclization; however, it should also be noted that peptides possessing other cyclization topologies may also be amenable for the lipidization-cationization motifs.

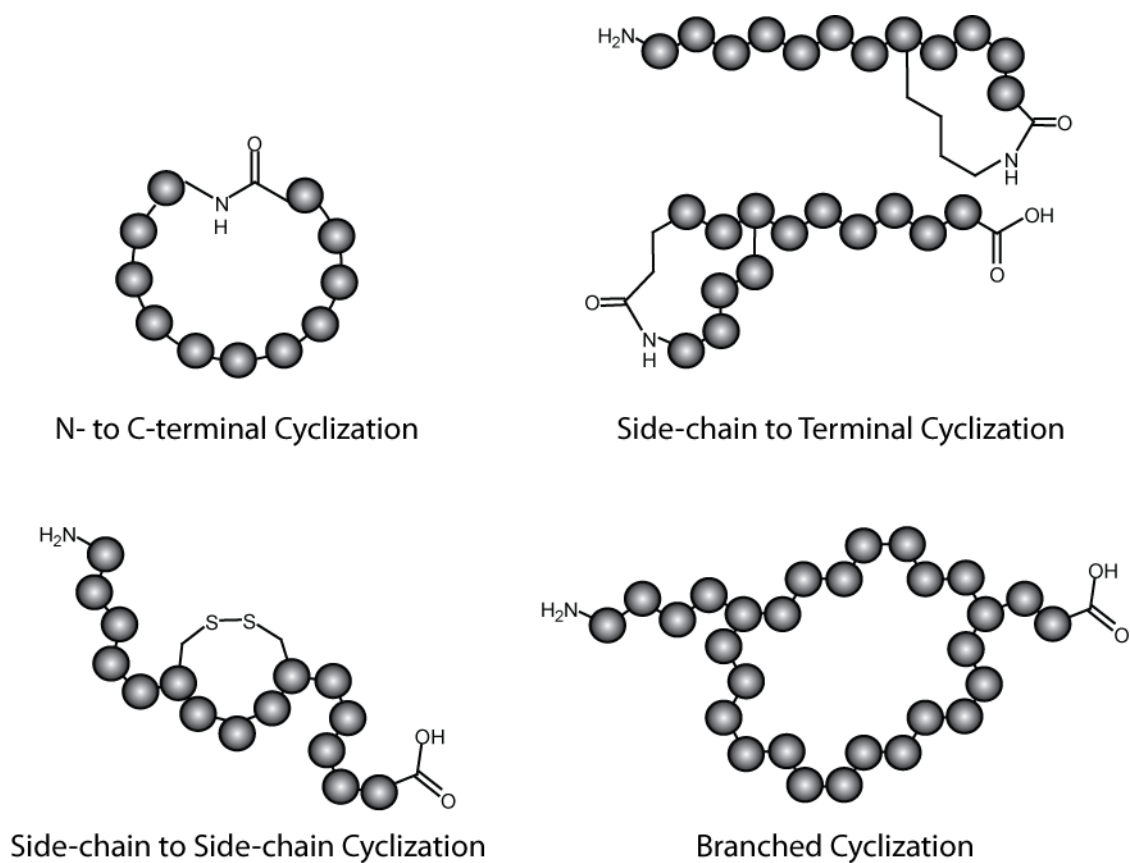


Figure 5.1. Schematic representations of different topologies exhibited by cyclized peptides. Figure was adapted Sewald and Jakubke (1).

5.2.2 Somatostatin and Erythropoietin

Somatostatin (SOM) was initially identified as a regulatory compound, inhibiting the release of certain hormones. Recently, somatostatin and somatostatin analogs have shown promise as analgesics, anticonvulsants and as anti-proliferative compounds (2-4). Both variants (SOM-14 and SOM-28) have been shown to exhibit similar biological effects, serving as high affinity ligands for their GPCR targets. SOM binds to one of five somatostatin receptor subtypes (sst_1 - sst_5) (5). The sst_2 and sst_4 receptor subtypes have been implicated in controlling seizure activity in rodent models (6). In efforts to discover the minimal number of residues required to elicit a biological effect, structure-activity studies were carried out. Through these efforts, the SRIF analog octreotide (Oct) was discovered. It was found that a minimal structure consisting of eight residues, constrained by a single disulfide bridge, exhibited increased metabolic stability, increased biological activity, and prolonged action (7). Moreover, octreotide was found to be selective for the sst_2 -receptor subtype (8). Despite the improvements conferred by octreotide over somatostatin, it was hypothesized in this work that modification of the octreotide framework would result in metabolically-stable, BBB-permeable analogs of somatostatin.

The idea of hormone-mediated regulation of red blood cell production has been known since the early 1900's. However, it was not until 1985 that the gene encoding this protein, erythropoietin (EPO), was first isolated and characterized (9). The initial role of this 166 amino acid glycoprotein (34 kDa) was found to be regulation of proliferation and differentiation of red blood cells (10, 11). More recently, a role for this protein in the

central nervous system as a neurotrophic factor and in controlling seizure activity was identified (12, 13).

Recently, peptide minimized analogs have been identified which could be chemically-synthesized and modified using solid phase peptide synthesis. In an attempt to develop multimeric EMPs, Vadas and co-workers developed both N- and C-terminally modified peptides (10). Using the N-EMP and C-EMP analogs as a template, we designed and synthesized a series of analogs possessing the lipidization-cationization motifs at both the N- and C-termini of erythropoietin mimetic peptides.

5.3 Materials and Methods

5.3.1 Design of Somatostatin and Erythropoietin Analogs

Containing Lipidization-Cationization Motifs

As mentioned earlier, octreotide was found to exhibit similar/improved physicochemical and pharmacological properties to those of SOM-14 and SOM-28 (7). Octreotide is essentially the C-terminal fragment of full-length SOM; it was therefore assumed that insertion of the lipidization-cationization motif at the N-terminus of octreotide would not interfere with receptor binding or activation. Furthermore, it has been previously reported that N-terminal glycosylation, PEGylation and lipidization of somatostatin analogs afforded ligands with comparable, or even increased, affinity for sst₂-receptors (14-16). Based on this information, a series of somatostatin analogs were designed that incorporated lipidization-cationization motifs attached to the N-terminus of octreotide. The somatostatin analog SOM-BBB1 (KKK_pK-Oct-NH₂) directly coupled the lipidization-cationization motif to the N-terminus of octreotide. This arrangement of three

Lys-residues and N^ε-palmitoyl-L-lysine was determined as the optimal lipidization-cationization motif for systemically-bioavailable galanin analogs (17). SOM-BBB2 (KKK_pG-Oct-NH₂) was designed to test the degree to which cationic character influenced biological activity of somatostatin analogs. This was accomplished by the [K4G] substitution, which effectively lowered the cationic character of this analog. SOM-BBB3 (KKK_p(Ahx)-Oct-NH₂) was designed to test whether increased distance between the lipidization-cationization motif and the bioactive fragment improved or attenuated pharmacological activity. SOM-BBB4 (KKK_p(Ahx)G-Oct-NH₂) maintained the spacing motif described for SOM-BBB3, but effectively switched the positioning of the palmitoyl motif relative to the peptide backbone. Our previous efforts with neuropeptide Y showed that insertion of an additional Ala-residue could have dramatic effects on the biological activity of the modified analogs (18). In SOM-BBB5, incorporation of polar PEG-type spacers was explored perhaps giving rise to somatostatin analogs that are active on peripheral neurons for the treatment of neuropathic pain (Figure 5.2).

Using peptide sequences obtained from phagemid mutagenesis libraries collected and screened by Wrighton and co-workers, a number of EMPs have been identified that exhibit similar physicochemical and pharmacological properties to that of the full-length protein (10, 19). Johnson and coworkers showed that EMP analogs N-terminally conjugated with PEG motifs could bind to erythropoietin receptors (EPOR) with micromolar affinities (20). Furthermore, in an attempt to construct multimeric analogs of EMPs, Vadas recently showed that modifications could be made to either the N- or C-terminal ends with similar effect (10) Using existing EMP scaffolds, and the fact that

these compounds can accommodate modifications at either terminus, we designed a series of erythropoietin analogs that contained lipidization-cationization motifs coupled directly to either the N- or C-terminus (EPO-BBB1 and EPO-BBB3). Additionally, the distancing and positioning of the lipoamino acid, with respect to the peptide backbone, was examined through insertion of a single Gly-residue between the lipidization-cationization motif and the EMP scaffold (EPO-BBB2 and EPO-BBB3) (Figure 5.3).

5.3.2 Solid Phase Peptide Synthesis

Synthesis of somatostatin and erythropoietin analogs was carried out using a Symphony automated peptide synthesizer (Protein Technologies, Inc). Syntheses were carried out at 50 μ mol scale using preloaded Amide-AM resins. Triple couplings of each amino acid (30, 30, and 40 min) were performed using 0.2 M PyBOP (benzotriazol-1-yl-oxytripyrrolidinophosphonium hexafluorophosphate), 0.4 M DIPEA (*N,N*-diisopropylethylamine), and 200 mM of each amino acid. Protected amino acids, including Fmoc-Lys(palmitoyl) and Fmoc-protected spacers were obtained commercially from Chem-Impex International. Peptides were cleaved from resin by treatment with reagent K (82.5% TFA, 5% water, 5% ethanedithiol, 2.5% thioanisole v/v, 75 mg/mL phenol) followed by vacuum filtration to separate peptide from resin, and finally precipitated with chilled methyl-*tert*-butyl ether. Crude peptides were then purified by preparative reversed-phase HPLC over a linear gradient of solvent B (90% acetonitrile in 0.1% TFA). Purities of separated fractions were assessed by analytical reversed-phase HPLC using a linear gradient of solvent B. HPLC fractions with peptide purities greater

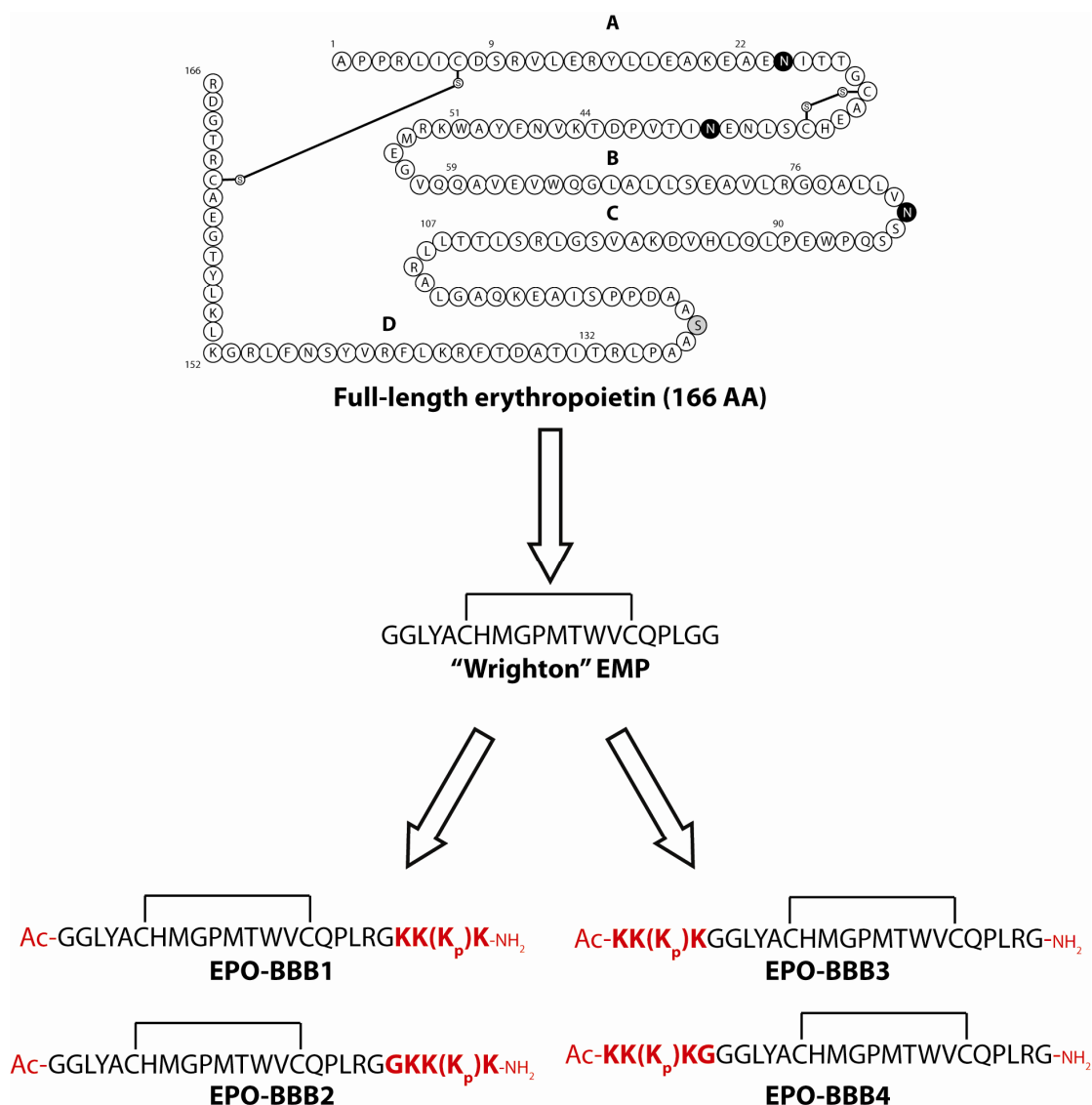


Figure 5.3 Design strategy for erythropoietin analogs containing lipidization-cationization motifs. Using an EMP scaffold described by Wrighton, erythropoietin analogs were designed that contained lipidization-cationization motifs at either the N- or C-termini. Consequences of the spacing/position of the modifications, relative to the bioactive fragment were explored through insertion of an additional Gly residue (19). (Ac) represents N-terminal acetylation; (K_p) denotes N^ε-palmitoyl-L-lysine.

than 95% were pooled and quantified by measuring UV absorbance at either 279.8 nm (SOM) or 274.6 (EPO). Molecular masses of all linear peptides were confirmed by MALDI-TOF MS.

5.3.3 Oxidation of Modified Somatostatin and Erythropoietin Analogs

Disulfide bond formation in somatostatin analogs was accomplished through oxidation of the linear peptide using CLEAR-OXTM resin (21, 22). Briefly, resin was prepared as described previously (22). Linear peptide was then reconstituted in 0.1 M Tris-HCl, pH 7.0 and was added to the pre-swelled resin. Peptides were incubated at 2 h at room temperature; after which, the oxidized peptide was removed from resin by vacuum-filtration. Completion of the oxidation reaction was verified by analytical reversed-phase HPLC and was confirmed by MALDI-TOF mass spectrometry.

Initial efforts to form the disulfide bridge in EPO analogs using CLEAR-OX resin were unsuccessful. EPO analogs were oxidized in solution in a manner similar to that described by Nielsen and coworkers (23). Briefly, linear peptide was reconstituted in $n\text{H}_2\text{O}$. Peptide was then added, at a final concentration of 20 μM , to a solution containing 30% acetonitrile, 0.1 mM GSSG, and 0.1 M Tris-HCl, pH 7.4. Oxidation was allowed to proceed for 6 h at room temperature. Reactions were quenched with formic acid (8% of total reaction volume) and peptides were purified by preparative reverse-phased HPLC using a linear gradient ranging from 5% to 95% solvent B in 30 min.

Following HPLC purification individual fractions were purified, pooled and masses of the folded peptides were confirmed by MALDI-TOF mass spectrometry.

5.4 Results and Discussion

Analogs of the cyclic peptides somatostatin and erythropoietin were synthesized using solid phase peptide synthesis. Following synthesis, peptides were cleaved from resin by treatment with reagent K, and were purified by analytical HPLC. Final yields of the purified linear peptides ranged between 8-10%, with respect to resin mass, for both SOM and EPO analogs. Somatostatin analogs were oxidized using the solid-support CLEAR-OX. Final yields of the modified somatostatin analogs ranged between 40 and 62.5% of correctly oxidized peptide. Conversely, using solution oxidation methods, nearly all of the purified linear EPO analogs was recovered as the completely oxidized peptide. Following HPLC purification of the oxidized peptides, MALDI-TOF mass spectrometry analysis was conducted to verify formation of the disulfide bridge. All analogs were observed to possess masses 2 Da lower than those of their linear counterparts, indicating disulfide bridge formation (Figure 5.4).

5.5 Conclusions

As illustrated here, lipidization-cationization motifs were applied to short, conformationally-constrained analogs of the cyclic peptides somatostatin and erythropoietin. These compounds were synthesized by solid phase peptide synthesis and disulfide bridge formation was accomplished by oxidation using both solution and solid support methods.

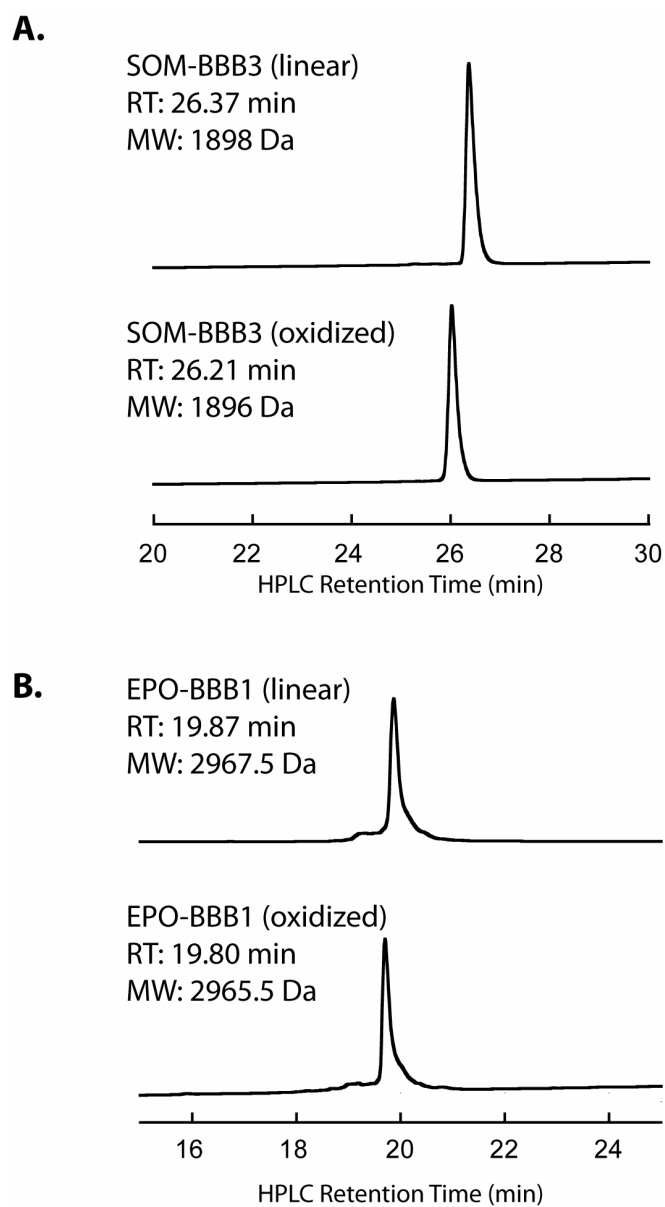


Figure 5.4 Oxidation of cyclic peptides containing lipidization-cationization motifs. Panel A illustrates representative HPLC traces of the somatostatin analog SOM-BBB3. In addition to differences in HPLC retention time, a decrease in mass was observed by MALDI-TOF. Panel B shows representative HPLC traces for oxidation of the EPO analog EPO-BBB1 with corresponding MALDI results.

Subsequent studies will focus on physicochemical and pharmacological characterization of the modified SOM and EPO analogs. For example, somatostatin is generally considered to possess poor systemic bioavailability. However, octreotide exhibited increased BBB-permeability, though it was still found to cross the BBB by passive diffusion and only at rates similar to those of albumin (24). Octreotide was also shown to possess increased serum half-life, $t_{1/2}(\text{SOM-14}) < 3 \text{ min}$ versus $t_{1/2}(\text{octreotide}) = 1.5 \text{ h}$ (25). It is anticipated, based on our previous findings, that these values may be further improved. Moreover, it is expected that lipidization-cationization motifs applied to the octreotide framework may result in systemically-active peptide analogs in mouse models of epilepsy. Likewise, it is recognized that further characterization of the EPO analogs must be undertaken to show improved characteristics of these compounds in comparison to existing EMPs. Efforts to determine the metabolic stabilities and logD values for SOM and EPO analogs are ongoing in an attempt to engineer analogs with improved characteristics.

5.6 References

1. Sewald, N., and Jakubke, H.-D. (2002) *Peptides: Chemistry and Biology*, Wiley-VCH Verlag GmbH, Weinheim.
2. Chrubasik, J., Meynadier, J., Scherpereel, P., and Wunsch, W. (1985) The effect of epidural somatostatin on postoperative pain, *Anesth. Analg.* *64*, 1085-1088.
3. Vezzani, A., and Hoyer, D. (1999) Brain somatostatin: A candidate inhibitory role in seizures and epileptogenesis, *Eur. J. Neurosci.* *11*, 3767-3776.
4. Weckbecker, G., Raulf, F., Bodmer, D., and Bruns, C. (1997) Indirect antiproliferative effect of the somatostatin analog octreotide on MIA PaCa-2 human pancreatic carcinoma in nude mice, *Yale J. Biol. Med.* *70*, 549-554.
5. Weckbecker, G., Lewis, I., Albert, R., Schmid, H. A., Hoyer, D., and Bruns, C. (2003) Opportunities in somatostatin research: Biological, chemical and therapeutic aspects, *Nat. Rev. Drug Discov.* *2*, 999-1017.
6. Tallent, M. K., and Qiu, C. (2007) Somatostatin: An endogenous antiepileptic, *Mol. Cell. Endocrinol.* *286*, 96-103.
7. Bauer, W., Briner, U., Doepfner, W., Haller, R., Huguenin, R., Marbach, P., Petcher, T. J., and Pless, J. (1982) SMS 201-995: A very potent and selective octapeptide analogue of somatostatin with prolonged action, *Life Sci.* *31*, 1133-1140.
8. Rajeswaran, W. G., Hocart, S. J., Murphy, W. A., Taylor, J. E., and Coy, D. H. (2001) Highly potent and subtype selective ligands derived by *N*-methyl scan of a somatostatin antagonist, *J. Med. Chem.* *44*, 1305-1311.
9. Szenajch, J., Wcislo, G., Jeong, J.-Y., Szczylik, C., and Feldman, L. (2010) The role of erythropoietin and its receptor in growth, survival and therapeutic response of human tumor cells From clinic to bench - a critical review, *Biochim. Biophys. Acta* *1806*, 82-95.
10. Vadas, O., Hartley, O., and Rose, K. (2008) Characterization of new multimeric erythropoietin receptor agonists, *Biopolymers* *90*, 496-502.
11. Boissel, J.-P., Lee, W.-R., Presnell, S. R., Cohen, F. E., and Bunn, H. F. (1993) Erythropoietin structure-function relationships, *J. Biol. Chem.* *268*, 15983-15993.
12. Kondo, A., Shingo, T., Yasuhara, T., Kuramoto, S., Kameda, M., Matsui, Y., Miyoshi, Y., Agari, T., Borlongan, C. V., and Date, I. (2009) Erythropoietin exerts anti-epileptic effects with the suppression of aberrant new cell formation in

- the dentate gyrus and upregulation of neuropeptide Y in seizure model of rats, *Brain Res.* *1296*, 127-136.
13. Campana, W. M., and Myers, R. R. (2001) Erythropoietin and erythropoietin receptors in the peripheral nervous system: changes after nerve injury, *Eur. J. Neurosci.* *18*, 1497-1506.
 14. Schottelius, M., Wester, H.-J., Reubi, J. C., Senekowitsch-Schmidtke, R., and Schwaiger, M. (2002) Improvement of pharmacokinetics of radioiodinated Tyr³-octreotide by conjugation with carbohydrates, *Bioconjugate Chem.* *13*, 1021-1030.
 15. Na, D. H., Lee, K. C., and DeLuca, P. P. (2005) PEGylation of octreotide: II. Effect of N-terminal mono-PEGylation on biological activity and pharmacokinetics, *Pharm. Res.* *22*, 743-749.
 16. Dasgupta, P., Singh, A. T., and Mukherjee, R. (1999) Lipophilization of somatostatin analog RC-160 improves its bioactivity and stability, *Pharm. Res.* *16*, 1047-1053.
 17. Bulaj, G., Green, B. R., Lee, H.-K., Robertson, C. R., White, K., Zhang, L., Sochanska, M., Flynn, S. P., Scholl, E. A., Pruess, T. H., Smith, M. D., and White, H. S. (2008) Design, synthesis, and characterization of high-affinity, systemically-active galanin analogues with potent anticonvulsant activities, *J. Med. Chem.* *51*, 8038-8047.
 18. Green, B. R., White, K. L., McDougle, D. R., Zhang, L., Klein, B., Scholl, E. A., Pruess, T. H., White, H. S., and Bulaj, G. (2010) Introduction of lipidization-cationization motifs affords systemically bioavailable neuropeptide Y and neurotensin analogs with anticonvulsant activities, *J. Pept. Sci.* *16*, 486-495.
 19. Wrighton, N. C., Farrell, F. X., Chang, R., Kashyap, A. K., Barbone, F. P., Mulcahy, L. S., Johnson, D. L., Barrett, R. W., Jolliffe, L. K., and Dower, W. J. (1996) Small peptides as potent mimetics of the protein hormone erythropoietin, *Science* *273*, 458-463.
 20. Johnson, D. L., Farrell, F. X., Barbone, F. P., McMahon, F. J., Tullai, J., Kroon, D., Freedy, J., Zivin, R. A., Mulcahy, L. S., and Jolliffe, L. K. (1997) Amino-terminal dimerization of an erythropoietin mimetic peptide results in increased erythropoietic activity, *Chem. Biol.* *4*, 939-950.
 21. Darlak, K., Long, D. W., Czerwinski, A., Darlak, M., Valenzuela, F., Spatola, A. F., and Barany, G. (2004) Facile preparation of disulfide-bridged peptides using polymer-supported oxidant CLEAR-OX, *J. Pept. Res.* *63*, 303-312.
 22. Green, B. R., and Bulaj, G. (2006) Oxidative folding of conotoxins in immobilized systems, *Protein Pept. Lett.* *13*, 67-70.

23. Nielsen, J. S., Buczek, P., and Bulaj, G. (2004) Cosolvent-assisted oxidative folding of a bicyclic α -conotoxin ImI, *J. Pept. Sci.* 10, 249-256.
24. Banks, W. A., Schally, A. V., Barrera, C. M., Fasold, M. B., Durham, D. A., Csernus, V. J., Groot, K., and Kastin, A. J. (1990) Permeability of the murine blood-brain barrier to some octapeptide analogs of somatostatin, *Proc. Natl. Acad. Sci.* 87, 6762-6766.
25. Werle, M., and Bernkop-Schnürch, A. (2006) Strategies to improve plasma half life time of peptide and protein drugs, *Amino Acids* 30, 351-367.

CHAPTER 6

PERSPECTIVES AND CONCLUSIONS

6.1 Perspectives

This work describes the first examples of peptidic ligands of GAL, NPY, and NPW that penetrate the BBB and are active in suppressing seizure activity following systemic administration. To overcome the issues that have traditionally precluded the development of peptide-based drugs (i.e., poor metabolic stability and low bioavailability), our lab successfully employed a novel strategy of the combination of lipidization and cationization towards the development of metabolically-stable, systemically-bioavailable analogs of galanin, neurotensin, neuropeptide Y, and neuropeptide W for the treatment of neuropathic pain and epilepsy. This work serves as proof-of-concept that through modification of the bioactive fragments of endogenous neuropeptides, receptor-specific peptide ligands with improved physicochemical and pharmacological characteristics could be constructed. Furthermore, we have found that through these modifications, analogs could be modified for specific targeting of their receptors in the CNS or PNS.

As illustrated in Figure 6.1, the strategy described in this thesis has broader potential beyond the development of peptide drugs for the treatment of pain or epilepsy.

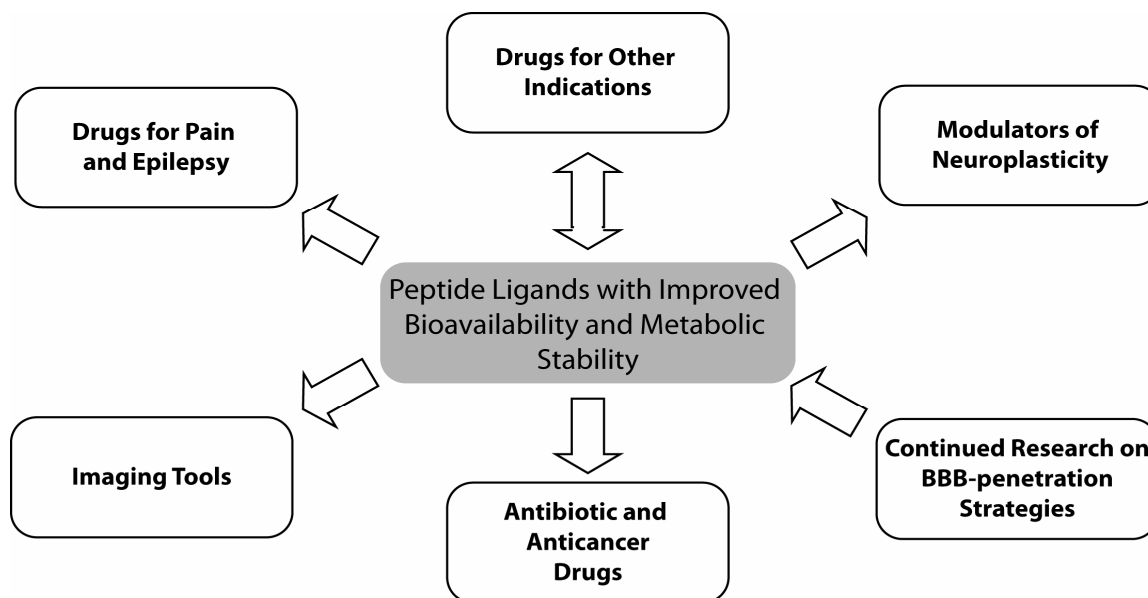


Figure 6.1 Potential outcomes/directions of the lipidization-cationization strategy.

First, using combinations of lipidization-cationization motifs, biologically-active peptides, can be modified to construct peptide-based therapeutics for a number of non-neurological disorders. Second, BBB-permeable neuropeptides could be used as tools for the study or treatment of the long-term effects of pain or epilepsy (synaptic neuroplasticity). Third, our work encourages an in-depth look at the combination of existing BBB-penetration strategies in an attempt to develop new peptide analogs with increased bioavailability. Fourth, extension of this technology to peptidic compounds such as non-ribosomal peptide (NRP) and ribosomal peptide (RP) natural products may result in the development of potent antimicrobial or anticancer drugs with improved bioavailability for the treatment of infections of the CNS or certain brain cancers. Finally, using BBB-permeable analogs containing labeling motifs (e.g., fluorescent labels, radiolabels, IR probes, etc.), may yield new tools for imaging regions/receptors in the brain that possess increased specificity for their CNS targets.

6.1.1 Drugs for Other Indications

There currently exists a great potential for the development of peptide-based drugs capable of specifically targeting receptors throughout the body for the treatment of a wide variety of human illnesses. As mentioned earlier, many GPCR targets of neuropeptides are expressed in tissues of both the CNS and PNS. Furthermore, many of these receptors are multifaceted in their biological function depending on their location. This is of particular interest in the development of peptide ligands for receptors implicated in non-neurological disorders. In addition to their roles as neuromodulatory

compounds, neuropeptides such as galanin, neuropeptide Y, and neuropeptide W have been also studied for their orexigenic (modulation of food intake) effects; modulated through receptors in other locations within the brain (1, 2). It is conceivable that through specific targeting of peptide analogs to the receptors that modulate orexigenesis, first-in-class treatments for disorders such as obesity, or even diabetes, could be developed. Moreover, we have previously shown that modifications made to the lipidization motif itself (i.e., altered chain length or PEGylation) could direct peptide analogs to receptors in the peripheral nervous system (3). This is of particular interest in the specific targeting of analgesic peptides such as opioid peptides, substance P, and neuropeptide FF to receptors in peripheral neurons (Table 6.1). Towards the development of peripherally-acting neuropeptides, special care must be taken to avoid unintended delivery to the CNS. In doing so, one avoids many of the adverse side effects that might result from interactions of these analgesic neuropeptides with their respective receptors in the brain (e.g., drowsiness, decreased cognitive function, respiratory depression, etc.).

6.1.2 Modulators of Neuroplasticity

Another promising outcome of this research may be in the development of new pharmacological tools to aid in studying synaptic plasticity of the nervous system (10). As a result of extended periods of neuropathic pain or seizure, expression of certain neuropeptides is altered (11). Expression levels of important anticonvulsant peptides (galanin, neuropeptide Y, etc.) are decreased; whereas de novo synthesis of proconvulsant neuropeptides (neurokinin B and substance P) is increased (11). The

Table 1. Examples of endogenous neuropeptides that may be modified for improved analgesic effect.

| Peptide | Structure | Target Receptor | Literature Reference |
|-----------------|--------------------------------|---|----------------------|
| Orphanin | FGGFTGARKSARKLANQ [^] | nociceptin/orphanin FQ peptide (NOP) receptor | (4) |
| Dynorphin-A | YGGFLRRIRPKLK [^] | κ -opioid receptor | (5) |
| Substance P | RPKQQFFGLM [#] | Neurokinin receptor subtype 1 (NK1R) | (6) |
| Neuropeptide FF | FLFQPQRF [#] | Neuropeptide FF receptor (NPFFR1) | (7) |
| Met-enkephalin | YGGFM [^] | δ -opioid receptor | (8) |
| Endomorphin-1 | YPYF [#] | μ -opioid receptor | (9) |

Selected endogenous peptides that may be modified to target peripheral neurons for antinociceptive effect. (^) denotes a carboxylated C-terminus; (#) denotes C-terminal amidation. Through attachment of lipidization-cationization motifs to the minimal number of residues necessary to elicit the peptides' biological effect, novel peptide-based analgesic compounds could be constructed.

maladaptive restructuring of proconvulsant and anticonvulsant peptides results in the inability of neuronal tissues to properly regulate excitatory/inhibitory behaviors (12). This often leads to persistent seizure activity or chronic pain states. Systemic administration of BBB-permeable anticonvulsant compounds could potentially compensate for the loss of important neuromodulatory compounds such as galanin, neuropeptide Y, and others. Moreover, BBB-permeable analogs may be explored for their disease modification properties. Through administration of the modified peptides, researchers could effectively alter the expression levels of other endogenous neuropeptides in the brain. With respect to neurological disorders such as pain or epilepsy, this could prove of great worth as a treatment that actually reverses the effects of such disorders.

6.1.3 Continued Research on Design of BBB-penetration Strategies

This research also encourages further exploration into alternative combination strategies for the development of CNS targeting peptides. Numerous strategies have been employed to increase serum stability and bioavailability of peptide-based drugs. All of the listed BBB-penetration strategies were shown to increase metabolic stability of the peptides; however, the effects of these modifications on logD values, as an indicator of the lipophilicity of the compounds, were varied (13, 14). It is therefore conceivable that any number of the aforementioned strategies could be employed simultaneously to increase serum stability, providing receptor binding/activation was not adversely affected. However, certain combinations of these strategies may lead to more

pronounced changes in logD values, and subsequent BBB-penetration of the modified peptides.

This work described the combination of lipidization and cationization for improved BBB-penetration. Based on our research, increased lipophilicity appears to be the major contributor for increased BBB-penetration. This modification likely increased BBB-penetration via passive diffusion as a direct result of increased lipophilicity of the peptide. Whereas, increased cationic character, in the context of oligo-Lys motifs, may have facilitated BBB-penetration through absorptive mediated endocytosis (15). However, we also showed that increased lipophilicity or increased cationic character alone did not facilitate efficient delivery of analogs into the brain (see Chapter 1); rather, the combination of these two modifications was required for systemic bioavailability (16). Liu and coworkers described the combination of increased N-terminal cationization and halogenation of endomorphin-1 for increased bioavailability (13). By itself, cationization actually decreases the overall lipophilicity of peptide drugs. However, in agreement with our findings, the combination of this chemical modification with a modification that increases lipophilic character (halogenation) resulted in endomorphin analogs with increased metabolic stability and improved BBB-penetration (13).

Based on the individual effects of each modification on logD, and overall BBB-permeability, it is hypothesized that increased lipophilicity is the primary contributor to increased BBB-penetration. As such, the conjugation of lipidization or halogenation (through addition of Cl or Br groups) motifs may have the greatest effects on CNS delivery. However, the combination of multiple strategies that increase lipophilicity is not likely viable due to decreased solubility and serum stability of the peptide analogs.

By combining these modifications with others that do not significantly contribute to peptide lipophilicity (glycosylation, cationization, or polymer conjugation), analogs may be designed that are capable of exploiting both active and passive transport mechanisms. Furthermore, it is conceivable that the combination of two, or more, strategies that do not increase logD values (cationization, glycosylation, or polymer conjugation) may prove effective in the construction of peptides that act specifically on the periphery. In conjunction with the lipidization-cationization strategy described in this work, Liu's work served as evidence that the combination of two or more of these strategies may be effective in developing peptide-based drugs for treatment of numerous indications both centrally and peripherally (Table 6.2).

6.1.4 Antibiotic and Anticancer Drugs

The lipidization-cationization strategy may not be entirely limited to endogenous neuropeptides. Recent interest has been drawn by the therapeutic potentials of peptidic compounds such as the non-ribosomal peptide (NRP) and ribosomal peptide (RP) natural products (21, 22). Many of these compounds have shown tremendous potential as therapeutics due to their antimicrobial or anticancer properties; unfortunately, a large number also possess poor systemic bioavailability (i.e., vancomycin) (23). Furthermore, NRP and RP natural products isolated from fungi or bacteria exhibit a large structural diversity, providing a large repertoire of peptide scaffolds from which novel peptide-based therapeutics could be generated. Using available structure-activity information for these compounds, lipidization-cationization motifs could be rationally-incorporated

Table 6.2 Strategies for improving CNS delivery of peptides.

| Strategy | Transport Mechanism | Serum Stability | logD | BBB-Permeability |
|------------------------------|--|-----------------|------|------------------|
| Lipidization (15) | Passive diffusion | ↑↑ | ↑↑ | ↑ |
| Structural Modification (15) | Passive diffusion | ↑↑ | N/A | ↑ |
| Nutrient Transport (15) | Various active transport mechanisms | ↑ | ↑ | ↑ |
| Prodrug Strategies (15) | Passive/active transport | ↑ | ↑ | ↑ |
| Cationization (17) | Absorptive mediated endocytosis | ↑ | ↓ | ↑ |
| Glycosylation (18) | Unknown; likely active transport (i.e. RAGE) | ↑ | ↓ | ↑ |
| Polymer Conjugation (19) | Passive diffusion | ↑ | ↓ | ↑↓ |
| Halogenation (20) | Passive diffusion | ↑ | ↑↑ | ↑ |

Table presents numerous strategies for increasing the BBB-permeability of peptide-based drugs. The effects of each modification on serum stability, lipophilicity (logD), and overall BBB-permeability are listed. This work explores the combination of two strategies for development of systemically-bioavailable neuropeptides. Based on our results, future efforts should be focused on combinations of multiple strategies.

towards the synthesis of NRP or RP natural product analogs with improved bioavailability. As a result BBB-permeable NRP/RP analogs could be constructed as first-in-class treatments for bacterial infections of the CNS like bacterial meningitis or bacterial encephalitis, or as treatments of neuroblastomas.

6.1.5 Imaging Tools

Another application of the lipidization-cationization strategy is the development of peptide-based imaging tools specifically targeted to the CNS. Recently, much effort has been devoted towards the creation of receptor-specific molecular probes for the imaging of tumors. Both radiolabeled and fluorescently-labeled analogs of neurotensin have been developed for diagnosis/imaging of tumors in the peripheral tissues; largely facilitated by the increased expression of neurotensin receptors on the surface of cancerous cells (24, 25). By engineering fluorescently-labeled peptide analogs that cross the BBB, peptide-based labeling systems may prove useful in specifically targeting/identifying neuropeptide receptor subtypes in the brain or spinal chord. Furthermore, BBB-permeable neuropeptide probes might also be used as contrasting agents for real-time imaging of brain tissues. This application would further compliment previous efforts with NT and NPW, while spurring further efforts towards developing Gal, NPW, SOM, etc. as imaging tools.

6.2 Conclusions

In summary of this section, the lipidization-cationization strategy was found broadly applicable across numerous endogenous neuropeptides (GAL, NT, NPY, and

NPW). This combination strategy resulted in multiple systemically-bioavailable peptide analogs (Gal-B2, NT-BBB1, NPY-BBB2, and NPW-B1) that were shown active in suppressing seizures in the 6 Hz psychomotor seizure model in mice. The anticonvulsant properties of these analogs were directly attributed to the improved metabolic stability and increased logD values, conferred by the lipidization-cationization motifs. It was also shown in previous sections that this approach could be further applied towards the synthesis and preparation of analogs of cyclic peptides such as somatostatin or erythropoietin. Lastly, this chapter has illuminated the larger potential of the lipidization-cationization strategy for the construction of peptide-based tools for the study and/or treatment of a wide range of indications beyond pain and epilepsy.

6.3 References

1. Adams, A. C., Clapham, J. C., Wynick, D., and Speakman, J. R. (2008) Feeding behaviour in galanin knockout mice supports a role of galanin in fat intake and preference, *J. Neuroendocrinol.* 20, 199-206.
2. Takenoya, F., Kageyama, H., Shiba, K., Date, Y., Nakazato, M., and Shioda, S. (2010) Neuropeptide W: a key player in the homeostatic regulation of feeding and energy metabolism?, *Ann. N. Y. Acad. Sci.* 1200, 162-169.
3. Zhang, L., Robertson, C. R., Green, B. R., Pruess, T. H., White, H. S., and Bulaj, G. (2009) Structural requirements for a lipoamino acid in modulating the anticonvulsant activities of systemically active galanin, *J. Med. Chem.* 52, 1310-1316.
4. Reinscheid, R. K., Ardati, A., Frederick, J., Monsma, J., and Civelli, O. (1996) Structure-activity relationship studies on the novel neuropeptide orphanin FQ, *J. Biol. Chem.* 271, 14163-14168.
5. Lai, J., Luo, M. C., Chen, Q., Ma, S., Gardell, L. R., Ossipov, M. H., and Porreca, F. (2006) Dynorphin A activates bradykinin receptors to maintain neuropathic pain, *Nat. Neurosci.* 9, 1534-1540.
6. De Felipe, C., Herrero, J. F., O'Brien, J. A., Palmer, J. A., Doyle, C. A., Smith, A. J., Laird, J. M., Belmonte, C., Cervero, F., and Hunt, S. P. (1998) Altered nociception, analgesia and aggression in mice lacking the receptor for substance P, *Nature* 392, 394-397.
7. Gicquel, S., Mazarguil, H., Desprat, C., Allard, M., Jean-Paul, D., Simonet, J., and Zajac, J.-M. (1994) Structure-activity study of neuropeptide FF: Contribution of N-terminal regions to affinity and activity, *J. Med. Chem.* 37, 3477-3481.
8. Audigier, Y., Mazarguil, H., Gout, R., and Cros, J. (1980) Structure-activity relationships of enkephalin analogs at opiate and enkephalin receptors: Correlation with analgesia, *Eur. J. Pharmacol.* 63, 35-46.
9. Zadina, J. E., Martin-Schild, S., Gerall, A. A., Kastin, A. J., Hackler, L., Ge, L. J., and Zhang, X. (1999) Endomorphins: Novel endogenous mu-opiate receptor agonists in regions of high mu-opiate receptor density, *Ann. N. Y. Acad. Sci.* 897, 136-144.
10. Sperk, G., Drexel, M., and Pirker, S. (2009) Neuronal plasticity in animal models and the epileptic human hippocampus, *Epilepsia* 50, 29-31.
11. Wasterlain, C. G., Mazarati, A. M., Naylor, D., Niquet, J., Liu, H., Suchomelova, L., Baldwin, R., Katsumori, H., Shirasaka, Y., Shin, D., and Sankar, R. (2002)

- Short-term plasticity of hippocampal neuropeptides and neuronal circuitry in experimental status epilepticus, *Epilepsia* 43, 20-29.
12. Vezzani, A., Schwarzzer, C., Lothman, E. W., Williamson, J., and Sperk, G. (1996) Functional changes in somatostatin and neuropeptide Y containing neurons in the rat hippocampus in chronic models of limbic seizures, *Epilepsy Res.* 26, 267-279.
 13. Liu, H.-M., Liu, X.-F., Yao, J.-L., Wang, C.-L., Yu, Y., and Wang, R. (2006) Utilization of combined chemical modifications to enhance the blood-brain barrier permeability and pharmacological activity of endomorphin-1, *J. Pharmacol. Exp. Ther.* 319, 308-316.
 14. Nelson, A. R., Borland, L., Allbritton, N. L., and Sims, C. E. (2007) Myristoyl-based transport of peptides into living cells, *Biochemistry* 46, 14771-14781.
 15. Witt, K. A., Gillespie, T. J., Huber, J. D., Egleton, R. D., and Davis, T. P. (2001) Peptide drug modifications to enhance bioavailability and blood-brain barrier permeability, *Peptides* 22, 2329-2343.
 16. Bulaj, G., Green, B. R., Lee, H. K., Robertson, C. R., White, K., Zhang, L., Sochanska, M., Flynn, S. P., Scholl, E. A., Pruess, T. H., Smith, M. D., and White, H. S. (2008) Design, synthesis, and characterization of high-affinity, systemically-active galanin analogues with potent anticonvulsant activities, *J. Med. Chem.* 51, 8038-8047.
 17. Tamai, I., Sai, Y., Kobayashi, H., Kamata, M., Wakamiya, T., and Tsuji, A. (1997) Structure-internalization relationship for adsorptive-mediated endocytosis of basic peptides at the blood-brain barrier, *J. Pharmacol. Exp. Ther.* 280, 410-415.
 18. Egleton, R. D., Mitchell, S. A., Huber, J. D., Palian, M. M., Polt, R., and Davis, T. P. (2001) Improved blood-brain barrier penetration and enhanced analgesia of an opioid peptide by glycosylation, *J. Pharmacol. Exp. Ther.* 299, 967-972.
 19. Tsusumi, Y., Onda, M., Nagata, S., Lee, B., Kreitman, R. J., and Pastan, I. (2000) Site-specific chemical modification with polyethylene glycol of recombinant immunotoxin anti-Tac(Fv)-PE38 (LMB-2) improves antitumor activity, and reduces animal toxicity, and immunogenicity, *Proc. Natl. Acad. Sci.* 48, 910-916.
 20. Gentry, C. L., Egleton, R. D., Gillespie, T., Abbruscato, T. J., Bechowski, H. B., Hruby, V. J., and Davis, T. P. (1999) The effect of halogenation on blood-brain barrier permeability of a novel peptide drug, *Peptides* 20, 1229-1238.
 21. Walsh, C. T. (2004) Polyketide and nonribosomal peptide antibiotics: Modularity and versatility, *Science* 303, 1805-1810.

22. McIntosh, J. A., Donia, M. S., and Schmidt, E. W. (2009) Ribosomal peptide natural products: Bridging the ribosomal and nonribosomal worlds, *Nat. Prod. Rep.* 26, 537-559.
23. Lamb, S. S., and Wright, G. D. (2005) Accessorizing natural products: Adding to nature's toolbox, *Proc. Natl. Acad. Sci.* 102, 519-520.
24. Alshoukr, F., Rosant, C., Maes, V., Abdelhak, J., raguin, O., Burg, S., Sarda, L., Barbet, J., Tourwé, D., Pelaprat, D., and Gruaz-Guyon, A. (2009) Novel neurotensin analogues for radioisotope targeting to neurotensin receptor-positive tumors, *Biconjug. Chem.* 20, 1602-1610.
25. Achilefu, S. (2004) Lighting up tumors with receptor-specific optical molecular probes, *Technol. Cancer Res. Treat.* 3, 393-409.